STUDIES ON THERMOPLASTIC ELASTOMERS FROM NATURAL RUBBER/POLYSTYRENE AND NATURAL RUBBER/POLYSTYRENE/ NATURAL RUBBER-GRAFT-POLYSTYRENE BLENDS

THESIS SUBMITTED TO
THE MAHATMA GANDHI UNIVERSITY
IN PARTIAL FULFILMENT OF THE REQUIREMENTS FOR
THE AWARD OF THE DEGREE OF

DOCTOR OF PHILOSOPHY
IN POLYMER CHEMISTRY
UNDER THE FACULTY OF SCIENCE

ASALETHA R.

RUBBER RESEARCH INSTITUTE OF INDIA
KOTTAYAM, KERALA, INDIA

AND

SCHOOL OF CHEMICAL SCIENCES
MAHATMA GANDHI UNIVERSITY
KOTTAYAM, KERALA, INDIA

JANUARY, 1998

. . . to my Parents

रबड़ बोर्ड

(वाणिज्य मन्त्रालय, भारत सरकार)

THE RUBBER BOARD

(Ministry of Commerce, Government of India)

रबड़ प्रसंस्करण विभाग

DEPARTMENT OF PROCESSING & PRODUCT DEVELOPMENT

Reply to be Addressed to
THE DIRECTOR (P & PD)

कोट्टयम–५, केरळ
KOTTAYAM – 686005
Kerala State

Ref No ...._

Date ...9.th.....Feb.(99

CERTIFICATE

This is to certify that the thesis entitled **Studies on Thermoplastic Elastomers from Natural Rubber/Polystyrene and Natural Rubber/Polystyrene/Natural Rubber-graft-Polystyrene Blends** is an authentic record of the research work carried out by **Ms. Asaletha R.** under the joint supervision and guidance of myself and Dr. Sabu Thomas, Reader, School of Chemical Sciences, Mahatma Gandhi University, in partial fulfilment of the requirements for the award of the degree of **Doctor of Philosophy** in Polymer Chemistry under the Faculty of Science of the Mahatma Gandhi University, Kottayam. The work presented in this thesis has not been submitted for any other degree or diploma earlier.   It is also certified that Ms. Asaletha R. has fulfilled the course requirements and passed the qualifying examination for the Ph.D. degree of the University.

Kottayam
January 1998

DR. M. G. KUMARAN
(Supervising Teacher)

Dr. SABU THOMAS B. Tech., Ph.D.

READER IN POLYMER SCIENCE & TECHNOLOGY
(Director, Regional Centre
School of Technology and Applied Sciences)
SCHOOL OF CHEMICAL SCIENCES
MAHATMA GANDHI UNIVERSITY
PRIYADARSHINI HILLS P. O.
KOTTAYAM - 686 560
KERALA, INDIA.

Mahatma Gandhi University

Date 9th Feb 1998

CERTIFICATE

This is to certify that the thesis entitled **Studies on Thermoplastic Elastomers from Natural Rubber/Polystyrene and Natural Rubber/Polystyrene/Natural Rubber-graft-Polystyrene Blends** is an authentic record of the research work carried out by **Ms. Asaletha R.** under the joint supervision and guidance of myself and Dr. M. G. Kumaran, Joint Director, Rubber Board, in partial fulfilment of the requirements for the award of the degree of **Doctor of Philosophy** in Polymer Chemistry under the Faculty of Science of the Mahatma Gandhi University, Kottayam. The work presented in this thesis has not been submitted for any other degree or diploma earlier. It is also certified that Ms. Asaletha R. has fulfilled the course requirements and passed the qualifying examination for the Ph.D. degree of the University.

Priyadarsini Hills
January 1998

DR. SABU THOMAS
(Supervising Teacher)

DECLARATION

I hereby declare that the thesis entitled **Studies on Thermoplastic Elastomers from Natural Rubber/Polystyrene and Natural Rubber/Polystyrene/Natural Rubber-graft-Polystyrene Blends** is a record of the research work carried out by me under the joint supervision and guidance of **Dr. M. G. Kumaran**, Joint Director, Rubber Board, Kottayam, and **Dr. Sabu Thomas,** School of Chemical Sciences, Mahatma Gandhi University, Kottayam. No part of this thesis has been presented for any other degree or diploma earlier.

Kottayam   ASALETHA R.
January 1998

ACKNOWLEDGEMENTS

Asaletha R.

SYMBOLS AND ABBREVIATIONS

$\dot{\gamma}_{wa}$	-	apparent shear rate at wall
$\dot{\gamma}_{w}$	-	shear rate at wall
Σ	-	area occupied by the copolymer at the interface
ρ	-	density
χ	-	interaction parameter
v	-	molar volume of solvent
η	-	shear viscosity
δ	-	solubility parameter
ϕ	-	volume fraction
$\Delta\gamma$	-	interfacial tension reduction
$\tau_{11}-\tau_{22}$	-	principal normal stress difference
ϕ_A	-	volume fraction of the polymer
ϕ_c	-	volume fraction of the copolymer
ΔG	-	standard free energy of mixing
ΔH_s	-	enthalpy
ΔS	-	entropy
τ_w	-	shear stress
ABS	-	acrylonitrile butadiene styrene copolymer
Ap	-	cross-sectional area of the piston
C_6H_6	-	benzene
$CaCl_2$	-	calcium chloride
CBS	-	N-cyclohexyl-2-benzothiazylsulphenamide
CCl_4	-	carbontetrachloride
$CHCl_3$	-	chloroform
CMC	-	critical micelle concentration
CP	-	chloroprene
D	-	diffusion coefficient
d	-	width at half height of the copolymer profile reduced by Kuhn statistical segment length
d_c	-	diameter of capillary
DCP	-	dicumyl peroxide
d_e	-	diameter of the extrudate
DRC	-	dry rubber content
DSC	-	differential scanning calorimetry
DTG	-	derivative thermogravimetry
E	-	activation energy

E_D	-	activation energy of diffusion
EMA	-	ethylene methacrylate
E_p	-	activation energy of permeation
EPDM	-	ethylene propylene diene monomer
EPM	-	ethylene propylene monomer
EVA	-	ethylene vinyl acetate
G	-	elastic shear modulus
GMA	-	glycidyl methacrylate
HEMA	-	hydroxy ethyl methacrylate
HPMA	-	hydroxy propyl methacrylate
HDPE	-	high density polyethylene
iBMA	-	isobutyl methacrylate
IPO	-	isopropenyl oxazoline
ISNR	-	Indian standard natural rubber
K_s	-	molar equilibrium sorption coefficient
L	-	interfacial thickness
l_c	-	length of the capillary
LDPE	-	low density polyethylene
m	-	mass of the copolymer
M	-	molecular weight of copolymer
M_c	-	molar mass between crosslinks
MEK	-	methyl ethyl ketone
MFI	-	melt flow index
M_L	-	series lower bound value
MMA	-	methyl methacrylate
M_s	-	mass of the penetrant molecule at equilibrium
M_U	-	parallel upper bound value
n'	-	flow behaviour index
NaOH	-	sodium hydroxide
NR	-	natural rubber
NRET	-	non-radiative energy transfer
P	-	permeability coefficient
PA	-	polyamide
PB	-	polybutadiene
PE	-	polyethylene
PET	-	polyethylene terephthalate
phr	-	parts per hundred rubber
PI	-	polyisoprene
PMMA	-	polymethyl methacrylate
PP	-	polypropylene
PPO	-	polyphenylene oxide
PS	-	polystyrene

PVC	-	poly(vinyl chloride)
Q	-	volume flow rate
Q_∞	-	moles of liquid by 100 g of the rubber at equilibrium
Q_t	-	moles of liquid by 100 g of the rubber at time t
R	-	universal gas constant
r	-	radius of the dispersed particle
S	-	sorption coefficient
SAN	-	styrene acrylonitrile rubber
SBR	-	styrene butadiene rubber
SBS	-	styrene butadiene styrene
SEBS	-	styrene ethylene butylene styrene
SIS	-	styrene isoprene styrene
SR	-	recoverable elastic shear strain
T	-	temperature on Kelvin scale
t	-	time
T_g	-	glass transition temperature
TG	-	thermogravimetry
TMTD	-	tetramethyl thiuram disulphide
TPEs	-	thermoplastic elastomers
UTM	-	universal testing machine
V_H	-	volume fraction of hard phase
VL	-	vulcastab
V_s	-	volume fraction of soft phase
Z_c	-	degree of polymerisation of copolymer

CONTENTS

Chapter 1

Introduction

1.1 Introduction

Over the last several years researchers all over the world have been trying to get new polymeric materials with specific properties for different applications. Since the field of new materials is highly exposed, scientists have turned their interest on to the modified forms like polymer blends, polymer composites, interpenetrating networks, etc. As a new and important challenge for researchers, polymer blends have gained a lot of interest and of course have become a new branch of macromolecular science. The blending technique is quite attractive due to the fact that already existing polymers can be used and thus the costly development of new polymers via copolymerisation or by the polymerisation of new monomers can be avoided. Since there is no generally accepted definition for polymer blends they are generally considered as the combination of two or more polymers. Polymer blends can be obtained by methods such as melt mixing, solution mixing, latex blending, etc. and these methods do not involve the formation of chemical bonds between the polymers. Blending is the simplest and cheapest route of combining the properties of different polymeric materials.

We can classify blends into three: miscible, partially miscible and immiscible. Miscibility can be defined in thermodynamic terms. For a binary blend to be miscible, the following conditions should be satisfied.

$$\Delta G_m < 0 \qquad (1.1)$$

$$\frac{\delta^2(\Delta G_m)}{\delta(\phi_2)^2} > 0 \qquad (1.2)$$

where ΔG_m is the free energy of mixing per unit volume and ϕ_2 is the volume fraction of component 2. In miscible polymer blends, molecular level mixing of the components is obtained and are characterised by a single phase morphology.

Immiscible blends do not satisfy the conditions proposed in equations (1) and (2) and show a two-phase morphology. In the case of partially miscible blends, the second criteria is not satisfied and will show either two phase or single phase morphology.

1.2   Incompatibility: problems and solutions

Only a very few polymers form truly miscible blends. These include poly(phenylene oxide)/polystyrene (PPO/PS), poly(vinyl chloride) (PVC)/polymeric plasticizers, etc.[1] Besides these there are a few polymer blends which are found to be compatible in solution. These include cellulose nitrate/poly(vinyl acetate), cellulose nitrate/poly(methyl methacrylate) and cellulose benzoate/polystyrene blends. The rest of the blends which are either partially miscible or immiscible, may undergo micro or macrophase separation, leading to heterophase polymer blends. This heterogeneity is highly unfavourable and this often leads to problems and reflects in the overall performance of the resultant material. Blending can give rise to morphologies that lead to certain specific characteristics. It is expected that this process can give rise to a material with proper balance of properties than that is obtainable with a single polymer. Practically it is difficult to get the expected combination of properties due to the fact that many of the polymers are thermodynamically immiscible and it is difficult to get a homogeneous product. In an immiscible blend, high interfacial tension and poor adhesion between the phases are generally observed. The high viscosities associated with such systems are responsible for poor dispersion and lack of stability to gross phase segregation. The low intermolecular force between the component phases which is responsible for the poor properties of incompatible blends, can be improved by increasing the interfacial area and adhesion between the phases. This can be achieved by the addition of a suitable compatibiliser. The interface between immiscible polymers in polymer blends can be schematically represented as shown in Figure 1.1.
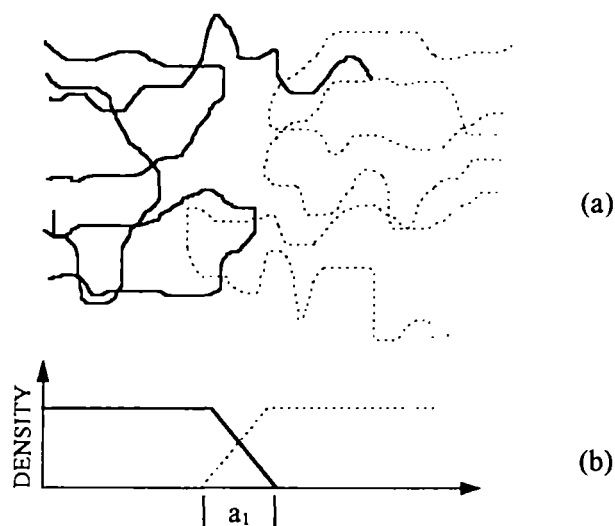
Figure 1.1. (a) Interface between immiscible polymers and (b) Interfacial density profile between immiscible polymers.

The term 'compatibility' is used extensively in the blend literature and is used synonymous with the term 'miscibility' on a thermodynamic sense. Compatible polymers are "polymer mixtures that do not exhibit gross symptoms of phase separation when blended" or "polymer mixtures that have desirable chemical properties when blended". However, on a technological sense, the former is used to characterise the ease of fabrication or the improvement in properties of the blend.[2-4]

1.3 Compatibilisation techniques

In a strict sense compatibility can be defined as molecular miscibility. In order to improve the compatibility in a heterogeneous polymer blend, compatibilisers are often added. Even though blending is an easy method for the preparation of TPEs, most of the TPE blends are immiscible and incompatible. Very often the resulting materials exhibit poor mechanical properties due to the

poor adhesion between the phases. Over the years, different techniques have been developed to alleviate this problem. One solution to this problem is the selection of the most suitable blending technique. By the proper selection of the processing technique either a co-continuous or interpenetrating phase morphology can be obtained which results in direct load sharing without the need for stress transfer across the phases. The second way is by the addition of a third component which is capable of interaction with the blend components, (e.g., block and graft copolymers and low molecular weight materials). The third way is to blend suitably functionalised polymers which are capable for specific interactions or chemical reactions. The functionalisation can be done in solution or in a compounding extruder[5] and may involve reactions like halogenation, sulfonation, hydroperoxide formation and in-situ formation of block and graft copolymers.

The in-situ formed copolymers act as very good compatibilisers in many systems. These are formed during compounding, mastication, polymerisation of one monomer in presence of another polymer etc. and have segments which are chemically identical to the homopolymers. Hajian et al.[6] reported the in-situ formation of styrene/ethylene graft copolymers during the mixing of PS and PE. Anderson[7] studied the compatibilising action of in-situ formed EPDM-g-MMA during the melt extrusion of EPDM and methyl methacrylate. The in-situ formation of compatibilisers employing functionalised polymers form the subject of several studies. Ide and Hasegawa[8] studied the effect of maleic anhydride grafted polypropylene in PP/PA-6 blend.

Block or graft copolymers which act as compatibilisers are of two types, reactive and non-reactive. Non-reactive ones have segments capable of specific interaction with each of the blend components. In reactive copolymers, segments are capable of forming strong covalent or ionic bonds with the blend components. Copolymers of both A-B type and A-C type can act as efficient compatibilisers in A/B system provided C is miscible with B. Tables 1.1 and 1.2 contain a few examples of polymer systems that are compatibilised through non-reactive and reactive copolymers, respectively.

Table 1.1. Compatibility through non-reactive copolymers.

Major component	Minor component	Compatibiliser
PE or PS	PS or PE	S-B, S-EP, S-I-S, S-I-HBD, S-EB-S, S-B-S, PS/PE-graft copolymers
PP	PS or PMMA	S-EB-S
PE or PP	PP or PE	EPM, EPDM
EPDM	PMMA	EPDM-g-MMA
PS	PA-6 or EPDM	PS/PA-6 block copolymers or S-EB-S or PPE
PET	HDPE	S-EB-S
PF	PMMA/PS	PF-g-MMA or PF-g-S
PVDF	PS/PPE	PS/PMMA block copolymer
PVC	PS or PE or PP	PCL/PS block copolymer or CFE
SAN	SBR	BR/PMMA block copolymer

Source: Ref. 1.

Table 1.2. Compatibility through reactive copolymers.

Major component	Minor component	Compatibiliser
ABS	PA-6/PA-6,6 copolymer	SAN/MA copolymer
PP or PS-6	PA-6 or PP	EPM/MA copolymer
PE	PA-6 or PA-6,6	Ionomers, carboxyl functional PE's
PP or PE	PET	PP-g-AA, carboxyl functional PE
PA-6	Acrylate rubber	EPM-g-MA

Source: Ref. 1.

Low molecular weight compounds can also act as compatibilisers in many polymer blends. Co-crosslinking, crosslinking and grafting reaction may involve in such systems and may lead to the formation of certain copolymers. Table 1.3 deals with such system involving low molecular weight compounds as compatibilisers.

Table 1.3. Compatibility through low molecular weight reactive compounds.

Major component	Minor component	Compatibiliser
Fluoro rubber, FPM	NBR or CHR	Triazine dithiol complex
PVC or LDPE	LDPE or PVC	Polyfunctional monomers plus peroxide
NBR	PP	NBR curative and interchain copolymer
PVC or PP	PP or PVC	Chlorinated paraffin
PPE	PA-6,6	Amino silane
NR	PA-6 or polyolefins	Peroxide and or polyfunctional monomers
PBT	EPDM-g-MA or MBS or NBR	Oligomers or epoxy silanes or polyfunctional epoxies

Source: Ref. 1.

1.4 Compatibilisation by block and graft copolymers—basic features

The efficiency of a copolymer, either block or graft, acting as the compatibiliser depends on its structure. One of the primary requirements to get maximum efficiency is that the copolymer should locate preferentially at the blend interface (Figures 1.2a, 1.2b and 1.2c).[9,10]
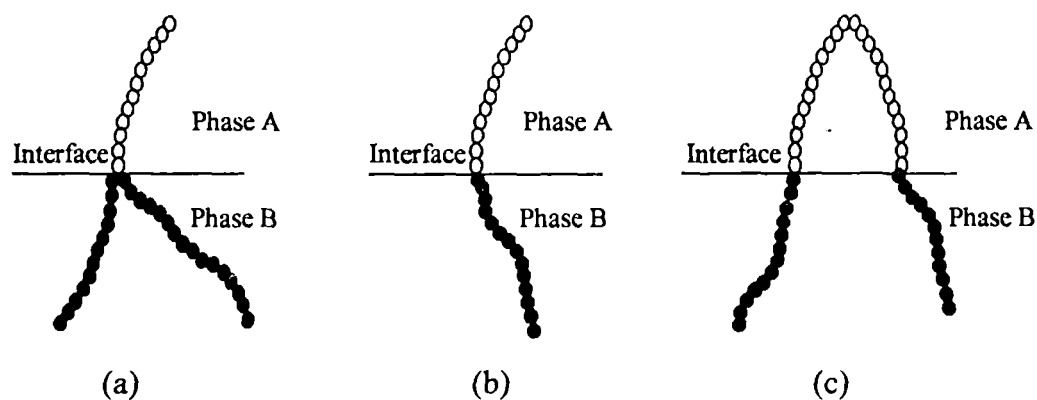
Figure 1.2. Conformation of the copolymer at the blend interface: (a) graft, (b) diblock and (c) triblock copolymers extending into the homopolymers.

Many researchers[11,12] found that conformational restraints are important and on this basis a block copolymer can be expected to be superior to graft copolymer. In the case of graft copolymer multiple branches should be avoided. Otherwise it would restrict the penetration of the backbone into the homopolymer phases. Among block copolymers, a diblock copolymer will be more effective than a triblock copolymer. Teyssie and coworkers[13] demonstrated that a tapered diblock is more efficient than a pure diblock with the same composition and molecular weight. Pure diblock copolymer contains highly incompatible sequences. These sequences segregate into domains and less mixing occurs. But tapered block copolymers do not form domains of their own and therefore provide strong adhesion. Compared to diblock, the tapered block copolymers can be easily dispersed due to their low viscosity. Chemical identity of the copolymer segment with the homopolymer phase is important. Even if there is no chemical identity between the copolymer segment and the homopolymer, copolymers can be kept equally efficient provided the segment is miscible with the homopolymer.

Another important requirement is that the copolymer should have the propensity to segregate into two phases. Further, the copolymer, both block and graft, should not be miscible as a whole in one of the homopolymer phases.

The amount of the copolymer (m) to be added into a binary blend depends on several factors and is given by[14]

$$m = 3\phi_A \, M/aRN \qquad\qquad (1.3)$$

where ϕ_A is the volume fraction of polymer A, R is the radius of dispersed particle A in a matrix B, N is the Avogadro's number, a is the area occupied by the copolymer and M is the molecular weight of the copolymer. For a copolymer to be fully efficient, its molecular weight (M) should be higher than the molecular weight of the homopolymers. Riess and Jolivet[12] studied the effect of molecular weight on solubilisation. When the homopolymer molecular weight is larger than that of the

corresponding block segment, homopolymer form a separate phase and is not solubilised into the domains of block copolymer. In the case of high molecular weight copolymers, the long segments are able to anchor the immiscible phases firmly. Besides all these arguments, there should be an optimum molecular weight when the cost-benefit of the resultant product is concerned. The emulsifying effect of block and graft copolymers in polystyrene/polyisoprene blends was demonstrated by Riess and Jolivet.[12] Mechanical properties of the incompatible blends can be enhanced by controlling the dispersed phase size and adhesion between the components, which can be achieved by the addition of a suitable copolymer. Molecular weight and composition are two important parameters which determine whether the copolymer will locate at the blend interface, in the continuous phase or in the dispersed phase. Block copolymers of equal segmental mass are more effective as compatibiliser than those of unequal segmental mass. In addition to the above mentioned parameters, various factors such as viscosity of the copolymer and its interaction with the homopolymers also play a major role in the compatibilisation process. There are various techniques for characterising the location of the copolymer. These include the use of copolymer with a fluorescent group, X-ray scanning microanalysis, TEM analysis of gel formed after crosslinking the elastomer phase by γ-radiation etc.[15]

1.5   Theories of compatibilisation

There are interesting theoretical studies in literature dealing with the compatibilsation of immiscible homopolymer blends by the addition of copolymers.

Noolandi and Hong[16,17] reported the interfacial properties of immiscible homopolymer blends in the presence of block copolymers. The emulsifying activity of a diblock copolymer in an incompatible homopolymer blend is comparable to the action of soap molecules at an oil-water interface. By the proper selection of the type and molecular weight of the block copolymer it is possible to locate the copolymer at the blend interface.

The state of the block copolymer in a phase separated homopolymer system is controlled by different parameters. The entropy of mixing of the block copolymers with homopolymers favours a random distribution of the copolymer. However, the localisation of block copolymers at the blend interface displaces the homopolymers away from each other and lowers the enthalpy of mixing. The enthalpy of mixing is further lowered by the tendency of the block copolymer to extent into its compatible homopolymer phases. The entropy loss is mainly due to the confinement of block copolymers to the blend interface. Further reduction in entropy arises from the restriction of the blocks to their respective homopolymer regions. A schematic representation of the interface between immiscible homopolymers containing a diblock copolymer is given in Figure 1.3.
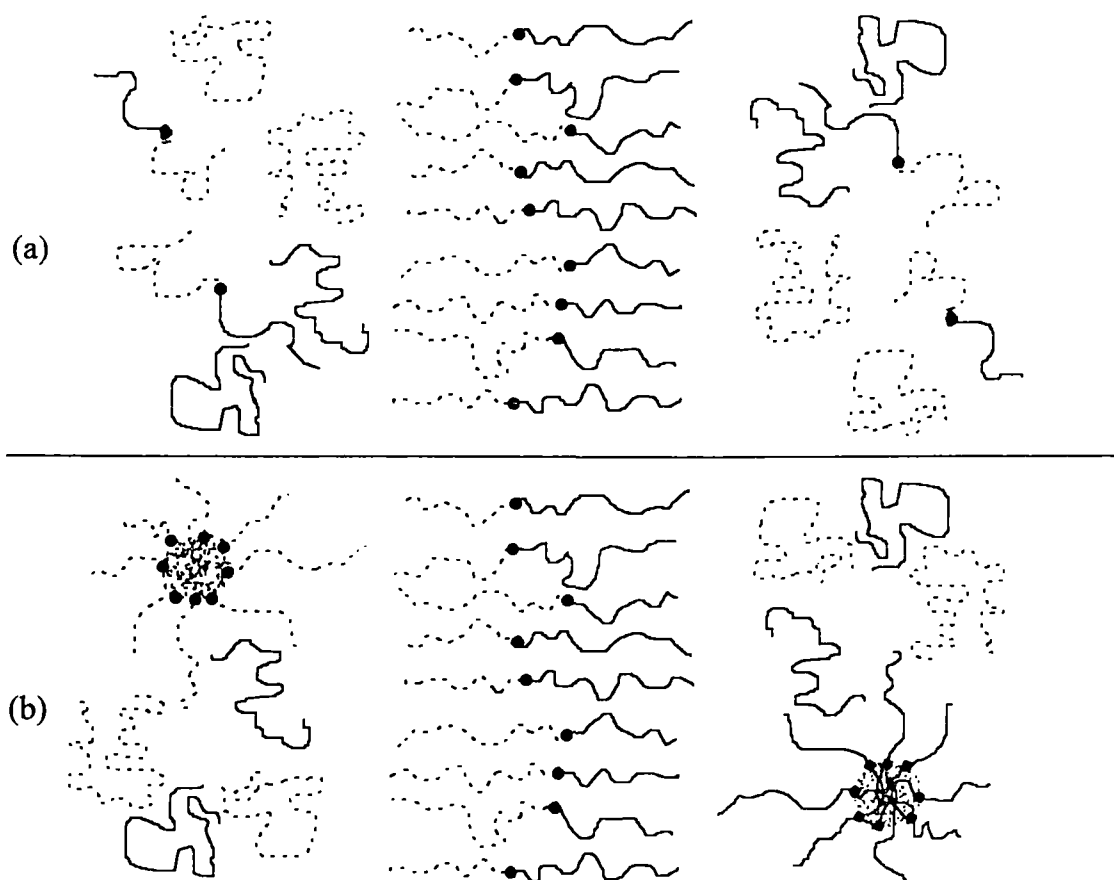
Figure 1.3. Schematic representation of the blend interface in an immiscible blend in presence of a compatibiliser (diblock copolymer): (a) diblock copolymer present at the interface as well as in the bulk, and (b) micelle formation in the bulk.

In Figure 1.3a some of the copolymers settle at the interface while some are randomly distributed among the homopolymer phases. In addition to the first one, Figure 1.3b shows the micelle formation due to copolymers.

Noolandi and Hong[17] calculated the reduction in interfacial tension with increase in concentration of the block copolymer for a range of homo and block copolymer molecular weights and comparison was made with the experimental results of Riess and coworkers[18] on the polystyrene-polybutadiene-copolymer-styrene system (PS-PBD-CopSBD-S). The reduction in interfacial tension with varying weight fraction of block copolymer for the above quaternary system for two different values of interaction parameters (χ_{AB}) is given in Figure 1.4. Blends with a lower interaction parameter shows higher values of interfacial tension compared to that with higher interaction parameter. In both cases as the weight fraction of the copolymer increases, the interfacial tension decreases.
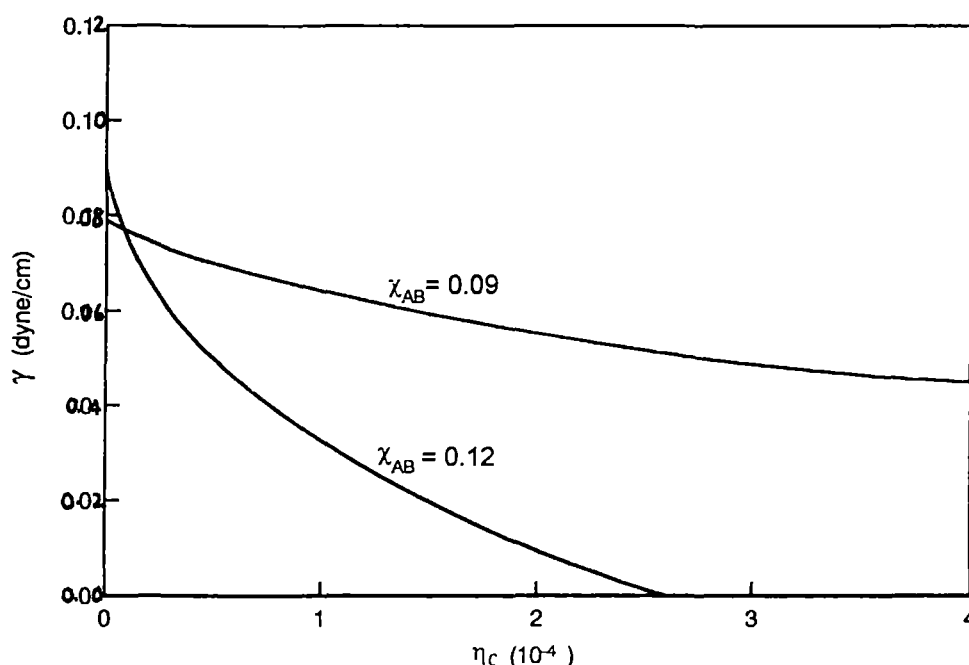
Figure 1.4. Calculated interfacial tension for the phase separated quarternary system (PS-PBD-CopSBD-S) with varying weight fraction (η_c) of block copolymer (Ref. 16).

Block copolymer molecular weight has a significant role on the reduced interfacial tension. The variation of reduced interfacial tension ($\Delta\gamma$) with copolymer molecular weight (Z_c) for different over all copolymer volume fraction is given in Figure 1.5 which predicts the linear dependence of $\Delta\gamma$ on Z_c. It was found that as the molecular weight increases, the reduced interfacial tension decreases. The volume fraction of the copolymer is also a controlling parameter, i.e., blends with higher volume fraction will have the minimum interfacial tension. One of the important findings from the theoretical results is that the interfacial tension for the above mentioned quaternary system was found to be disappeared for a few concentration of the compatibilisation. This is because some of the copolymer is found to be settled at the interface, while the rest is randomly dispersed in the bulk phase.
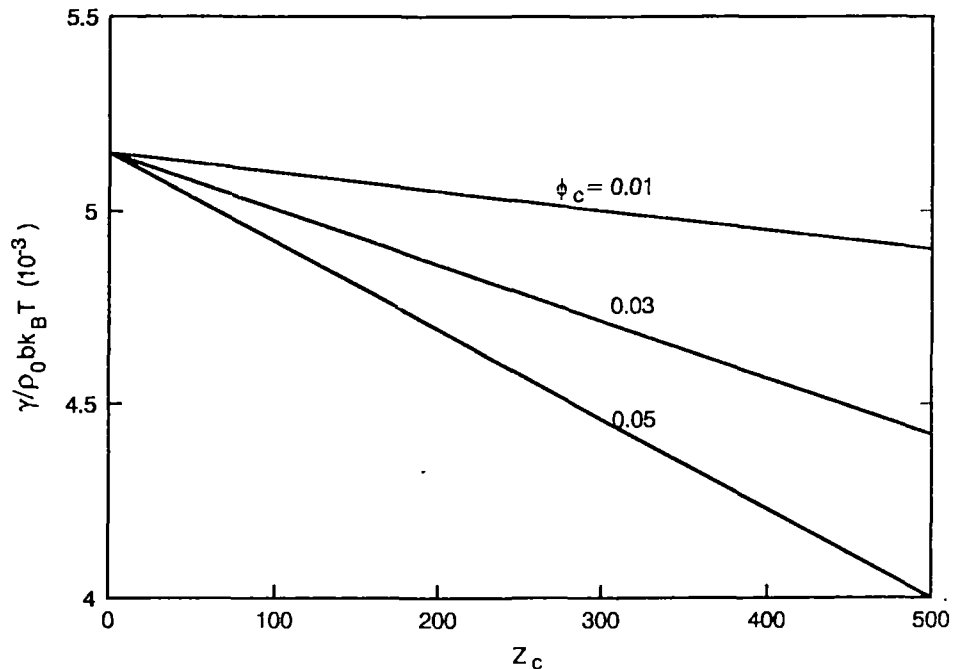
Figure 1.5. Variation of interfacial tension with copolymer molecular weight for different overall copolymer volume fraction (ϕ_c) (Ref. 17).

Noolandi and Hong developed a theoretical equation to study the behaviour of block copolymer in immiscible homopolymer blends. When a block copolymer is added, it gets localised at the interface and the homopolymer profiles were broadened with increasing copolymer concentration and molecular weight. A statistical thermodynamic theory is used to derive the Mean-field equations for a ternary system of two immiscible homopolymers, diluted with a solvent in the presence of a diblock copolymer. Then the mean field equation is solved to get the reduction in interfacial tension and found that the reduction in interfacial tension with increasing copolymer concentration and molecular weight is due to the reduction in interaction energy of the block copolymers at the interface. The interfacial tension reduction is given by the equation.

$$\Delta\gamma = d\phi_c \left[\left(\tfrac{1}{2} \chi + 1/Z_c \right) - 1/Z_c \exp Z_c \chi /2 \right] \tag{1.4}$$

where $\Delta\gamma$ = interfacial tension reduction

ϕ_c = bulk volume fraction of the copolymer

d = width at half height of the copolymer profile reduced by Kuhn statistical segment length in the system

Z_c = degree of polymerisation of copolymer

χ = Flory-Huggin's interaction parameter.

Simple expression for the interfacial tension showed an exponential dependence on the copolymer molecular weight and interaction parameter.

The interesting features of the results of equation (1.4) are worth discussing. The exponential dependence on the block copolymer molecular weight and homopolymer volume fraction gives us an awareness about the effectiveness of using large molecular weight diblocks as surfactants in immiscible blends. The predictions of these theories also provide us information about the linear dependence of the interfacial tension on block copolymer volume fraction.

The length of the blocks in a block copolymer is a controlling parameter towards the interfacial activity in immiscible blends. Block copolymer with shorter

blocks along with better mixing can avoid micelle formation due to shorter reptation times.

The theoretical predictions of Noolandi and Hong have been testified by Anastasiadis *et al.*[19,20] They have reported the compatibilising effect of block copolymers added to the polymer/polymer interface. The compatibiliser used is poly(styrene-block-1,2-butadiene) and its influence on polystyrene/poly(styrene-block-1,2-butadiene) was studied. The interfacial tension was found to be decreased upon the addition of the compatibiliser followed by a levelling off at higher concentration of the copolymer (above CMC). Similar to the studies of Noolandi and Hong, here also the interfacial tension decreases with increase in concentration of the compatibiliser as shown in Figure 1.6. It was found that a 40% reduction in interfacial tension is observed with 1.29% of the compatibiliser. Addition of any excess amount of the compatibiliser is a waste because it will not reduce the interfacial tension rather it may adversely effect the blend properties via micelle formation.
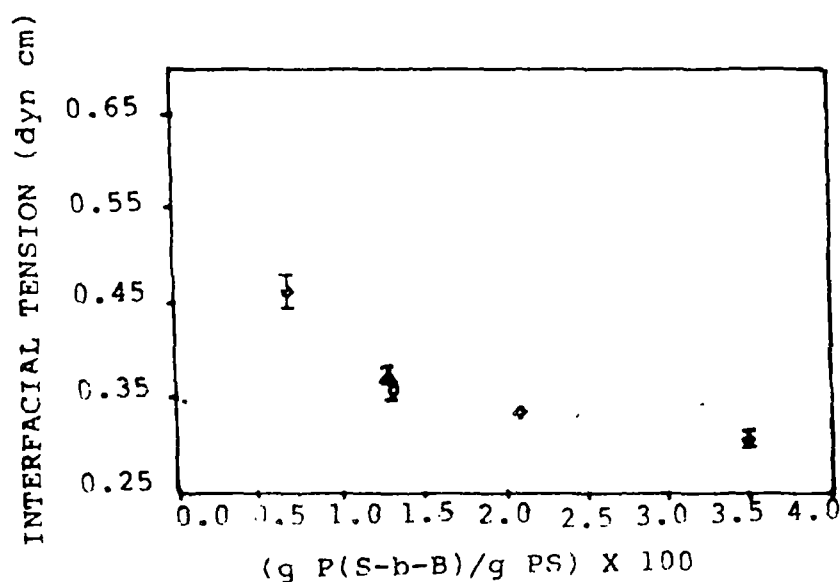
Figure 1.6.   Variation in interfacial tension with concentration of compatibiliser [P(S-b-B) diblock copolymer] (Ref. 20).

The emulsifying effects of block copolymers in incompatible polymer blends was reported by Leibler.[21,22] According to this blending with block or graft copolymer is a widely accepted method to control the overall blend properties by reducing the dispersed domain size. In order to study the interfacial activity of block copolymers, it is necessary to study the properties of the interfacial film. There are different molecular parameters like molecular weight of homo and copolymers, copolymer composition, degree of incompatibility etc. which control the overall compatibility of immiscible blends. According to Leibler, by the proper selection of copolymers it is possible to obtain low interfacial tension. By locating at the blend interface, the copolymer will separate unlike homopolymer species and reduce the number of unfavourable contacts between the homopolymers. The interfacial tension (γ) is the difference of two contributions and can be represented as follows:

$$\gamma = \gamma_0 - \gamma_1 \tag{1.5}$$

where γ_0 represents the interfacial energy due to the non-homogeneity of the overall monomer content. The second term γ_1 is the decrease of interfacial tension due to the effect of the preferential location of the copolymer at the blend interface.

For a flat interface with surface area (A), the interfacial thickness (D) and interfacial tension (γ_0) are given by

$$D = \frac{a}{\sqrt{6\chi}} \tag{1.6}$$

$$\gamma_0 = \left(\frac{KT}{a^2}\right)\sqrt{\chi/6} \tag{1.7}$$

where χ is the interaction parameter and a is the monomer length. Leibler discussed the formation of thermodynamically stable droplet phase in which one of the homopolymers is solubilised and protected by an interfacial film. In order to get

such a system, the copolymer should be highly symmetric. The condition for a symmetric copolymer is as follows:

$$\frac{V_A^3}{R_{GA}^2} = \frac{V_B^3}{R_{GB}^2} \tag{1.8}$$

where V_A and V_B are the molar volumes, and R_{GA} and R_{GB} are the radii of gyration of the A and B blocks, respectively.

1.6   Thermoplastic elastomers (TPEs)

Thermoplastic elastomers are materials which combine the easy processability of thermoplastics and elastic behaviour of rubbers. They can be processed by the conventional plastic processing techniques such as injection moulding, blow moulding, sheet extrusion, etc. but they develop final rubber-like properties immediately on cooling. At normal temperatures, TPEs possess the characteristic resilience and recovery from extension of crosslinked elastomers but exhibit plastic flow at elevated temperatures. The elastic behaviour is associated with certain interchain secondary valence forces of attraction which have the effect of typical conventional covalent crosslinks. At elevated temperature, the secondary bonds dissociate and the polymer exhibits thermoplastic behaviour.

TPEs have many processing advantages over the conventional vulcanised rubbers. The various vulcanisation techniques are not required and only very little compounding is needed. Conventional rubbers on the other hand, must be vulcanised to give useful properties. This is a rather irreversible and slow process and takes place only on heating. However, in the case of thermoplastics, the transition from a processable melt to a solid rubber-like object is rapid, reversible and takes place on cooling. Thermoplastic processing techniques like blow moulding, heat welding, etc. which are unsuitable for conventional rubbers can be applied successfully to TPEs. The short processing cycle involved consumes only very low amount of energy. Processing of scraps which are considered as a waste

in conventional system can be made possible here. However, TPEs possess certain disadvantages such as high creep and set on prolonged use and will melt only at elevated temperatures. Thermoplastic elastomers have received commercial importance recently. They are replacing many of the conventional rubbers as well as thermoplastics.

TPEs can be mainly classified into five groups. These are (1) TPEs from rubber/plastic blends, (2) polystyrene-elastomer block copolymers, (3) polyurethane-elastomer block copolymers, (4) polyamide-elastomer block copolymers, and (5) polyether-elastomer block copolymers.

Most important category among these is TPEs from blends of rubbers and plastics. These have certain typical advantages over the other TPEs. These can be prepared either by the melt mixing of plastics and rubbers in an internal mixer or by solvent casting from a suitable solvent. The commonly used plastics and rubbers include polypropylene (PP), polyethylene (PE), polystyrene (PS), nylon, ethylene propylene diene monomer rubber (EPDM), natural rubber (NR), styrene butadiene rubber (SBR), butyl rubber, nitrile rubber (NBR), etc. By the proper selection of rubbers and plastics and by controlling their ratios, the required properties can be easily achieved. The overall performance of the resultant TPEs can be improved by changing the phase structure and crystallinity of plastics and also by the proper incorporation of suitable ingredients such as fillers, crosslinkers and interfacial agents.

1.7   Compatibilisation studies on thermoplastic elastomer blends

There are a large number of studies related to the compatibilisation of TPE blends by the addition of copolymers, (both block and graft) and by dynamic crosslinking.

It is known that when suitably chosen graft copolymers are added in small quantities to immiscible polymers, the graft copolymer behaves as classical

surfactants, similar to soap molecules at an oil-water interface.[14] The segments of the graft copolymer should be chemically identical or compatible with those in the immiscible blends. Lundstedt and Bevilacqua[23] showed that if graft copolymer of styrene to rubber was made which in turn was simply blended with PS, significant increase in impact strength was produced.

Teyssie et al.[13] reported a large number of systems, in which beneficial effects of polymeric emulsifiers in polymer blends have been illustrated. Teyssie clearly demonstrated that the copolymer is uniformly absorbed at the interface between two polymers. Hughes and Brown[24] have studied the influence of styrene grafted poly(ethyl acrylate) on the phase separation of blends of poly(ethyl acrylate) and polystyrene in a common solvent. Addition of graft copolymer of poly(ethyl acrylate) and styrene did not give two liquid layers.

Park et al.[25] reported the synthesis of poly(chloroprene-co-isobutyl methacrylate) and its compatibilising effect in immiscible polychloroprene/ poly(isobutyl methacrylate) blends. A block copolymer of chloroprene (CR) and isobutyl methacrylate (iBMA) [poly(CR-co-iBMA)] and a graft copolymer of iBMA and polychloroprene [poly(CR-g-iBMA)] were prepared for comparison. Blends of CR and PiBMA are prepared by the solution casting technique using THF as the solvent. The morphology and glass transition temperature behaviour indicated that the blend is an immiscible one. It was found that both the copolymers can improve the miscibility, but the efficiency is higher in the case of poly(CR-co-iBMA) than poly(CR-g-iBMA).

Oommen and Thomas[26-28] studied the interfacial activity of natural rubber-g-poly(methyl methacrylate) in incompatible NR/PMMA blends. Graft copolymer of NR and PMMA was prepared using a redox initiator consisting of cumene hydroperoxide and tetraethylene pentamine. Mechanical and morphological properties of the blends with and without the compatibiliser were studied and it was found that the mechanical properties increase with increasing concentration of the graft copolymer. Morphological data are in agreement with the mechanical data. They further studied the effect of casting solvent, mode of addition of

compatibiliser, molecular weight of homo and copolymers, etc. on the morphological and mechanical properties. The experimental results were compared with the theoretical predictions of Noolandi and Hong.

Fayt et al.[29] reported the characterisation and control of interfaces in the incompatible polymer blends. For this, they have adopted techniques like electron microscopy, thermal transition analysis, non radiative energy transfer (NRET) etc. They have illustrated the exciting potentialities offered by diblock copolymers in high performance polymer blends. Chu et al.[30] correlated viscosity, morphology and compatibility of PS/PB blends. Effect of styrene/butadiene triblock copolymer in PS/PB blend was studied and found that the domain size decreased with increase of compatibiliser loading. The blending methods influenced the morphology due to the difference in the extent of mixing.

Dynamic crosslinking as a means to improve the impact strength and other mechanical properties of polypropylene/elastomer blends has been discussed in detail by Inoue.[31] All these blends contain 80% PP and 20% elastomer. Elastomers include EPDM, SBS and SIS and the crosslinking system comprised of N,N'-m-phenylene-bis-maleimide and 6-ethoxy-2,2,4-trimethyl-1,2-dihydroquinoline or poly(2,2,4-trimethyl-1,2-dihydroquinoline). Impact strength and other mechanical properties like tensile strength at yield, ultimate elongation, flexural modulus, etc. showed remarkable increase after crosslinking. This is due to the increase of interfacial adhesion caused by the PP-graft elastomers located at the blend interface.

Interfacial adhesion and thereby compatibility can be enhanced by the selective crosslinking reaction in polymer blends. Inoue and Suzuki[32] reported the properties of dynamically crosslinked PP/EPDM blends using N,N'-m-phenylene-bismaleimide/poly (2,2,4-trimethyl-1,2-dihydroquinoline) system. Increase in interfacial adhesion leads to an improvement in izod impact strength. Various other mechanical properties like tensile strength at yield, ultimate elongation and flexural modulus were also studied before and after the crosslinking reaction.

Krulis et al.[33] also described the dynamic crosslinking as a route to improve the mechanical properties. It was found that high impact strength is obtained in PP/EPDM blends by the slow curing with sulphur. Thiuram disulphide N-(cyclohexylthio)phthalimide was used as an inhibitor of curing and its effect on the impact strength of dynamically cured PP/EPDM blends has been studied. It was also found that one step method of blend preparation has a favourable effect on the impact strength of the resultant blend system.

Compatibilisation along with dynamic vulcanisation techniques have been employed in thermoplastic elastomer blends of poly(butylene terephthalate) and ethylene propylene diene rubber by Moffett and Dekkers.[34] The in-situ formation of graft copolymer can be obtained by the use of suitably functionalised rubbers. By the usage of conventional vulcanising agents for EPDM, the dynamic vulcanisation of the blend can be achieved. Optimum effect of compatibilisation along with dynamic vulcanisation can be obtained only when the compatibilisation is done before the rubber phase was dispersed.

Ha[35] has shown that in polypropylene/HDPE/ dynamically cured EPDM, the cured EPDM acts as a compatibiliser to HDPE/PP system. Blending was done in two ways. EPDM was cured first and then blended with PP and HDPE. In the second case, EPDM was cured in presence of PP and HDPE using DCP as vulcanising agent. In EPDM rich composition, mechanical properties were increased with increasing the concentration of DCP, whereas in PP rich composition, reverse was the case.

Dynamic vulcanisation as a method to improve the mechanical properties of NR/PE blends has been discussed in detail by Choudhury et al.[36] In all the compositions, the DCP cured blends showed better properties than the corresponding unvulcanised samples. This work further demonstrated the use of EPDM, chlorinated polyethylene, chlorosulphonated PE, maleic anhydride modified polyethylene and blends of epoxidised natural rubber/sulphonated EPDM as compatibilisers in NR/LDPE blends.

Kim *et al.*[37] prepared a binary blend of polypropylene/ethylene propylene diene monomer rubber and a ternary blend of PP/EPDM/ poly(ethylene-co-methacrylic acid) ionomer. The rheological. mechanical and morphological properties of these blends were analysed. Two kinds of ionomers, i.e., ionomer A and ionomer B neutralised with different metal ions (Na^+ and Zn^{2-}, respectively) were used and their concentration varied from 5–20% based on the total amount of PP and EPDM. It was found that rheological and morphological properties of the binary and ternary blends showed much variation due to the compatibilising effect of the ionomer. Na-neutralised ionomer (Ionomer A) showed a compatibilising effect and the effect was prominent at 5 wt % of the ionomer concentration. Effect of ionomer concentration on the storage modulus of PP/EPDM blends is given in Figure 1.7. It was seen that the ternary blends with 5 wt % of ionomer A, showed better properties than other blends. The effect of ionomer concentration on the mechanical properties of PP/EPDM blends was also studied. It is seen that the tensile strength and modulus showed a maximum at 5 wt % of both ionomer A and B and thereafter the properties decrease at higher ionomer loading. The properties are higher for the ternary blends containing Zn^{2-} neutralised ionomer (ionomer B) than that containing ionomer A. On the other hand, addition of ionomers reduced the elongation at break regardless of the ionomer type.

Frequency (rad/sec)
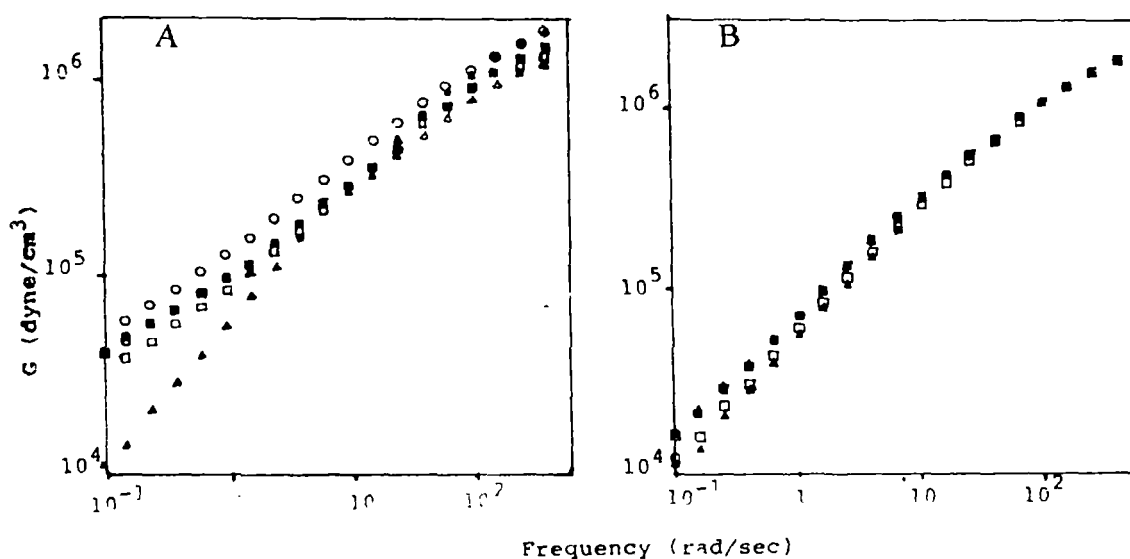
Figure 1.7. Effect of ionomer concentration on storage modulus: (A) PP50-EP50/IA and (B) PP50-EP50/IB [▲ 0 wt %, ○ 5 wt %, □ 10 wt %, △ 15 wt %].

The structure-property relationship of graft copolymers based on an elastomeric backbone poly(ethyl acrylate)-g-polystyrene was studied by Peiffer and Rabeony.[38] The copolymer was prepared by the free radical polymerisation technique and found that the improvement in properties depends upon factors like number of grafts/chain, graft molecular weight, etc. It was shown that mutually grafted copolymers produce a variety of compatibilised ternary blends.

Coran and Patel[39] selected a series of TPEs based on different rubbers and thermoplastics. Three types of rubbers EPDM, EVA and NBR were selected and the plastics include PP, PS, SAN and PA. It was shown that the ultimate mechanical properties such as stress at break, elongation and elastic recovery of these dynamically cured blends increased with the similarity of the rubber and plastic in respect to the critical surface tension for wetting and with the crystallinity of the plastic phase. Critical chain length of the rubber molecule, crystallinity of the hard phase (plastic) and the surface energy are a few parameters used in the analysis. Better results are obtained with a crystalline plastic material when the molecular length of the rubber is low. The other two conditions which are to be satisfied are (1) the surface energies of the plastic and rubber should not be very high, (2) both rubber and plastic should not decompose in presence of the other during melt mixing.

In the case of NBR/nylon blends it was reported that the addition of the curative m-phenylene-bis-maleimide, improved the strength and stiffness of the blend. An attempt to compare the effect of different curatives m-phenylene bismaleimide and dimethylol phenolic compounds was also reported. Nylon-NBR graft molecules formed during crosslinking will induce better homogenisation in the system which leads to overall enhancement of the blend performance.

In addition to dynamic vulcanisation, technological compatibilisation technique was also adopted by Coran and Patel[40] to obtain thermoplastic vulcanisate having good mechanical properties and elastic recovery.

Swelling of thermoplastic elastomeric vulcanisates using a model EPDM/PP blend in various solvents like cyclohexane, butyl acetate, methyl ethyl ketone (MEK), etc. was studied by Coran and Patel.[41] Blends were vulcanised both by dynamic and by static means and the mechanical properties like ultimate tensile strength, Young's modulus, ultimate elongation, hardness etc. were determined in each case. All the properties except elongation at break (EB) are higher for dynamically vulcanised samples. Static samples are not processable with the typical thermoplastic processing techniques, whereas the dynamically cured samples can be moulded. The amount of swelling of the thermoplastic vulcanisates was found to be less than the average swelling of the rubber and plastic. It was also noted that the vulcanisates prepared by the dynamic vulcanisation technique swell less than those prepared by static means.

Riess *et al.*[42] have discussed the polystyrene (PS)/polyisoprene (PI) blend and the corresponding PS-b-PI as a model system for rubber modified thermoplastics. The emulsifying effect of the block copolymer is evaluated by checking the transparency of the polymer blend. The transparency of an incompatible PS/PI system having different refractive indices can be obtained by reducing the particle size of the dispersed phase below a certain level. This may be possible by the compatibilising action of the block copolymer.

Frounchi and Burford[43] studied the effect of styrene block copolymer as a compatibiliser in isotactic polypropylene/ABS blends. The effects of four different block copolymers, styrene-butadiene-styrene (SBS), styrene-isoprene-styrene (SIS), styrene-ethylene-butylene-styrene (SEBS), and a slightly maleated functionalised SEBS were compared. It was found that in PP-rich blends, a marginal improvement in mechanical properties was obtained. However, in ABS-rich blends, no improvement was obtained.

Elliot[44] has reported that interfacial adhesion in NR/PP blend can be enhanced by the addition of small amounts of HDPE. Addition of HDPE does give some improvement in the notched izod impact strength of NR/PP blend

(Figure 1.8). The effect of HDPE on the impact modification of NR/PP is associated with the improved crystallinity of PP due the presence of HDPE. During the mill mixing of NR and PP, chain scission occur to give polymeric radicals which on reaction with the added multifunctional radical acceptor may give graft copolymer and that in turn can act as a compatibiliser in NR/PP system.
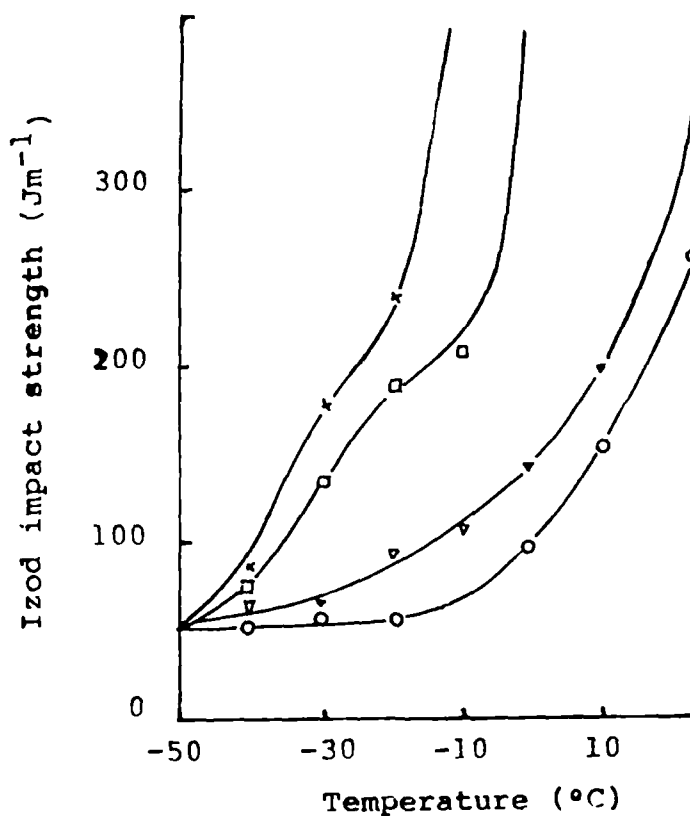
Figure 1.8. Variation of izod impact strength upon the addition of HDPE [O 20/80 NR/PP homopolymer; ∇ 20/67/13 NR/PP homopolymer/HDPE; □ 15/85 NR/PP copolymer; × 15/75/10 NR/PP copolymer/HDPE].

Compatibility and various other properties like morphology, crystalline behaviour, structure and mechanical properties of natural rubber/polyethylene blends were investigated by Qin et al.[45] Polyethylene-b-polyisoprene acts as a successful compatibiliser for this system. Mechanical properties of the blends were improved upon the addition of the block copolymer. The copolymer locates at the interface, and thus reduces the interfacial tension which is reflected in the

mechanical properties. As the amount of graft copolymer increases, tensile strength and elongation at break increase and then levels off. Morphological studies of these blends revealed that the compatibilisation was very effective in decreasing the interfacial tension and increasing the adhesion between the two phases.

Wang and Chen[46] studied the compatibility problems of incompatible NBR/PVC blends. Poly(vinylidene chloride-co-vinyl chloride) was reported to act as an efficient interfacial agent. Blends of PVC, NBR and the copolymer were prepared by the solution casting technique using THF as a solvent. Improvement in mechanical properties can be achieved in NBR/PVC blend by the addition of different types of rubbers.[47] These rubbers include NR, SBR and BR. Replacement of a certain percentage of NBR by other rubbers will improve the mechanical properties and at the same time reduce the cost of the blend.

Compatibility of immiscible PP/NBR blends was improved by the reactive compatibilisation technique using various modified polypropylenes. In this study glycidyl methacrylate (GMA), 2-hydroxyethyl methacrylate (HEMA), 2-hydroxypropyl methacrylate (HPMA), t-butylaminoethyl methacrylate (TBAEMA), dimethylaminoethyl methacrylate and 2-isopropenyl-2-oxazoline (IPO) were used as the modifiers. It was found that IPO and GMA are effective in compatibilising the PP/NBR blends.[48] The compatibilisation of NBR/PP[49] and NBR/HDPE blends has been reported by Thomas and coworkers.[50] High impact polystyrene (PS) can be obtained from PS and EPDM by the coupling of EPDM and PS in the mixing chamber of a Haake plastograph. Lewis acids were added to the melt and found that rubber became crosslinked or it was coupled with the PS molecules and improvement in mechanical properties was observed.[51] Santra et al.[52] have reported the in-situ compatibilisation of low density polyethylene and polydimethyl siloxane rubber blends using ethylene-methyl acrylate copolymer as a chemical compatibiliser. Ethylene methacrylate (EMA) reacted with the rubber to form EMA-grafted rubber during the melt mixing which acts as the compatibiliser. They have conducted the dynamic mechanical analysis,

adhesion studies and phase morphology and found that 6 wt % of the compatibiliser was found to be the optimum quantity required for effective compatibilisation.

Els and McGill[53] reported the action of maleic anhydride on polypropylene/polyisoprene blends. A graft copolymer was formed *in-situ* through the modifier which later enhanced the overall performance of the blend. Scott and Macosko[54] studied the reactive and non-reactive compatibilisation of nylon/ethylene propylene rubber blends. The non-reactive polyamide/ethylene propylene blends showed poor interfacial adhesion between the phases. The reactive polyamide/ethylene propylene-maleic anhydride modified blends showed excellent adhesion and much smaller dispersed phase domain size.

Greco *et al.*[55] studied the effect of reactive compatibilisation technique in ethylene propylene rubber/polyamide-6 blends. Binary blends of polyamide-6/ethylene propylene rubber (EPR) and ternary blend of polyamide-6/EPR/EPR-g-succinic anhydride were prepared by melt mixing technique and the influence of the degree of grafting of (EPR-g-SA) on morphology and mechanical properties of the blends was studied.

1.8   Scope of the work

TPEs from blends of NR and PS are a new class of materials which will combine the positive aspects of both NR and PS. Natural rubber is characterised by good elastic properties, good resilience, damping behaviour but poor chemical resistance and processability. On the other hand, polystyrene exhibits superior processing characteristics even though it is extremely brittle. The NR/PS blends exhibit good processability, impact strength, good flexibility and rubbery nature. However, to our knowledge, till date no detailed study has been made on the morphology and properties of NR/PS blends.

Inspite of the positive aspects described above for NR/PS blends, the performance of NR/PS blends is not up to the expectations. This is because these blends are immiscible and incompatible and are characterised by a narrow

interface, coarse morphology, high interfacial tension, poor physical and chemical interactions across the phase boundaries. Detailed investigations have revealed that the compatibilisation of these blends is essential to alleviate these problems. Until now, no systematic study has been made on the compatibilisation of NR/PS blends. In this thesis, a detailed work has been carried out to study the influence of a graft copolymer (NR–graft–PS) on the compatibilisation of NR/PS blends. The important objectives of the present work are detailed below.

1.8.1 Effect of processing conditions on morphology and mechanical properties

The morphology of the blends is one of the controlling parameters which determine the ultimate properties of the blends. There is the existence of different types of morphologies like dispersed/matrix, co-continuous, interpenetrating structure, etc. By the proper selection of the processing technique, either a co-continuous or interpenetrating phase morphology can be obtained which results in direct load sharing without the need for stress transfer across the blend phases. During the day-to-day encounter, materials will be subjected to varying deformations. In this respect, characterisation of mechanical properties is really important. The engineering design of the final products are also related to the mechanical properties of the materials. TPEs from blends of NR and PS have been prepared by melt mixing and solution casting techniques. Morphology and mechanical properties were compared in both the cases and found that the morphology depends on the processing conditions i.e., whether the samples are prepared by the melt mixing or by solution casting technique. In the latter case three solvents were compared to study the interaction between the solvent and the polymer. Different theoretical models have been used to fit the experimental mechanical data. It was found that solution casted samples showed superior properties compared to melt mixed ones.

1.8.2 Compatibilising action of NR-graft-PS on morphology and mechanical properties

The compatibilising action of NR-g-PS on the morphology and mechanical properties has been analysed in detail. The graft copolymer has been prepared by the ^{uu}Co-γ-irradiation technique and characterised by FTIR and NMR spectroscopic analysis. The effect of addition of the copolymer on the morphology of the blend was studied in detail with special reference to the effect of graft copolymer concentration, homopolymer and copolymer molecular weight, mode of addition of the copolymer, casting solvents, etc. The mechanical properties like stress–strain behaviour, tensile strength, tear strength, impact strength have been studied. Attempts have also made to correlate the mechanical properties with the morphology of the system. The experimental results were compared with the theories of Noolandi and Hong[15] and attempts were made to establish the conformation of the graft copolymer at the interface.

1.8.3 Melt rheological properties

Complete knowledge of the melt flow behaviour of the blends over a wide range of shear rate, shear stress and temperature is highly important to get a thorough understanding of the processing operations and to improve the quality and quantity of the product manufactured. The rheological behaviour of both melt mixed and solution casted blends were studied and compared. NR and PS possess different melt viscosities and in order to standardise the processing conditions for their blends, it is necessary to study the effect of shear stress at different temperatures on the viscosity. Hence the effect of blend composition, temperature, shear stress and compatibiliser loading on shear viscosity was studied. Melt elastic parameters like die swell, principal normal stress difference and recoverable shear strain are essential parameters to explain the ultimate properties of the products that

can be prepared from the blend. Finally, master curves have been constructed at different temperatures using modified shear viscosity and shear rate functions.

1.8.4 Stress relaxation measurements

Stress relaxation is an important tool to study the viscoelastic behaviour of polymeric materials which explores the decay of stress with time at constant strain. Stress-relaxation characteristics of NR/PS blends have been investigated in terms of relative stress as a function of logarithmic time. The effects of blend composition, compatibiliser loading, strain level and temperature have been studied in detail. Both the relaxation rate and relaxation mechanism are much influenced by these parameters which provided an insight into the viscoelastic nature of these blends.

1.8.5 Dynamic mechanical thermal analysis

The dynamic mechanical behaviour of rubber based materials are of much relevance since these materials are subjected to various types of dynamic deformations. The dynamic mechanical properties were studied to provide an idea about the various types of structural motions and thermal transitions in polymers. The viscoelastic behaviour of NR/PS blends has been investigated using dynamic mechanical thermal analysis techniques. The experiments were carried out to study the dynamic mechanical properties like tan δ, storage modulus and loss modulus in the presence and absence of the graft copolymer. The experimental values were compared with various theoretical models. The cole-cole plots and the time-temperature super position curves were constructed at different compatibiliser loading and temperatures.

1.8.6 Thermal properties

Thermogravimetric analysis were carried out to study the thermal stability and oxidative degradation of NR/PS blends with and without the addition of graft copolymer. The miscibility of the blends were studied using DSC and the glass

transition temperatures were analysed in the presence and absence of the copolymers.

1.8.7 Swelling studies

Since NR/PS blends could be utilised for the transport of solvents, the sorption and diffusion of solvents namely petrol, mineral turpentine and diesel through NR/PS blends were investigated. Swelling parameters were studied with special reference to the effect of blend ratio, temperature, solvent and vulcanising systems. From the temperature dependence of diffusivity, the activation energy for the different processes were computed. The experimental values were compared with different theoretical predictions.

1.9 References

1. M. Xanthos, *Polym. Eng. Sci.*, **28**, 1392 (1988).

2. D. R. Paul, C. E. Vinson and C. E. Locke, *Polym. Eng. Sci.*, **12**, 157 (1972).

3. A. J. Yu, *Multicomponent Polymer Systems* (Ed., N. A. J. Platzer), Adv. Chem. Ser., Vol. 99, Amer. Chem. Soc., Washington, DC, 1971., p. 2.

4. N. G. Gaylord, *Copolymers, Polyblends and Composites* (Ed., N. A. J. Platzer), Adv. Chem. Ser., Vol. 142, Amer. Chem. Soc., Washington, DC, 1975, p. 76.

5. C. S. Tucker and R. J. Nicholas, *S. P. E. ANTEC Tech. Papers*, **33**, 117 (1987).

6. M. Hajian, C. Sadrmohaghegh and G. Scott, *Eur. Polym. J.*, **20**, 135 (1984).

7. P. G. Anderson, *U. S. Patent*, **4**, 476, 283 (1984).

8. F. Ide and A. Hasegawa, *J. Appl. Polym. Sci.*, **8**, 963 (1974).

9. S. Thomas and R. E. Prud'homme, *Polymer*, **33**, 4260 (1992).

10. Z. Oommen, M. R. G. Nair and S. Thomas, *Polym. Eng. Sci.*, **36**, 151 (1996).

11. G. Riess, J. Kohler, C. Tournut and A. Banderet, *Makromol. Chem.*, **101**, 58 (1967).

12. G. Riess and Y. Jolivet, *Copolymers, Polyblends and Composites*, (Ed., N. A. J. Platzer), Adv. Chem. Ser., Vol. 142, Amer. Chem. Soc., Washington, DC, 1975, p. 243.

13. R. Fayt, R. Jerome and Ph. Teyssie, *J. Polym. Sci. Polym. Phys. Edn.*, **20**, 2209 (1982).

14. D. R. Paul and S. Newman, Eds., *Polymer Blends*, Vol. 1, Academic Press, New York, 1978, Ch. 12.

15. O. Olabisi, L. M. Robeson and M. T. Shaw, *Polymer Polymer Miscibility*, Academic Press, New York, 1979.

16. J. Noolandi and K. M. Hong, *Macromolecules*, **15**, 482 (1982).

17. J. Noolandi and K. M. Hong, *Macromolecules*, **17**, 1531 (1984).

18. P. Gaillard, M. Ossenbach-Sauter and G. Riess, *Makromol. Chem. Rapid Commun.* **1**, 771 (1980).

19. S. H. Anastasiadis, I. Gancarz and J. T. Koberstein, *Macromolecules*, **21**, 2980 (1988).

20. S. H. Anastasiadis, I. Gancarz and J. T. Koberstein, *Macromolecules*, **22**, 1449 (1989).

21. L. Leibler, *Makromol. Chem. Macromol. Symp.*, **16**, 1 (1988).

22. L. Leibler, *Macromolecules*, **15**, 1283 (1982).

23. O. W. Lundstedt and E. M. Bevilacqua, *J. Polym. Sci.*, **24**, 297 (1957).

24. L. J. Hughes and G. L. Brown, *J. Appl. Polym. Sci.*, **7**, 59 (1963).

25. C. K. Park, C. S. Ha, J. K. Lee and W. J. Cho, *J. Appl. Polym. Sci.*, **50**, 1239 (1993).

26. Z. Oommen and S. Thomas, *Polymer Bulletin*, **31**, 623 (1993).

27. Z. Oommen and S. Thomas, *J. Appl. Polym. Sci.*, **65**, 1245 (1997).

28. Z. Oommen, S. Thomas, C. K. Premalatha and B. Kuriakose, *Polymer*, **38**, 5611 (1997).

29. R. Fayt, R. Jerome and Ph Teyssie, *Polym. Eng. Sci.*, **27**, 328 (1987).

30. Line-Hwa Chu, Shang-Her Guo and Hsieng-Cheng Tseng, *J. Appl. Polym. Sci.*, **49**, 179 (1993).

31. T. Inoue, *J. Appl. Polym. Sci.*, **54**, 723 (1994).

32. T. Inoue and T. Suzuki, *J. Appl. Polym. Sci.*, **56**, 1113 (1995).

33. Z. Krulis, I. Fortelny and J. Kovar, *Collect. Czech. Chem. Commun.*, **58**, 2642 (1993).

34. A. J. Moffett and M. E. J. Dekkers, *Polym. Eng. Sci.*, **32**, 1 (1992).

35. Chang Sik Ha, *J. Appl. Polym. Sci.*, **37**, 317 (1989).

36. N. R. Choudhury, P. P. De and A. K. Bhowmick, *Thermoplastic Elastomers from Rubber-Plastic Blends*, Ellis Horwood, England, 1990, Ch. 3, p. 79.

37. Y. Kim, Chang-Sik Ha, T. Kang, Y. Kim and W. Cho, *J. Appl. Polym. Sci.*, **51**, 1453 (1994).

38. D. G. Pieffer and M. Rabeony, *J. Appl. Polym. Sci.*, **51**, 1283 (1994).

39. A. Y. Coran and R. Patel, *Rubber Chem. Technol.*, **54**, 892 (1981b).

40. A. Y. Coran and R. Patel, *Rubber Chem. Technol.*, **55**, 116 (1982a).

41. A. Y. Coran and R. Patel, *Rubber Chem. Technol.*, **55**, 1063 (1982b).

42. G. Riess, P. Bahadur and H. Hurtrez, *Encyclopedia Polymer Science and Engineering*, 2nd edn., Vol. 2, John Wiley and Sons, New York, 1985, p. 324.

43. M. Frounchi and R. P. Burford, *Iranian J. Polym. Sci. Technol.*, **2**, 59 (1993).

44. D. J. Elliot, *Thermoplastic Elastomers from Rubber-Plastic Blends*, Ellis Horwood, England, 1990, Ch. 4, p. 121.

45. Chuan Qin, J. Yin and B. Huang, *Polymer*, **31**, 663 (1990).

46. Y. Wang and S. Chen, *Polym. Eng. Sci.*, **21**, 47 (1981).

47. K. E. George, Rani Joseph, D. Joseph Francis and K. T. Thomas, *Polym. Eng. Sci.*, **27**, 1137 (1987).

48. N. C. Liu, H. Q. Xie and W. E. Baker, *Polymer*, **34**, 4680 (1993).

49. S. George, R. Joseph, K. T. Varughese and S. Thomas, *Polymer*, **36**, 4405 (1995).

50. J. George, R. Joseph, K. T. Varughese and S. Thomas, *J. Appl. Polym. Sci.*, **57**, 449 (1995).

51. E. Mori, B. Pukanszky, T. Kelen, F. Tudos, *Polymer Bulletin*, **12**, 157 (1984).

52. R. N. Santra, B. K. Samantaray, A. K. Bhowmick and G. B. Nando, *J. Appl. Polym. Sci.*, **49**, 1145 (1993).

53. C. Els and W. J. McGill, *Plast. Rubb. Comp. Proc. Appl.*, **21**, 115 (1994).

54. C. E. Scott and C. W. Macosko, *International Polym. Proc.*, **10**, 1 (1995).

55. R. Greco, M. Malinconico, E. M. Celli, G. Ragosta and G. Scarinzi, *Polymer*, **28**, 1185 (1987).

Chapter 2
Experimental Techniques

---

*The details of the materials used and
experimental techniques adopted in the present
investigation are given in this chapter*

2.1 Materials

2.1.1 Natural rubber (NR)

Natural rubber in the form of crumb rubber (ISNR-5, Indian Standard Natural Rubber-5) collected from the Rubber Research Institute of India, Kottayam, Kerala, India, was used in this study. The specification parameters for ISNR–5 grade natural rubber are given in Table 2.1 and this satisfies the requirements of the Bureau of Indian standard's specifications. The natural rubber samples, NR_5, NR_{10} and NR_{15} are obtained by mastication of NR for 5, 10 and 15 min respectively in a two roll mixing mill. The physical characteristics of these different NR samples are given in Table 2.2. Basic properties such as molecular weight, molecular weight distribution, non-rubber constituents etc. are affected by clonal variation, season, use of yield stimulants, methods of preparation etc.[1,2] and hence rubber from the same lot has been used in a particular experiment.

Table 2.1. Specifications for ISNR-5 grade NR.

Parameters	Limit	Actual value
Dirt Content (% by mass, Max)	0.05	0.03
Volatile matter (% by mass, Max)	0.80	0.70
Nitrogen content (% by mass, Max)	0.65	0.40
Ash content (% by mass, Max)	0.60	0.48
Initial plasticity (Po, Min)	30	40
Plasticity Retention Index (PRI, Min)	60	75

2.1.2 Polystyrene (PS)

Polystyrene was supplied by Poly. Chem. Ltd., Bombay, India. Polystyrenes of two grades were used and the characteristics are given in Table 2.2.

Table 2.2. Characteristics of the materials used.

Material	Density (g/cm^3)	Solubility parameter $(cal/cm^3)^{1/2}$	Molecular weight $(\overline{Mn})$
NR_0	0.90	7.75	7.79×10^5
NR_5	0.90	7.75	3.70×10^5
NR_{10}	0.90	7.75	2.49×10^5
NR_{15}	0.90	7.75	1.62×10^5
PS_1	1.04	8.56	3.51×10^5
PS_2	1.04	8.56	2.07×10^5
G_1 (NR-g-PS)	-	-	3.95×10^5
G_2 (NR-g-PS)	-	-	1.01×10^5
$CHCl_3$	-	9.3	-
CCl_4	-	8.6	-

2.1.3 Graft copolymer (NR-g-PS)

The graft copolymer of NR and PS was prepared by polymerising styrene in rubber latex using $^{60}Co-\gamma$–radiation as the initiator.[3] Styrene monomer was made into an emulsion which was then mixed with NR latex of known dry rubber content (DRC) at room temperature and exposed to $^{60}Co-\gamma$radiation for 16 h. The dose rate was 0.1166 Mrad/min. The free homopolymers NR and PS were removed from the crude sample by soxhlet extraction with petroleum ether and methyl ethyl ketone (MEK), respectively. The graft copolymer so obtained was dried in a vacuum oven for a period of 48 h. The graft copolymer obtained was masticated for 0 and 5 min

respectively and are designated as G_1 and G_2. The characteristics of these different grades are given in Table 2.2.

2.1.4 Solvents

Chloroform, benzene and carbontetrachloride were supplied by BDH, Chemicals Ltd. Petrol, diesel and mineral turpentine used in the sorption studies were of analytical grade. The characteristics of the solvents used are given in Table 2.3.

Table 2.3. Characteristics of the solvents.

Solvent	Density (g/cm^3)	Mol. wt $(\overline{Mn})$	BP $(°C)$	Solubility parameter $(Cal/cm^3)^{1/2}$
$CHCl_3$	1.48	118	61.70	9.30
CCl_4	1.59	152	76.54	8.60
C_6H_6	0.87	78	80.10	9.20
Petrol	0.83	246	300	-
Diesel	0.78	170	200	-
Mineral turpentine	0.71	100	95	-

2.1.5 Other chemicals

Styrene monomer for graft copolymer preparation was supplied by BDH Chemicals Ltd. It was washed with 10% NaOH solution to remove the inhibitor, followed by water and finally dried over $CaCl_2$. The stabiliser, VL (vulka stab) used to maintain the stability of NR latex during graft copolymer preparation was obtained from Rubber Research Institute of India supplied by Bayer India Ltd.

2.2   Preparation of the blends

2.2.1   Melt mixed NR/PS blends

- Blends of NR and PS were prepared using a Brabender Plasticorder (Model T-300A) with a rotor speed of 80 rpm at $160^{\circ}C$. PS was melted for two minutes. This was followed by the addition of NR and the mixing was continued for further 5 min. After mixing, the blend was taken out and pressed in a mould in the hot condition itself. The pressed material was then compression moulded at $160^{\circ}C$ for 4 min. in specially designed moulds. The melt mixed samples are denoted as M_0, M_{30}, M_{40}, M_{50}, M_{60}, M_{70} and M_{100} where 'M' stands for melt mixing and the subscripts indicate the proportion of NR in the blend. In the case of dynamically vulcanised melt mixed samples M will be followed by D, S and M, respectively to denote curative such as dicumyl peroxide (DCP), sulphur and mixed systems (i.e., MD, MS and MM, respectively). The formulations of the mixes are given in Table 2.4.

Table 2.4.   Compounding recipe (parts per 100 parts of rubber by weight).

Ingredients	Sulphur system	Mixed system	DCP system
NR	100	100	100
Stearic acid	1	1	1
Zinc oxide	5	5	5
CBS*	1	1	-
TMT**	0.8	0.8	-
DCP***	-	3	6.25 (40% active)
Sulphur	2.5	1	-

*N-cyclohexyl-2-benzothiazyl sulphenamide
**Tetramethylthiuram disulphide
***Dicumyl peroxide

2.2.2 Solution casted NR/PS blends

NR and PS were blended together in a common solvent (CHCl$_3$, C$_6$H$_6$ or CCl$_4$). In all the cases the concentration of the solution was kept as 5%. Natural rubber, polystyrene and the graft copolymer were mixed in a common solvent, kept overnight and then stirred for eight hours with a magnetic stirrer. Films were casted on a glass plate and dried in a vacuum oven at 80°C for 48 h, and then at 120°C for a further 4 h. The solution casted samples were denoted as S$_0$A, S$_{30}$A, S$_{40}$A, S$_{50}$A, S$_{60}$A, S$_{70}$A, S$_{100}$A, S$_0$B, S$_{30}$B, S$_{40}$B, S$_{50}$B, S$_{60}$B, S$_{70}$B, S$_{100}$B, S$_0$C, S$_{30}$C, S$_{40}$C, S$_{50}$C, S$_{60}$C and S$_{70}$C, S$_{100}$C, where 'S' stands for solution casting, the subscripts indicate the amount of NR in the blend and the letters A, B and C stand for samples prepared from benzene, chloroform and CCl$_4$, respectively. The solution casted samples (50/50 NR/PS) compatibilised with the graft copolymer are represented as SG$_a$, SG$_b$, SG$_c$ and SG$_d$, where a, b, c and d stand for 1.5, 3, 4.5 and 6 wt % of compatibiliser, respectively.

2.3 Characterisation of blend properties

2.3.1 Mechanical properties

In this case a minimum of five specimens per sample were tested for each property and the average of these values was reported.

(a) Tensile strength, modulus and elongation at break

These three parameters were determined at 25°C according to ASTM D 638 specification, using dumb–bell shaped specimens, at a crosshead speed of 50 mm/min. The test pieces were punched out from the moulded sheets or from the casted sheets using a C–type die. The thickness of the dumb-bell specimen (C-type) was measured using a thickness gauge. The experiments were carried out in a Zwick universal testing machine (UTM) model 1474 and the values were

recorded on a strip chart recorder. The Young's modulus was determined from the linear portion of the stress–strain curve.

(b) Tear strength

The tear strength of the samples was tested as per ASTM–D–(624–8L) test method, using 90° angle test specimen which were punched out from the moulded or casted sheets. The instrument and the experimental conditions are the same as in the case of tensile strength testing.

(c) Izod impact strength

The Izod impact strength was measured using Ceast Impact tester (Model 6545/000) according to the ASTM D 256 specification. The dimensions of the specimen used were 6.13 x 1.20 x 1.23 cm and the impact energy was obtained by the difference in the potential energy of the falling hammer before and after impact.

2.3.2 Morphology of the blends

In the case of solution casted samples the morphology of the samples were examined under an optical microscope (Model–Leitz Diaplan). For that very thin samples were made on specimen glass and dried it in a vacuum oven at 80°C for 48 h and then at 120°C for a further 4 h. The domain size has been measured using an image analyser. In the case of melt mixed samples, morphological studies were carried out using scanning electron microscope (Model JEOL–JSM–35C). For this, the samples were fractured in liquid nitrogen to avoid the possibility of phase deformation. The minor phase of the blend was preferentially extracted using MEK for PS and petroleum ether for NR. The cut edges of the samples were then kept in oven at 50°C for 48 h. The dried surfaces of the samples were gold coated and then

examined by SEM. About two hundred domains selected at random were considered for the domain size measurements.

2.3.3 Melt flow studies

(a) Rheological measurements

The rheological measurements were carried out using viscotester (1500 version 2.0 model) with different plunger speeds of 0.06–20 mm/min. A capillary die of length/diameter (l_c/d_c) of 30 was used and the melts were extruded at 150, 160, 170°C for different piston speeds. The test samples were placed inside the barrel of the extrusion assembly and forced down into the capillary with the piston attached to the moving crosshead. After a warming up period of 4 min, the melt was extruded through the capillary at pre-selected speeds of the crosshead. The height of the melt within the barrel was kept the same in all the experiments. Force corresponding to different piston speeds was recorded using a strip chart recorder assembly. The force and crosshead speed were converted into shear stress (τ_w) and shear rate ($\dot{\gamma}_w$) at wall respectively, using the following equations involving the geometry of the capillary and piston.

$$\tau_w = \frac{F}{4Ap(l_c / d_c)} \tag{2.1}$$

$$\dot{\gamma}_w = \frac{(3n'+1)32Q}{4n'\pi d_c^3} \tag{2.2}$$

where F is the force applied at a particular shear rate. A_p the cross-sectional area of the piston, l_c the length of the capillary die, d_c the diameter of the capillary, Q the volume flow rate and n' the flow behaviour index which is given by

$$n' = \frac{d(\log \tau_w)}{d(\log \dot{\gamma}_{wa})} \tag{2.3}$$

and was determined by the regression analysis of the values of τ_w and $\dot{\gamma}_{wa}$ obtained from the experimental data. The shear viscosity (η) was calculated as,

$$\eta = \frac{\tau_w}{\dot{\gamma}_w} \qquad (2.4)$$

(b) Die swell measurements

The extrudates from the capillary were collected carefully, without any deformation. The diameter of the extrudate was measured using an optical microscope (Model Leitz-Diaplan). An average of ten readings was taken as the diameter (d_e) of the extrudate. Die swell was calculated as the ratio of the diameter of the extrudate to that of the capillary (d_e/d_c).

(c) Extrudate morphology analysis

Morphology analysis of the extrudate was carried out by etching the minor blend phase using a suitable solvent. The cryogenically fractured extrudate was immersed in petroleum ether for 48 h for the preferential extraction of NR and in methyl ethyl ketone for the extraction of polystyrene. The samples were then dried in a hot air oven and the extracted surface was examined with a scanning electron microscope (Model JEOL-JSM 35C). The surface characteristics of the extrudates at different shear rates was studied by optical microscopy.

(d) Melt flow index (MFI)

Melt flow index i.e., the weight of polymer in grams extruded in 10 min through a capillary was determined using Ceast modular flow index (Model 6542/000) as per ASTM-D 1239-73. The applied load in all the cases was 2.16 kg. The measurement was carried out at 250°C.

2.3.4 Stress relaxation studies

For this study, dumb-bell shaped specimens (ASTM D412; type C) were taken. Stress relaxation measurements were carried out in a Zwick universal testing machine (Model 1474). The samples were pulled to a desired strain level using a crosshead speed of 5 mm/min and the decay in stress as a function of time was recorded. The decay in stress has been evaluated as a function of blend composition, strain level and compatibiliser loading. The test was carried out at room temperature. The ratio σ_t/σ_0 was plotted against logarithm of time (log t) where σ_t and σ_0 are the stress at time t and zero respectively.

2.3.5 Dynamic mechanical thermal analysis

The dynamic mechanical properties of NR, PS and NR/PS blends both compatibilised and non–compatibilized were measured using a dynamic mechanical thermal analyser (Polymer Laboratories DMTA MK-II). The instrument measures dynamic moduli (both storage and loss moduli) and the damping of the specimen under an oscillatory load as a function of temperature. The experiment was conducted at a dynamic strain of 0.325% and at frequencies, 0.1, 1, 10, 50 and 100 Hz. Liquid nitrogen was used to achieve subambient temperature and a programmed heating rate of $1\,^{\circ}C$ min^{-1} was used. Mechanical loss factor tan δ and dynamic moduli (E' and E") were calculated with a microcomputer. Samples of dimension 70 x 10 x 2.5 mm were prepared for testing. The storage modulus E' and the loss modulus E" are obtained from E* and δ using the following equations.

$$E" \quad = E* \, Sin \, \delta \qquad\qquad (2.5)$$

$$E' \quad = E* \, Cos \, \delta \qquad\qquad (2.6)$$

where E* is the dynamic complex modulus.

The loss tangent

$$tan \, \delta \quad = E" / E' \qquad\qquad (2.7)$$

2.3.6 Thermal studies

(a) Thermogravimetric analysis (TGA)

Thermogravimetric analysis (TGA) and derivative thermogravimetric analysis (DTG) were carried out in a Schimadzu DT-40 analyser in nitrogen atmosphere. Samples were scanned from 30-750°C at a heating rate of 10°C/min.

(b) Differential scanning calorimetry (DSC)

The thermal behaviour of the blends was studied with the help of a Perkin-Elmer DSC thermal analyser. The samples were inserted into the apparatus at room temperature and immediately heated to 200°C at a heating rate of 40°C min^{-1} and kept for 1 min at this temperature in order to remove the volatile impurities. The samples were quenched to -80°C at a rate of 320°C/min and then heated to 130°C at a heating rate of 10°C/min in helium atmosphere. The glass transition temperature of each sample was taken as the midpoint of the step in the scan.

2.3.7 Swelling studies

Circular samples were punched out from the vulcanised sheets using a sharp edged steel die of 2 cm diameter. The thickness of the samples was measured with an accuracy of ± 0.001 cm using a dial gauge. The samples were soaked in liquids taken in sorption bottles kept at constant temperatures. At regular intervals, they were taken out and weighed carefully in an electronic balance (Shimadzu, Libror AEn–210, Japan) with an accuracy of ± 0.0001 g. The samples were replaced into the bottles containing the liquids and the process is continued until the samples attained equilibrium swelling. The experiments were repeated at 28, 48 and 58°C.

2.4   References

1.   A. Subramanyam, *Rubber Chem. Technol.*, **45**, 346 (1972).

2.   A. Subramanyam, *Proc. of the RRIM Planters Conference, Kualalumpur,* 255, 1971.

3.   W. Cooper, P. R. Sewell, and G. Vaughan, *J. Polym. Sci.,* **41**, 167 (1959).

Chapter 3

Effect of Processing Conditions on Morphology and Mechanical Properties

The morphology and properties of TPEs have been extensively reported. Morphology and properties of polymer blends are strongly affected by the processing conditions. The effects of mixing procedure on morphology, mechanical and impact properties of nylon6/rubber/modified rubber blends have been studied by Cimmino and coworkers.[1] Morphology-property relationships in polycarbonate based blends were studied by Kunori and Geil.[2] Processing-morphology relationship of compatibilised polyolefin/polyamide blends was reported by Willis and Favis.[3] Nishi and coworkers[4] have shown that, processing technique has much influence on the blend properties. Solution casted blend has given a lower Tg value compared to the corresponding melt mixed sample. Bank *et al.*[5] have shown that the casting solvent used in the preparation of the blend influences the compatibility and related properties of polystyrene (PS)-poly(vinyl methyl ether) (PVME) mixtures. Favis[6] studied the effects of processing parameters such as time of mixing, rotor speed etc. on the morphology of an immiscible binary blend of polypropylene and polycarbonate. The effect of different processing methods on the mechanical properties, structure and morphology of natural rubber/low density polyethylene blends were studied by Qin *et al.*[7] .

The aim of the present work is to investigate the influence of processing conditions on the morphology and mechanical properties of NR/PS blends. The properties of the TPE blends very much depend on the way in which the blends are prepared. The morphology of the blends is one of the controlling parameters which determine the ultimate properties of the TPE blends. Different types of morphologies like dispersed/matrix, co-continuous, interpenetrating structures

could be generated by the control of viscosity, composition and processing conditions. Thus by the proper selection of the processing techniques, the phase morphology can be varied and this will be reflected in the ultimate properties of the blends. In this chapter the effect of different processing conditions on the morphology and mechanical properties of NR/PS blends have been reported. The influence of dynamic vulcanisation using sulphur, peroxide and mixed systems on the morphology-mechanical property relationship of NR/PS blends has also been analysed in detail in this chapter.

3.1 Results and discussion

The properties of NR/PS blends prepared by different processing techniques have been compared. Melt mixed and solution casted samples showed significant differences in their properties. Among the solution casted samples itself, the nature of casting solvents influences both the mechanical and the morphological properties.

3.1.1 Processing characteristics

The processing characteristics of the blends have been studied from the time-torque and time-temperature curves obtained during the mixing in the plasticorder. Several authors have used the plastographs to analyse the processing characteristics of blends.[8-10] The variations in mixing torque with time during the blend preparation have been recorded. Figure 3.1 shows the Brabender (torque vs. time) curve of the melt mixed NR/PS blends. In all the cases, the mixing torque increases with increase in mixing time and finally decreases indicating a good level of mixing. The highest torque is exhibited by pure NR and the torque decreases as the rubber content decreases. This is associated with the high viscosity of natural rubber (NR) compared to polystyrene (PS).
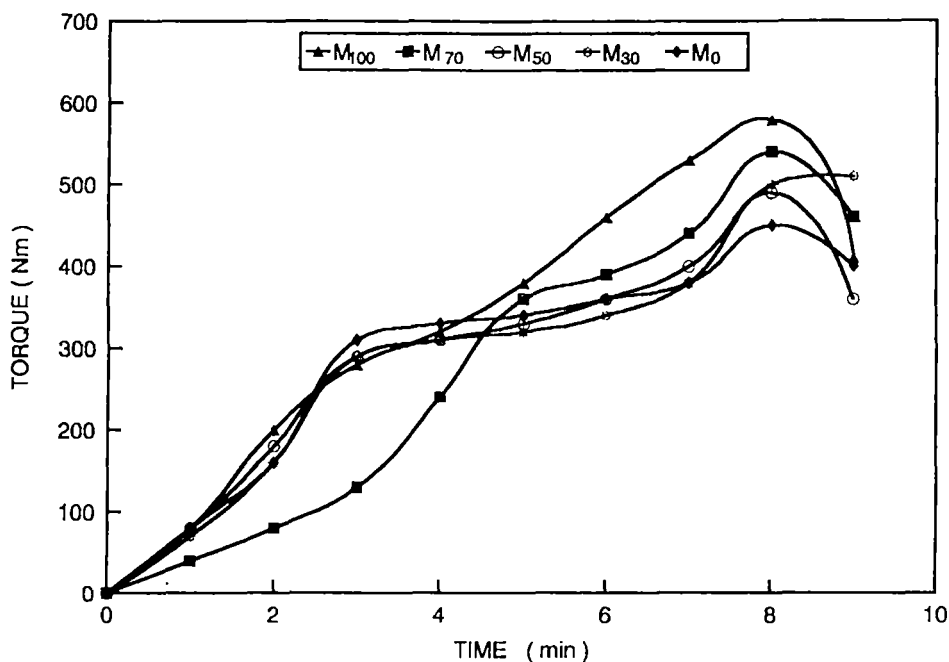
Figure 3.1. Brabender plastographs of NR/PS blends showing the variation of mixing torque with time of mixing (Uncured).

The variation in mixing temperature with time is given in Figure 3.2. In the case of homopolymers NR and PS, initially there is a drop in temperature due to the introduction of the material into the mixing chamber and then it increases with time due to the melting of the concerned material. In the case of blends, two temperature drops are observed. Initially the temperature falls due to the introduction of the plastic phase. Then the temperature increases as the melting of plastic occurs. Addition of rubber causes the second drop in temperature value. Again as the mixing progresses, the temperature increases.
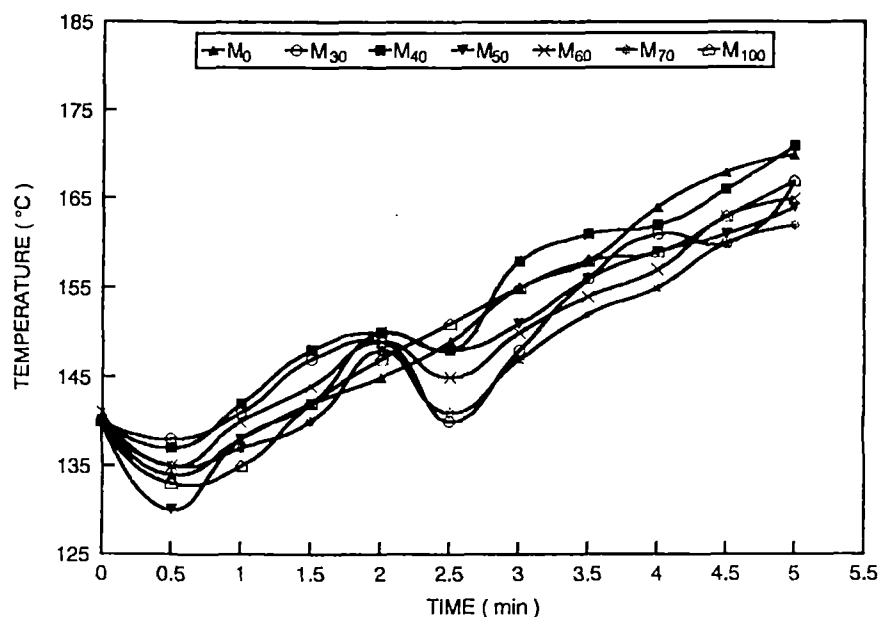
Figure 3.2. Brabender plastographs of NR/PS blends showing the variation of mixing temperature with time (Uncured).

The Brabender time-torque curves for dynamically cured NR/PS blends (sulphur system) are given in Figure 3.3. In all the cases, two peaks are obtained. The first peak is associated with the increase in viscosity due to the melting of the blend components, followed by a decrease which is an indication of the complete melting of the phases. Again there is an increase in the torque due to an increase in viscosity as a result of dynamic crosslinking. In the case of peroxide and mixed systems also, the same trend is observed. In all the three different blend systems (i.e., sulphur, mixed and peroxide) the dynamically cured samples show a higher mixing torque compared to uncured samples (Figure 3.1).
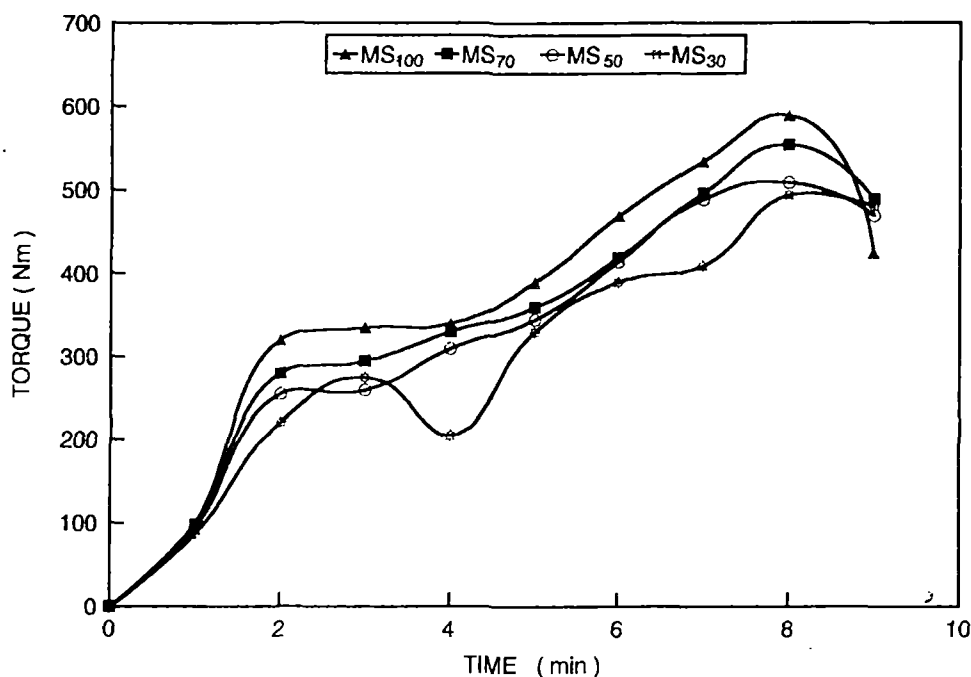
Figure 3.3. Brabender plastographs of NR/PS blends showing the variation of mixing torque with time of mixing (Dynamically cured).

3.1.2 Morphology of the blends

It was reported by Danesi and Porter[11] that under similar processing conditions, blend composition and viscosity differences of the components determine the blend morphology. The component which is having the high volume fraction and low viscosity has a tendency to become continuous relative to that of the other component. Optical micrographs of different solution casted NR/PS blends using benzene, chloroform and carbon tetrachloride are given in Figures 3.4, 3.5 and 3.6, respectively. In 30/70 NR/PS blends ($S_{30}A$, $S_{30}B$ and $S_{30}C$) natural rubber forms the dispersed phase and PS forms the continuous phase. In 70/30 NR/PS blends ($S_{70}A$, $S_{70}B$ and $S_{70}C$) polystyrene forms the dispersed phase. In 30/70 blends, the size of NR domains is higher compared to that of PS domains in 70/30 blends. This is due to coalescence of the NR domains. Coalescence of domains is possible at higher concentrations of one of the components and has been reported by many authors.[12-14] It is seen that in all the three different solvent systems, as the amount of NR increases from 30-40 wt % the dispersed domain size

increases. Beyond 50 wt % NR, phase inversion of NR takes place from dispersed to continuous phase and PS becomes the dispersed phase and the domain size decreases. However, it is believed that blends exhibit a partial–co-continuous morphology between 40 and 60 wt % of NR, i.e., dispersed and co-continuous morphologies co-exist. Therefore, the domain size was measured based on the available dispersed phase morphology. The number average domain diameters for different blend systems are given in Table 3.1.

(a)

(b)

(c)
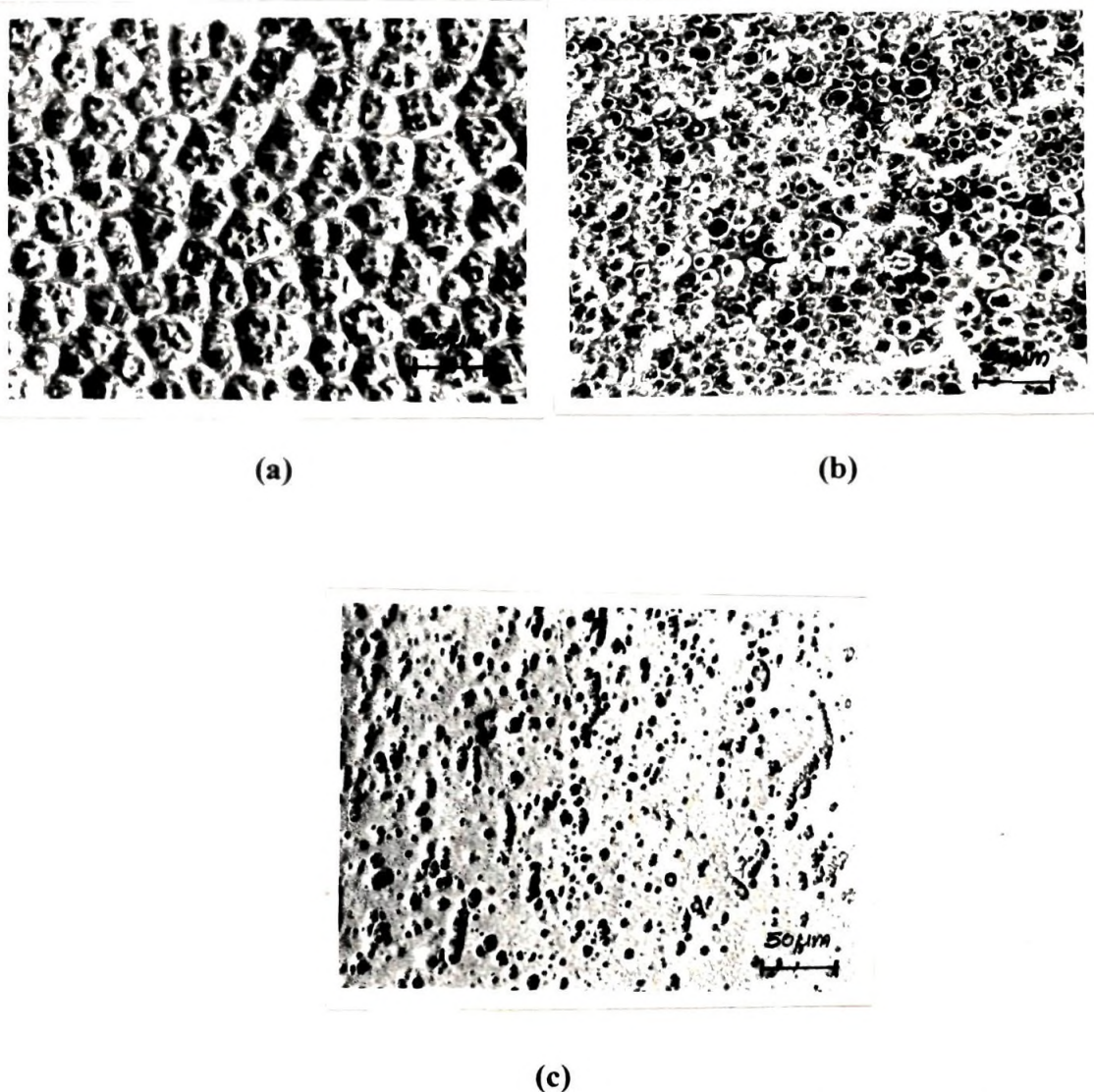
Figure 3.4. Optical micrographs of solution casted 30/70 NR/PS blends (a) $CHCl_3$, (b) CCl_4 and (c) C_6H_6.

(a)

(b)

(c)
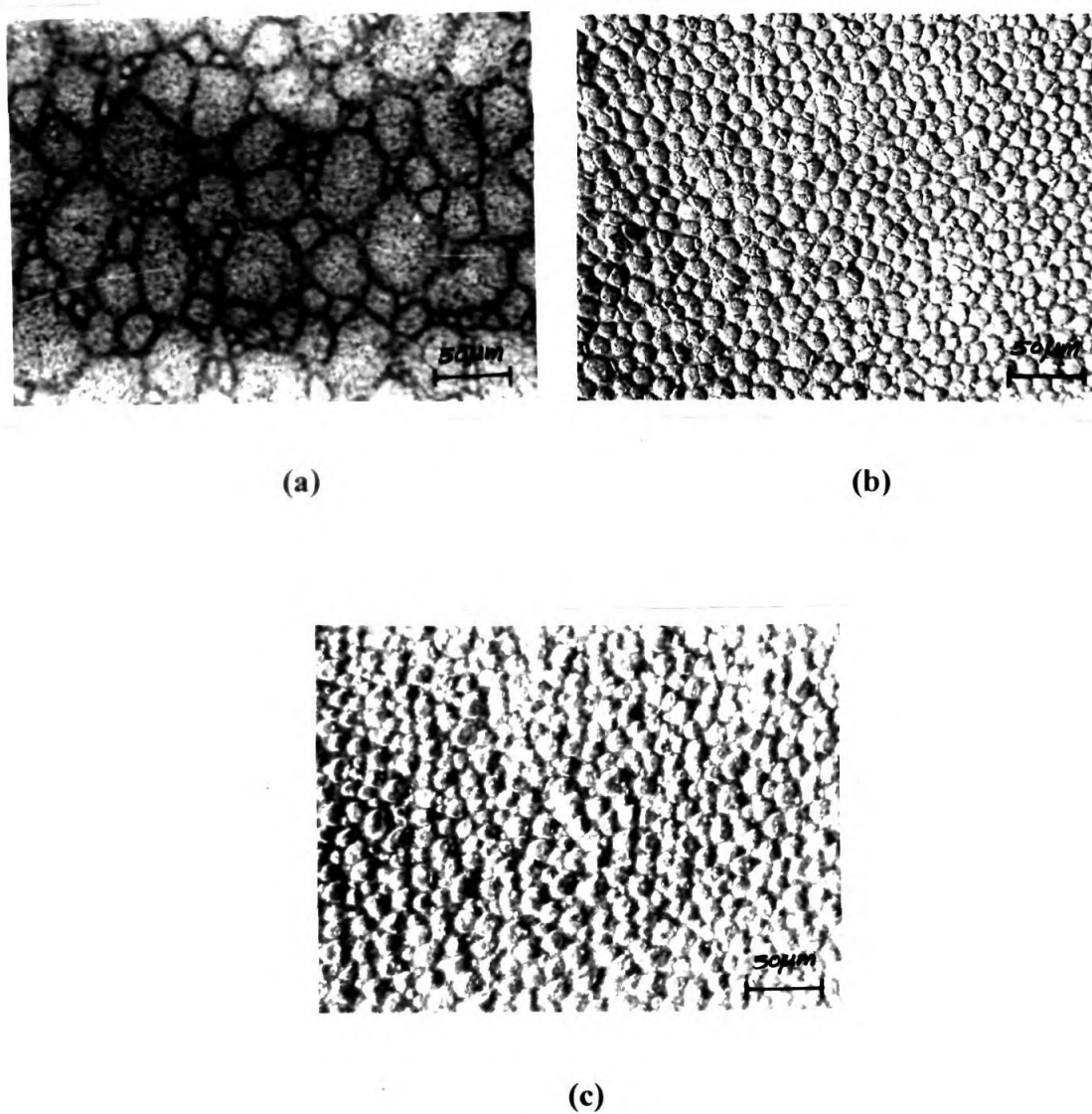
Figure 3.5. Optical micrographs of solution casted 50/50 NR/PS blends (a) CHCl$_3$, (b) CCl$_4$ and (c) C$_6$H$_6$.

(a)

(b)

(c)
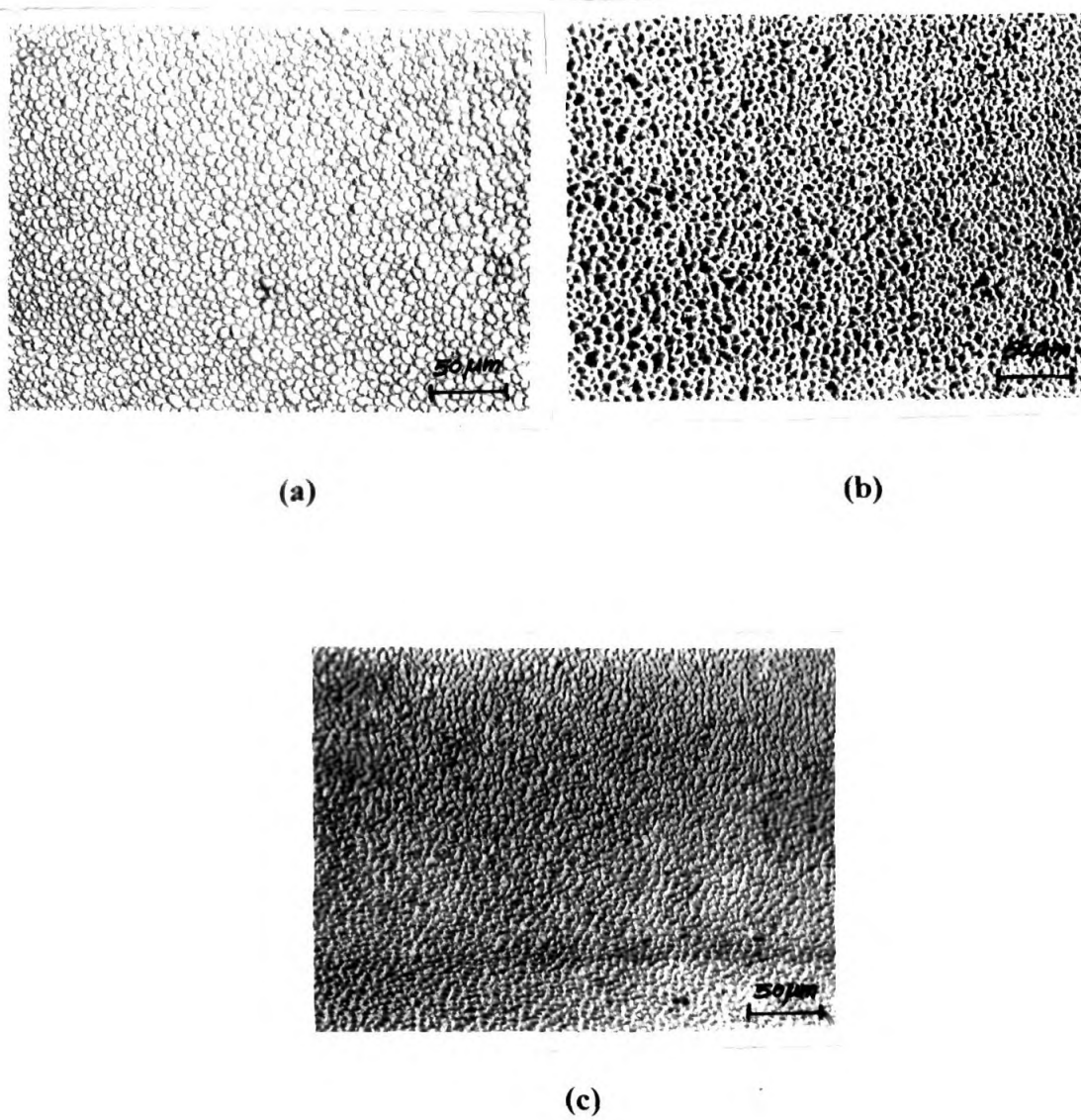
Figure 3.6. Optical micrographs of solution casted 70/30 NR/PS blends (a) $CHCl_3$, (b) CCl_4 and (c) C_6H_6.

Table 3.1.   Number average domain diameter for solution casted NR/PS blends (μm).

Solvent	30/70	40/60	50/50	60/40	70/30
CHCl$_3$	13.11	17.14	14.11	13.45	3.94
CCl$_4$	5.69	7.63	4.83	9.50	2.79
C$_6$H$_6$	3.22	3.36	4.14	5.00	2.17

Comparing the three solvent systems, CHCl$_3$ casted blends show the highest domain size followed by CCl$_4$ and C$_6$H$_6$ for all compositions. The domain size distribution of solution casted blends are given in Figures 3.7–3.9 for different blend compositions. The polydispersity is higher for blends casted from chloroform as evidenced by the large width of the distribution curve. The C$_6$H$_6$ casted blends show the lowest polydispersity and CCl$_4$ casted blends occupy the intermediate position as in the case of domain size (Table 3.2). The trend is the same in all the three different blend systems. The differences in morphology with respect to different casting solvents are associated with the extent of polymer-solvent interaction. This has been addressed by the pioneering studies of Robard and Patterson[15] both theoretically and experimentally. Since the solvent preferentially interacts with one of the components, the morphologies are different. The preferential interaction of solvent with one of the components has been investigated by Thomas and coworkers recently.[16,17] The degree of molecular mixing and its influence on the extent of interactions will be different in different solvent casted system. When the same blend is casted with different solvents, different molecular environments are obtained. For some polymer pairs, the solvent can significantly influence the polymer-polymer compatibility phenomenon. In solution, the conformation of polymers varies with solvent. As a result, the interactions responsible for compatibility of components are altered and will be reflected in the overall performance of the blend system. In different solvent systems, a wide variety of intermolecular contacts are possible ranging from microphase separation to true molecular aggregation. The effects of neighbouring interactions as well as

intermolecular phase boundaries will be different in different solvents. As a result, the total properties of the blend will be altered.[5]
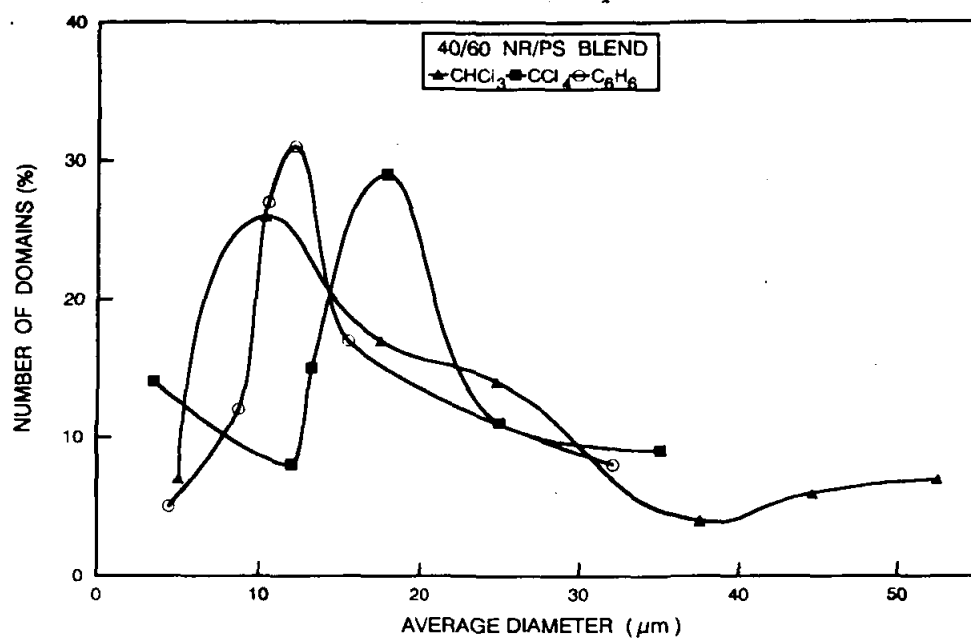
Figure 3.7.   Domain size distribution of 40/60 NR/PS blends.
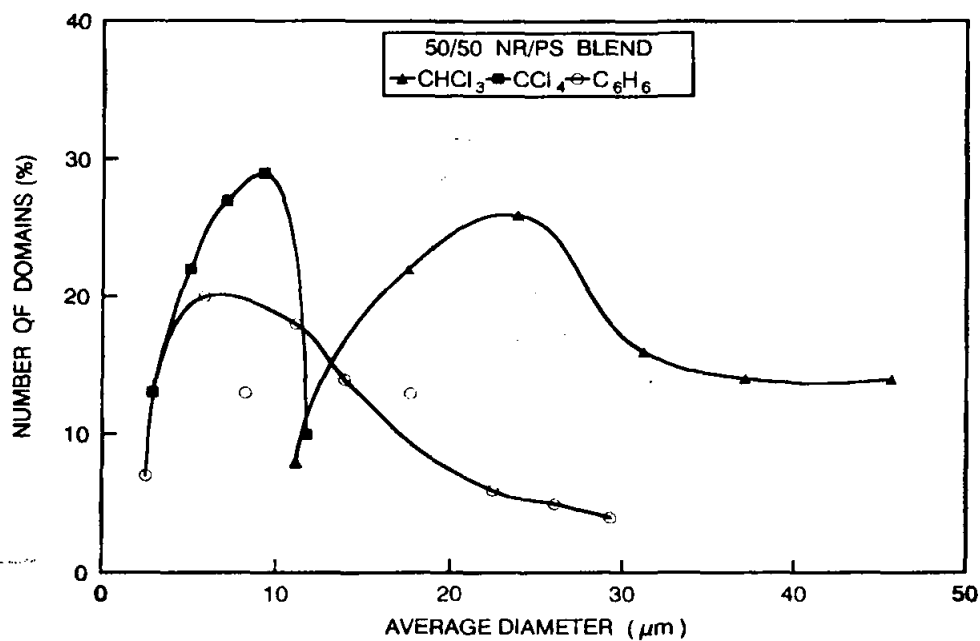
Figure 3.8.   Domain size distribution of 50/50 NR/PS blends.
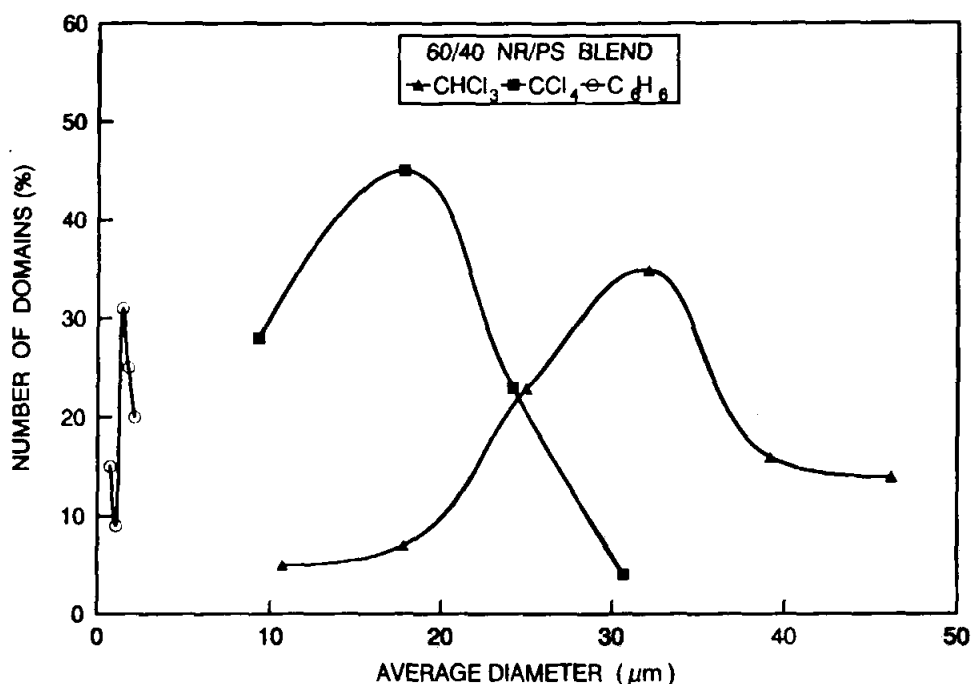
Figure 3.9.   Domain size distribution of 60/40 NR/PS blends.

Table 3.2.   Polydispersity index (PDI) values of different NR/PS blends.

Solvents	40/60	50/50	60/40
CHCl₃	1.24	1.14	1.09
CCl₄	1.36	1.13	1.11
C₆H₆	1.22	1.32	1.09
Melt	1.46	1.26	1.46

Scanning electron micrographs of melt mixed NR/PS blends are given in Figure 3.10. The morphology could be understood from these micrographs. In Figures 3.10a (30/70 NR/PS) and 3.10b (40/60 NR/PS) NR phase has been preferentially etched out by petroleum ether and in Figure 3.10d (60/40 NR/PS) and 3.10e (70/30 NR/PS), PS phase has been etched out by methyl ethyl ketone. In the first two cases, NR is the dispersed phase and in the last two cases PS is the dispersed phase.

(a)

(b)

(c)

(d)

(e)
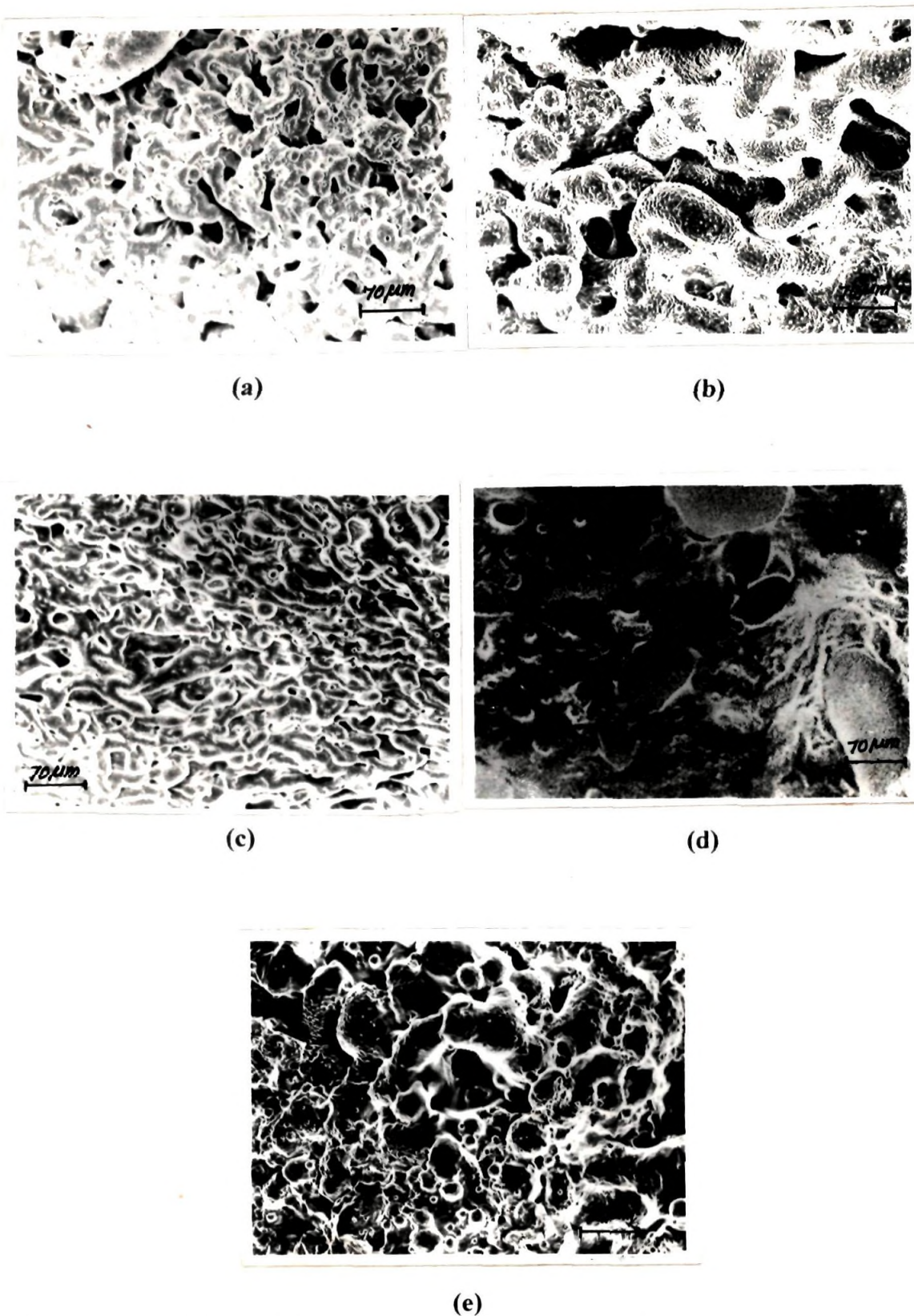
Figure 3.10.   Scanning electron micrographs of melt mixed NR/PS blends: (a) 30/70, (b) 40/60, (c) 50/50, (d) 60/40 and (e) 70/30 NR/PS blends.

From 40/60 to 60/40 range, a partial co-continuous morphology is observed. The variation in dispersed domain size with blend composition is the same as in the case of solution casted blends (Figure 3.11). As discussed earlier the increase in dispersed domain size with increasing proportion of that component is associated with the coalescence or recombination of the dispersed domains.[18-20]
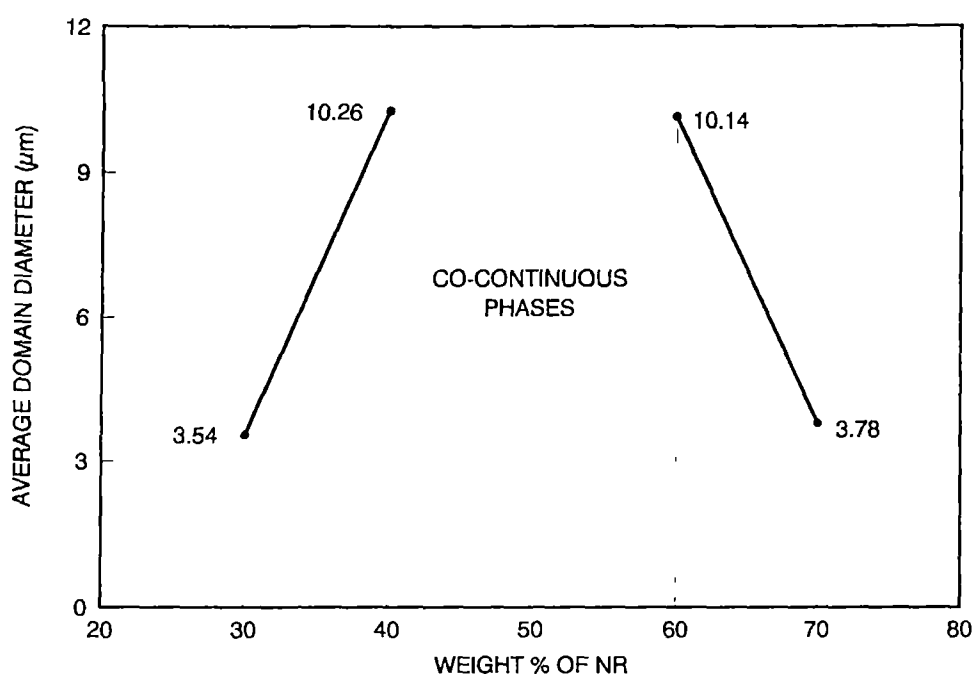
Figure 3.11. Effect of blend composition on the dispersed domain size (melt mixed).

3.1.3 Mechanical properties

The stress-strain curves of blends both melt mixed and solution casted (chloroform) are given in Figures 3.12 and 3.13, respectively. These curves illustrate the deformation pattern of different blends and homopolymers. There are some differences in the deformation behaviour between melt mixed and solution casted samples. In the cases of melt mixed NR/PS blends (Figure 3.12) the stress-strain curve of PS is similar to that of brittle plastic materials. Addition of NR changes the nature of the curve considerably. In the case of 30/70 and 50/50 NR/PS blends, both elastic and inelastic regions could be distinguished. In the

stress-strain curves, slight yielding tendency can be observed which decreases as the rubber content increases. It is seen that the initial modulus reduced considerably while coming down to 70/30 NR/PS blend. The stress-strain behaviour of both NR and high NR blend, i.e., 70/30 NR/PS blend is similar to that of a typical uncrosslinked elastomer.
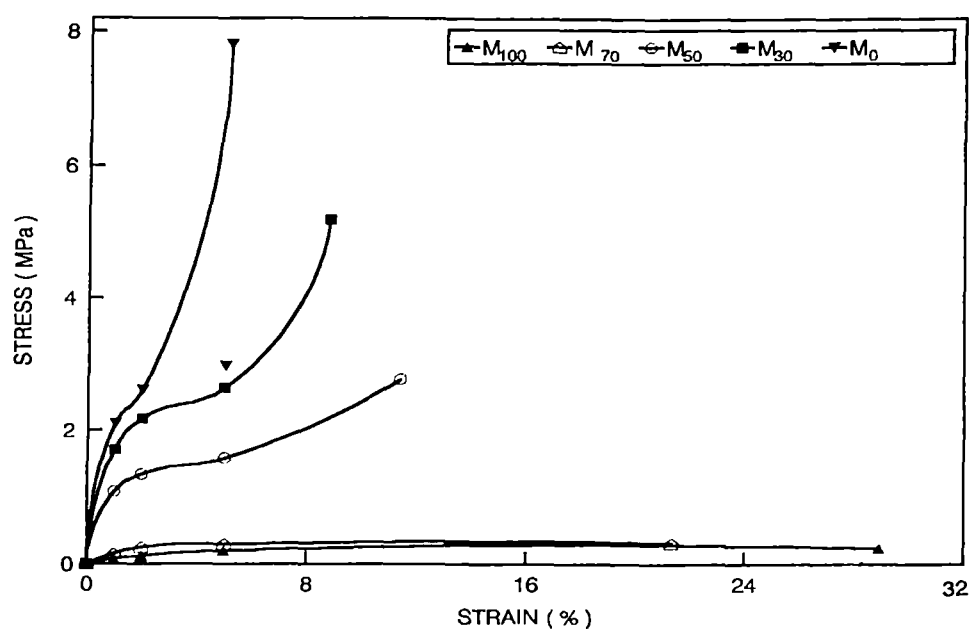
Figure 3.12.   Stress-strain curves of melt mixed NR/PS blends.
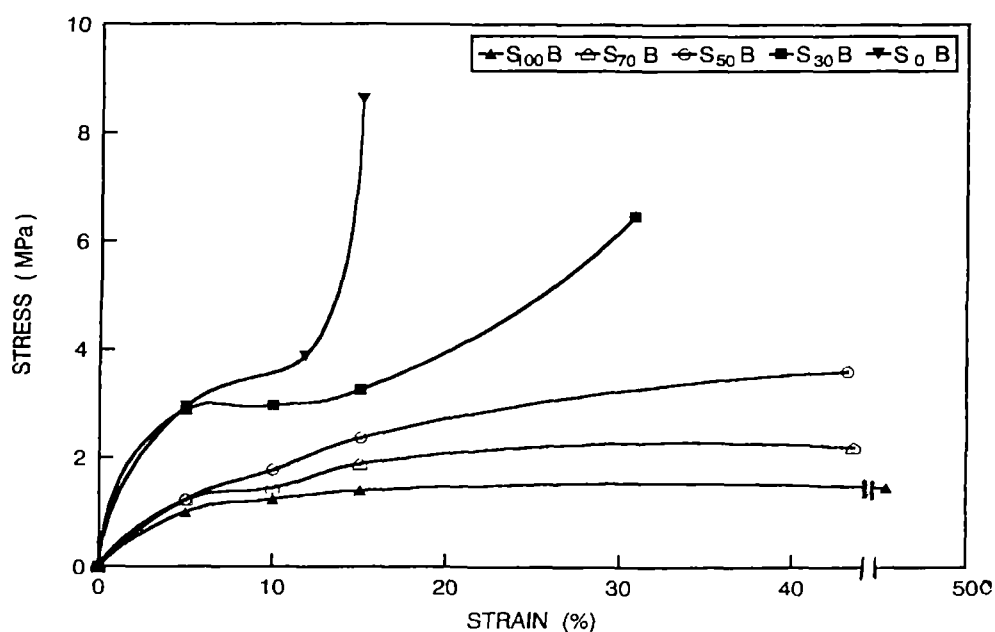
Figure 3.13.   Stress-strain curves of solution casted (CHCl₃) NR/PS blends.

In the case of solution (CHCl₃) casted blends, the stress-strain behaviour (Figure 3.13) shows a slight deviation from that of the melt mixed blends. Even the homopolymers NR and PS showed deviation from those of the corresponding melt blended systems. Compared to melt mixed samples, the initial moduli are lower in the case of PS and high plastic blends and the yielding was increased. In the case of NR and high NR blends, the initial moduli increased compared to that in melt mixed blends. In all the cases the ultimate strength is higher in the case of solution casted blends. Generally the solution casted samples showed higher moduli compared to melt mixed ones and this can be accounted in terms of the degradation that is possible during melt mixing at high temperature.

Figure 3.14 shows the variation of elongation at break (EB) and Young's modulus as a function of blend ratio for the chloroform casted blends. The low value of elongation at break for the blends can be explained on the basis of poor adhesion between the two phases in the blend. Up to 50 wt % of NR, Young's modulus value is higher compared to the latter stages. This is because PS forms the continuous phase and hence high Young's modulus value is observed. Beyond this level, phase inversion takes place, NR becomes the continuous phase and the modulus decreases. It can be seen that as the weight percentage of NR increases, the elongation at break increases and the Young's modulus decreases. In both cases, sharp changes in properties are observed beyond 50 wt % of NR where phase inversion takes place. Similar observations have been reported by Danesi and Porter.[11] It is interesting to note that both properties show negative deviation, i.e., the blends show moduli and elongation at break which are below the additivity line. Blends of NR and PS are incompatible and the high interfacial tension leads to poor interfacial adhesion between the blend components. This is responsible for the negative deviation.
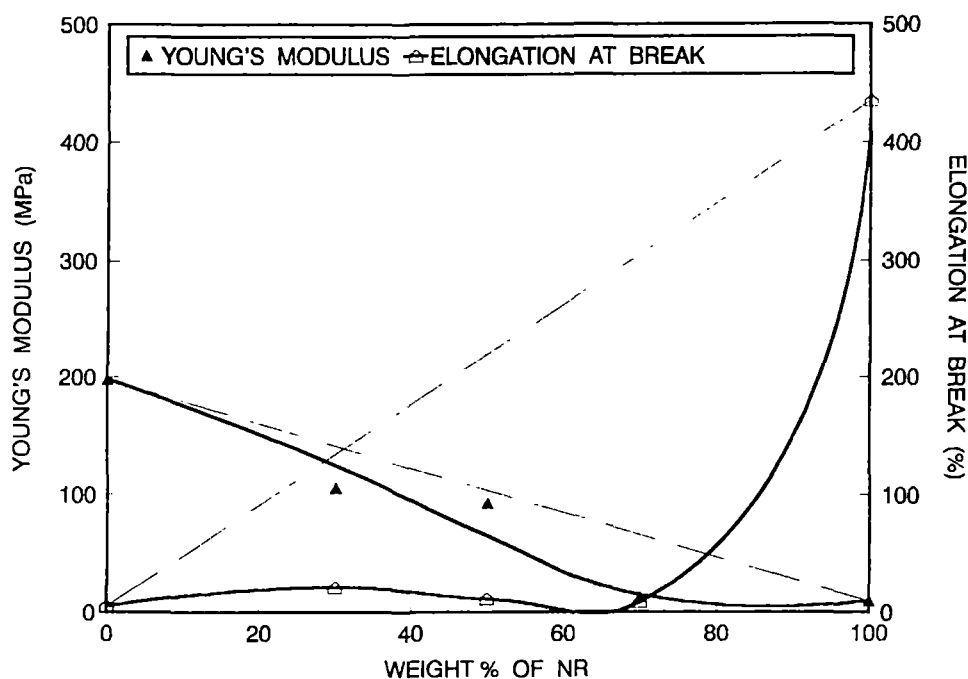
Figure 3.14.   Effect of composition of NR on elongation at break and Young's modulus

Natural rubber/polystyrene blends prepared by the solution casting technique showed much variation in properties compared to the melt mixed samples. The properties were different with respect to the nature of the casting solvents. Figure 3.15 shows the effect of weight per cent of NR on tensile strength of NR/PS blends prepared by both melt and solution mixing techniques. Since the NR/PS blends are immiscible and incompatible, generally the tensile strength values are lower than the additivity value. Both in melt and solution casted samples, pure polystyrene exhibits the maximum tensile strength and pure natural rubber shows the minimum. The blends occupy the intermediate positions. In fact many of them show negative deviation. The tensile strength in general decreases as the weight per cent of NR increases. In the case of melt mixed blends, up to 40 wt % NR the fall in tensile strength is gradual because in this region PS is the matrix and NR is the dispersed phase. Between 40 to 60 wt % NR, the value falls to a low level. In this region, a partial co-continuous phase morphology is observed. From 60 wt % NR onwards, the value is very low because at this stage NR becomes the continuous matrix and

PS forms the dispersed phase. Compared to solution casted blends, tensile strength is higher in the case of melt mixed blends up to 40 wt % NR and beyond this the value is below that of solution casted ones. This is because at higher NR loading, there is a rise in the mixing torque which enhances mechanical degradation of the resulting blend. Among the solution casted blends, C_6H_6 casted blends show the maximum value and this is in agreement with the lower domain size and low polydispersity values exhibited by C_6H_6 casted blends. Compared to chloroform casted blends, CCl_4 casted blends exhibit lower domain size and polydispersity. In spite of this, they exhibit poor tensile strength and this may be due to the occlusion of the last traces of solvent due to the high boiling point of CCl_4 (B.P. 77°C). At 100% NR, all the three systems show almost identical values.
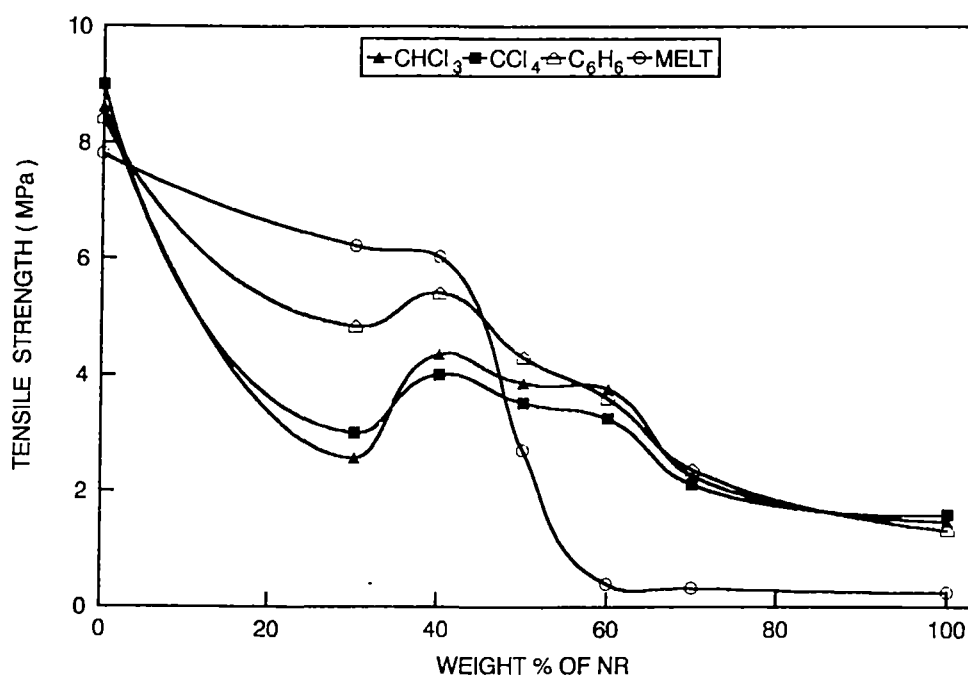
Figure 3.15. Variation of tensile strength with weight per cent of NR.

The effect of weight per cent of NR on tear strength is given in Figure 3.16. In the case of C_6H_6 and CCl_4 casted systems, tear strength decreases sharply up to 50 wt % of NR and thereafter only a marginal decrease in strength is observed. In the case of $CHCl_3$ casted system, the decrease in strength with weight per cent of NR is not sharp as in the former cases. Above 50 wt % NR, the $CHCl_3$ casted systems show much higher tear strength compared to CCl_4 and C_6H_6 casted systems. This is because in the other two cases due to the high boiling points (77 and 80°C for CCl_4 and C_6H_6 respectively) the solvent may occlude in the blend especially at higher NR loading and at this stage NR forms high viscous continuous phase. In the case of melt mixed samples, the tear strength is much lower than the solution casted samples up to 50 wt % of NR and thereafter the values are slightly higher or comparable to the solution casted samples (CCl_4 and C_6H_6). The change in mechanical property is not linear with blend composition. As explained earlier the observed change in slope is due to the phase inversion taking place in the blend as a function of composition. Table 3.3 shows the tensile impact strength of both melt and solution casted NR/PS blends. As the weight per cent of NR increases, impact strength of samples increases. In the case of melt mixed samples, the value is low compared to solution casted blends. In solution casted systems, C_6H_6 casted samples show higher values compared to CCl_4 and $CHCl_3$ casted systems. The impact strength of rubber modified plastics depend on rubber particle size, interparticle distance and interface adhesion. The C_6H_6 casted blends exhibit lowest domain size and hence the highest value of impact strength. In the case of 50/50 NR/PS blends, the value of impact strength is higher because at this state a partial co-continuous morphology is observed. Beyond that NR becomes the matrix and PS becomes the dispersed phase and hence the impact strength increases.
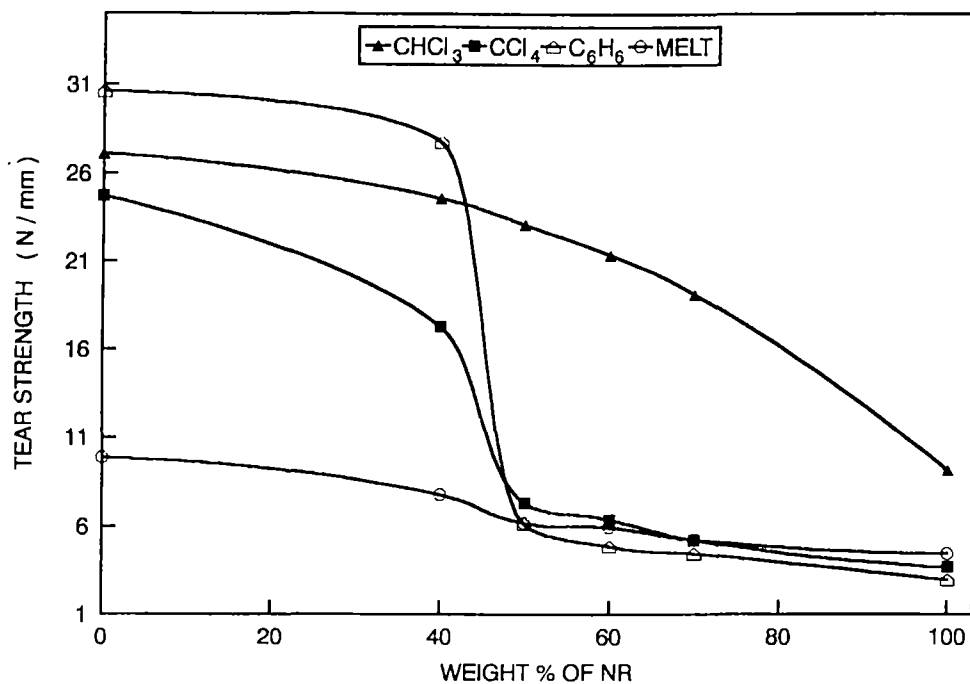
Figure 3.16. Variation of tear strength with weight per cent of NR.

Table 3.3. Tensile impact strength of different NR/PS blends (J/m).

Sample	0/100	30/70	40/60	50/50	60/40	70/30
C_6H_6	800	11000	11600	28860	16500	16666
CCl_4	300	7900	11300	21300	12000	28500
$CHCl_3$	900	9800	17000	23500	19272	34000
Melt	941	1420	1666	1850	2715	3710

Comparing the melt mixed and solution casted systems, the latter gives better properties generally. It may be due to the fact that, in the melt mixing process, the homopolymers undergo degradation due to high temperature (160°C) and shear (80 rpm) employed during the preparation of the blend. The molecular weight values for NR and PS before and after the melt mixing process proved that the blend has undergone considerable degradation during the melt mixing process.

Before and after mixing, the values for $\overline{M}_w$ for NR were 7.79 x 10^5 and 4.70 x 10^5, respectively and those for PS were 3.51 x 10^5 and 2.08 x 10^5, respectively. Moreover, the molecular level mixing is possible in solution casted samples compared to melt mixed ones. Within the solution casted category, $CHCl_3$ casted blends show better properties in many of the systems followed by C_6H_6 and CCl_4 casted blends. This is associated with the different extent of solvent-polymer interactions in the blend as explained earlier.

Different models like parallel, series, Halpin-Tsai, Coran's and Takayanagi model have been used to predict the mechanical properties of these blends. The highest-upper- bound parallel model is given by the rule of mixtures.

$$M \quad = \quad M_1\phi_1 + M_2\phi_2 \tag{3.1}$$

where M is any mechanical property of the blend. M_1 and M_2 are the mechanical properties of components 1 and 2, respectively and ϕ_1 and ϕ_2 are their corresponding volume fractions. In this model, the components are arranged parallel to one another so that an applied stress elongates each component by the same amount. In the lowest-lower bound series model, the blend components are arranged in series and the equation is given as follows,

$$1/M \quad = \quad \phi_1/M_1 + \phi_2/M_2 \tag{3.2}$$

Parameters M, M_1, M_2, ϕ_1, and ϕ_2 are the same as in the upper-limit model. According to the Halpin-Tsai equation,[21,22]

$$M_1/M = \frac{1 + A_iB_i\phi_2}{1 - B_i\phi_2} \tag{3.3}$$

where

$$B_i \quad = \quad \frac{(M_1/M_2) - 1}{(M_1/M_2) + A_i} \tag{3.4}$$

In this model subscripts 1 and 2 correspond to the continuous and dispersed phases respectively. The constant A_i = 0.66 when elastomers form the dispersed phase in

continuous hard matrix. On the other hand, if the hard material forms the dispersed phase in a continuous elastomer matrix, then $A_i = 1.5$. In the case of incompatible blends, generally the experimental value is between the parallel upper bound (M_U) and the series lower bound (M_L) values.

According to Coran's Model,[23]

$$M = f(M_U - M_L) + M_L \tag{3.5}$$

where f is varying between 0-1.

$$f = V_H^n (n V_S + 1) \tag{3.6}$$

where n is related to phase morphology. V_H and V_S are the volume fractions of the hard and soft phase respectively.

According to Takayanagi[24] model

$$M = (1-\lambda) M_1 + \lambda \{[(1-\phi)/M_1] + (\phi/M_2)\} \tag{3.7}$$

where M_1 is the property of the matrix phase; M_2, the property of the dispersed phase; and $\phi\lambda$ is the volume fraction of the dispersed phase and is related to the degree of series-parallel coupling.

The degree of parallel coupling of the model can be expressed by

$$\% \text{ parallel} = [\phi(1-\lambda)/(1-\phi\lambda)] \times 100 \tag{3.8}$$

Figures 3.17 and 3.18 show the experimental and theoretical curves of tensile and tear strength, respectively of the melt mixed blends. It can be seen that the experimental data are close to Halpin-Tsai model in the case of tear strength both at low and high rubber content. In the case of tensile strength, at low rubber content the experimental data is close to parallel model and at high rubber content it is close to Coran's model in which n = 2.
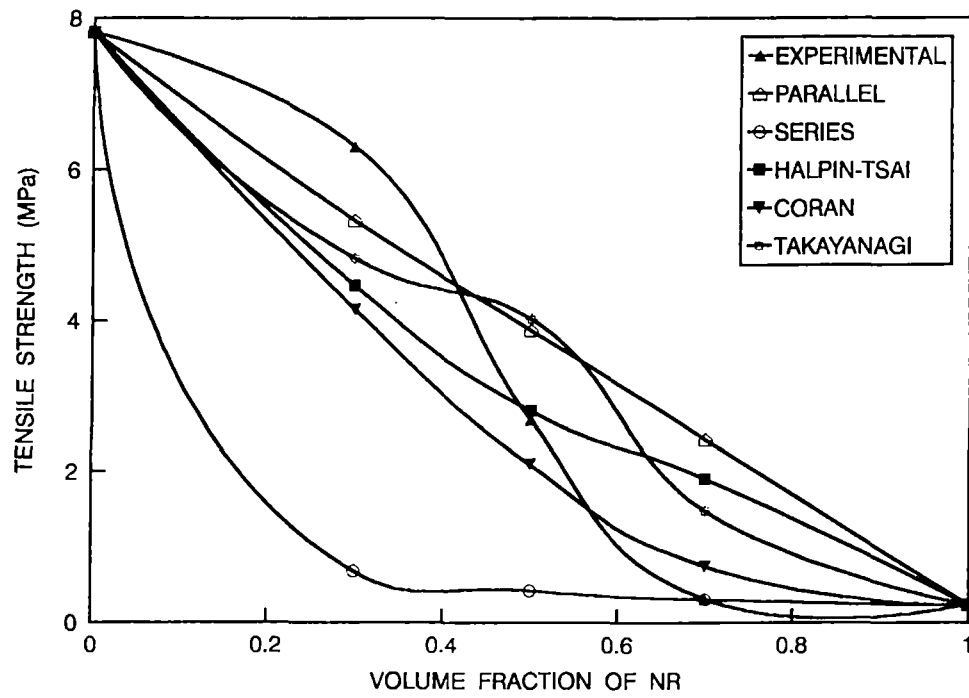
Figure 3.17. Theoretical modelling of tensile strength.
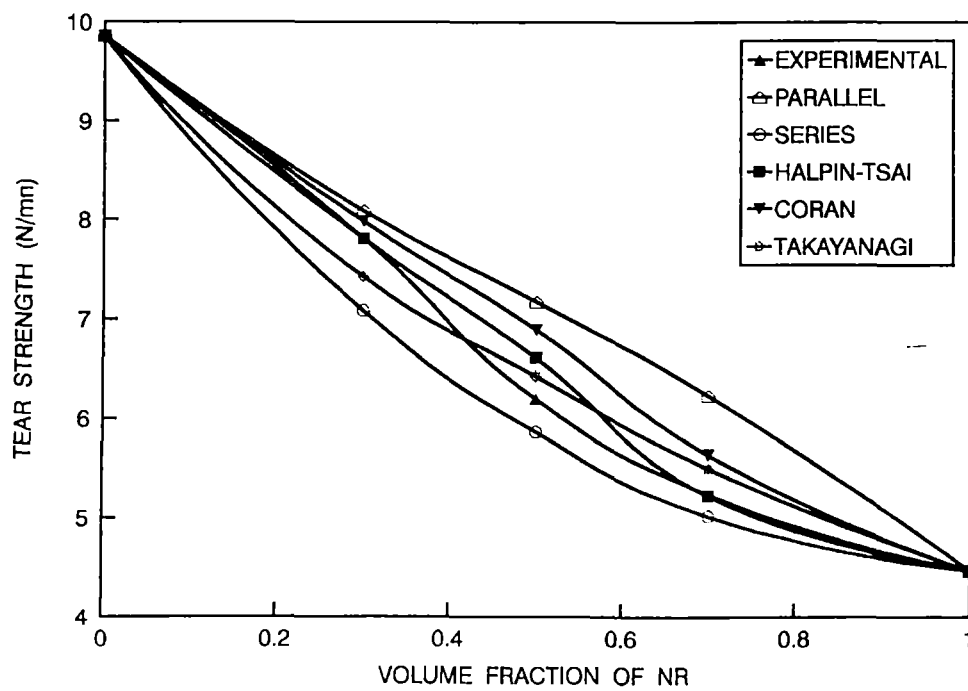
Figure 3.18. Theoretical modelling of tear strength.

3.1.4 Dynamic vulcanisation

The dynamically vulcanised plastic/rubber blends represent a new class of thermoplastic elastomers whose principal features are the ability to be melt processed as thermoplastic and the outstanding elastic recovery after mechanical deformation. The overall performance of the thermoplastic elastomers is thus enhanced upon dynamic vulcanisation. Vulcanisation process modifies the morphology of the system, i.e., a uniform and fine distribution of rubber particles in thermoplastic matrix is obtained.[25,26] This can be schematically represented in Figure 3.19.
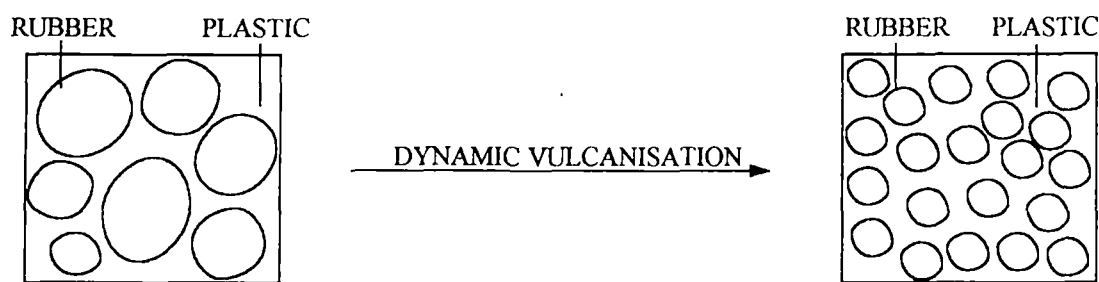
Figure 3.19. Schematic representation of blend morphology showing the uniform distribution of particles upon dynamic crosslinking.

During dynamic crosslinking, the rubber phase is dispersed in the continuous plastic phase and the particle size increases in the order DCP < mixed < sulphur systems. The transformation of morphology of 70/30 NR/PS blends during dynamic crosslinking is schematically presented in Figure 3.20a. During dynamic crosslinking phase inversion takes place and the continuous rubber phase is dispersed as particles in the plastic phase. When dynamic crosslinking is carried out on systems where rubber is already in the dispersed state, no phase inversion takes place, but rubber phase is more finely dispersed. This is schematically shown in Figure 3.20b. In 30/70 and 40/60 NR/PS blends, rubber is already in the dispersed stage in continuous PS phase. As explained earlier here phase inversion does not takes place. Figures 3.21a, b, and c show the scanning electron micrographs of 30/70 NR/PS blends vulcanised by sulphur, mixed and peroxide systems respectively and this shows the variation in dispersed domains size. Here NR forms the dispersed phase in continuous PS matrix.

CROSSLINKED
NR PARTICLE

CONTINUOUS
PS PHASE

DCP SYSTEM

CONTINUOUS   DISPERSED
NR PHASE   PS PHASE

CROSSLINKED
NR PARTICLE

CONTINUOUS
PS PHASE

DYNAMIC CROSSLINKING
PHASE INVERSION

MIXED SYSTEM

NR/PS 70/30

CROSSLINKED
NR PARTICLE

CONTINUOUS
PS PHASE

(a)   SULPHUR SYSTEM

CROSSLINKED
NR PARTICLE

CONTINUOUS
PS PHASE

DCP SYSTEM

CONTINUOUS   DISPERSED
PS PHASE   NR PHASE

CROSSLINKED
NR PARTICLE

CONTINUOUS
PS PHASE

DYNAMIC CROSSLINKING
NO PHASE INVERSION

MIXED SYSTEM

NR/PS 30/70

CROSSLINKED
NR PARTICLE

CONTINUOUS
PS PHASE

(b)   SULPHUR SYSTEM

Figure 3.20.   Schematic   representation   of   dynamically   vulcanised   NR/PS   blend
morphology: (a) 70/30, (b) 30/70 NR/PS blend.

(a)   (b)

(c)
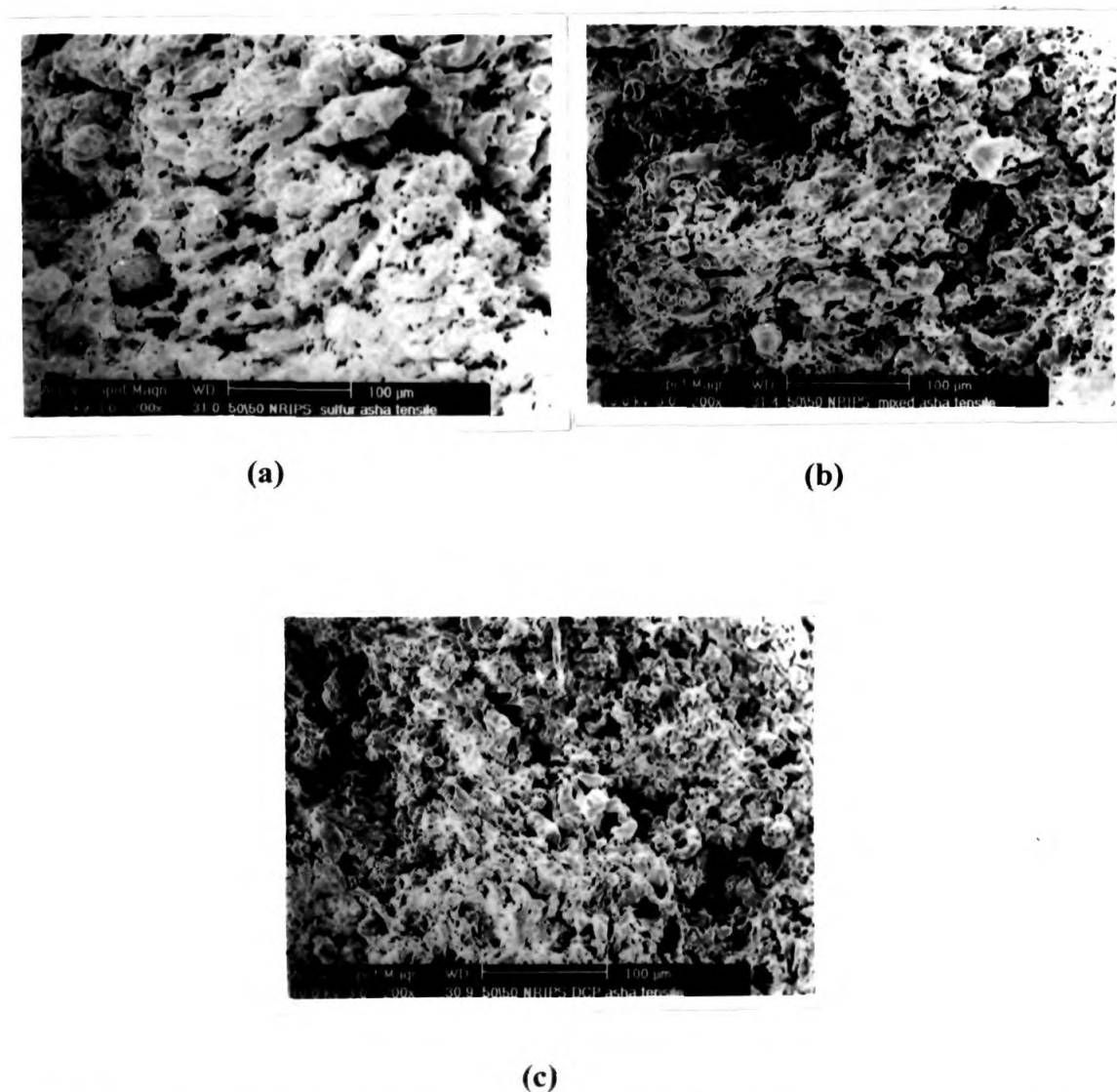
Figure 3.21.   Scanning electron micrographs of dynamically cured 30/70 NR/PS blends: (a) sulphur, (b) mixed and (c) peroxide.

The different crosslinks possible during dynamic crosslinking using sulphur, peroxide and mixed systems are given in Figure 3.22.   The mono, di and polysulphidic linkages in sulphur system impart high chain flexibility to the polymer network.   In the DCP system only rigid C-C linkages are present and in mixed system all these mono, di, polysulphidic and C-C linkages are present.   The

effect of dynamic vulcanisation on various mechanical properties have been studied in three different blend systems namely, 30/70, 40/60 and 50/50 NR/PS blends. The effects of different vulcanising systems such as sulphur, peroxide and mixed systems on mechanical properties are given in Table 3.4.

(a)
PEROXIDE
(DCP)

C-C linkages

(b)
SULPHUR

Mono, di and polysulphidic linkages
(Predominantly polysulphidic x > 3)

(c)
MIXED

Mixed linkages (x > 3)
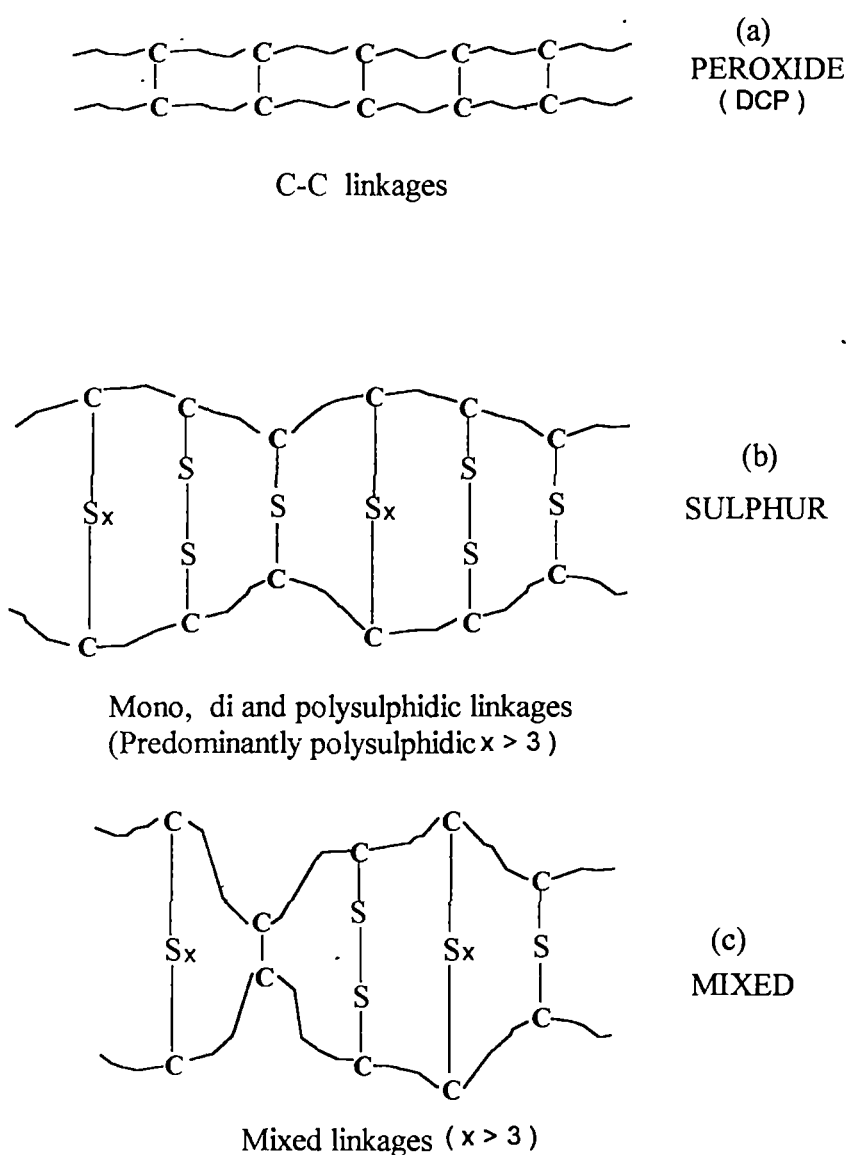
Figure 3.22.   Structure of the network formed by different vulcanising techniques: (a) peroxide, (b) sulphur and (c) mixed systems.

Table 3.4. Mechanical properties of uncrosslinked and dynamically crosslinked melt mixed NR/PS blends.

Sample	Tensile strength (MPa)	Elongation at break (%)	Young's modulus (MPa)
30/70 NR/PS	6.26	10.18	105
30/70 NR/PS/S	12.8	3.43	800
30/70 NR/PS/DCP	12.4	5.97	690
30/70 NR/PS/S/DCP	11.70	4.3	858
40/60 NR/PS	6.13	13.18	97
40/60 NR/PS/S	11.01	6.11	520
40/60 NR/PS/DCP	11.40	4	590
40/60 NR/PS/S/DCP	3.81	21	375
50/50 NR/PS	2.7	11.4	91
50/50 NR/PS/S	12.8	6.9	400
50/50 NR/PS/DCP	4.2	5	280
50/50 NR/PS/S/DCP	3.1	3	90

In almost all the cases, the mechanical properties of the dynamically vulcanised blends are higher compared to uncured samples. This can be related to the morphology and crosslink density of different vulcanised samples. It is possible to estimate the degree of crosslinking in various systems by determining the volume fraction of solvent swollen samples (V_r) which is determined by the equation (Table 3.5).[27]

$$\phi = \frac{W_1 / \rho_1}{W_1 / \rho_1 + W_2 / \rho_2} \qquad (3.9)$$

where W_1 and ρ_1 are the weight and density of the polymer sample respectively and W_2 and ρ_2 are the weight and density of the solvent, respectively. The sulphur system shows the minimum value of crosslink density and the peroxide system the maximum value. The mixed system occupies the intermediate position.

Table 3.5.   Volume fraction (V$_r$) of NR/PS blends.

Sample	Volume fraction (V$_r$)
Sulphur	0.2096
Mixed	0.2225
Peroxide	0.2752

The high value of tensile strength in DCP system is attributed to the fine particle size of the dispersed rubber phase and higher value of crosslink density. The Young's modulus values of different NR/PS blends are also given in Table 3.4. In all the cases the dynamically cured samples show higher modulus compared to uncured ones. Among all the different vulcanised systems, the 30/70 NR/PS blends show the maximum value of Young's modulus whereas the 50/50 blends show the minimum value because of the decrease in the amount of PS in the blend. The stress-strain curves for different NR/PS (dynamically cured) blends are given in Figure 3.23. The 50/50 NR/PS blends show lower moduli compared to 30/70 NR/PS blends.
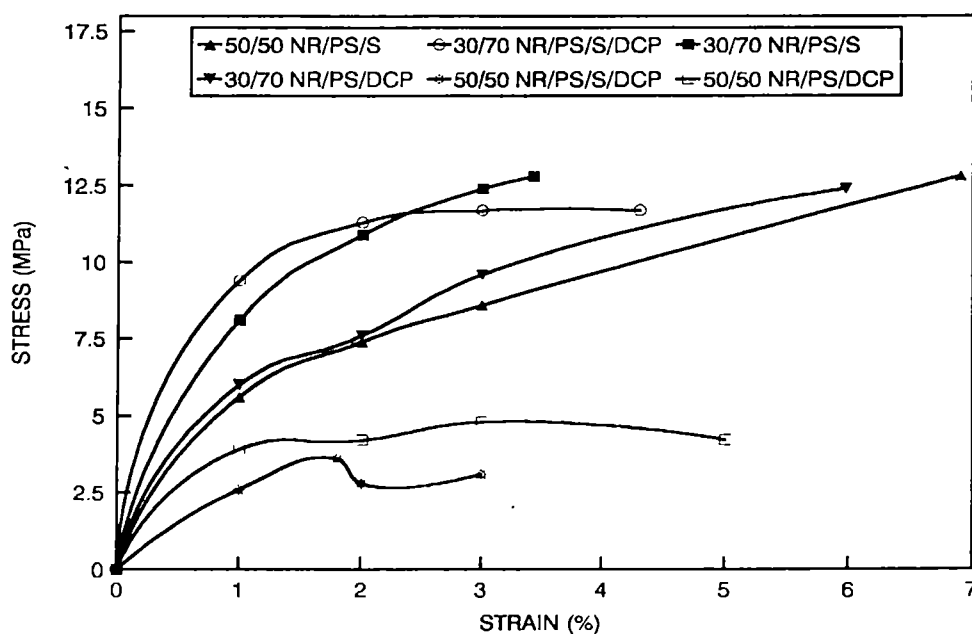
Figure 3.23.   Stress-strain behaviour of dynamically cured NR/PS blends.

The tensile impact strength values of different vulcanised systems are given in Table 3.6. Except in 30/70 NR/PS blend, the dynamically cured samples show values higher than those of uncured samples. As the rubber content increases from 30/70 to 50/50 NR/PS the impact strength increases in all the three different vulcanising systems. The sulphur system shows the maximum value for impact strength followed by mixed and peroxide system and can be related to the high flexibility of polysulphidic linkages. In all the cases, NR is the dispersed phase in the continuous thermoplastic matrix. However, in 50/50 blend NR exists as both dispersed and continuous phase, i.e., a partial co-continuous morphology is observed.

Table 3.6. Tensile impact strength of unvulcanised and dynamically vulcanised NR/PS blends (J/m).

Sample	30/70	40/60	50/50
Sulphur	1280	2180	4000
Mixed	1190	1770	2620
Peroxide	1090	1340	2170
Unvulcanised	1420	1666	1850

3.2 References

1. S. Cimmino, F. Coppola, L. D'orazio, R. Greco, G. Maglio, M. Malinconico, C. Mancarella, E. Martuscelli, and G. Ragosta, *Polymer,* **27**, 1874 (1986).

2. T. Kunori, and P. H. Geil, *J. Macromol. Sci. Phys.,* B1, **8**(1), 93 (1980).

3. J. M. Willis and B. D. Favis, *Polym. Eng. Sci.,* **28**, 1416 (1988).

4. T. Nishi, T. K. Kwei and T. T. Wang, *J. Appl. Polym. Sci.,* **46**, 4157 (1975).

5. M. Bank, J. Leffingwell and C. Thies, *Macromolecules,* **4**, 43 (1971).

6. B. D. Favis, *J. Appl. Polym. Sci.,* **39**, 285 (1990).

7. C. Qin, J. Yin, and B. Huang, *Rubber Chem. Technol.,* **63**, 77 (1989).

8. C. E. Scott, and C. W. Macosko, *Polymer,* **35**, 5425 (1994).

9. S. George, R. Joseph, K. T. Varughese, and S. Thomas, *Polymer*, **36**, 23, 4405 (1995).

10. S. S. Dagli, N. Xanthos and J. A. Beisenberger, *Polym. Eng. Sci.*, **34**, 1723 (1994).

11. S. Danesi, and R. S. Porter, *Polymer*, **19**, 448 (1978).

12. C. S. Ha, W. J. Cho, Y. S. Hur and S. C. Kin, *Polymers for Advanced Technologies*, **2**, 31 (1990).

13. A. P. Plachocki, S. S. Dagli and R. D. Adrews, *Polym. Eng. Sci.*, **30**, 741 (1990).

14. C. K. Park, C. S. Ha, J. K. Lee and W. J. Cho, *J. Appl. Polym. Sci.*, **50**, 1239 (1993).

15. A. Robard and D. A. Patterson, *Macromolecules*, **10**, 1021 (1977).

16. Z. Oommen, M. G. Nair and S. Thomas, *Polym. Eng. Sci.*, **36**, 151 (1996).

17. Z. Oommen and S. Thomas, *Polym. Bullet.* **31**, 623 (1993).

18. H. Varghese, S. S. Bhagawan, S. S. Rao and S. Thomas, *Eur. Polym. J.*, **31**, 957 (1995).

19. K. C. Dao, *Polymer*, **25**, 1527 (1984).

20. S. Thomas, B. R. Gupta and S. K. De, *J. Vinyl Technol.*, **9**, 71 (1987).

21. L. E. Nielson, *Rheol. Acta*, **13**, 86 (1974).

22. J. C. Halpin, *J. Compos. Mater.*, **3**, 732 (1970).

23. A. Y. Coran, *Hand Book of Elastomers—New Development and Technology* (Eds., A. K. Bhowmick and H. L. Stephens), Marcel Dekker, NY, 1988, p. 249.

24. S. George, N. R. Neelakantan, K. T. Varughese and S. Thomas, *Polym. Sci. Part B: Polym. Phys.*, **35**, 2309 (1997).

25. F. S. Liao, A. C. Su and T. C. J. Hsu, *Polymer*, **35**, 2579 (1994).

26. B. Kuriakose, S. K. De, S. S. Bhagawan, R. Sivaramakrishnan and S. K. Athithan, *J. Appl. Polym. Sci.*, **32**, 5509 (1986).

27. S. R. Jain, V. Sekhar and V. N. Krishnamurthy, *J. Appl. Polym. Sci.*, **48**, 1515 (1993).

Chapter 4

Compatibilising Effect of Graft Copolymers on Morphology and Mechanical Properties

Even though blending is an easy method for the preparation of TPEs, most of the TPE blends are immiscible and incompatible. Very often the resulting materials exhibit poor mechanical properties due to the poor adhesion between the phases. Over the years different techniques have been developed to alleviate this problem. These include (1) the addition of a third homopolymer or graft or block copolymer which is miscible with the two phases (physical compatibilisation), (2) the introduction of covalent bonds between the homopolymer phases (reactive compatibilisation). There are several studies in literature in which the addition of copolymer increases the technological compatibility of immiscible polymer pairs. Incorporation of a copolymer usually improves the interaction between the constituent homopolymers and thereby slows down the phase separation process.[1-4] It was reported by Paul[5] that the copolymer addition will provide finer dispersion, improved interfacial adhesion, stability against gross segregation and will reduce the interfacial tension. Several researchers have reported the compatibilising ability of copolymers in immiscible blends.[6-10]

In this chapter, we report on the compatibilisation of thermoplastic elastomers from blends of natural rubber (NR) and polystyrene (PS) which are highly incompatible. Till date no serious attention has been made on the compatibilising action of copolymers in these blends. The effects of addition of graft copolymer (NR-g-PS) of NR and PS on the mechanical and morphological properties of NR/PS blends have been analysed. The influence of copolymer concentration, molecular weight of homo and copolymers, mode of addition and nature of casting solvents on the morphology and properties of the blends has been investigated quantitatively. Attempts were made to deduce the graft copolymer conformation at the blend interface. Finally, the experimental results were compared with the current theories of Noolandi and Hong.

4.1 Results

4.1.1 Graft copolymer characterisation

Graft copolymer (NR-g-PS) was characterised by FTIR spectroscopy, H^1NMR spectroscopy and gravimetric methods. The grafting efficiency and percentage of PS grafted were 49 and 20% respectively. This has been estimated by gravimetric analysis as reported earlier.[11]

FTIR spectrum (Figure 4.1) shows peaks at 3026 and 2855 cm^{-1} which correspond to aromatic C-H stretching in PS. Peaks at 1601 and 1541 cm^{-1} correspond to C=C stretching of aromatic ring of PS. A strong peak at 698 cm^{-1} stands for the monosubstituted benzene ring along with the characteristic absorptions of the NR group at 837 and 889 cm^{-1}. The peaks at 1452 and 1375 cm^{-1} correspond to the aliphatic C-H stretching in NR.
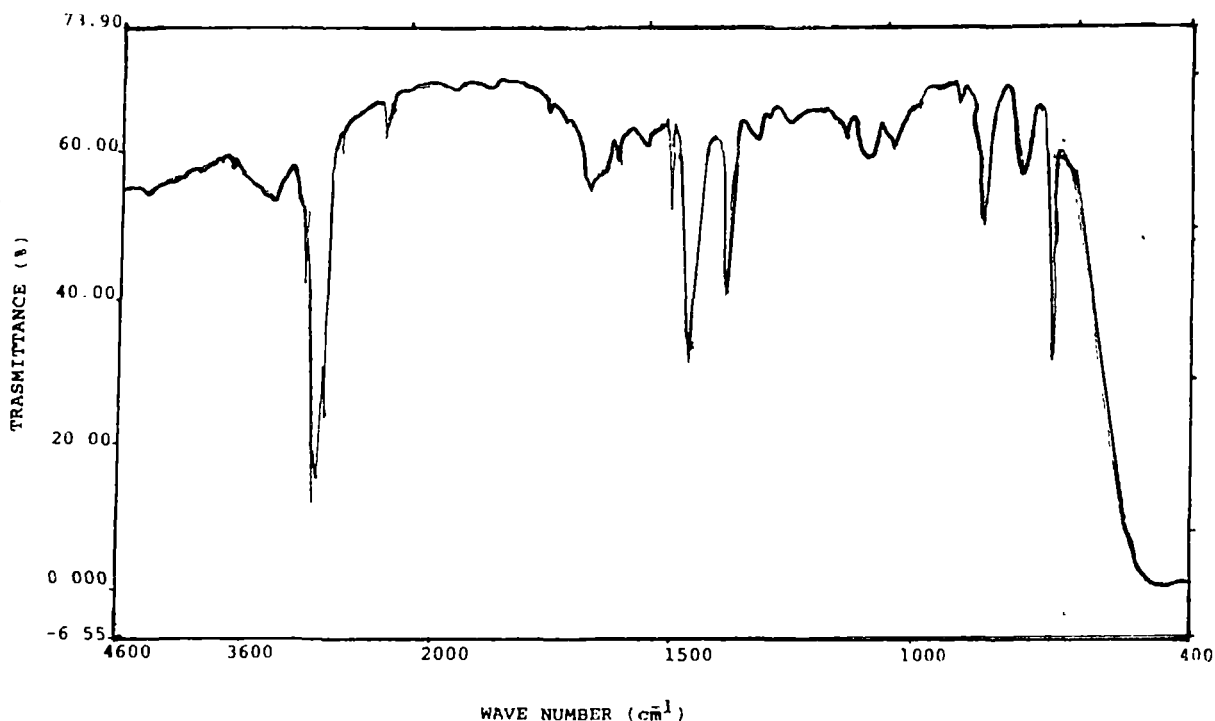
Figure 4.1. FTIR spectrum of the graft copolymer.

The H^1NMR spectrum (Figure 4.2) obtained at 90 MHz shows chemical shifts at 1-2, 4.6-4.8, 6.6 ppm corresponding to alkyl protons of NR, vinyl protons and aromatic protons of polystyrene respectively.
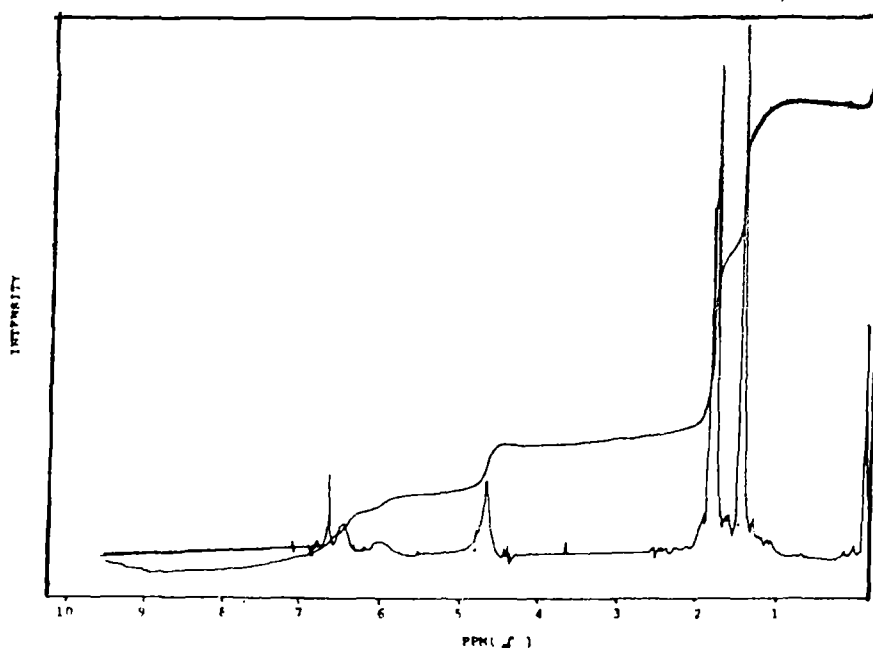
Figure 4.2.   H¹NMR spectrum of the graft copolymer.

4.1.2 Morphological studies

(a)   Effect of graft copolymer concentration

NR/PS blends are completely immiscible and incompatible. Large polystyrene domains are dispersed in the continuous NR matrix. The compatibility of the above system can be improved by the addition of a compatibiliser, i.e., a graft copolymer (NR-g-PS)of NR and PS. It was seen that the size of the dispersed polystyrene domains decreases with increasing percentage of the graft copolymer. Figure 4.3 shows the optical microphotographs of 50/50 NR/PS blends (CHCl₃ casted) with and without the addition of the copolymer. In this blend, PS is the continuous phase and NR found to be both dispersed and continuous. The number average domain size measurements were done by noting the diameter of about 200 domains at random in each blend system. The domain diameters were based on the available dispersed phase morphology. The average domain size decreases with increasing concentration of the compatibiliser and finally gets levelled off at higher concentrations (Figure 4.4). This levelling point can be considered as the apparent critical micelle concentration (CMC), i.e., concentration of the copolymer at which

micelles are formed. This sort of micelle formation is highly undesirable. The CMC values were in fact estimated from the intersection of the straight line drawn in the low concentration and the levelling off line at high concentration (Figure 4.4). It is important to indicate that generally CMC is estimated from the plot of interfacial tension versus copolymer concentration. Since the interfacial tension is directly proportional to the domain size, the estimation of CMC from the plot of domain size versus concentration is justified.[12]

(a)   (b)

(c)   (d)
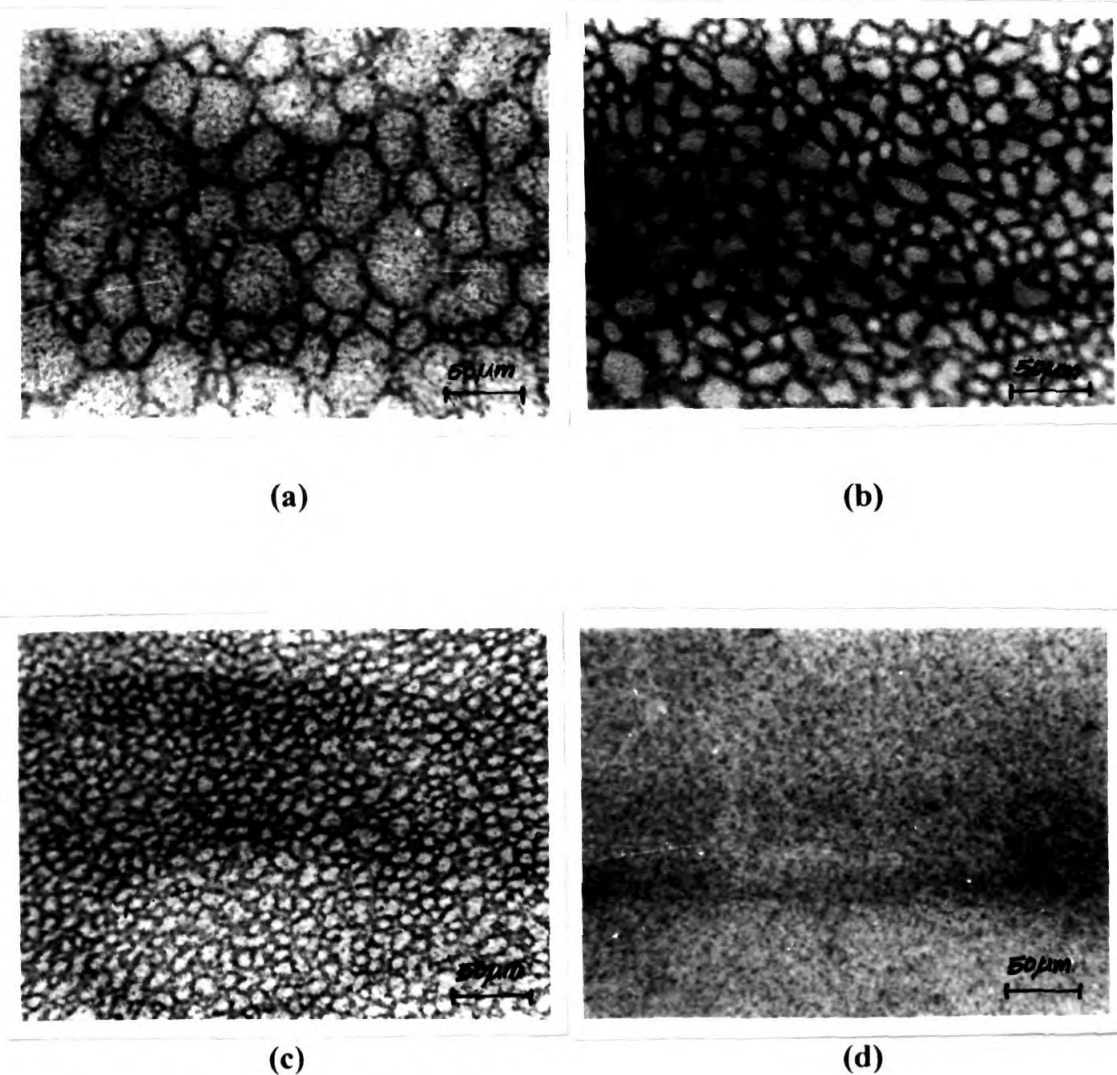
Figure 4.3.   Optical microphotographs of 50/50 NR/PS blend with (a) 0% (b) 1.5% (c) 3% (d) 4.5% graft copolymer.
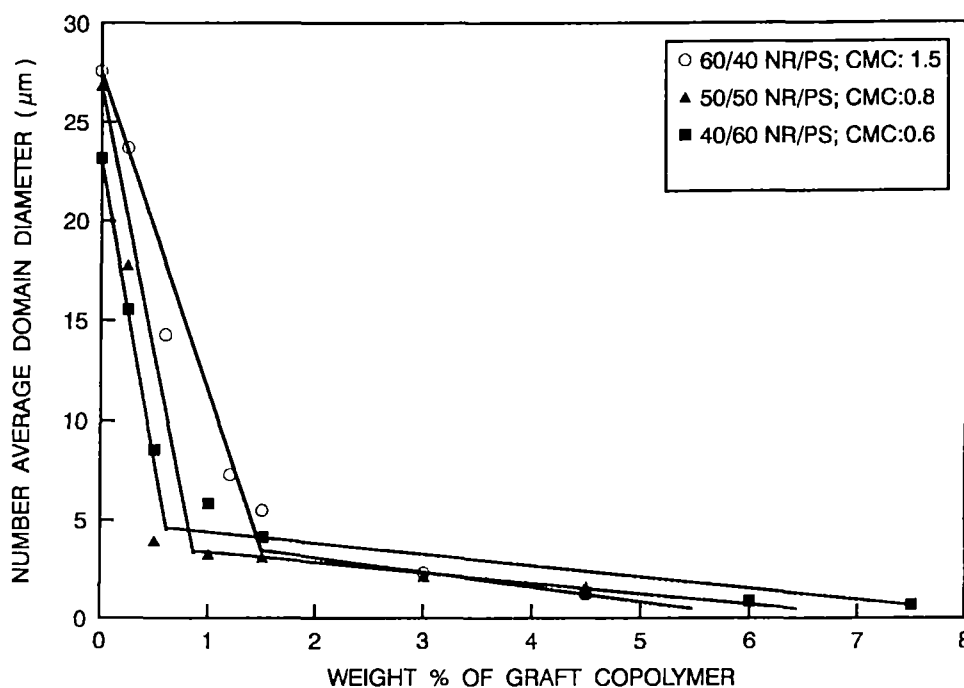
Figure 4.4. Effect of copolymer concentration on the number average domain diameter of the dispersed phase of different NR/PS blends.

When the 50/50 blend is analysed, it can be found that the levelling point (CMC) is at 0.8% compatibiliser loading. The domain size of the blend without graft copolymer is found to be 20.23 μm. Addition of 1.5% graft copolymer reduces the domain size to 3.493 μm, i.e., a reduction of 82.7% occurs. Addition of another 1.5% causes a reduction of 38% in the domain size. Finally the domain size levels off at higher concentrations of the copolymer. In the case of 60/40 and 40/60 NR/PS blends the percentages of graft copolymer required to saturate the interface (i.e., CMC) are 1.5 and 0.6%, respectively.

The domain size distribution for 50/50 NR/PS blend with and without the addition of the compatibiliser is given is Figure 4.5. Table 4.1 gives the standard deviation values of the blend (50/50 NR/PS) with the addition of the copolymer. These values decrease with increase in loading of the copolymer. The noncompatibilised blend contains large number of bigger particles. The

polydispersity is higher for blend without compatibiliser and is much reduced at higher concentration of the compatibiliser which is evident from the width of the distribution curve. Similar studies have been reported by Willis et al.[13] and Djakovic et al.[14]
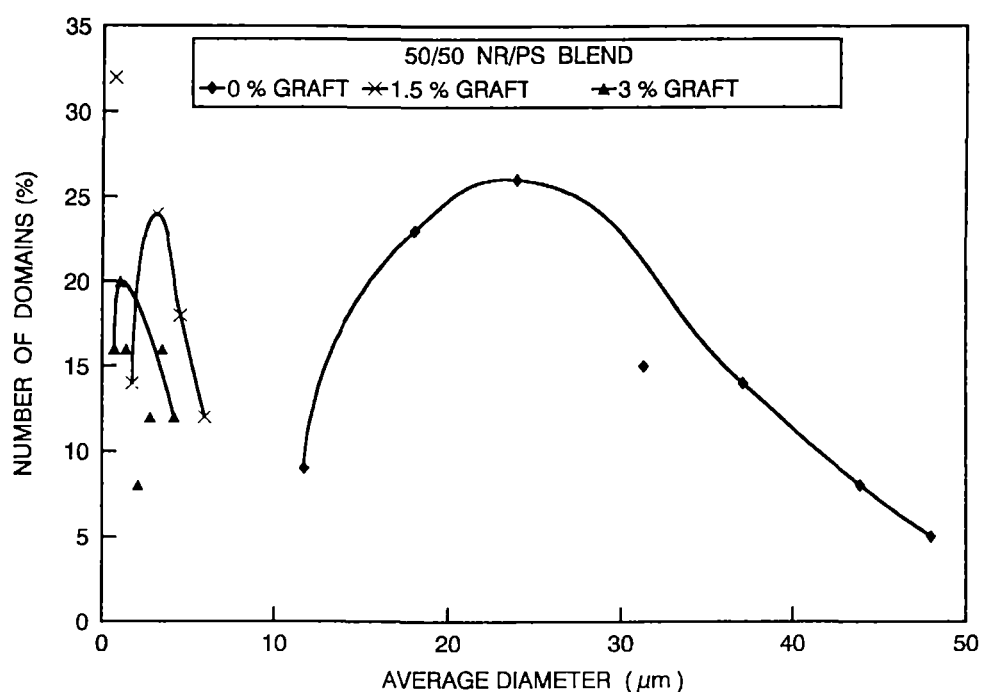
Figure 4.5. Effect of copolymer concentration on the number average domain size distribution of 50/50 NR/PS blends.

Table 4.1. Standard deviation values of 50/50 NR/PS blends.

Graft copolymer (%)	Average domain size (μm)	Standard deviation
0.5	3.5	25.45
1.5	3.4	24.95
3	2.1	7.40
4.5	1.6	11.70
6	0.9	2.15

Figure 4.6 shows the effect of compatibiliser on the interparticle distance of dispersed domains in the 50/50 NR/PS blend. The interparticle distance decreases with increasing concentration of the compatibiliser and finally levels off at higher compatibiliser loading.
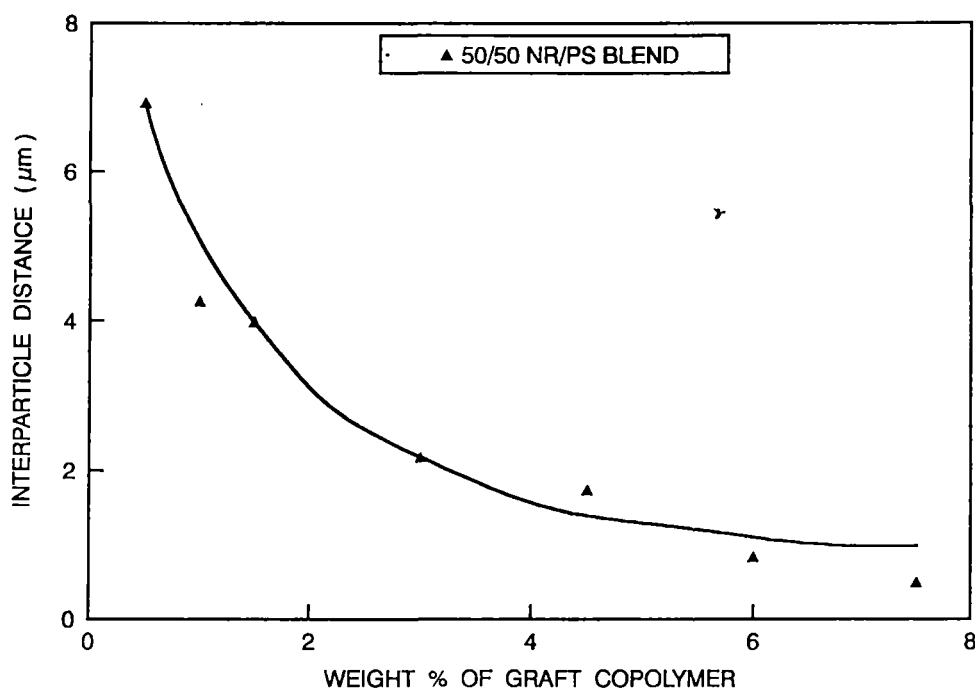
Figure 4.6. Effect of copolymer concentration on the interparticle distance of the dispersed phase of 50/50 NR/PS blend.

(b) *Effect of molecular weights of homo and graft copolymers*

The compatibilising effect depends very much on the molecular weight of the homopolymer. Generally, the amount of the graft copolymer required for compatibilisation is proportional to the   molecular weight of the homopolymer. Natural rubber of molecular weights, $NR_0 = 7.79 \times 10^5$, $NR_5 = 3.7 \times 10^5$, $NR_{10} = 2.49 \times 10^5$, $NR_{15} = 1.62 \times 10^5$ and polystyrene of molecular weights $PS_1 = 3.51 \times 10^5$ and $PS_2 = 2.073 \times 10^5$ were used to study the effect of molecular weight of homopolymer on the compatibilising action of the graft copolymer.

The amount of graft copolymer required to saturate unit volume of the interface (CMC) was found to decrease with decrease in molecular weight (Figures 4.7 and 4.8) of the homopolymers. The influence of molecular weight of polystyrene on the CMC values is given in Table 4.2.
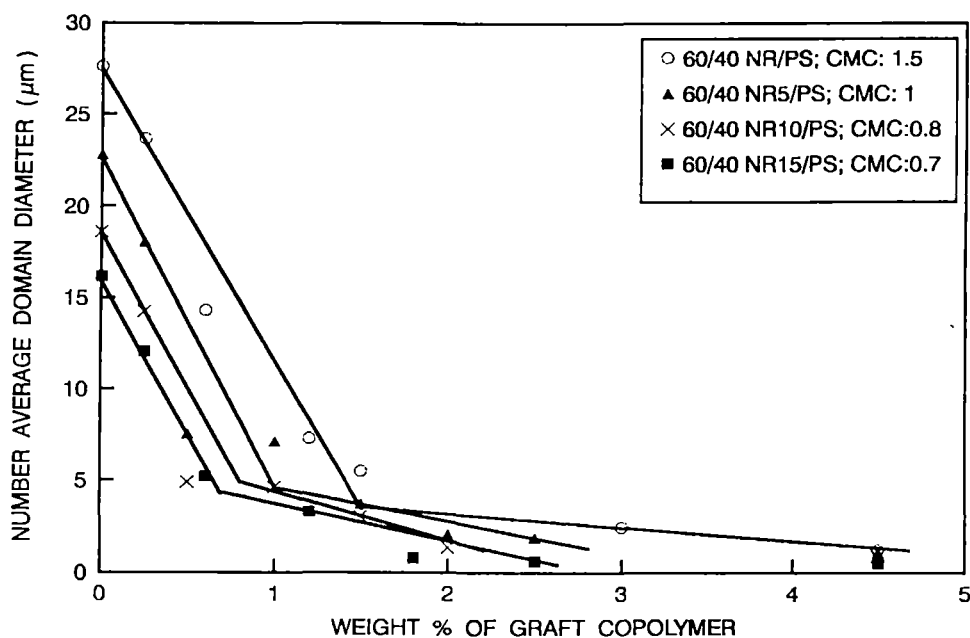
Figure 4.7. Influence of molecular weight of NR on CMC values.
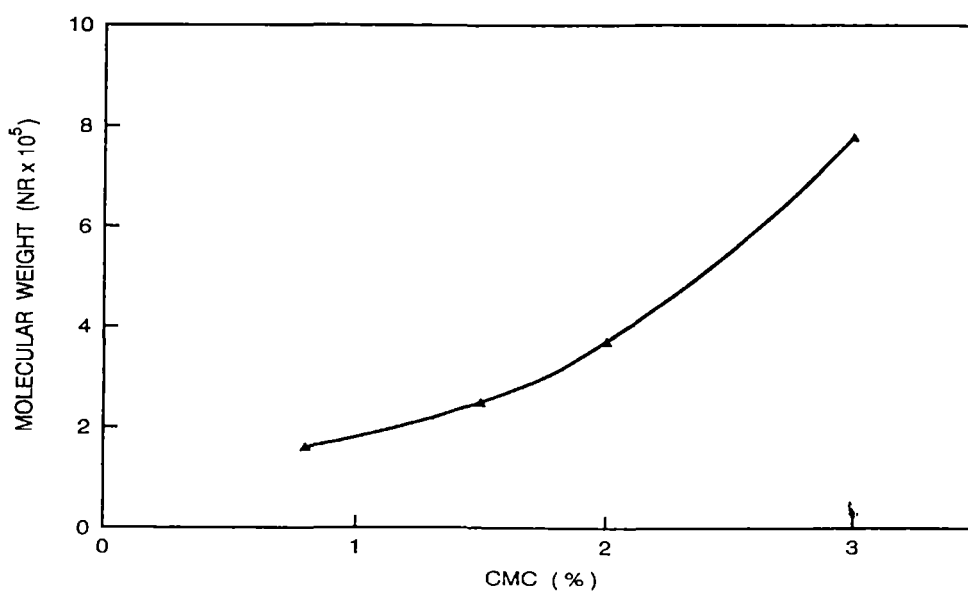
Figure 4.8. Effect of molecular weight of NR on CMC.

Table 4.2. Effect of molecular weight of PS on CMC values.

Sample	Mol. wt of PS ($\overline{Mn}$)	CMC (%)	Domain radius at CMC (μm)
PS$_1$	3.51×10^5	1.5	1.80
PS$_2$	2.07×10^5	1.2	1.28

Molecular weight of the copolymer (NR-g-PS) also influences the interfacial saturation point. Graft copolymers of molecular weight $G_1 = 3.95 \times 10^5$ and $G_2 = 1.009 \times 10^5$ have been used in this work. The amount of graft copolymer needed for interface saturation decreases with increase in molecular weight of the compatibiliser. The critical micelle concentration was found to be 1.5% in the case of 60/40 NR/PS blends compatibilised with sample G_1. The same blend system with sample G_2 gives a higher value for CMC i.e., 3% compatibiliser was required to saturate unit volume of the blend interface.

(c)   Effect of mode of addition of graft copolymer

Morphology of the blend depends very much on the mode of preparation of the blends. Variation in the conditions of blend preparation can change the morphology. Cimmino et al.[15] have observed a drastic change in the domain size of nylon/rubber blends when prepared in two steps compared to one step mixing.

The two step mixing can be done in two ways. In the first method, the solution of the dispersed phase (PS) is mixed with the compatibiliser and then blended with the matrix polymer (NR). In the second case the matrix polymer is mixed with the compatibiliser and then blended with the dispersed polymer. In both cases the solutions obtained were then evaporated to get thin films. Preblending the compatibiliser with the dispersed phase (PS) is found to improve the interaction between the copolymer and the dispersed phase.

The particle size and CMC of NR_0/PS blend were measured in the two step mixing and compared the values with those of one step mixing. In the case of 60/40 NR/PS blend the CMC was obtained as 1.5% graft copolymer (one step). When the copolymer was preblended with the dispersed phase the CMC was attained at 1.3% graft copolymer loading and there is much reduction in the domain size of the dispersed phase. In one step mixing the particle diameter of the dispersed domains at 1.5% graft copolymer loading was found to be 5.08 μm whereas in two step mixing the corresponding value was 3.70 μm and at 2.5% graft loading the values were 2.45 and 1.84 μm, respectively. When the matrix polymer was preblended with the copolymer, the CMC was the same as in the case of one step mixing (1.5%) but the dispersed domain size was reduced (Table 4.3).

Table 4.3. Dispersed phase radius (r) at CMC and Σ values of the system.

Polymer blends	Solvent	CMC (%)	Radius at CMC (μm)	Area Σ (nm^2)
40/60 (NR_0/PS_1/G_1)	$CHCl_3$	0.6	1.30	100.90
50/50 (NR_0/PS_1/G_2)	$CHCl_3$	0.8	1.71	71.90
60/40 (NR_0/PS_1/G_1 1 step mixing)	$CHCl_3$	1.5	2.54	30.98
60/40 (NR_0/PS_1/G_1 2 step mixing NR to PS+G)	$CHCl_3$	1.3	1.85	49.10
60/40 (NR_0/PS_1/G_1 2 step mixing PS to NR+G)	$CHCl_3$	1.5	2.45	32.12
60/40 (NR_0/PS_1/G_1)	CCl_4	1.1	1.30	82.55
60/40 (NR_0/PS_1/G_2)	$CHCl_3$	3.0	0.65	15.46
60/40 (NR_5/PS_1/G_1)	$CHCl_3$	1.0	2.36	50.02
60/40 (NR_{10}/PS_1/G_1)	$CHCl_3$	0.8	2.45	60.08
60/40 (NR_{15}/PS_1/G_1)	$CHCl_3$	0.7	2.60	64.97

The above findings reveal that the mode of addition of the compatibiliser has an important role in the morphology of the blends. Compared to one step mixing, in two step mixing i.e., preblending the compatibiliser with the dispersed phase, the amount of the compatibiliser that is diffused into the interface can be increased and the distance travelled by the compatibiliser to reach the blend interface can be minimised. This leads to better interfacial interaction of the compatibiliser and results in a finer morphology. A speculative model has been given to illustrate this behaviour in Figure 4.9.
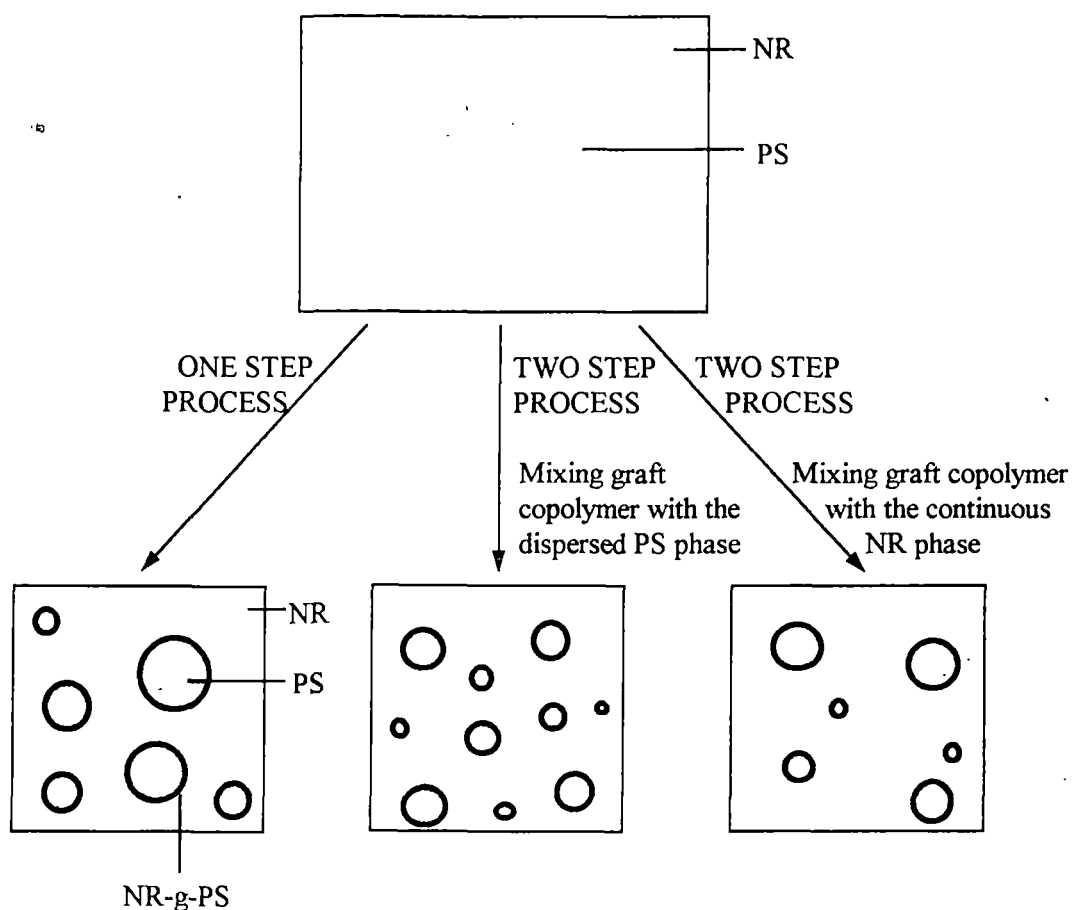
Figure 4.9.   Speculative model illustrating the compatibilisation efficiency under different mode of addition of copolymer.

(d)   Effect of casting solvents

Casting solvent has an important role in the morphology of blends. The same blend system can give different morphologies in different casting solvents. Two solvents were selected for comparison, namely chloroform and carbon tetrachloride. There is much difference in the domain size between the two solvent systems. Film casted from carbon tetrachloride shows a finer morphology compared to that of chloroform casted film (Figure 4.10). The difference in the behaviour is due to the difference in the level of interaction between the copolymer and solvent. This has been well addressed by the pioneering studies of Patterson et al.[16]

(b)

(c)   (d)
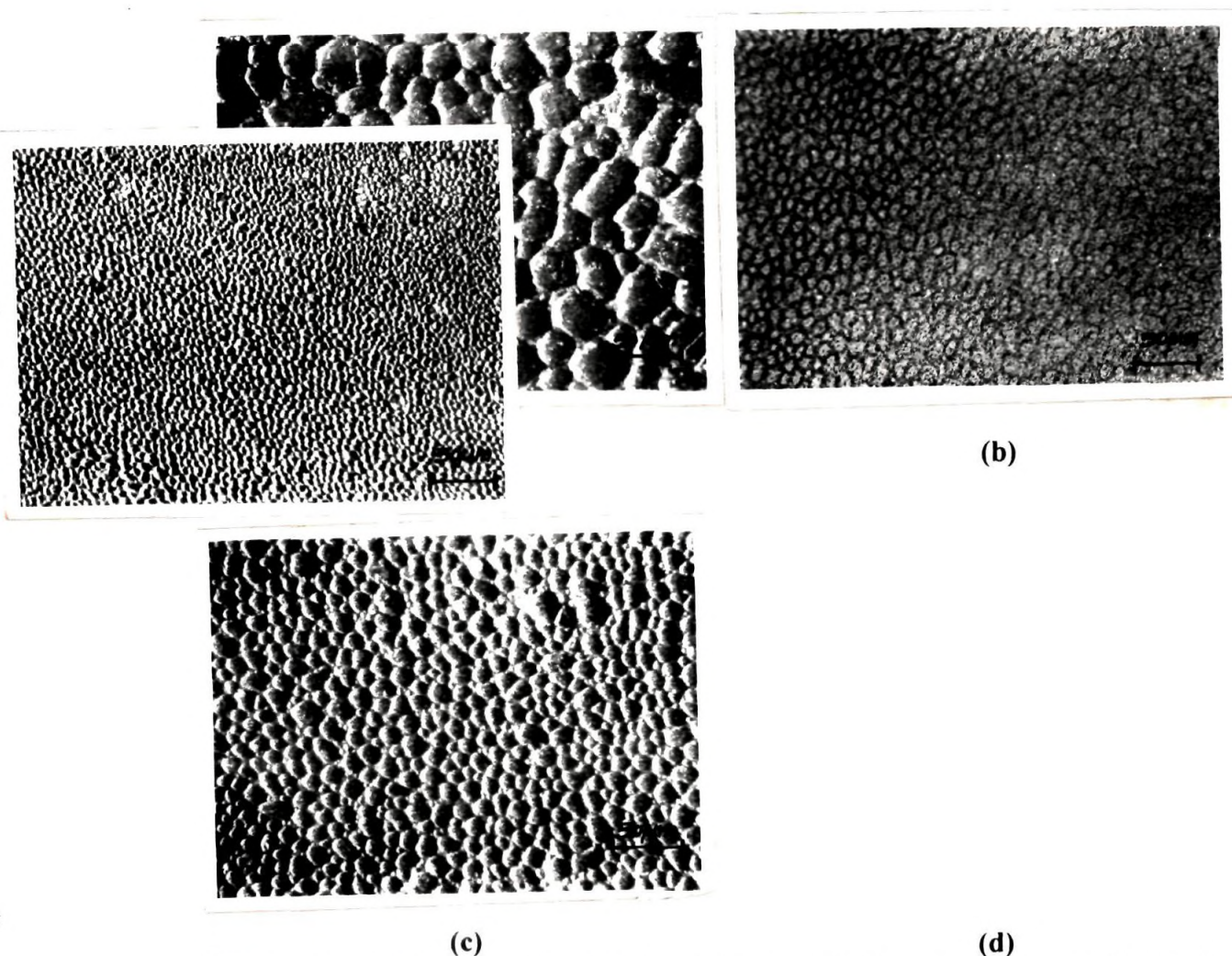
Figure 4.10.   Optical microphotographs of CCl$_4$ and CHCl$_3$ casted films (60/40 NR/PS blend) containing (a) 0% graft, CCl$_4$ (b) 1.2% graft, CCl$_4$ (c) 0% graft, CHCl$_3$ (d) 1.2% graft, CHCl$_3$.

In both cases, the addition of graft copolymer reduces the domain size.[17] The concentration of the graft copolymer required to saturate unit volume of the interface (CMC-1.1%) is less for carbon tetrachloride casted film than that for chloroform casted film (CMC-1.5%). The size of the dispersed domains of the non-compatibilised blends of chloroform casted and carbon tetrachloride casted films are 27.6 and 17.6 μm, respectively. This behaviour is due to the fact that the solubility parameter of CCl_4 ($\delta = 8.6$) is close to those of the polymers (PSδ = 8.56, NRδ = 7.75) than to that of $CHCl_3$ ($\delta = 9.3$).

4.1.3 Mechanical properties

The morphology has a significant role on the mechanical properties of the blends. Many research studies have been reported on the morphology-mechanical property relationships of polymer blends. Paul and coworkers[18] have studied the mechanical properties of PE/PVC blends containing chlorinated PE as compatibiliser. Mechanical properties of nylon/PP was studied by Ide and Hasegawa.[19] Locke and Paul[20] studied the improvement in mechanical properties of PS/PE blends by the addition of graft copolymer. In all the above cases, the graft copolymer improved the interfacial adhesion and hence the mechanical properties of the blends too.

The influence of graft copolymer on tensile strength and modulus was studied. Figure 4.11 shows the variation in tensile strength and modulus with percentage of the compatibiliser. The tensile strength and modulus increase with the addition of the copolymer and finally levelled off at higher concentrations (Table 4.4). The impact strength increases up to 3% compatibiliser loading and then decreases at higher concentration (Table 4.4). These changes are in accordance with the morphology of the blends. Addition of the copolymer results in an improvement in tensile strength, modulus and impact strength due to the enhanced interfacial adhesion between PS and NR.
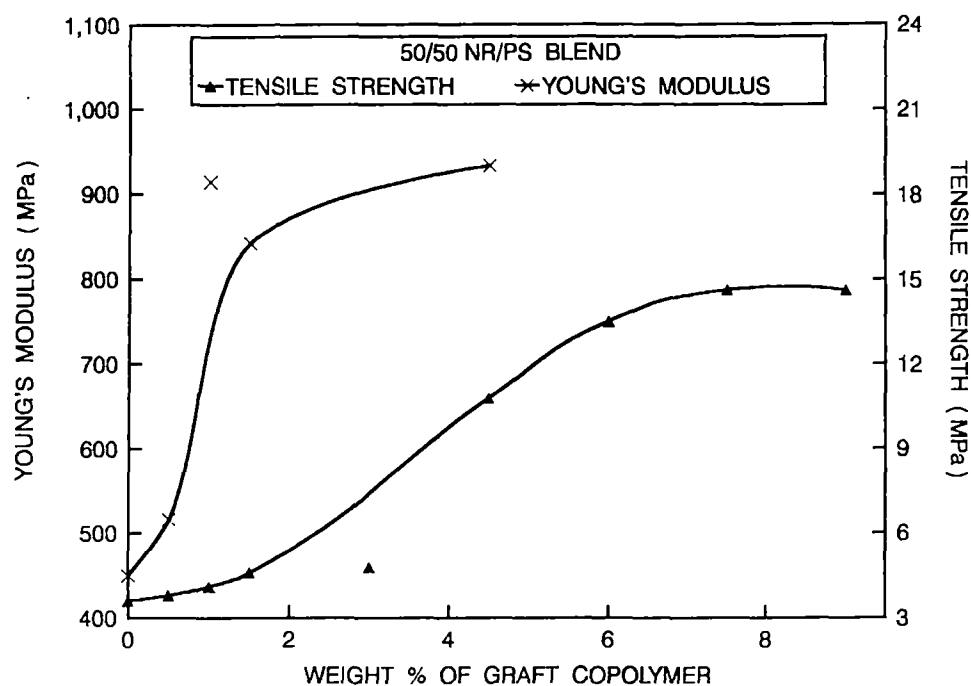
Figure 4.11. Effect of copolymer concentration on the tensile strength and Young's modulus of NR/PS blend (CHCl₃).

Table 4.4. Mechanical properties of 50/50 NR/PS blends.

Graft copolymer (%)	Stress at different elongations (MPa)			Tensile strength (MPa)	Elongation at break (%)	Tensile impact strength (J/m²)
	15%	30%	50%			
0	1.24	1.78	2.37	3.6	454	0.30×10^5
1	-	-	-	-	-	1.43×10^5
1.5	1.54	1.82	2.45	3.86	194	1.64×10^5
3	1.96	2.05	2.75	4.50	190	2.10×10^5
4.5	1.99	2.28	3.07	10.10	252	1.63×10^5
6	2.56	2.78	3.24	13.24	247	1.39×10^5

4.2   Discussion

In the case of heterogeneous polymer blends, several research studies have been done on the compatibilising action of the block and graft copolymers. The high interfacial tension that exist between the phases which is responsible for macrophase separation can be reduced by the addition of the compatibiliser. There are different parameters which govern the interfacial saturation. These include molecular weight of the homopolymers, molecular weight of the copolymer, its structural details, mode of addition of compatibiliser, processing conditions, affinity of the copolymer for the dispersed phase, orientation of the copolymer at the blend interface, etc.

The experimental and theoretical studies on the compatibilisation of immiscible blends report on the so-called interfacial saturation by the addition of copolymers. For example in the case of polyethylene/ natural rubber blends[21] 5% of the compatibiliser (polyethylene-b-polyisoprene) was found to be sufficient for interfacial saturation. The compatibilising action of poly(styrene-b-1,2-butadiene) in heterogeneous polystyrene/1,2-polybutadiene blends was reported by Koberstein and coworkers.[22] Interfacial tension reduced with copolymer addition up to CMC and thereafter levelled off at higher concentration. Beyond CMC, further addition of the copolymer leads to micelle formation.

Willis and Favis[23] reported that about 5% of the ionomer is sufficient for polyolefin/polyamide blend system for interfacial saturation. Fayt, Jerome and Teyssie[24,25] found equilibration of domain size by the addition of 0.5–1.0% by weight of the compatibiliser. The recent studies of Thomas and Prud'homme[26] and Oommen *et al.*[27] also report on the interfacial saturation by the addition of copolymers in PS/PMMA and NR/PMMA systems, respectively. The theoretical predictions of Noolandi and Hong[28-30] indicated that micellar aggregation of the

copolymer takes place at the interface of the blend beyond a critical concentration of the copolymer, i.e., CMC.

Almost all the experimental and theoretical studies related to the compatibilisation of heterogeneous blends including the present work suggest that there is a critical concentration of the compatibiliser (CMC) required to saturate the blend interface beyond which addition of the compatibiliser leads to undesirable micelle formation which very often reduces the total performance of the blend system.

One can also explain the interfacial saturation point using Taylor's equation.[13]

$$W_e = \frac{\eta m \, dn \, \dot{\gamma}}{2 \, \dot{\gamma}_{12}} \qquad (4.1)$$

where W_e is the critical Weber number, ηm is the viscosity of the matrix, γ is the shear rate, γ_{12} is the interfacial tension and dn is the number average diameter of the dispersed phase. On the addition of the compatibiliser, the interfacial tension decreases and there is a consequent particle break down (deformation). However, at a particular compatibiliser loading there is a balance of interfacial tension and particle deformation. Thus, there is a critical value of W_e below which no particle deformation occurs and at this point, the compatibiliser occupies the maximum interfacial area. Therefore there is a maximum quantity of the compatibiliser required to saturate the blend interface and beyond this level further addition of compatibiliser will not reduce the particle size any more. Willis and Favis[31] and White[32] have also reported similar observations.

The compatibiliser added to a heterogeneous blend locates at the interface and reduces the interfacial energy. Based on thermodynamics, Noolandi and Hong[28-30] developed an expression for interfacial tension reduction. According to which the interfacial tension reduction $\Delta\gamma$ in a heterogeneous binary blend A/B upon the addition of a copolymer A-b-B is given by

$$\Delta\gamma = d\,\phi_c\left[\left(\frac{1}{2}\chi + \frac{1}{Z_c}\right) - \frac{1}{Z_c}\exp^{Z_c\chi/2}\right] \tag{4.2}$$

where 'd' is the width at half height of copolymer profile reduced by Kuhn statistical segment length, χ is the Flory-Huggins interaction parameter between the A and B segments of the AB copolymer, Z_c is the degree of polymerisation of the copolymer. According to this theory, the interfacial tension reduction, $\Delta\gamma$ is proportional to copolymer volume fraction ϕ_c until the system reaches CMC. However beyond CMC $\Delta\gamma$ levels off with ϕ_c. Although this expression was developed for block copolymers, our recent investigations indicated that this theory can be applied to graft copolymers as well.[27] Since interfacial tension reduction is directly proportional to particle size reduction Δd, it can be shown that

$$\Delta d = Kd\phi_c\left[\left(\frac{1}{2}\chi + \frac{1}{Z_c}\right) - \frac{1}{Z_c}\exp\left(Z_c\frac{\chi}{2}\right)\right] \tag{4.3}$$

where K is the proportionality constant. The plot of experimental values of Δd vs. ϕ_c is given in Figure 4.12. It can be seen that at low concentration of the compatibiliser Δd decreases linearly with copolymer loading and at high concentration Δd levels off as indicated by Noolandi and Hong.
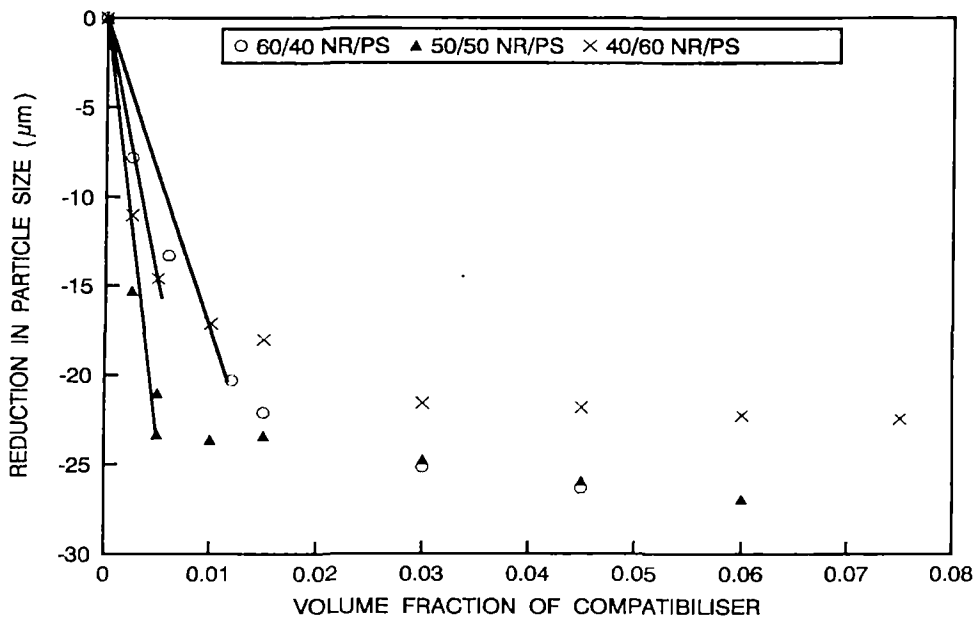
Figure 4.12.   Effect of volume fraction of compatibiliser on particle size reduction.

Valuable information can be obtained by calculating the area, Σ, occupied by the copolymer molecule at the blend interface. Let us consider a binary blend that contains a volume fraction ϕ_A of polymer A as spherical domains of radius r in a matrix B. The total interfacial area per unit volume of the original blend is equal to $3\phi_A/r$. If each copolymer molecule occupies an area, Σ, at the interface, the mass m of the copolymer required to saturate unit volume of the blend is given by the equation[5]

$$\Sigma = \frac{3 \phi_A M}{m r N} \tag{4.4}$$

where M is the molecular weight of the copolymer and N is the Avogadro's number. In the present study since CMC is the interfacial saturation point, it would be reasonable to consider CMC as the value of m.

Radius of the dispersed domain at CMC, CMC values, (m values) and Σ are given in Table 4.3. The CMC values are estimated from Figure 4.12 by the intersection of the straight line drawn at the low concentration and the levelling of line at high concentration.

It can be noticed that the area occupied by the compatibiliser molecule at the interface (Σ) increases as the molecular weight of the homopolymer decreases (Figure 4.13). The Σ values also depend on the mode of addition of the compatibiliser to the blend system. In the two step process where the copolymer is preblended with the dispersed phase, the Σ value is 49.10 nm^2. This indicates that the interaction of the copolymer and homopolymer is higher in two step process as compared to that in one step process ($\Sigma = 30.98$ nm^2). Greater interaction increases the interfacial area and reduces the interfacial tension. Casting solvent can also influence the Σ values. In the case of CCl_4, Σ value is higher (82.55 nm^2) compared to that of chloroform (30.98 nm^2). In a good solvent like CCl_4, interaction between the copolymer and homopolymer is higher than that in chloroform and hence the interfacial area occupied by the copolymer is higher.

Similarly, the copolymer molecular weight is also a controlling parameter. When the copolymer molecular weight is reduced, the interaction between the copolymer and homopolymer is reduced. Hence the area (Σ = 15.46 nm^2) occupied by the copolymer (mol. wt 1.009 x 10^5) at the interface is lower than that (Σ = 30.98 nm^2) of the copolymer (mol. wt 3.95 x 10^5) which is having a higher molecular weight.
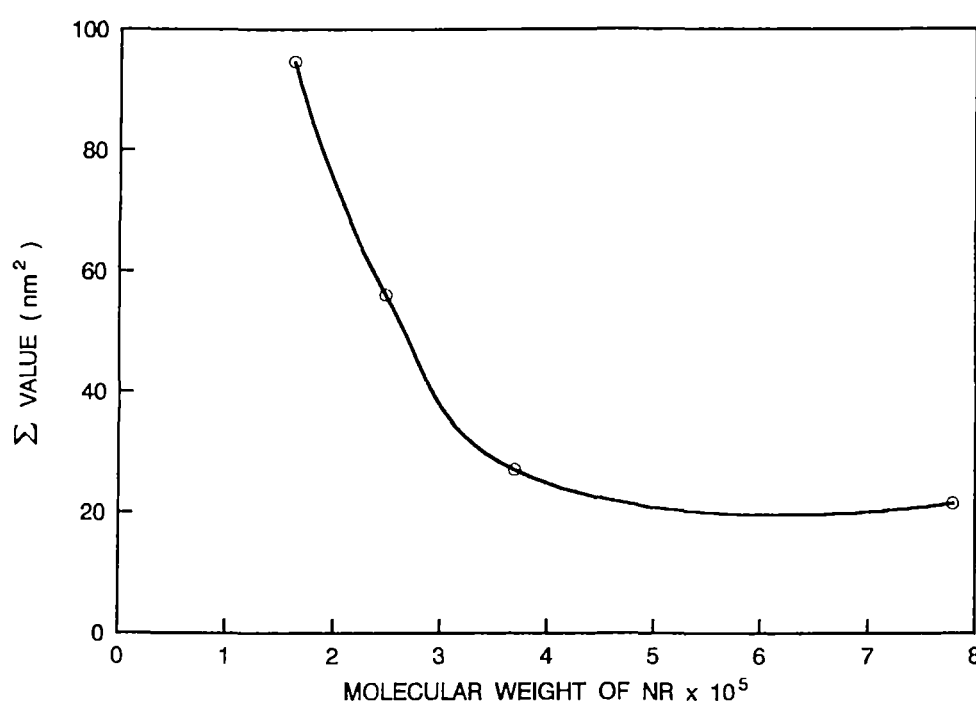
Figure 4.13. Effect of homopolymer (NR) molecular weight on Σ values.

One can also comment on the conformation of the copolymer based on Σ values. Figure 4.14 represents the different physical models representing the conformation of the copolymer at the blend interface. First model (Figure 4.14a) indicates a conformation in which the graft copolymer extends into the corresponding homopolymer phases. In such a case the occupied area at the interface is the cross sectional area of the extended copolymer molecule. This is approximately equal to 0.6 nm^2. In the second model (Figure 4.14b) copolymer lies flat at the interface and here the occupied area is the lateral surface area of the entire copolymer molecule. This value is approximately 106 nm^2 which was

calculated from the experimental values of the root mean square radius of gyration of PS block of the copolymer as reported in literature.[26]

(a)

(b)

(c)
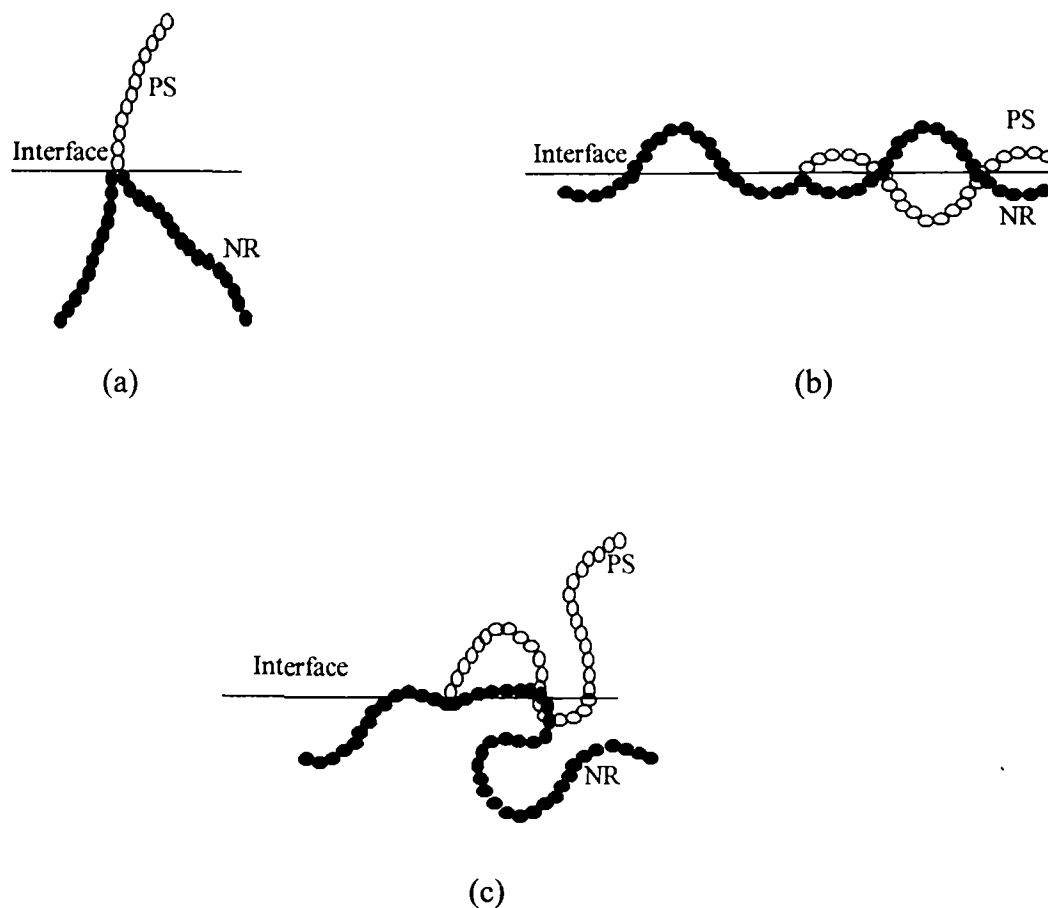
Figure 4.14. Physical models representing the conformation of copolymer at the interface: (a) fully extended model, (b) completely flat, and (c) intermediate suggested model.

A comparison of the experimental and calculated values of interfacial area gives the actual conformation of the copolymer at the blend interface. The experimental values of Σ as obtained from equation (4.4), lie between 15.46-100.90 nm^2 (Table 4.3). This is intermediate to those of the two models (0.6 and 106 nm^2) reported in the literature. This suggests that the actual conformation

of the copolymer at the blend interface is neither fully extended nor completely flat. The actual position can be represented by Figure 4.14c, in which a portion of the copolymer remains at the interface and rest penetrates into the corresponding homopolymer phases. This model is in agreement with the model suggested by Oommen and Thomas.[27] However, by controlling the physical parameters such as molecular weight of the homo and copolymer, mode of preparation of the blends, casting solvents, etc., one can dictate the area occupied by the copolymer at the interface. For example, as the molecular weight of the copolymer increases or the molecular weight of the homopolymer decreases, the area occupied by the copolymer at the interface increases (Table 4.3). For example, copolymer G1 occupies an area 30.98 nm^2, which is much higher than that by G2 which occupies an area of 15.46 nm^2.

It is also important to consider the fact that as the molecular weight of the copolymer increases, macromolecular interactions such as chain entanglement hinder the complete penetration of each segment into the corresponding homopolymer phases. This suggests that the copolymer cannot penetrate completely into the homopolymer phases and therefore, it is expected that part of the copolymer may be staying at the interface. This could lead to an increase in interfacial thickness and would be maximum in the case of copolymers having the highest molecular weight. According to Wu[12] interfacial tension (γ_{12}) and interfacial thickness (L) are related by the following equation.

$$\gamma_{12} = 7.6/L^{0.86} \qquad (4.5)$$

This indicates that the superior compatibilising action of the high molecular weight graft copolymer is associated with the larger increase in interfacial thickness and consequent reduction in interfacial tension. Russel et al.[33] have also reported that addition of copolymer increases the interfacial thickness of PS/PMMA blends. In this study the interfacial thickness was measured by neutron reflectivity. The thickness of the interface was increased by 50% by the addition of the copolymer. Recently, experimental results of Anastasiadis et al.[34] also support the conformation

represented in Figure 4.14c. They have reported on the compatibilising action of poly(styrene-b-1,2-butadiene) in PS/1,2-poly(butadiene) and found that about 24% of the contour length of the copolymer chain is located at the blend interface and the rest penetrates into the corresponding homopolymer phases.

4.3 References

1.   G. E. Molau, *Block Polymers* (Ed., S. L. Aggarwal), Plenum Press, New York, p. 79, 1970.

2.   G. E. Molau and H. Keskkula, *Appl. Polym. Symp.*, **7**, 35 (1968).

3.   G. E. Molau, *J. Polym. Sci.*, **A3**, 1267 (1965).

4.   G. E. Molau, *J. Polym. Sci.*, **A3**, 4235 (1965).

5.   D. R. Paul, *Polymer Blends* (Eds., D. R. Paul and S. Newman), Academic Press, New York, Ch. 12,1978.

6.   G. Riess, J. Kohler, C. Tournut and Banderet, *Makromol. Chem.*, **58**, 101 (1967).

7.   T. Inoue, T. Soen, T. Hashimoto and H. Kawai, *Macromolecules*, **3**, 87 (1970).

8.   M. Moritani, T. Inoue, M. Motegi and H. Kawai, *Macromolecules*, **3**, 433 (1970).

9.   H. T. Patterson, K. H. Hu, T. H. Grindstaff, *J. Polym. Sci. Part C*, **34**, 31 (1971).

10.   P. Gailard, Sauter M. Ossenbach and G. Riess, *Makromol. Chem. Rapid Commun.*, **1**, 771 (1980).

11.   M. Goni, Gurru Chaga, J. Sam Roman, M. Valero and G. M. Guzman, *Polymer*, **34**, 512 (1993).

12.   S. Wu, *Polym. Eng. Sci.*, **27**, 335 (1987).

13.   J. M. Willis and B. D. Favis, *Polym. Eng. Sci.*, **28**, 1416 (1988).

14.   L. Djakovic, P. Dokie, P. Radivojevic, I. Sefer and V. Sovilij, *Colloid Polym. Sci.*, **265**, 993 (1987).

15.   S. Cimmino, F. Coppola, L. D'Orazio, R. Greco, G. Maglio, M. Malinconico, C. Mancarella, E. Martusceli and G. Ragosta, *Polymer*, **27**, 1874 (1986).

16.   A. Robard and D. A. Patterson, *Macromolecules*, **10**, 1021, (1977).

17.   R. Asaletha, M. G. Kumaran and S. Thomas, *Polym. Plast. Technol. Eng.*, **34(4)**, 633 (1995).

18.   D. R. Paul, C. E. Locke and C. E. Vinson, *Polym. Eng. Sci.*, **13**, 202 (1973).

19.   F. Ide and A. Hasegawa, *J. Appl. Polym. Sci.*, **18**, 963 (1974).

20.   C. E. Locke and D. R. Paul, *J. Appl. Polym. Sci.*, **13**, 2791 (1973).

21.   C. Qin, J. Yin and B. Huang, *Polymer*, **31**, 663 (1990).

22.   S. H. Anastasiadis, I. Gancarz and J. T. Koberstein, *Macromolecules*, **21**, 2980 (1988).

23.   J. M. Willis and B. D. Favis, *Polym. Eng. Sci.*, **30**, 1073 (1990).

24.   R. Fayt, R. Jerome and Ph. Teyssie, *J. Polym. Sci. Polym. Phys. Edn.*, **20**, 2209 (1982).

25.   R. Fayt, R. Jerome and Ph. Teyssie, *Polym. Eng. Sci.*, **27**, 328 (1987).

26.   S. Thomas and R. E. Prud'homme, *Polymer*, **33**, 4260 (1992).

27.   Z. Oommen, M. R. G. Nair and S. Thomas, *Polym. Eng. Sci.*, **36**, 151 (1996).

28.   J. Noolandi, *Polym. Eng. Sci.*, **24**, 70 (1984).

29.   J. Noolandi and K. M. Hong, *Macromolecules*, **15**, 482 (1982).

30.   J. Noolandi and K. M. Hong, *Macromolecules*, **17**, 1531 (1984).

31.   B. D. Favis and J. M. Willis, *J. Polym Sci. Part B, Polym. Phys.* **28**, 2259 (1990).

32.   J. L. White, *Polym. Eng. Sci.*, **13**, 46 (1973).

33.   T. P. Russel, A. Menelle, W. A. Hamilton, G. S. Smith, S. K. Satija and C. F. Majkrzak, *Macromolecules*, **24**, 5721 (1991).

34.   S. H. Anastasiadis, I. Gancarz and J. T. Koberstein, *Macromolecules*, **22**, 1449 (1989).

Chapter 5

Melt Rheological Properties

Melt flow studies of polymers are highly important in order to optimise the processing conditions and in designing processing equipments like injection moulding machines, extruders and dies required for various products. During the processing, the polymer or the blend may undergo various changes. Better knowledge of the processing faults and defects will help to introduce the suitable remedies to minimise the processing problems.[1] Melt rheological studies give us valuable viscosity data which will be helpful in optimising the processing conditions.

A large number of studies have been reported on the melt flow behaviour of elastomers and their blends. Danesi and Porter[2] reported on the rheology-morphology relationships in the blends of isotactic polypropylene and ethylene propylene rubbers. Akhtar et al.[3] reported on the rheological behaviour and extrudate morphology of thermoplastic elastomers from natural rubber and high density polyethylene. Gupta et al.[4] have studied the various rheological aspects of blends of polypropylene with ABS and LDPE and correlated it with the morphology studies. Melt rheological behaviour of natural rubber/ethylene vinyl acetate copolymer blends was studied by Koshy et al.[5]

In the present chapter, the rheological behaviour of NR/PS blends with and without the addition of the compatibiliser (NR-g-PS) has been presented. Melt flow characteristics such as shear viscosity, flow behaviour index, melt elasticity, extrudate deformation, etc. have been studied with special reference to the effect of blend ratio, compatibiliser loading, temperature, shear-stress, blending techniques, etc. The elastic parameters like principal normal stress difference and recoverable elastic shear strain were calculated and the extrudate morphology has been studied. The role of the compatibiliser on the morphology and processing behaviour of the blends was analysed. Finally, master curves were generated using the modified viscosity and shear rate functions that contain melt flow index as a parameter.

5.1   Results and discussion

5.1.1   Effect of shear stress and blend ratio on viscosity

Figure 5.1 shows the flow curves of NR/PS blends at 160°C made by solution casting technique using chloroform as the casting solvent. As shear stress increases, the viscosity in all cases decreases, indicating the pseudoplastic flow behaviour.
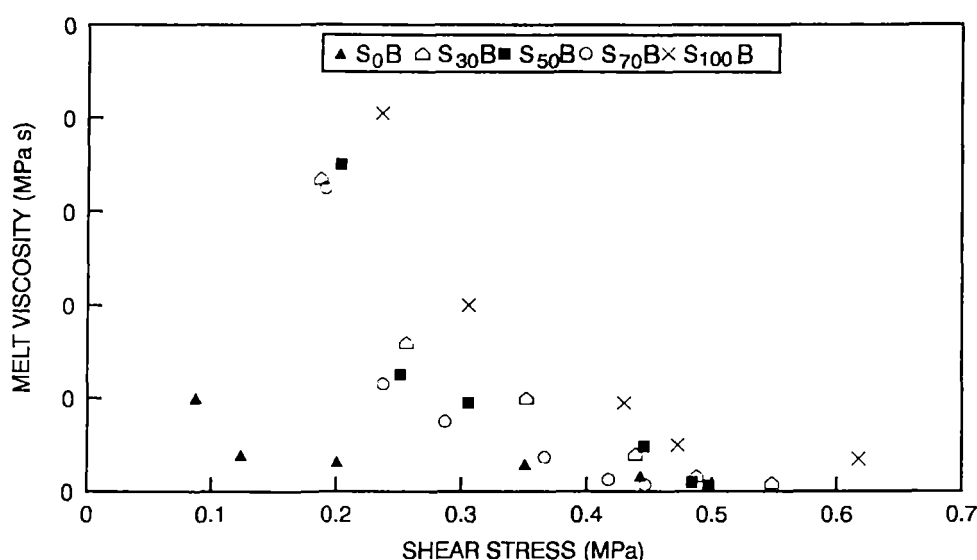
Figure 5.1.   Variation of shear viscosity with shear stress of solution (CHCl₃) cast blends.

At zero shear, the molecules are randomly oriented and highly entangled and therefore exhibit high viscosity. Under the application of shearing force, the polymer chains orient resulting in the reduction of shear viscosity and exhibit pseudoplastic behaviour. The reduction in viscosity at higher shear rate is also due to the decrease in particle size of the dispersed domains (Figure 5.2). During extrusion, the dispersed particles under the action of shearing force undergo deformation which leads to the breakdown of the particles. Figures 5.2a and 5.2b correspond to non-compatibilised 50/50 NR/PS blends and Figures 5.2c and 5.2d are the corresponding compatibilised blends at two different shear rates 57.6 and 115.2 sec⁻¹, respectively. It was found that the average domain diameter was reduced from 0.781 to 0.361 μm as the shear rate increases from 57.6 to 115.2 sec⁻¹.

The domain size diameter was found to be decreased upon compatibilisation. The domain distribution of the blends at different shear rates are given in Figure 5.3. It is seen that as the shear rate increases the distribution curves narrow down indicating a fine distribution of the particles. According to Munstedt[6] at low shear rate, the dispersed plastic phase (plastic phase is the minor one) will form a wall structure around the rubber matrix. As the stress exceeds a minimum called yield stress, this wall structure breaks down and viscosity decreases. It is also possible that in the case of blends, the decrease in viscosity with increase of shear stress is due to the shearing away of the dispersed phase of the blend.

(a)

(b)

(c)

(d)
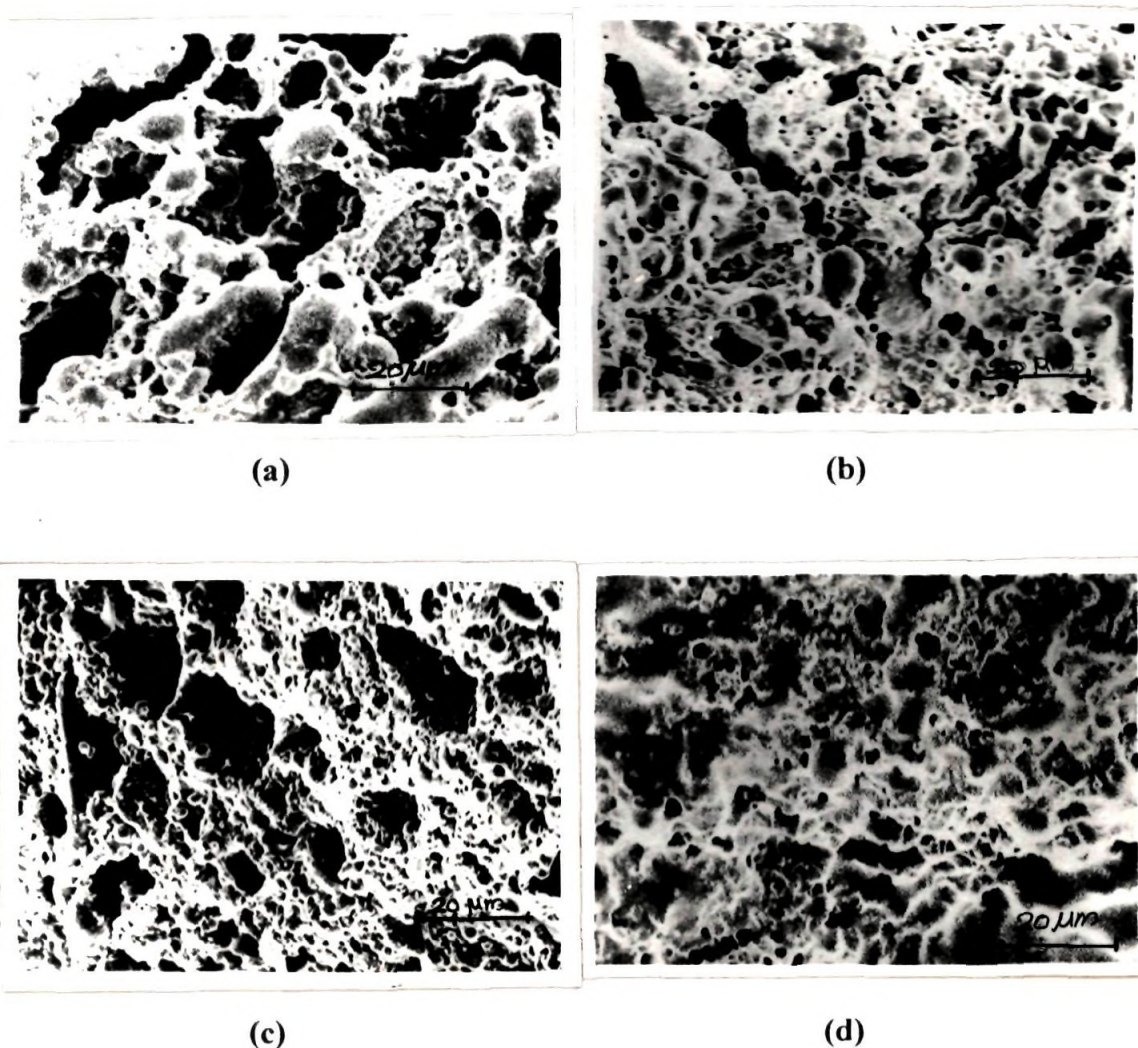
Figure 5.2. SEM photographs of extrudate of 50/50 NR/PS blends (solution casted) at different shear rates: (a) non-compatibilised at 57.6 sec^{-1}, (b) non-compatibilised at 115.2 sec^{-1}, (c) compatibilised at 57.6 sec^{-1}, and (d) compatibilised at 115.2 sec^{-1}).
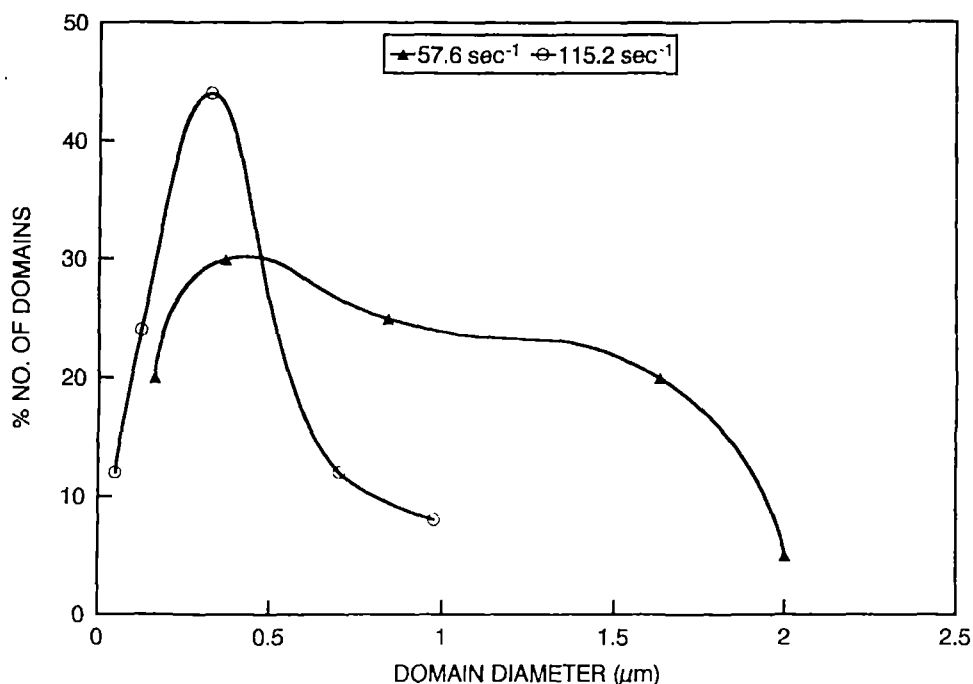
Figure 5.3. Distribution curves for 50/50 NR/PS (melt mixed) blends in the absence of copolymer at different shear rates.

The flow curves (Figure 5.1) indicate that the viscosity of the blends are non-additive functions of the viscosities of component polymers. This can be well understood from the variation of viscosity with the weight percentage of NR at low and high shear rates as presented in Figure 5.4. NR always exhibits a slightly higher viscosity than PS. At lower shear rate, the viscosities of the blends are higher than those of the homopolymers. At the low shear region (≤ 60 sec^{-1}) up to 50 wt % NR, the viscosity of the blends increases and thereafter it decreases. In the region up to 50 wt % NR, there may arise strong interactions among the dispersed NR domains. This leads to the clustering of the domains. As a consequence a reversible structural build-up arises which leads to an increase in viscosity. This sort of positive deviation in the viscosity of polymer blends has been reported by

many researchers.[7-11] An increase in viscosity at a lower shear region in the case of elastomer—modified thermoplastics has been reported by Lee.[9] Ablasova[10] reported that the viscosity of polyoxymethylene (POM)/copolyamide (CPA) goes through a maximum at low shear stress level and through a minimum at high shear stress level. On the other hand in the present system, a negative deviation is observed at the high shear rate region (Figure 5.4).
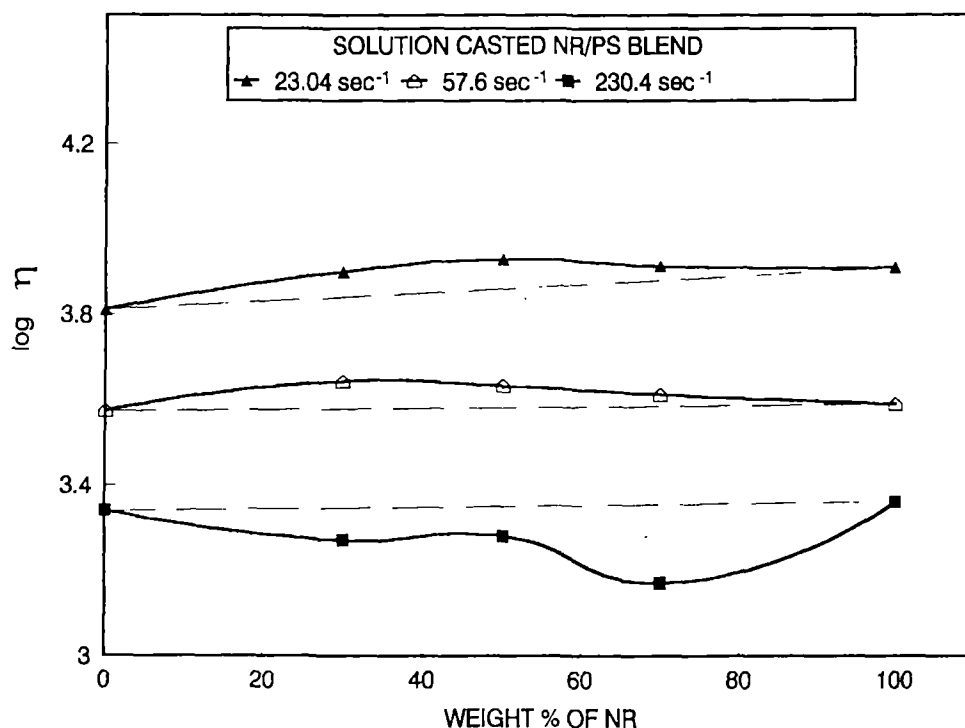
Figure 5.4. Variation of shear viscosity with weight per cent of NR of solution casted blends at different shear rates.

This is because, at high shear rate, the structure breaks down and the interaction between the dispersed NR domains are reduced. A speculative model is given in Figure 5.5 to illustrate the structural build-up and breakdown at low and

high shear rate region. The negative deviation in viscosity of polymer blends at high shear rate has been reported by many researchers. Varughese et al.[12] reported similar reduction in viscosity in ENR/PVC blends. Khanna and Congdon[13] also reported a reduction in viscosity in the case of PVC/hytrel blends.

AT LOW SHEAR REGION: AT HIGH SHEAR REGION:
STRUCTURAL BUILD UP   STRUCTURAL BREAK UP
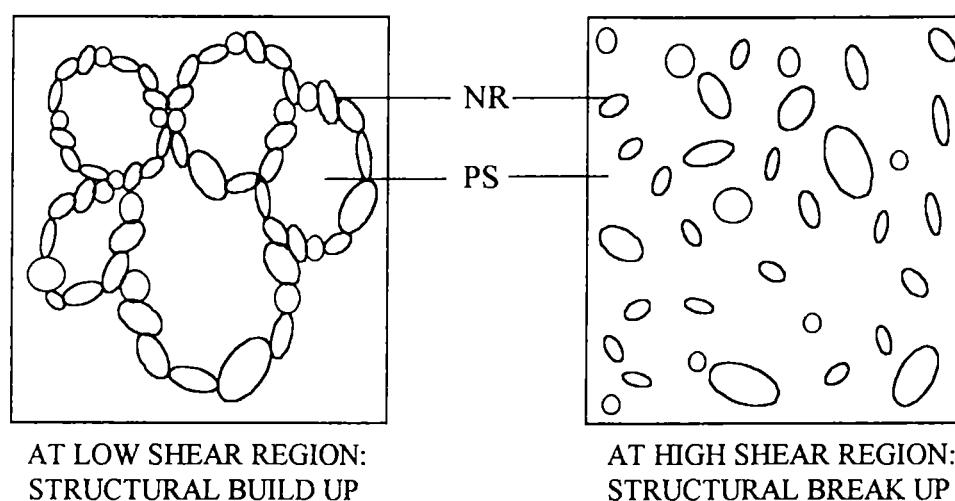
Figure 5.5.   Speculative model illustrating the structural build up and breakdown at low and high shear rate region.

Since NR/PS blend is an incompatible system, it exhibits a two phase morphology. In the absence of the compatibiliser the interface is highly mobile, weak and unstable. This is schematically represented in Figure 5.6a. Therefore, application of shear force leads to high extent of inter layer slip between the phases and this results in a viscosity which is lower than those of the component polymers.

(a) IN THE ABSENCE OF COPOLYMER:

INTERFACE

PS

NR

- NARROW AND MOBILE INTERFACE
- BIG DISPERSED PHASE SIZE
- HIGH INTERFACIAL TENSION
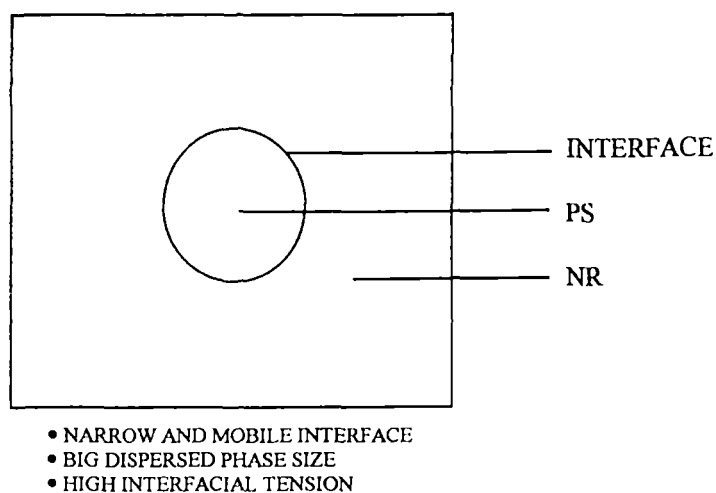
(b) IN THE PRESENCE OF COPOLYMER—BELOW CMC:

COPOLYMER

PS
COPOLYMER

NR

- BROAD AND LESS MOBILE INTERFACE
- SMALL DISPERSED PHASE SIZE
- SMALLER INTERFACIAL TENSION
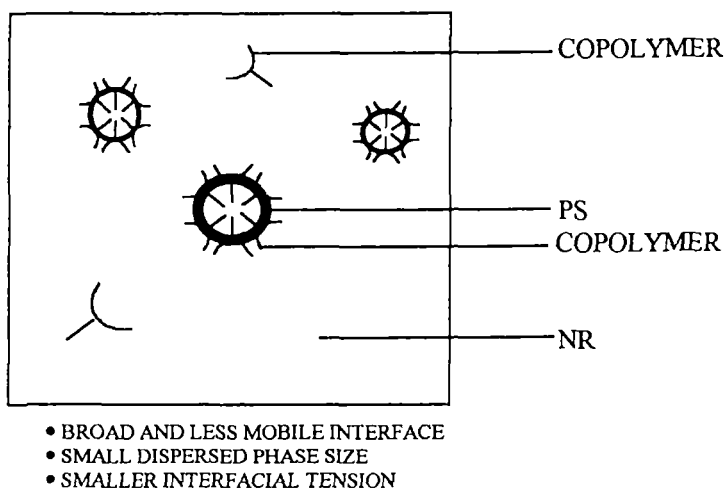
(c) IN THE PRESENCE OF COPOLYMER—ABOVE CMC:

PS

MICELLES

COPOLYMER
NR

- BROAD AND LESS MOBILE INTERFACE
- SMALL DISPERSED PHASE SIZE
- SMALLER INTERFACIAL TENSION
- MICELLER AGGREGATION
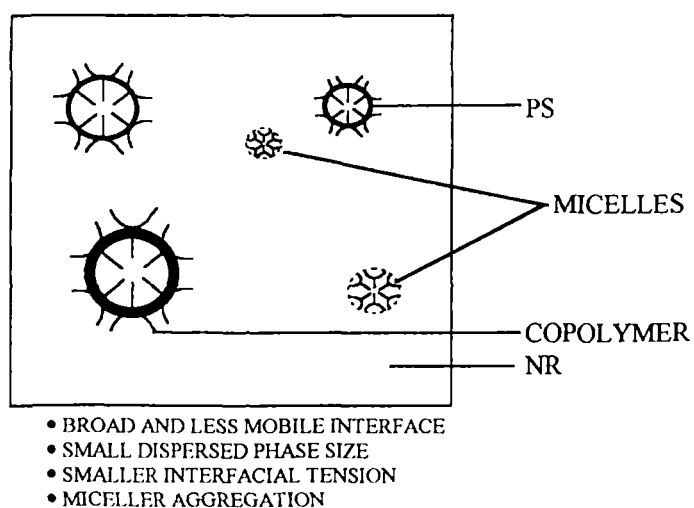
Figure 5.6.   Schematic representation of the morphology in the absence and presence of a compatibiliser (copolymer).

The experimental viscosity data can be compared with the theoretical values calculated by various models. According to Utracki and Sammut[14] positive or negative deviation of the experimentally measured viscosity from the theoretically calculated (log additivity rule) one is an indication of strong or weak interactions between the phases of the blend. According to this,

$$\ln (\eta_{app}) \text{ blend} = \sum_i W_i \ln (\eta_{app})i \qquad (5.1)$$

where W_i is the weight fraction of the ith component of the blend. Immiscible blends are expected to show negative deviation and miscible blends a positive deviation.

Different models can be used to calculate the viscosity of the blend. According to series model

Model 1 $\eta_{mix} = \eta_1\phi_1 + \eta_2\phi_2$ \qquad (5.2)

where η_1 and η_2 are the viscosities of component 1 and 2, and ϕ_1 and ϕ_2 are their volume fractions.

According to Hashin's upper and lower limit models, viscosity can be calculated as follows.

Model 2 $\eta_{mix} = \eta_2 + \dfrac{\phi_1}{1/(\eta_1 - \eta_2) + \phi_2/(2\eta_2)}$ \qquad (5.3)

Model 3 $\eta_{mix} = \eta_1 + \dfrac{\phi_2}{1/(\eta_2 - \eta_1) + \phi_1/(2\eta_1)}$ \qquad (5.4)

A free volume state model developed by Mashelkar and coworkers[15] can be applied in our system too. Accordingly,

Model 4 $\ln \eta_{mix} = \dfrac{\phi_1(\alpha - 1 - \gamma\phi_2)\ln\eta_1 + \alpha\phi_2(\alpha - 1 + \gamma\phi_1)\ln\eta_2}{\phi_1(\alpha - 1 - \gamma\phi_2) + \alpha\phi_2(\alpha - 1 + \gamma\phi_1)}$ \qquad (5.5)

where η_1, η_2, ϕ_1 and ϕ_2 are the viscosities and volume fractions of the components 1 and 2, respectively. The α and γ values were calculated as explained in the literature.[15] The experimentally observed values at a shear rate of 23.04 and

230.4 sec^{-1} are found to be in between that calculated by different models as shown in Figures 5.7 and 5.8, respectively. At 23.04 sec^{-1}, except at 50 wt % NR, the experimental values are close to Model IV. At 50 wt % NR, the experimental value is close to Model III. At 230.4 sec^{-1}, the experimental values are close to Model IV up to 40 wt % NR. At 50 wt % NR, it is close to Model I and above that it shows deviation from the different models.
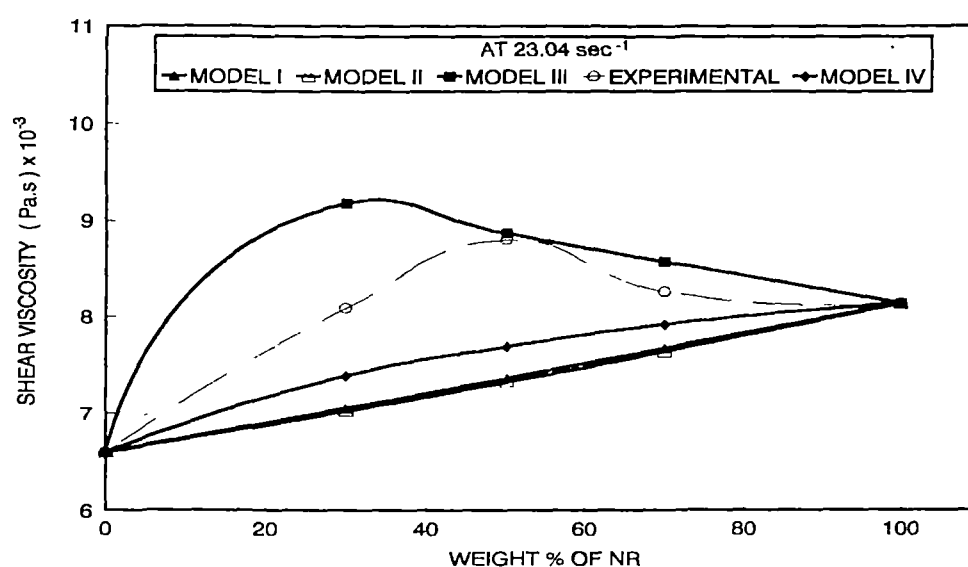
Figure 5.7.   Comparison of experimental shear viscosity with theoretical predictions at a shear rate of 23.04 sec⁻¹.
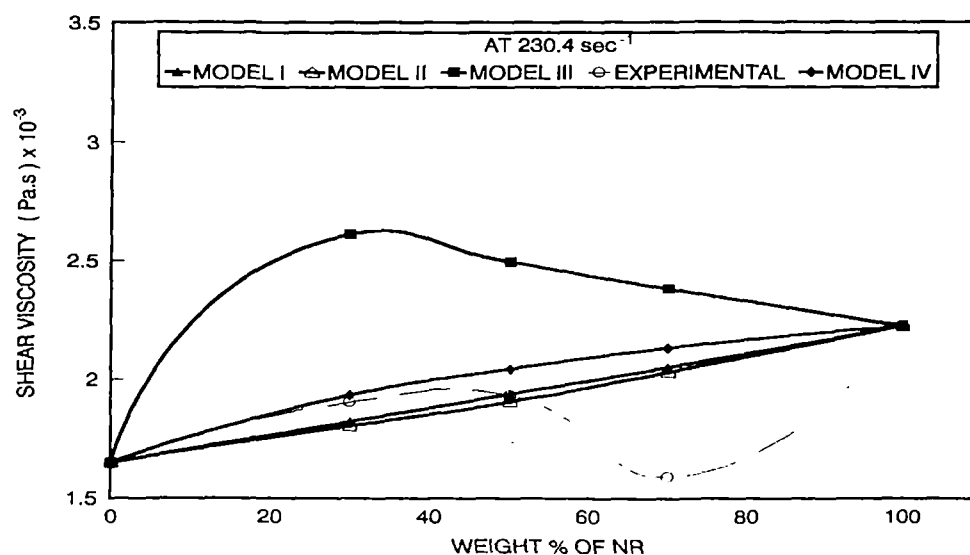
Figure 5.8.   Comparison of experimental shear viscosity with theoretical predictions at a shear rate of 230.04 sec⁻¹.

5.1.2 Effect of processing techniques and blend ratio on viscosity

. Blends of NR and PS can be prepared either by solution casting technique using chloroform as the casting solvent or by the melt mixing process in a Brabender plasticorder. The viscosity values are very much influenced by the method of preparation.

Effect of blend ratio and blending technique on shear viscosity can be understood from Figures 5.1 and 5.9. Solution casted blends show a higher shear viscosity than melt mixed samples (Table 5.1). This is further presented in Figures 5.4 and 5.10. As in solution casted blends, the melt mixed samples also show shear rate dependent positive and negative deviation in viscosity.
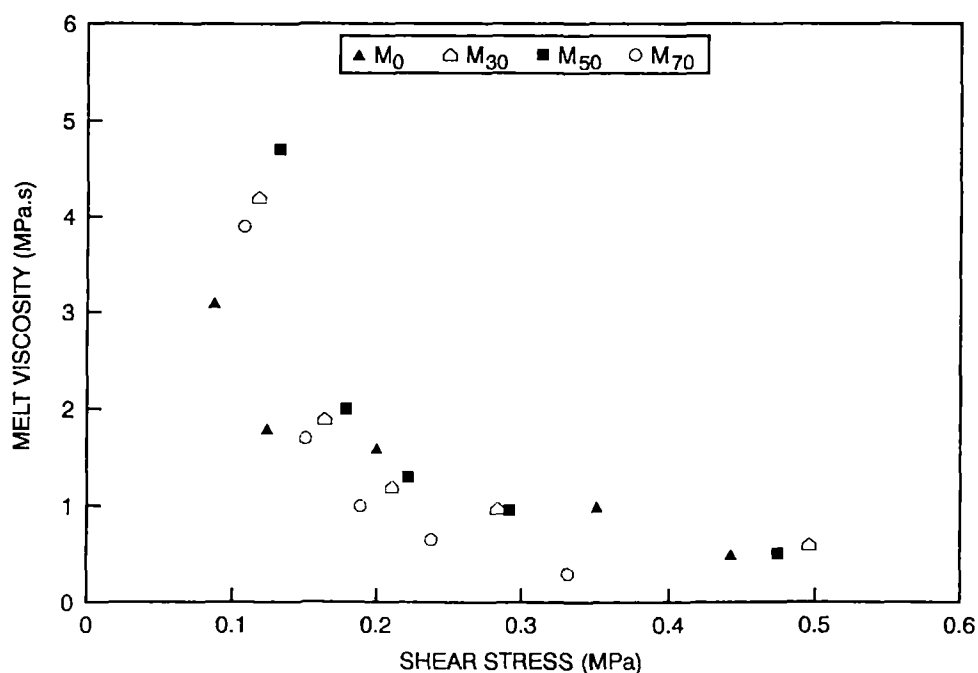
Figure 5.9.   Variation of shear viscosity with shear stress of different melt mixed blends.
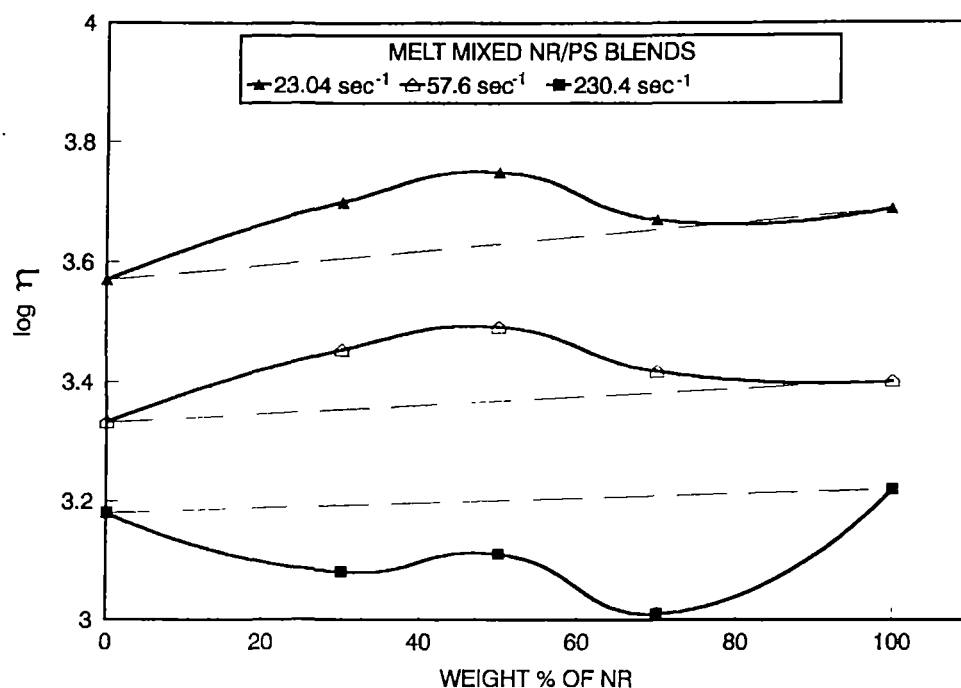
Figure 5.10. Variation of shear viscosity with weight per cent of NR of melt mixed blends at different shear rates.

Table 5.1. Shear viscosity of melt and solution casted samples.

Wt % of NR	Sample	Shear viscosity (Pa.s)			
		23.04 sec^{-1}	57.60 sec^{-1}	230.40 sec^{-1}	576 sec^{-1}
30	Melt	5.11×10^3	2.83×10^3	1.23×10^3	8.46×10^2
	Solution	8.08×10^3	4.44×10^3	1.90×10^3	8.61×10^2
50	Melt	5.74×10^3	3.09×10^3	1.29×10^3	8.23×10^2
	Solution	8.79×10^3	4.36×10^3	1.93×10^3	8.40×10^2
70	Melt	4.68×10^3	2.60×10^3	1.03×10^3	5.75×10^2
	Solution	8.25×10^3	4.12×10^3	1.59×10^3	7.24×10^2

Both in melt mixed and solution casted systems, the viscosity decreases with increase of shear stress indicating pseudoplastic behaviour. As compared to solution casted blends, in melt mixed ones degradation of NR and PS due to high temperature and shear is possible. It is well known that both natural rubber and

polystyrene undergo degradation under the application of high temperature and shear. The molecular weight values for NR and PS before and after the melt mixing process indicate that the component polymers have undergone considerable degradation during the melt mixing process. Before and after mixing, the values for $\overline{M}_n$ for NR were 7.79×10^5 and 4.70×10^5, respectively and those for PS were 3.51×10^5 and 2.08×10^5, respectively. This indicates extensive degradation of the material during melt mixing.

5.1.3 Effect of compatibiliser loading on viscosity and extrudate morphology

The effect of compatibiliser loading on the shear viscosity at three different shear rates is given in Figure 5.11. As the compatibiliser loading increases, the shear viscosity increases, followed by a decrease at higher loading. The MFI measurements also showed a similar trend as can be seen in the coming section. The increase in viscosity upon the addition of the compatibiliser indicates the higher interfacial interaction between the components at the interface.
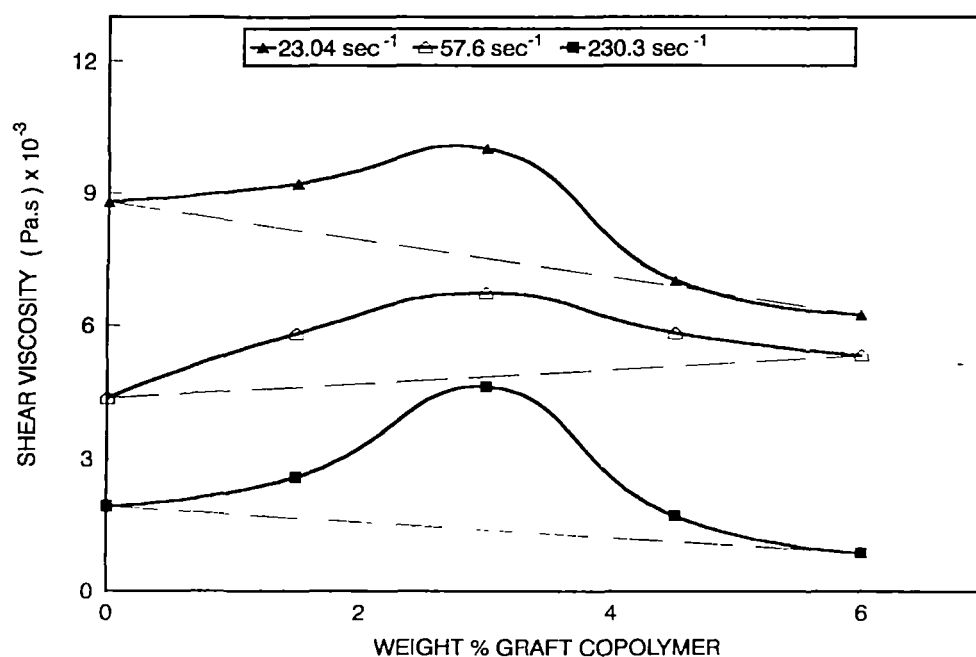
Figure 5.11. Variation of shear viscosity with percentage graft copolymer (50/50 NR/PS) solution casted blends.

In fact the compatibiliser decreases the interfacial tension and the interaction between NR and PS is greatly enhanced. The graft copolymer locates at the blend interface and thereby holds the two phases together. The localisation of the compatibiliser at the interface makes the interface less mobile, more broad and stable. This has been schematically shown in Figure 5.6. Willis and Favis[16] reported an increase of viscosity upon the addition of a compatibiliser in immiscible binary blends. In the case of incompatible blend, due to the presence of a sharp interface and poor interaction between the homopolymer phases there occurs high extent of inter layer slippage between the phases. Upon the addition of the graft copolymer interfacial interaction between the phases increases and there will be less slippage at the interface. Upon the addition of 3% graft copolymer viscosity increases and thereafter it decreases at higher graft loading (Figure 5.11). This is due to the fact that in the absence of the copolymer, NR/PS blend is highly incompatible and the interface adhesion is very poor. The graft copolymer addition decreases the interfacial tension and this leads to a reduction in the dispersed phase size and an increase in interfacial adhesion. In addition to the increase in interfacial adhesion, the presence of the graft copolymer at the blend interface broadens the interface region through penetration of the copolymer chains into the adjacent phases which stabilises the blend morphology against coalescence. Graft copolymer addition increases the interfacial adhesion as evidenced by a decrease in the interfacial energy. The interfacial tension in NR/PS blend has been calculated using the following equation.[17]

$$\frac{G\,\eta_m a_n}{v} = \left(\frac{4\eta_d}{\eta_m}\right)^{0.84} \tag{5.6}$$

where G is the shear rate, v is the interfacial tension, η_m and η_d are the viscosities of the continuous and dispersed phases, respectively, and a_n is the average size of the dispersed phase domains. It can be seen that the interfacial tension decreases with the increase of copolymer loading (Figure 5.12).
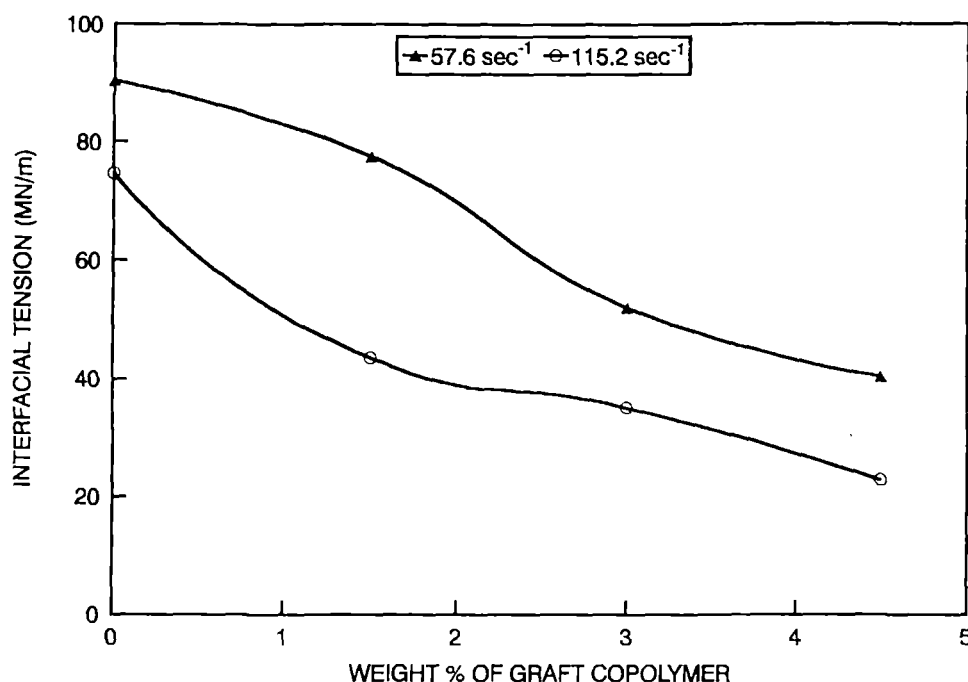
Figure 5.12. Calculated interfacial tension as a function of graft loading.

From Figure 5.11 it can be seen that at high graft copolymer loading viscosity of the system decreases. This is due to the fact that by the incorporation of 3% of copolymer, the interface is fully saturated. The system reaches the so-called critical micelle concentration (CMC), the attainment of CMC has been addressed by several authors experimentally and theoretically.[18,19] Further addition of the copolymer creates micelle formation in the continuous phase. This is schematically shown in Figure 5.6c. The large number of micelles in the continuous phase has a plasticising effect on the flow behaviour of the blends. This leads to a decrease in viscosity.

The SEM photographs of the extrudate cross section of 50/50 NR/PS blends are given in Figure 5.13 at 23.04 sec^{-1}. Large dispersed domains are seen in 50/50 NR/PS blends in the absence of copolymer (Figure 5.13a). Upon the addition of the graft copolymer the domain size decreases (Figures 5.13b and 13c).

(a) (b)

(c)
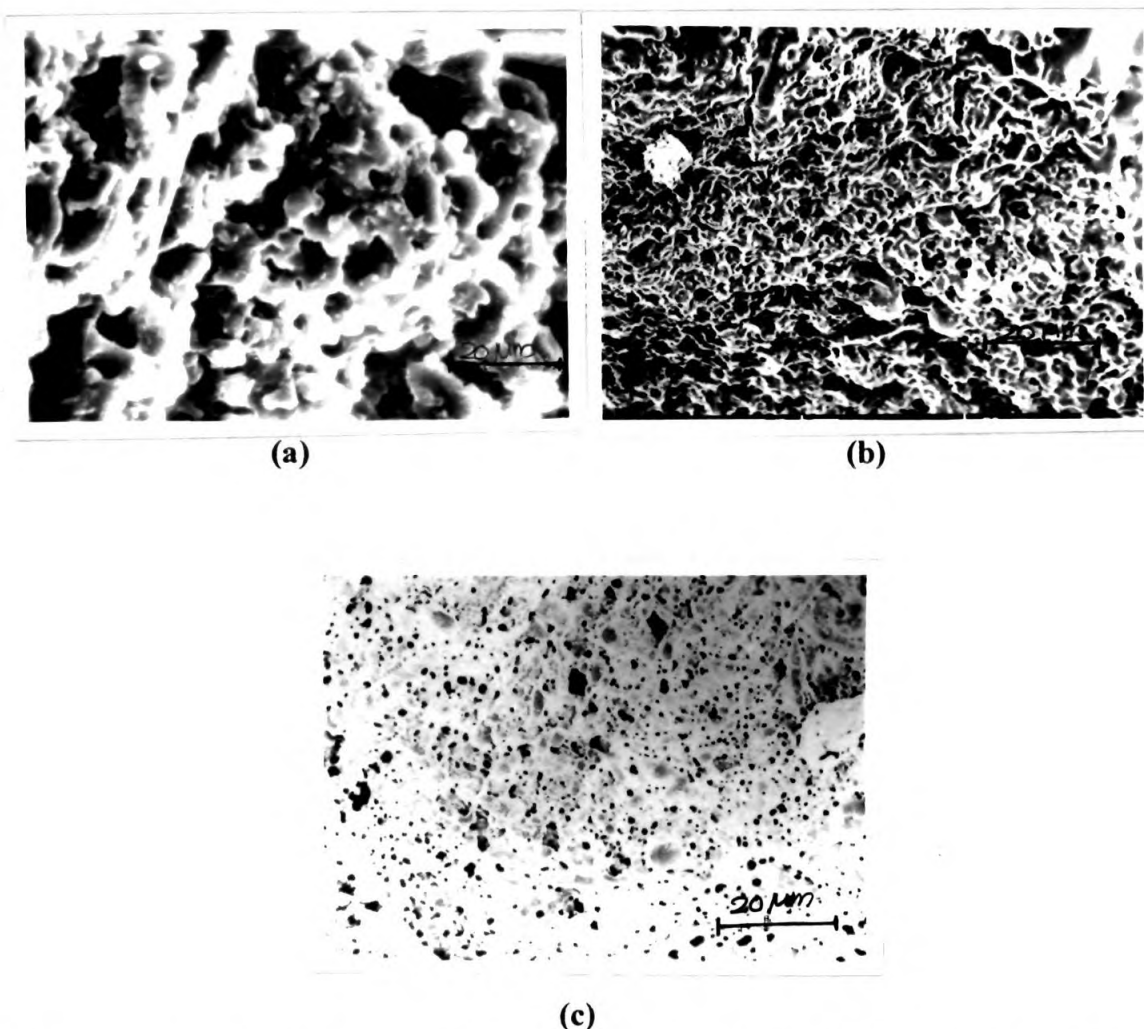
Figure 5.13.   SEM photographs of extrudate of solution casted 50/50 NR/PS blends: (a) 0%, (b) 1.5% and (c) 3% graft copolymer.

The number average domain diameter was measured and plotted the same against percentage graft copolymer added (Figure 5.14).   It is done by taking the diameters of about 200 domains.   It can be seen that there is a sharp decrease in diameter upon the addition of the compatibiliser followed by a levelling off at higher loading. The interparticle distance of 50/50 NR/PS blends also reduces by the addition of the compatibiliser followed by levelling off at higher loading (Figure 5.15).   From these observations, we can calculate the optimum amount of compatibiliser required to saturate unit volume of the blend interface (called CMC-critical micelle concentration).   The CMC value has been estimated by the intersection of the straight lines obtained at low concentration and levelling of line

at higher concentration (Figure 5.14) and is found to be 1.8% for 50/50 NR/PS blend system. Beyond CMC further addition of the compatibiliser makes no difference in the domain size and hence interfacial tension. The shear viscosity of the 50/50 blend is also plotted in Figure 5.14 as a function of copolymer loading. Up to 3% graft loading the shear viscosity increases, reaches a maximum and then it decreases.
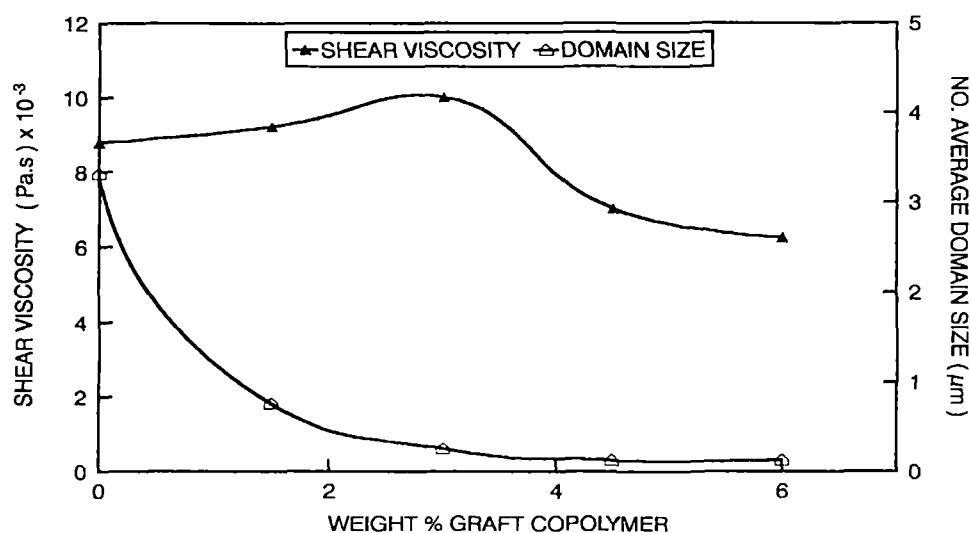
Figure 5.14. Variation of number average domain diameter and shear viscosity at 23.04 sec⁻¹ as a function of graft copolymer concentration (50/50 NR/PS solution casted blends).
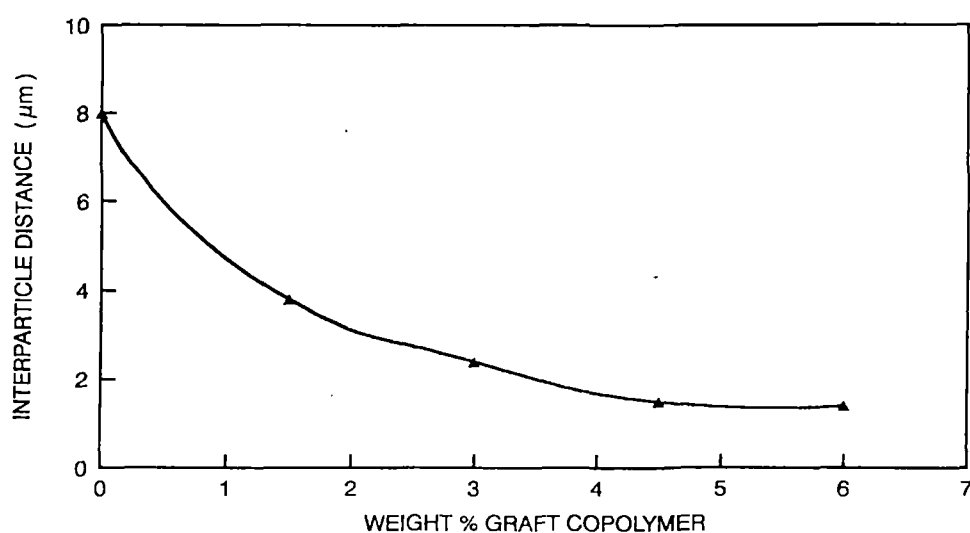
Figure 5.15. Variation of interparticle distance as function of graft copolymer concentration (50/50 NR/PS solution casted blends).

5.1.4 Effect of temperature and shear stress on viscosity

The variation of shear viscosity with temperature of 50/50 NR/PS blends is given in Figure 5.16. It is clear that as the temperature increases from 150-160°C, the viscosity decreases, both in melt mixed and solution casted samples and thereafter increases. Effect of temperature on shear viscosity of compatibilised 50/50 NR/PS blends (solution casted graft loading 4.5%) is also given in Figure 5.16. In this case, both shear viscosity and shear stress decrease first and then increase at high temperature. This is because as the temperature increases the initial fall in viscosity is due to the degradation of the material. Thereafter it increases because the material may undergo crosslinking at high temperature. In order to understand the influence of temperature on viscosity, Arrhenius plots at a constant shear rate were drawn (Figure 5.17). In the Arrhenius plots, log η is plotted versus 1/T. In the Arrhenius equation, η is related to the absolute temperature (T) by the following equation.

$$\eta = A e^{-E/RT} \qquad (5.7)$$

where A is a constant characteristic of the polymer, E is the activation energy and R is the universal gas constant. The Arrhenius plots of the samples at two different shear rates (23.04 sec^{-1} and 230.45 sec^{-1}) are given in Figure 5.17. The activation energies of blends calculated from the slopes of these plots are given in Table 5.2. The activation energy of a material provides valuable information on the sensitivity of the material towards the change in temperature. The higher the activation energy the more temperature sensitive the material will be. Activation energy of solution mixed sample is higher than melt mixed sample. By the addition of the compatibiliser, activation energy decreases. This means that the blends become less temperature sensitive in presence of the compatibiliser. Such information is highly useful in selecting the temperature for processing during the product manufacture.
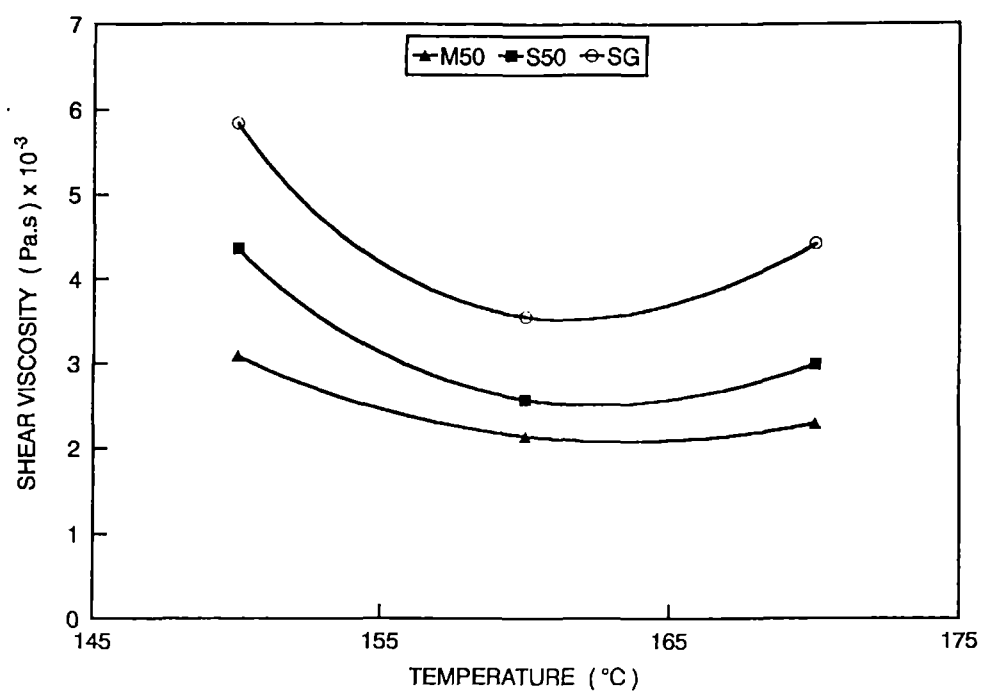
Figure 5.16. Effect of temperature on shear viscosity of different blends (50/50 NR/PS blends).
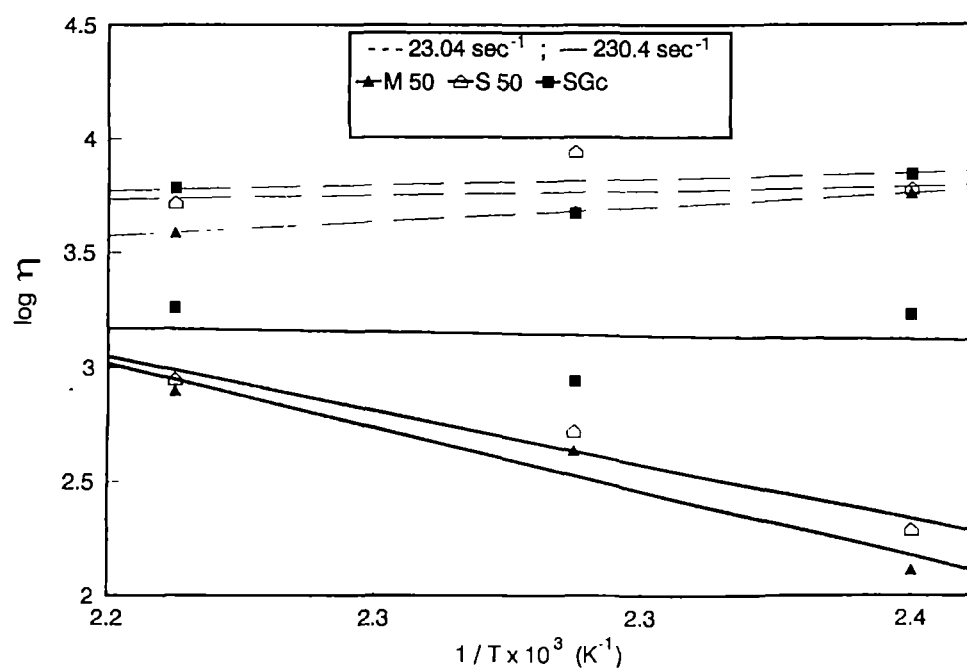
Figure 5.17. Arrhenius plots for different NR/PS blends

Table 5.2. Activation energy of blends.

Sample	Activation energy (cal/mole)
M_{50}	2242.2
S_{50}	4567.4
SG_c	3093.5

5.1.5 Flow behaviour index (n')

The effects of temperature and blend ratio on the flow behaviour indices of the samples were studied in detail. The extent of pseudoplasticity or non-Newtonian behaviour of the materials can be understood from n' values. Pseudoplastic materials are characterised by n' below 1.

Flow behaviour index values of NR/PS blends both melt mixed and solution casted systems are given in Table 5.3. All the mixes are non-Newtonian pseudoplastic fluids characterised by n' below 1. The flow behaviour index of PS is greater than that of NR both in melt and solution casted samples. In both melt and solution casted blends, as the amount of polystyrene decreases, the value of n' decreases. Melt mixed samples show a high value of n' compared to solution casted ones at 150°C and this is because during melt mixing degradation may occur to the samples. This indicates a low pseudoplastic nature of the melt mixed blend as compared to solution casted one. The effect of temperature on n' of 50/50 NR/PS blend is given in Table 5.4. Here also, melt mixed samples show high value for n' compared to solution casted ones and as the temperature increases, the value of n' decreases in both cases. Hence it is concluded that the pseudoplasticity of NR/PS blends increases with increase in temperature and increase in weight percentage of NR. A similar trend of decreasing values of n' with increase in temperature has been reported elsewhere.[20,21] The effect of compatibiliser loading and temperature on the n' value of NR/PS blends are given in Tables 5.5 and 5.6, respectively. Here

also, in all the cases value of n' is below 1 indicating a non-Newtonian pseudoplastic nature. As the compatibiliser loading increases n' value increases. This suggests that the system becomes less pseudoplastic as compatibiliser loading increases. The effect of temperature on n' is the same as that of non-compatibilised NR/PS blends.

Table 5.3. n' at 150°C.

Sample	n'
M_0	0.4078
M_{30}	0.3682
M_{50}	0.3238
M_{70}	0.3060
M_{100}	0.2998
S_0	0.3171
S_{30}	0.2949
S_{50}	0.2866
S_{70}	0.2333
S_{100}	0.2019

Table 5.4. n' of 50/50 blend.

Temperature (°C)	Melt	Solution
150	0.3238	0.2866
160	0.2926	0.2387
170	0.2614	0.1908

Table 5.5.   n' of compatibilised system (50/50) at 150°C.

Wt % of compatibiliser	n'
0	0.2866
1.5	0.2942
3	0.3174
4.5	0.3743

Table 5.6.   n' of 50/50 NR/PS + 4.5% graft.

Sample temperature (°C)	n'
150	0.3743
160	0.3731
170	0.2754

5.1.6   Extrudate deformation studies

Figures 5.18 and 5.19 are the optical photographs of the extrudates which show the extrudate deformation of the blends with and without the compatibiliser respectively at two different shear rates.   Solution casted blends show high distortion compared to melt mixed samples both at low and high shear rate regions. Most of the extrudates have smooth surfaces at low shear rates. At high shear rates, the extrudate surface exhibits different degree of distortion. At high shear rate the surface is not as smooth as in the case of low shear rates. These extrudates have rough surfaces and have non-uniform diameter. This is associated with the melt fracture which occurs at high shear forces where the shear stress exceeds the strength of the melt.[1] The presence of the compatibiliser reduces the extrudate

deformation because it makes blend rigid and hence exhibits a low degree of distortion.
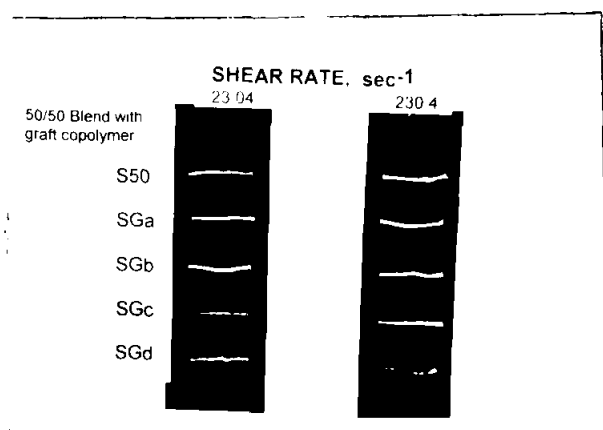
Figure 5.18.   Extrudate deformation at different shear rates as a function of compatibiliser loading (50/50 NR/PS solution casted blends).
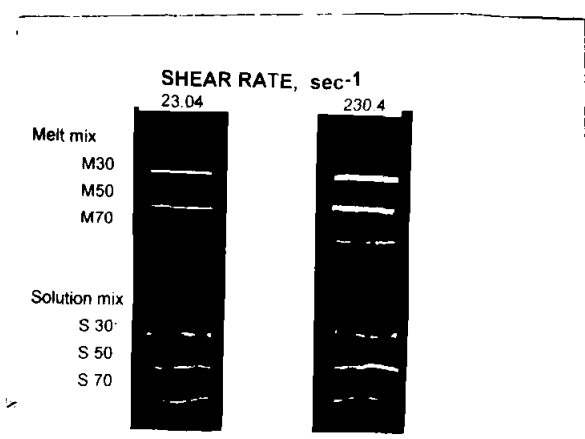
Figure 5.19.   Extrudate deformation at different shear rates as a function of blend composition (50/50 NR/PS melt mixed and solution casted blends).

5.1.7 Melt elasticity

The important parameters which characterise the elasticity of polymer melts are die swell (d_e/d_c), principal normal stress difference ($\tau_{11}-\tau_{22}$), recoverable elastic shear strain (S_R) and the elastic shear modulus (G).

Die swell ratio (d_e/d_c) is the ratio of the extrudate diameter (d_e) to the diameter of the capillary (d_c). The principal normal stress difference ($\tau_{11}-\tau_{22}$) is calculated from the die swell and shear stress according to Tanner's equation.[22]

$$\tau_{111} - \tau_{22} = 2\tau_w \, [2(d_e/d_c)^6 - 2]^{1/2} \qquad\qquad (5.8)$$

Recoverable elastic shear strain (S_R) is given by

$$S_R = (\tau_{11}-\tau_{22})/2 \, \tau_w \qquad\qquad (5.9)$$

(a) Die swell

Table 5.7 shows the die swell ratio of melt mixed, solution casted and compatibilised NR/PS blends at two shear rates at 150°C. For all the mixes, die swell increases with increase in shear rate. In fact within the capillary the molten polymer under shear will maintain orientation of polymer chains and when it emerges from the die recoiling of chains occurs leading to the phenomenon of die swelling. This phenomenon is due to the relaxation imposed in the capillary and factors like chain breaking, stress relaxation, crosslinking, presence of fillers and plasticisers etc. which control the elastic recovery. The effect of temperature on the die swell value of 50/50 NR/PS blends is given in Table 5.8. Both in melt mixed and solution casted blends (non-compatibilised) die swell increases with increase of temperature, whereas in the compatibilised system die swell decreases with increase of temperature. Comparing solution casted and melt mixed samples, at lower shear rate, solution casted blend shows higher value of d_e/d_c due to the high molecular weight of NR in the blend. But at higher shear rate a reverse trend is obtained because of the molecular breakdown of NR. In both melt mixed and

solution casted blends, as the amount of NR increases the value of d_e/d_c decreases in most cases. The die swell values increase with the addition of compatibiliser (Table 5.7). However, among the compatibilised blends there is no regular trend in the value of d_e/d_c with increasing compatibiliser concentration.

Table 5.7.   Die swell (d_e/d_c) value at 150°C.

Shear rate (sec^{-1})	M_{30}	M_{50}	M_{70}	S_{30}	S_{50}	S_{70}	SG_a	SG_b	SG_c	SG_d
23.04	1.35	1.36	1.30	1.82	1.45	1.56	1.57	1.58	1.55	1.71
230.4	2.31	2.06	1.45	2.24	1.84	1.61	1.87	1.79	1.71	1.89

Table 5.8.   Die swell at shear rate of 2.304×10^1.

Temperature (°C)	M_{50}	S_{50}	SG_c
150	1.36	1.45	1.55
160	1.48	1.52	1.49
170	1.51	1.75	1.43

(b)   Principal normal stress difference $(\tau_{11}\text{-}\tau_{22})$

Table 5.9 shows the value of principal normal stress difference of melt mixed, solution casted and compatibilised blends at 150°C and at a shear rate of 230.4 s^{-1}. Both in melt mixed and solution casted blends, principal normal stress-difference decreases with increase of rubber content. Values are higher for solution casted samples compared to the corresponding melt mixed ones. The incorporation of the compatibiliser decreases the principal normal stress values. In fact, the higher values of normal stress difference indicates greater elastic recovery or high melt elasticity.   Upon the addition of the compatibiliser, the blend becomes less deformable and hence exerts greater resistance to flow i.e., it exhibits higher melt viscosity. The effect of temperature on principal stress difference is given in Table 5.10. The values decrease with the increase of temperature for both melt mixed and

solution casted blends. The compatibilised blends show no regular trend in the value of principal normal stress difference.

Table 5.9. Melt elasticity values at 150°C (shear rate 2.303 x 10^1 sec^{-1}).

Sample	Principal normal stress difference ($\tau_{11}-\tau_{22}$) (N/m^2)	Recoverable shear strain (SR)
M$_{30}$	99.05 x 10^5	17.48
M$_{50}$	73.31 x 10^5	12.31
M$_{70}$	19.38 x 10^5	4.07
S$_{30}$	139.80 x 10^5	15.93
S$_{50}$	78.07 x 10^5	8.76
S$_{70}$	42.24 x 10^5	8.76
SG$_a$	67.26 x 10^5	9.21
SG$_b$	59.57 x 10^5	7.98
SG$_c$	48.33 x 10^5	13.59
SG$_d$	20.65 x 10^5	9.43

Table 5.10. Effect of temperature on melt elasticity.

Sample	Temperature (°C)	Principal normal stress difference ($\tau_{11}-\tau_{22}$) (N/m^2)	Recoverable shear strain (SR)
M$_{50}$	150	73.31 x 10^5	12.31
	160	41.77 x 10^5	9.36
	170	25.28 x 10^5	6.92
S$_{50}$	150	78.07 x 10^5	8.76
	160	47.81 x 10^5	7.71
	170	24.71 x 10^5	6.04
SG$_c$	150	48.33 x 10^5	13.59
	160	22.14 x 10^5	6.95
	170	30.81 x 10^5	7.64

(c)   Recoverable shear strain (S_R)

Recoverable shear strain, a measure of the elastic energy stored in the system is given in Table 5.9. The excess energy stored may be converted to surface free energy which leads to extrudate deformation.[7] The behaviour of S_R is the same as that of principal normal stress difference except that in the case of compatibilised systems. In the case of compatibilised system S_R decreases first, then increases and finally decreases at high graft loading. The effect of temperature is the same as that of principal normal stress differences.

5.1.8   Melt flow index (MFI)

Melt flow index provides valuable information about the flow behaviour of materials. Table 5.11 shows the MFI values of melt mixed, solution casted and compatibilised 50/50 NR/PS blends. MFI experiments were done at 250°C. It is found that MFI values decrease with increase of rubber content both in melt mixed and solution casted samples. Solution casted samples show lower values compared to melt mixed samples. This is because in solution casted samples, viscosity is higher compared to melt mixed samples. As the viscosity increases the MFI value decreases. These results are in agreement with the capillary rheometer data. It is already seen that in the case of compatibilised blends, viscosity increases upon the addition of graft copolymer (up to 3 wt %) and thereafter it decreases. MFI values of compatibilised blends support this trend. MFI values decrease with increase of graft loading up to 3 wt % graft copolymer, then increase with increase in graft loading.

Table 5.11.   Melt flow index (MFI) of blends at 250°C.

Sample	M_{30}	M_{50}	M_{70}	S_{30}	S_{50}	S_{70}	$SG_{(a)}$	$SG_{(b)}$	$SG_{(c)}$
MFI (g/10 min)	2.2086	2.1898	1.7814	1.482	1.376	0.602	0.716	0.651	1.237

Shenoy *et al.*[23] adopted a method to coalesce rheograms of resin grades and the master curve thus plotted can be successfully used for the estimation of rheographs of polymer waste from the knowledge of MFI of the material. Bhagawan *et al.*[24] demonstrated a master curve in the case of 1,2-polybutadiene with different fillers and the rheogram coalesce smoothly into a single curve. Recently Thomas *et al.*[25,26] presented the master curves in which the rheogram coalesced smoothly into a single curve. In Figures 5.20 and 5.21 modified shear viscosity [$\log \eta \text{MFI}/\rho$] is plotted against modified shear rate [$\log \rho v/\text{MFI}$] for compatibilised and non-compatibilised systems respectively. In both cases, the curves coalesce smoothly into a single curve. It is very important to add that simply by knowing the MFI of the sample, rheograms of any system can be constructed using the master curve.
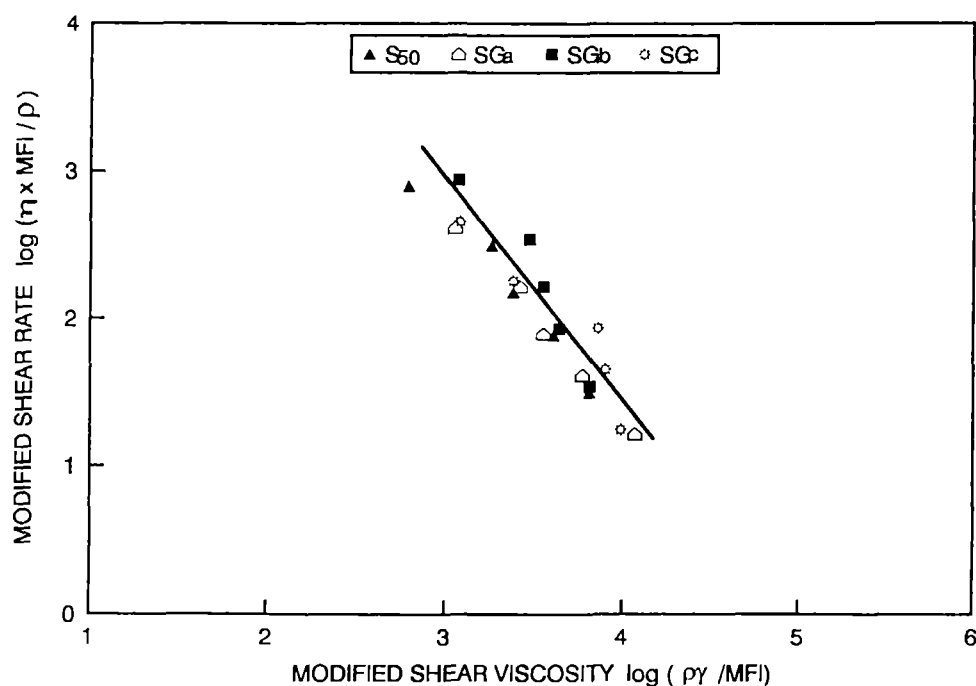
Figure 5.20. Master curve of modified shear viscosity vs. modified shear rate for compatibilised system.
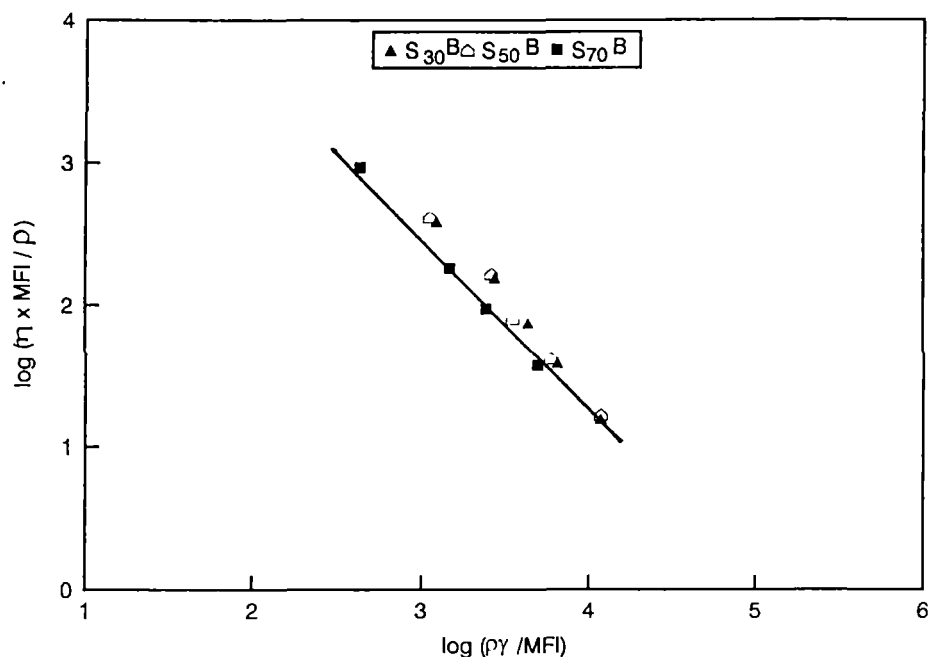
Figure 5.21. Master curve of modified shear viscosity vs. modified shear rate as a function of blend composition.

5.2 References

1. J. A. Brydson, *Flow Properties of Polymer Melts*, George Godwin Ltd., London, 2nd Edition, 1981, Ch. 1.

2. S. Danesi and R. S. Porter, *Polymer*, **19**, 448 (1978).

3. S. Akhtar, B. Kuriakose, P. P. De and S. K. De, *Plast. Rubber Process. Appli.*, **7**, 11 (1987).

4. A. K. Gupta, A. K. Jain and S. N. Maiti, *J. Appl. Polym. Sci.*, **38**, 1699 (1989).

5. A. T. Koshy, B. Kuriakose, S. Thomas, C. K. Premalatha and S. Varghese, *J. Appl. Polym. Sci.*, **49**, 901 (1993).

6. H. Munstedt, *Polym. Eng. Sci.*, **21**, 259 (1981).

7. L. A. Goettler, J. R. Richwine and F. J. Wille, *Rubber Chem. Technol.*, **55**, 1448 (1982).

8. L. A. Utracki, *Polym. Eng. Sci.*, **23**, 602 (1983).

9. T. S. Lee, *Proceedings of the 5th International Conference on Rheology*, University Park Press, Battimore, MD, Vol. 4, 1970, p. 421.

10. T. I. Ablasova, *J. Appl. Polym. Sci.*, **19**, 1781 (1975).

11. T. Fujimura, and K. Iwakura, *Kobunshi Roubunshu*, **31**, 617 (1974).

12. K. T. Varughese, P. P. De and S. K. Sanyal, *J. Vinyl Technol.*, **10(4)**, 166 (1988).

13. S. K. Khanna and W. I. Congdon, *Polym. Eng. Sci.*, **23**, 627 (1983).

14. L. A. Utracki, P. Sammut, *Polym. Eng. Sci.*, **28**, 1405 (1988).

15. R. Sood, M. G. Kulkarni, A. Dutta and R. A. Mashelkar, *Polym. Eng. Sci.*, **28**, 20 (1988).

16. J. M. Willis and B. D. Favis, *Polym. Eng. Sci.*, **28**, 1416 (1988).

17. S. Wu, *Polym. Eng. Sci.*, **27**, 335 (1987).

18. S. H. Anastasiadis, Spiros, I. Gancarz and J. T. Koberstein, *Macromolecules*, **22**, 1449 (1989).

19. J. Noolandi and K. M. Hong, *Macromolecules* **17**, 1531 (1984).

20. S. Thomas, B. Kuriakose, B. R. Gupta and S. K. De, *Plast. Rubber Process Appli.*, **6**, 85 (1986).

21. D. R. Saini and A. V. Shenoy, *J. Macromol. Sci. Phys.*, **B22(3)**, 437 (1983).

22. R. I. Tanner, *J. Polym. Sci.*, **14**, 2067 (1970).

23. A. V. Shenoy, S. Chattopadhyay and V. M. Nadkarni, *Rheol. Acta*, **22**, 90 (1983).

24. S. S. Bhagawan, D. K. Tripathy and S. K. De, *Polym. Eng. Sci.*, **28**, 648 (1988).

25. Z. Oommen, S. Thomas, C. K. Premalatha and B. Kuriakose, *Polymer*, **38**, 5611 (1997).

26. J. George, S. S. Bhagawan and S. Thomas, *J. Thermal Analysis*, **47**, 1121 (1996).

Chapter 6

Stress Relaxation Studies

The development of polymer based products, requires a deep knowledge on the mechanical response of the material as a function of time and temperature. To assess the service life of any product, accelerated tests can be carried out so that the effect of both temperature and time can be obtained within a short time interval. Generally creep and stress relaxation measurements are the widely employed standard test methods for this purpose. The long-term characteristics of the polymer based products can be predicted from the results of stress-relaxation experiments because they represent the basic time dependent response of the material.[1] According to Denby,[2] it is possible to correlate creep, stress relaxation and recovery for both textile polymers and other viscoelastic polymers.

Mijovic[3] studied the effect of physical ageing on the viscoelastic properties of compatible PMMA/SAN polymer blends. It was found that the slope of the stress relaxation curve does not change with change in composition, ageing temperature or ageing time. The stress-relaxation behaviour of polyacetal-thermoplastic polyurethane elastomer blends has been reported by Kumar et al.[4]

Till date no systematic studies have been reported on the stress relaxation behaviour of natural rubber/polystyrene blends although this blend can be used in dynamic applications. In the present chapter, the stress-relaxation behaviour of natural rubber/polystyrene blends with and without the addition of the compatibiliser, i.e., natural rubber-graft-polystyrene has been reported. The relaxation behaviour was also studied with special reference to the effects of strain level, blend ratio and ageing.

6.1 Results and discussion

The results of stress relaxation experiments are presented as linear plots of σ_t/σ_0 vs. log time, where σ_t is the stress at a particular time t and σ_0 is the stress at t = 0.

6.1.1 Effect of strain level

Linear plots of (σ_t/σ_0) vs. log t of 60/40 natural rubber/polystyrene blends at different strain levels (50, 100 and 150%) are given in Figure 6.1. In all the cases, the rate at which the initial strain attained is kept constant. The relaxation patterns of the samples were studied at different strains. There is only marginal variation in the rate of relaxation at all extensions. It is seen that in all cases, the experimental points fall on two intersecting straight lines. Two different straight lines will intersect at a point at which the relaxation mechanism changes from one mode to another. The time corresponding to this point is known as the cross over time. The values of crossover time are 1819, 622 and 2411 sec for samples, C, I and J, respectively. The slopes and intercepts of the two straight lines are given in Table 6.1 which were obtained by the linear regression analysis method. The difference in the values of slopes and intercepts indicate that the mechanism of relaxation operates in two ways; one that operates at shorter time and another that is prominent at the later stages of relaxation. Initial slope (i.e., relaxation rate) is nearly the same for all the 3 strain levels. The slope and location of the second process depend on strain level. The contribution by the earlier process of relaxation has been calculated as reported by Mackenzie and Scanlan[5] by dividing the differences of the two intercepts by the intercept of the first line at t = 1 sec. From Table 6.1 it is seen that as the strain level increases from 50% (sample J) to 150% (sample C) the contribution of the early process increases from 13.1 to 26.9% in the case of non-compatibilised blend and this can be attributed to the high interfacial tension across the phase boundary.
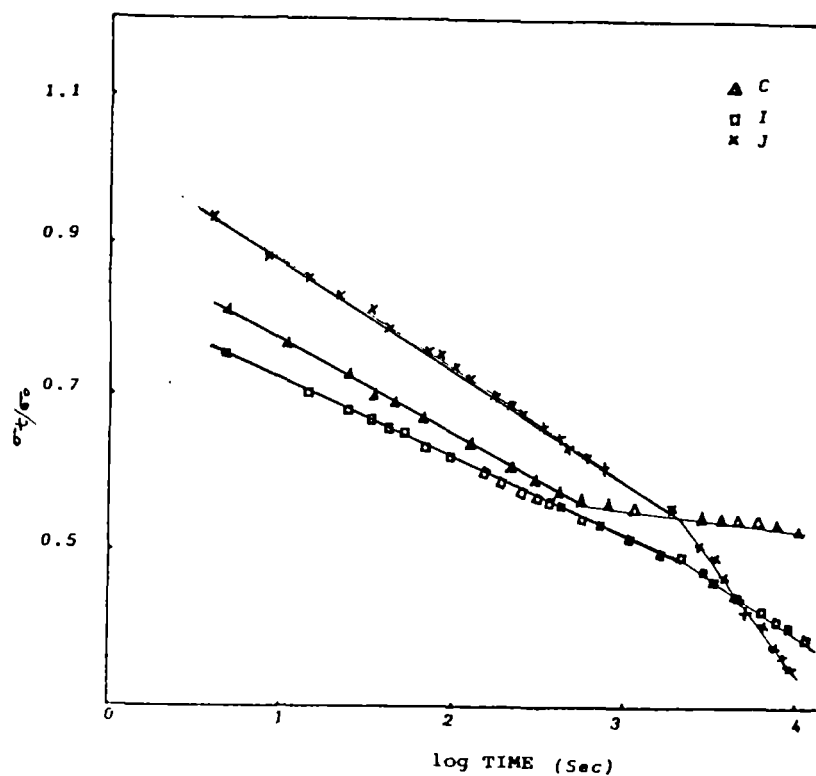
Figure 6.1. Effect of strain level on the stress relaxation pattern of 60/40 NR/PS blend: (C) 150%, (I) 100% and (J) 50%.

Table 6.1. Results of Stress Relaxation Measurements.

Sample	Slope (−ve)			Intercept			Contri-bution to initial mechanism (%)	Cross-over time (s)
	Initial	Inter-mediate	Final	Initial	Inter-mediate	Final		
A	0.0979	-	0.0572	0.9893	-	0.8655	12.5	762
B	0.0978	-	-	0.9937	-	-	-	
C	0.1285	-	0.2253	1.0126	-	1.2858	26.9	1819
D	0.1147	-	0.0367	0.9316	-	0.6789	27.1	1698
E	0.0943	-	0.1035	0.9458	-	0.9650	20.0	2411
F	0.1182	0.8089	0.0989	0.9403	3.1842	0.7043	25.1	1718 3383*
G	0.1191	-	0.0671	0.9412	-	0.8128	42.9	87
H	0.9698	-	9.0641	0.0997	-	0.0569	13.6	171
I	0.1086	-	0.0725	0.9437	-	0.8193	-	622
J	0.1200	-	0.1865	0.9318	-	-	13.1	2411

*Second cross overtime.

The stress relaxation behaviour can be related to the morphology of the blend. In 60/40 NR/PS blends where NR is the continuous matrix and PS is the dispersed phase, the initial stage relaxation is due to the continuous NR matrix which is slow compared to the relaxation due to PS dispersed phase.

6.1.2 Effect of composition

Figure 6.2 shows the stress relaxation curves of different NR/PS blends of varying composition. In the case of 50/50 blend, the experimental points fall on a single straight line, whereas in the other two cases, (i.e., curve A – 40/60 NR/PS and curve C – 60/40 NR/PS blends) the experimental points fall on two intersecting straight lines, indicating that the relaxation process follows two different mechanisms. In the case of 40/60 NR/PS blend, it was shown that NR is the dispersed phase and PS forms the continuous phase. In the case of sample C (60/40 NR/PS blend) the reverse is true and hence the relaxation due to NR increases. From Figure 6.2 it is observed that the behaviour of 50/50 blend is different from the others.
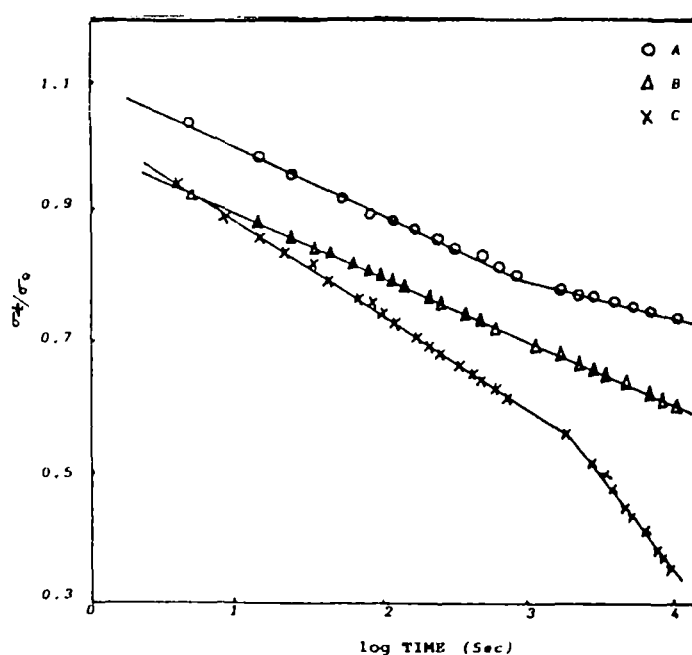
Figure 6.2. Effect of composition on the stress relaxation pattern of different NR/PS blends at a strain level of 150%: (A) 40/60, (B) 50/50 and (C) 60/40 NR/PS blend.

The relative stress decay is found to be a linear function of log T over the time scale studied. This indicates a single relaxation mechanism for the 50/50 blend, unlike 60/40 and 40/60 blends. The difference in behaviour can be understood in terms of the morphology of the blend.

Figure 6.3 shows the morphology of different NR/PS blends varying in composition. Figures 6.3a and 6.3c represent 40/60 and 60/40 NR/PS blends where NR and PS forms the dispersed phase, respectively. In Figure 6.3a, the dispersed rubber domain size is higher compared to the dispersed plastic domains in Figure 6.3c and this is due to the coalescence of the rubber domains (Table 6.2).

(a)

(b)

(c)
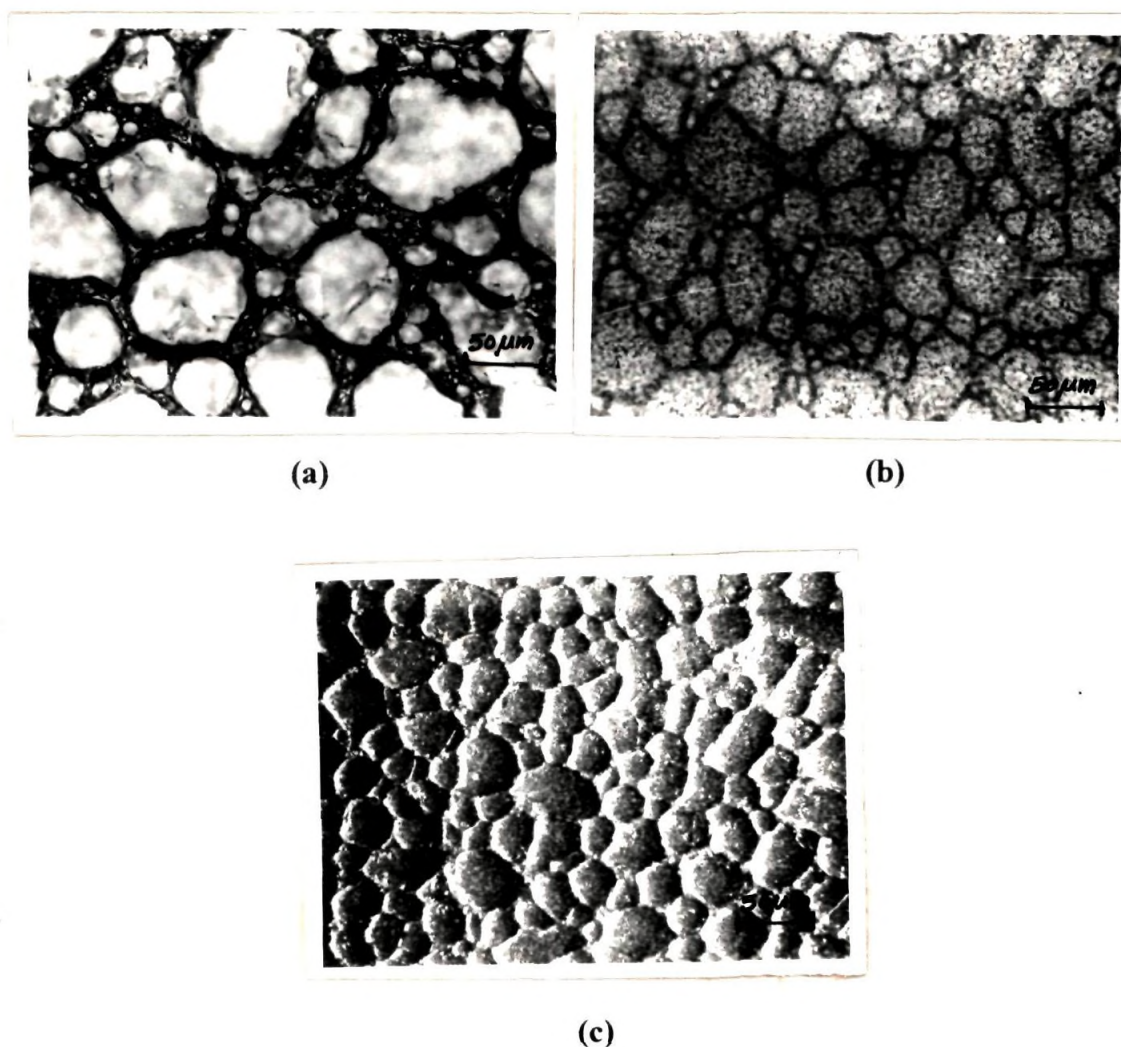
Figure 6.3.   Optical microphotographs of (a) 40/60, (b) 50/50 and (c) 60/40 NR/PS blends.

Due to the low viscosity of PS phase as compared to NR, the coalescence of the NR domains is favoured. For the 50/50 NR/PS blend, there is a tendency for the components to form a co-continuous morphology and this accounts for the single phase relaxation mechanism shown by the 50/50 NR/PS blend (Figure 6.3b). The 50/50 NR/PS blend shows a partial co-continuous morphology, i.e., both dispersed and co-continuous phases exist.

**Table 6.2.** Polydispersity Index (PDI) of Different NR/PS Blends

Samples	Polydispersity index	Average domain diameter (μm)
40/60	1.24	17.14
50/50*	1.14	14.11
60/40	1.09	13.45

*The size has been measured based on the available domains in the semi-co-continuous structure.

The stress relaxation rate can be analysed by measuring the slope and intercept of the relaxation curve. The slope, intercept, crossover time and the contribution to initial mechanism for different NR/PS blends have been calculated as explained earlier and are given in Table 6.1. It is observed from the table that the rate of stress relaxation is highest in 60/40 NR/PS blend. The relaxation rate decreases as the amount of NR decreases from 60/40 to 40/60 NR/PS blends because the overall relaxation process depends more upon the rubber content. This is further supported by the polydispersity index (PDI) values which are given in Table 6.2. The crossover time changes from 762 to 1819 sec as the matrix phase changes from PS to NR. This is due to the difference in the amount of NR which contributes largely to the relaxation process. It is seen from Table 6.1 that the contribution to initial mechanism changes from 12.5 to 26.9% as the continuous phase changes from PS to NR.

6.1.3 Effect of compatibiliser loading

Figure 6.4 shows the stress-relaxation curves of 50/50 NR/PS blends with varying amounts of the compatibiliser i.e., natural rubber-graft-polystyrene copolymer. It is observed that the relaxation pattern of compatibilised blend is different from that of non-compatibilised one. In the case of non-compatibilised blend, the experimental points fall on a single straight line, indicating that the mechanism of relaxation operates by a single mechanism. For the compatibilised blends (Samples D and E) the experimental points fall on two intersecting straight lines. This is due to the fact that the partially co-continuous morphology is transformed into a matrix/dispersed morphology upon compatibilisation. Compared to non-compatibilised blend, the compatibilised blends show an increase in the rate of relaxation because in these two cases, the compatibiliser added will be located at the blend interface and enhances the interaction between the two phases. Coming to sample F i.e., 50/50 NR/PS blend with 4.5% compatibiliser, the graft copolymer form micelles which reduces the blend properties and thereby a different relaxation pattern is observed. A three stage mechanism is shown at higher loading of compatibiliser. The rate of relaxation is higher compared to blends with lower graft loading. In the case of compatibilised blends (Samples D, E and F) the contribution to early process is nearly constant because of enhanced interfacial adhesion between the blend components. The first cross-over time in the case of sample F is less (1718 sec) compared to that of sample E (2411 sec) and is related to the formation of undesirable micelles. The second cross over time in this case is higher (3383 sec) and leads to a third mechanism which is due to the micelle formation.
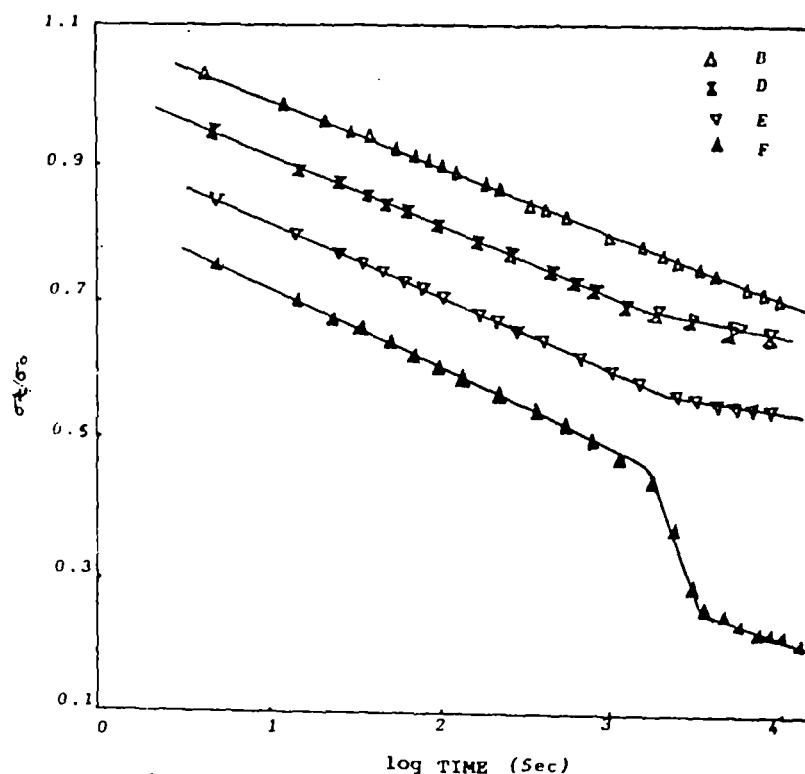
Figure 6.4. Effect of compatibiliser loading on the stress relaxation pattern of 50/50 NR/PS blends: (B) 0%, (D) 1.5%, (E) 3% and (F) 4.5% graft copolymer.

6.1.4 Effect of ageing

In order to study the effect of ageing, the relaxation measurements have been made using samples subjected to ageing at 50 and 70°C for 4 days. The dependence of relative stress on log T is shown in Figure 6.5. In the case of unaged 50/50 NR/PS blends, a single relaxation mechanism operates whereas in the case of aged samples operates in two stages (i.e., G and H). The rates of relaxation for the aged and unaged samples are shown in Table 6.1. In the case of aged samples, the rate of relaxation is high in the initial stage compared to later stages. In the aged samples, the initial increase in relaxation rate is due to the degradation of the rubbery phase on ageing. The later stages of relaxation is due to the plastic phase. The slopes and intercepts of these different stages are given in Table 6.1 and show that ageing produces interesting effects on the stress-relaxation of the blends. It was observed that the variation of slope at different stages of relaxation, is gradual both at 50 and 70°C. The slope value indicates that the rate of

of sample G the cross over time is less (87 sec) compared to sample H (171 sec) and it is due to the fact that the former case the matrix phase will undergo degradation at a faster rate compared to the latter one.
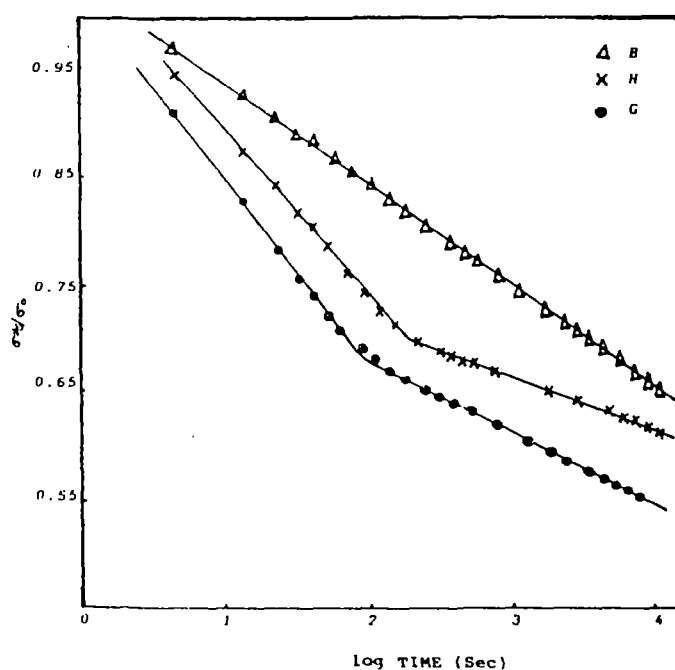
Figure 6.5. Effect of ageing on the stress relaxation pattern of 50/50 NR/PS blends: (B) 30°C, (H) 50°C and (G) 70°C.

6.2 References

1. R. F. Fedors, S. Y. Chung and S. D. Hong, *J. Appl. Polym. Sci.*, **30**, 2551 (1985).

2. E. F. Denby, *J. Text. Inst.*, **65**, 239 (1974).

3. J. Mijovic, S. T. Devine and Taiho, *J. Appl. Polym. Sci.*, **39**, 1133 (1990).

4. G. Kumar, Arindam, N. R. Neelakantan and N. Subramanian, *J. Appl. Polym. Sci.*, **50**, 2209 (1993).

5. C. I. Mackenzie and J. Scanlan, *Polymer*, **25**, 559 (1984).

Chapter 7

Dynamic Mechanical Properties

Miscibility and phase behaviour of polymer blends are of crucial importance in many applications. Dynamic mechanical thermal analysis (DMTA) is a widely accepted method for studying the structure - property relations in polymers. The viscoelastic data can be successfully used to study the miscibility in polymer blends in terms of changes in Tg (glass transition temperature) of the components of the blends. Miscible blends will have a single and sharp glass transition temperature intermediate between those of the individual polymers. In the case of border line miscibility, broadening of the transitions will occur, whereas two separate transitions corresponding to the constituents may occur in the case of completely immiscible blends. Generally the dynamic mechanical properties are expressed in terms of storage modulus, loss modulus, damping factor and these depend on crystallinity, structure and extent of crosslinking The performance of most of the rubber products is related to their dynamic properties which is a very important consideration when rubber compounds are designed for components to be used in dynamic applications.

Several studies have been carried out on the dynamic mechanical properties of polymer blends. Schneider and Wirbser[1] have reported the dynamic mechanical behaviour of miscible poly(vinyl methyl ether)/polystyrene blends. The viscoelastic behaviour of these blends shows peculiarities which are closely related to the observed composition dependence of the glass transition temperatures. Morphology and dynamic mechanical properties of polypropylene/elastomer (EPDM) blends and polypropylene block copolymer have been investigated by Karger-Kocsis and Kiss.[2]

In these blends as the concentration of EPDM increases, the storage modulus (E') of the blends decreases. The dynamic mechanical spectrum shows two separate damping peaks and have a two phase morphology indicating that the blend is an incompatible one. Toy and coworkers[3] have carried out the dynamic mechanical and morphological studies in styrene butadiene styrene (SBS)/low and high molecular weight polybutadiene (PB) blends. It was concluded that the dynamic mechanical relaxation of blends of block copolymers and homopolymers can be attributed to the relaxation behaviour of the individual components in the blend. The effect of diblock copolymers as compatibilisers on the dynamic mechanical properties of polyethylene/polystyrene (PE/PS) blend was reported by Brahimi et al.[4] According to their investigations, the addition of pure and tapered diblock copolymer enhances the phase dispersion and interphase interactions and the addition of excess compatibiliser creates micelles. Santhra et al.[5] have reported the dynamic mechanical properties of LDPE/PDMS. The effect of addition of ethylene-methyl acrylate copolymer as a compatibiliser was studied in detail and found that the Tg values were shifted by the addition of the compatibiliser.

The rubber products generally undergo dynamic stress during service and therefore their behaviour under dynamic loading is highly important. But until now no systematic study has been reported on the dynamic mechanical properties of NR/PS blends. The main objectives of the present study is to investigate the effects of blend ratio, frequency and compatibiliser loading on the dynamic mechanical properties of NR/PS blends. The properties have been evaluated as a function of temperature and frequency. Attempts were made to correlate the dynamic mechanical properties with the morphology of blends. Various theoretical models such as series, parallel, Halpin-Tsai, Coran's, Takayanagi, Kerner and Kunori were used to assess the experimental dynamic mechanical properties.

7.1 Results and discussion

7.1.1 Effect of frequency

The dynamic mechanical properties of NR/PS blends were analysed from -70 to 140°C at different frequencies (0.1, 1, 10, 50 and 100 Hz). The variation of tan δ with temperature (-70 to 30°C) at different frequencies of 50/50 NR/PS blends are given in Figure 7.1. The tan δ values increase with increase of temperature up to the glass transition temperature of NR and thereafter it levels off in the plateau region. As the temperature increases further (from -10°C onwards) it shows an increasing tendency with temperature. At -60°C, 50/50 NR/PS blend at 0.1 Hz shows the maximum value for tan δ and that at 100 Hz shows the minimum value. At -30°C the trend is exactly the reverse and again at 20°C the initial trend is retained. As the frequency increases from 0.1 to 100 Hz, the glass transition peak of NR phase shifts towards the high temperature region. The variation in Tg value of the NR phase with frequency is given in Table 7.1.
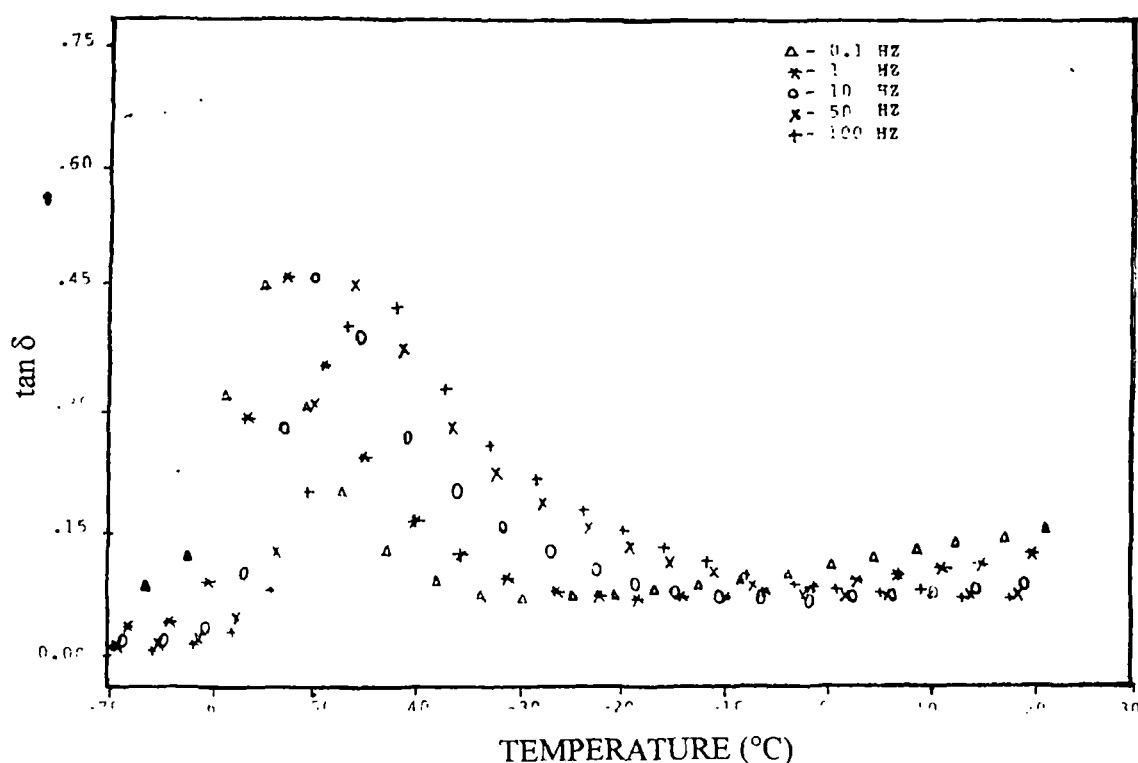

Figure 7.1. Variation of tan δ with temperature at different frequencies for 50/50 NR/PS blends (-70 to 30°C).

Table 7.1. Variation of Tg values (°C) upon graft loading from tan δ curves (50/50 NR/PS blends).

% graft copolymer	Frequency (Hz)									
	Due to NR					Due to PS				
	0.1	1	10	50	100	0.1	1	10	50	100
0	-55	-53	-49	-45	-41	104	110	115	120	122
1.5	-55	-53	-45	-44	-42	104	114	114	117	120
3	-54	-52	-49	-43	-42	104	108	115	118	121
4.5	-53	-51	-46	-42	-40	118	122	124	125	127

The activation energy, E for the glass transition of NR phase of the blends can be calculated from the Arrhenius equation.

$$f = f_0 \exp(-E/RT) \qquad (7.1)$$

where f is the measuring frequency, f_0 is the frequency when T approaches infinity and T is the temperature corresponding to the maximum of the tan δ curve. The Arrhenius plots of 50/50 NR/PS blends in which log frequency is plotted versus the reciprocal of temperature in kelvin scale are given in Figures 7.2 and 7.3 respectively in the low and high temperature region. Activation energies calculated from these plots are given in Table 7.2.

Table 7.2. Arrhenius energy of activation of NR/PS blends.

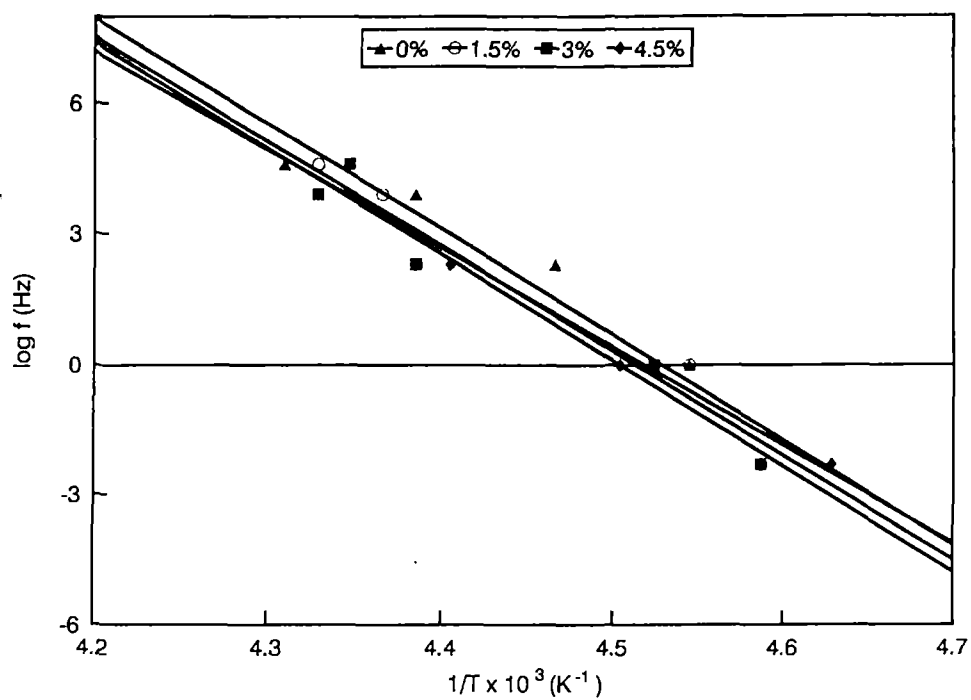| Composition (NR/PS)	ΔE (kJ/mol) (Due to NR)	ΔE (kJ/mol) (Due to PS)
40/60	-	493
50/50	202	480
60/40	-	443
50/50/1.5% graft	200	564
50/50/3% graft	203	474
50/2550/4.5% graft	188	432

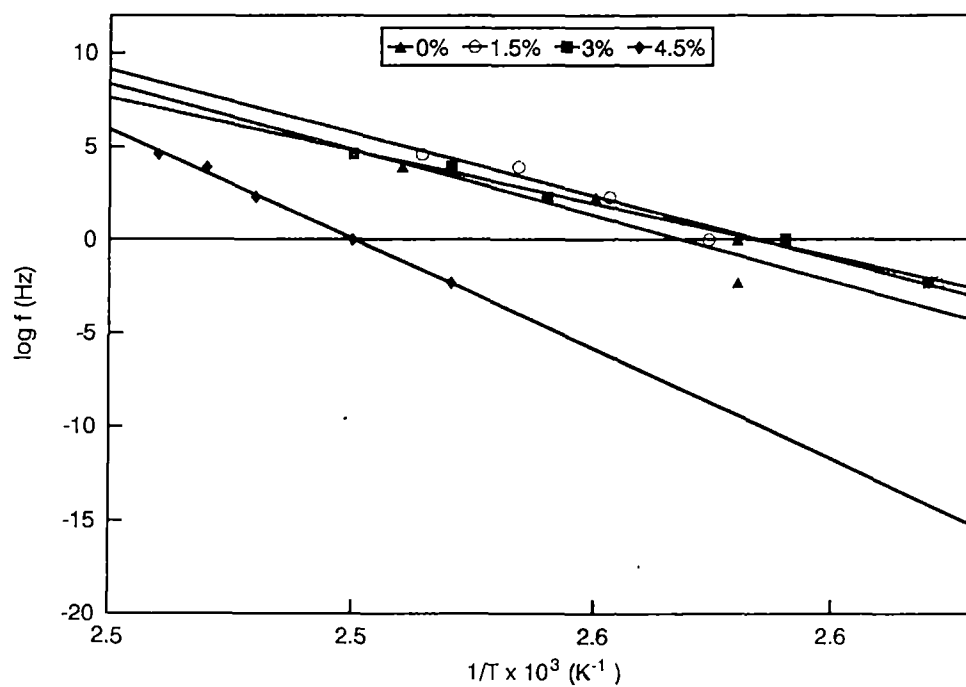Figure 7.2.   Arrhenius plots of log frequency vs. 1/T x 10³ (due to NR).

Figure 7.3.   Arrhenius plots of log frequency vs. 1/T x 10³ (due to PS).

The activation energy of 50/50 NR/PS blend due to NR is lower than that due to PS. The variation of tan δ with temperature (20 to 140°C) at different frequencies for 50/50 NR/PS blends is given in Figure 7.4. It is seen that at all frequencies the tan δ values increase with increase in temperature up to the glass transition of polystyrene (transition zone) and thereafter it decreases. Throughout the temperature range, the tan δ values decrease with increase of frequency. The tanδ curves of the blends show peaks corresponding to the glass transition temperature (Tg) of polystyrene. Here also as the frequency increases from 0.1 to 100 Hz, the glass transition peak of PS phase shifts to high temperature region. The variation in Tg value of PS phase with frequency is given in Table 7.1. The variation of tan δ with frequency for different NR/PS blends at 80°C are given in Figure 7.5. Here, as the frequency increases the tan δ values decrease. The 60/40 blends show the maximum value and 40/60 blends show the minimum value. In all the three cases, tan δ value levels off beyond 50 Hz.
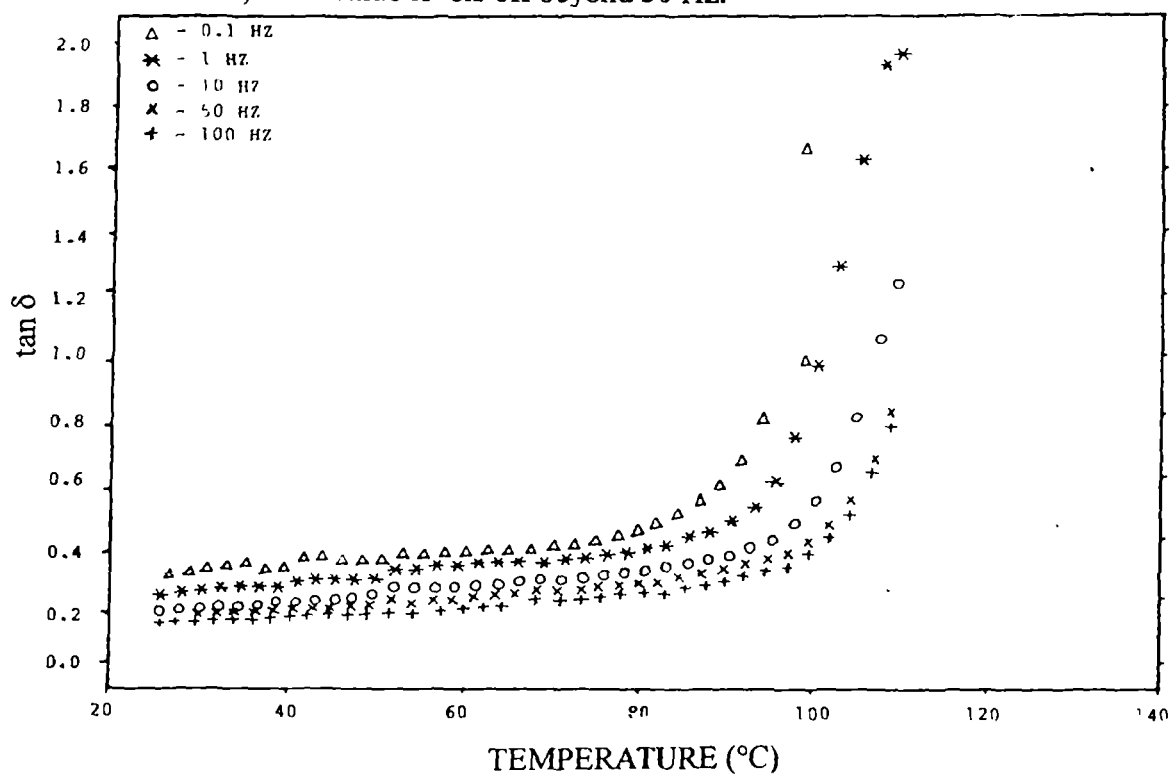
Figure 7.4.   Variation of tan δ with temperature at different frequencies for 50/50 NR/PS blends (20 to 140°C).
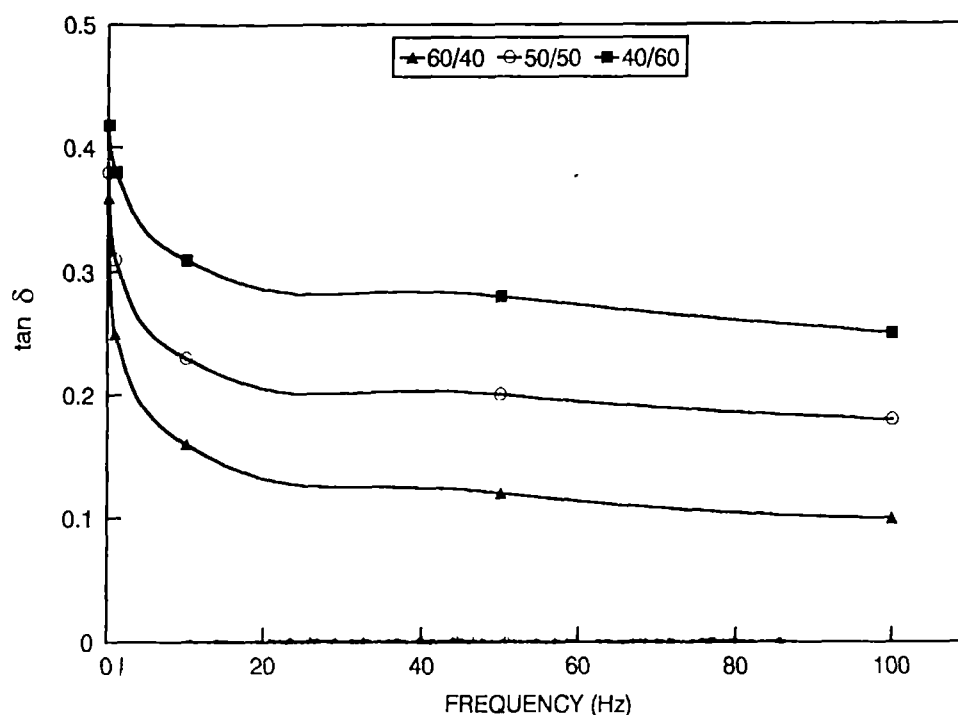
Figure 7.5. Variation of tan δ with frequency for different NR/PS blends at 80°C

Variation of storage modulus (E′) with temperature for 50/50 NR/PS blend for the temperature range of -70 to 30°C at different frequencies is given in Figure 7.6. The curves at all the frequencies have three distinct regions; a glassy region, a transition region and a rubbery region. In the glassy region, the storage modulus do not show much variation with frequency. However, in the transition region, the storage modulus values show an increasing tendency with frequency. In the rubbery region, again the variation of storage modulus with frequency is less pronounced. At all frequencies, storage modulus decrease with increase in temperature due to the decrease in the stiffness of the sample.
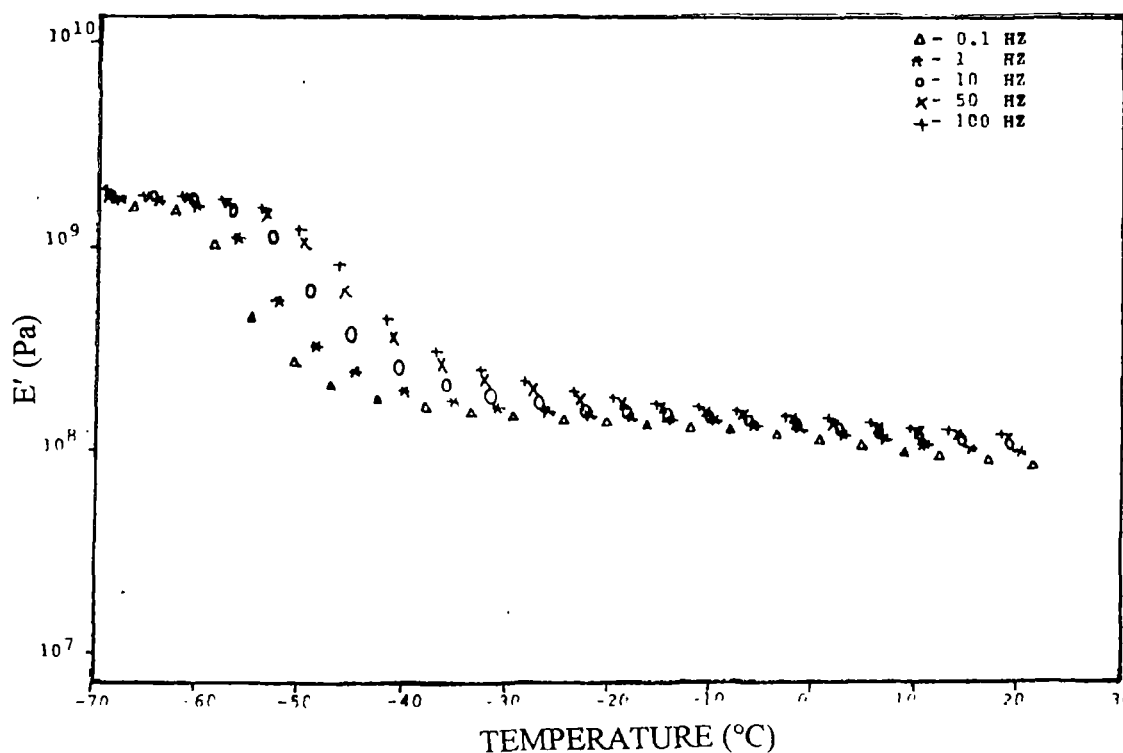
Figure 7.6. Variation of storage modulus with temperature at different frequencies for 50/50 NR/PS blends (-70 to 30°C).

Similar observations are obtained in the high temperature region also. Figure 7.7 shows the variation of storage modulus (E') with temperature for 50/50 NR/PS blend for the temperature range (20 to 140°C) at various frequencies. In all cases, the storage modulus decreases with increase of temperature. The fall in the value of E' is drastic around the glass transition temperature of polystyrene. As the frequencies increases from 0.1 to 100 Hz, the storage modulus values increase . Figure 7.8 shows the variation of storage modulus with frequency at 80°C for different NR/PS blends. Here as the frequency increases E' values increase and levels off at higher frequencies. The 40/60 blends show the maximum value of E' and the enhancement in modulus with frequency is more pronounced in this case. The 60/40 blend show the minimum value and 50/50 blend occupy the intermediate position.
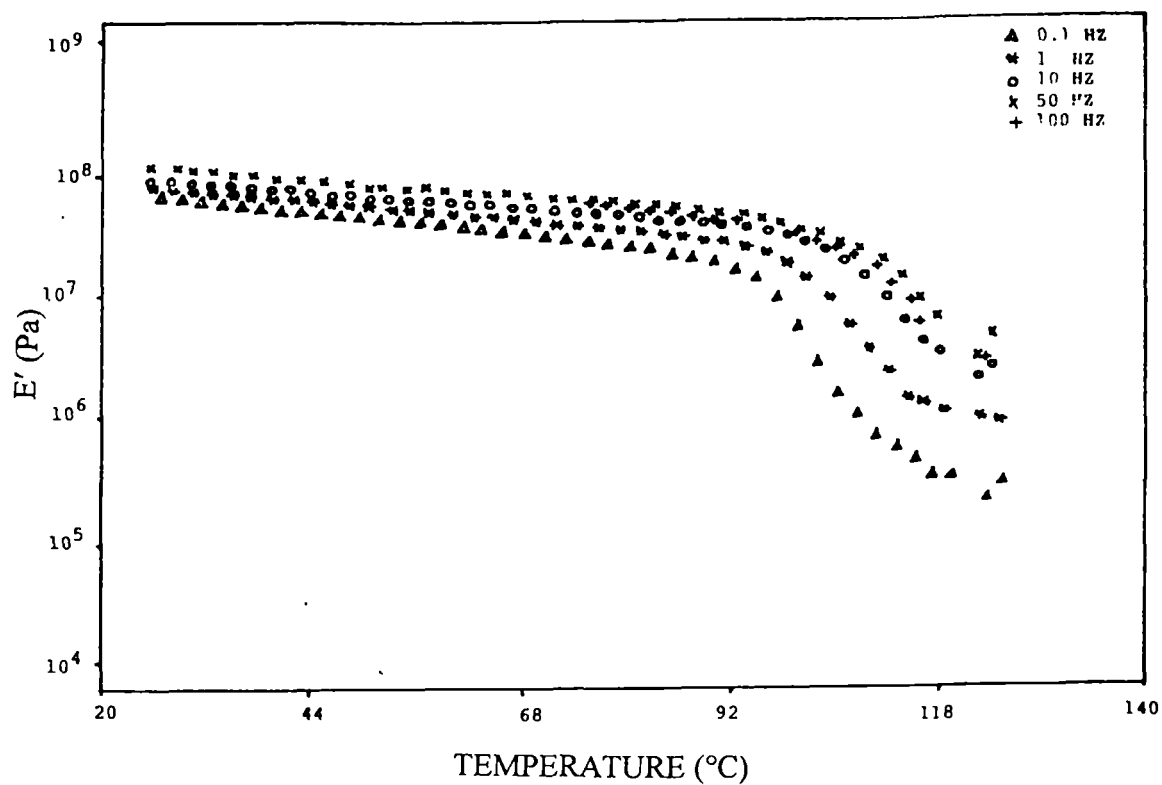
Figure 7.7. Variation of storage modulus with temperature at different frequencies for 50/50 NR/PS blends (20 to 140°C).

Figure 7.8. Variation of storage modulus with frequency for different NR/PS blends at 80°C.

Variation of loss modulus (E″) with temperature in the range of -70 to 20°C is given in Figure 7.9. Around the Tg region of NR phase, i.e., -70 to -60°C, the E″ values decrease with increase of frequency and then the trend is reversed. As the frequency is increased from 0.1 to 100 Hz, the E″ peak temperature of NR transition shifts towards the high temperature region. The Tg values obtained from the E″ vs. temperature plots are always lower than those obtained from the tan δ_max (Tables 7.1 and 7.3).
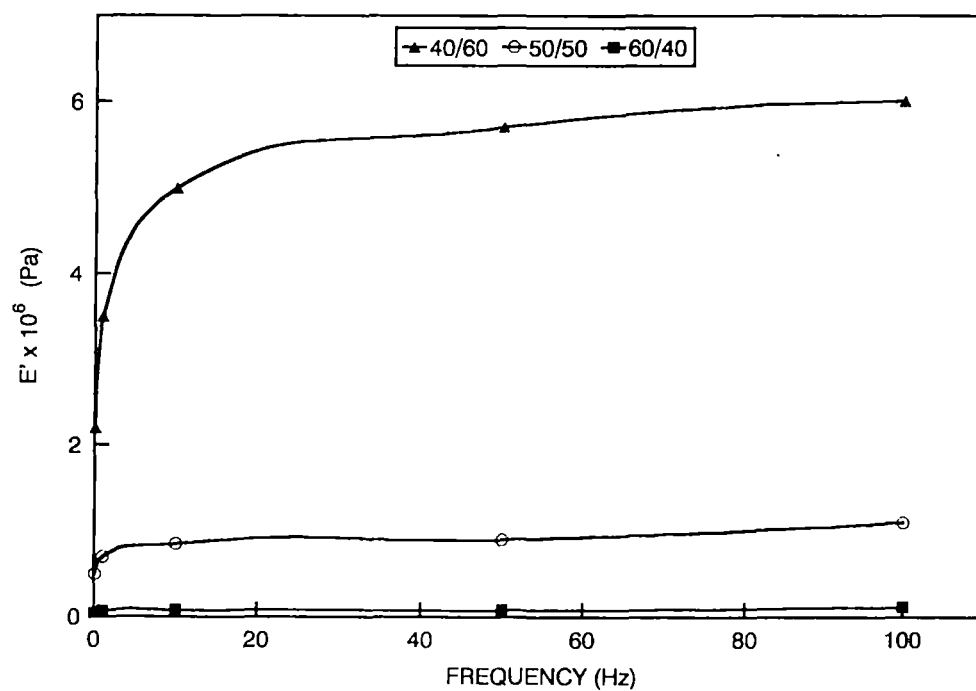

Figure 7.9.   Variation of loss modulus with temperature at different frequencies for 50/50 NR/PS blends (-70 to 30°C).

Table 7.3.   Variation of Tg values of 50/50 NR/PS blends upon graft loading from E″ curves.

% graft copolymer	Frequency (Hz)								
	Due to NR					Due to PS			
	0.1	1	10	50	100	0.1	1	10	50	100
0	-58	-56	-53	-49	-45	100	108	112	116	120
1.5	-59	-53	-49	-48	-46	101	109	111	115	115
3	-59	-56	-53	-49	-47	100	104	110	116	117
4.5	-58	-54	-50	-48	-47	115	117	120	121	123

Variation of loss modulus (E″) with temperature in the range (20 to 140°C) is given in Figure 7.10. In the plateau region, the loss modulus values decrease with increase of frequency and around the glass transition of polystyrene the trend is reversed. At high frequency, the modulus increases slightly with temperature and around the Tg of polystyrene it shows a slight decrease in the value of loss modulus. However, at lower frequency, the modulus shows a levelling off up to the glass transition of polystyrene and around the Tg of polystyrene it shows a sharp fall in value. The variation of loss modulus with frequency (Figure 7.11) is similar to the variation of storage modulus with frequency. Except in 40/60 NR/PS blend, as the frequency increases, the loss modulus values decrease and from 50 Hz onwards it levels off. In the case of 40/60 NR/PS blend, the loss modulus value increases up to 10 Hz and then it falls suddenly to a low value. In the case of non-compatibilised blends, the activation energy of transition due to PS phase decreases from 40/60 to 60/40 NR/PS blends. This is attributed to the decrease in the Tg of the blends having higher NR content.
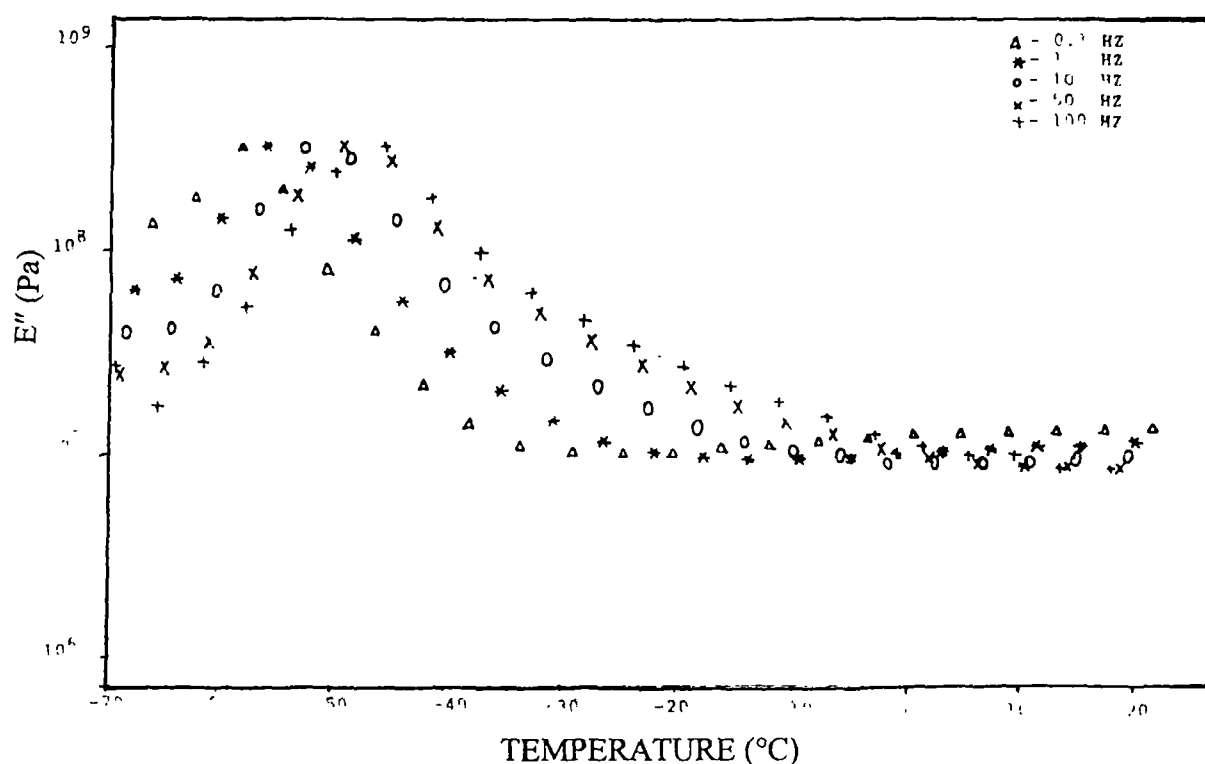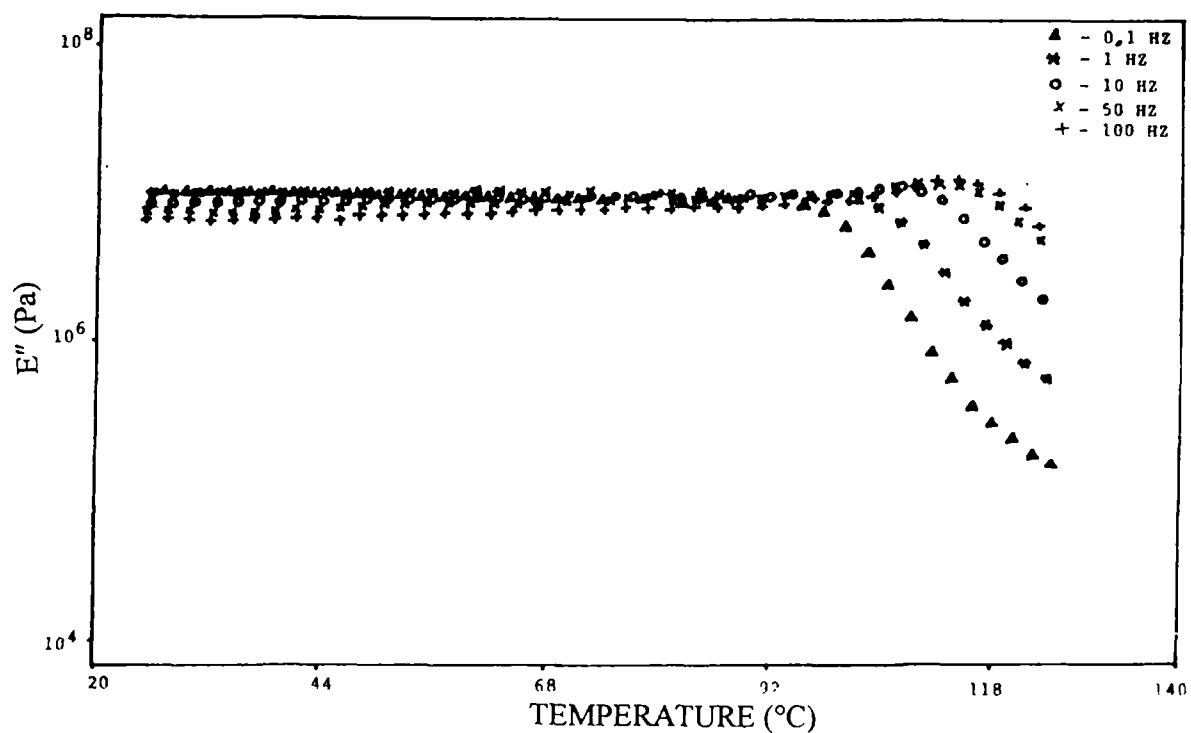
Figure 7.10.   Variation of loss modulus with temperature at different frequencies for 50/50 NR/PS blends (20 to 140°C).
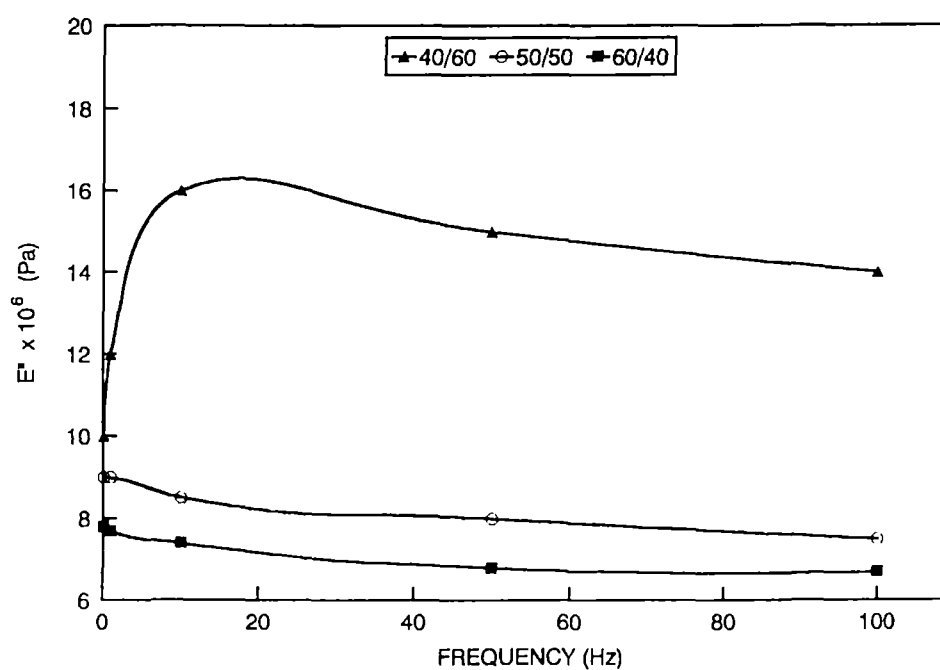
Figure 7.11.   Variation of loss modulus with frequency for different NR/PS blends at 80°C.

7.1.2 Effect of blend composition

In order to study the effect of composition on dynamic mechanical properties, the experiments were carried out in the temperature range of 20 to 140°C. The effect of composition on the tan δ values of various NR/PS blends at a frequency of 0.1 Hz is given in Figure 7.12.
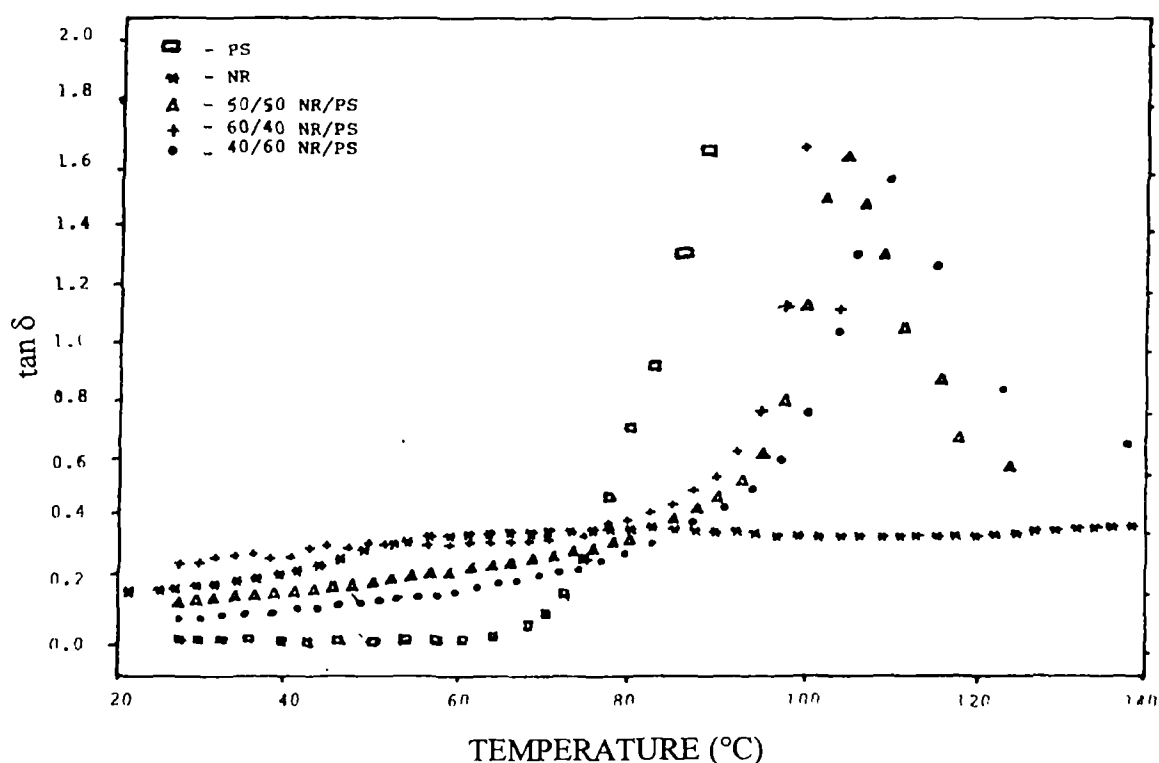
Figure 7.12. Variation of tan δ with temperature for different NR/PS blends at a frequency of 0.1 Hz (20-140°C).

Here the damping curves of the blends show a trend similar to that of polystyrene. At the low temperature region, the tan δ values of the blends are higher than that of polystyrene. However, at the high temperature region, the reverse will be the case. The damping curve of natural rubber is different from that of polystyrene and their blends. In this case, the curve is almost parallel to the temperature axis. Comparing the tan δ curves of 40/60, 50/50 and 60/40 NR/PS blends, as the NR content increases, the transition peak due to PS shifts towards the

low temperature region. The glass transition temperature (Tg) was selected at the peak position of tan δ curve. The tan δ_{max} values due to polystyrene increase as the NR content increases (Figure 7.13). The Arrhenius activation energies due to PS phase of different NR/PS blends are given in Table 7.2. It is found that the activation energy values increase from 40/60 to 60/40 NR/PS blends and is attributed to the increase in the amount of PS.
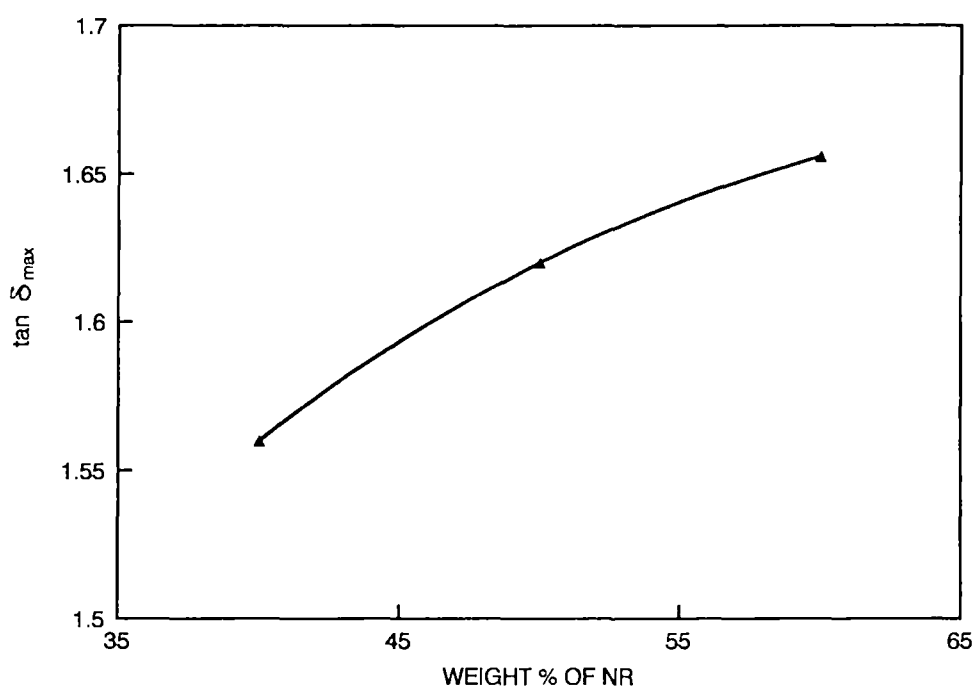
Figure 7.13. Variation of tan δ_{max} with wt % of NR.

The influence of temperature on the storage modulus of various NR/PS blends at a frequency of 0.1 Hz is given in Figure 7.14. Between the temperature range 20-80°C, the blends show modulus in between that of the components. It was reported by many researchers[4] that if no other interactions are present between the two phases, one can predict a modulus for the blend somewhere between the moduli of the individual components. As in the case of blend components, the modulus of the blends decreases with increase in temperature. Compared to NR, polystyrene shows a very high modulus. At 70°C, the storage modulus of PS shows

a sudden fall. This is due to the fact that the system approaches glass transition. Above 100°C the values fall below the modulus of NR and this may be due to the melting of polystyrene. The storage modulus of the blends decreases with increase of temperature in all cases. In the case of pure polystyrene and the blends, the modulus curves have three distinct regions namely, rubbery, transition and viscous regions. Both in the rubbery and transition regions, the modulus decreases with temperature and it levels off in the viscous region. The storage modulus of NR is almost unaffected by temperature. In all the cases, throughout the temperature range, storage modulus increases with increase of polystyrene. The variation of loss modulus (E″) with temperature for different NR/PS blends at a frequency of 0.1 Hz is given in Figure 7.15. Here also, the loss modulus curve of NR is unaffected by temperature. The loss modulus value decreases with increase of PS content at the low temperature region (glassy region) and the trend is reversed in the transition region.
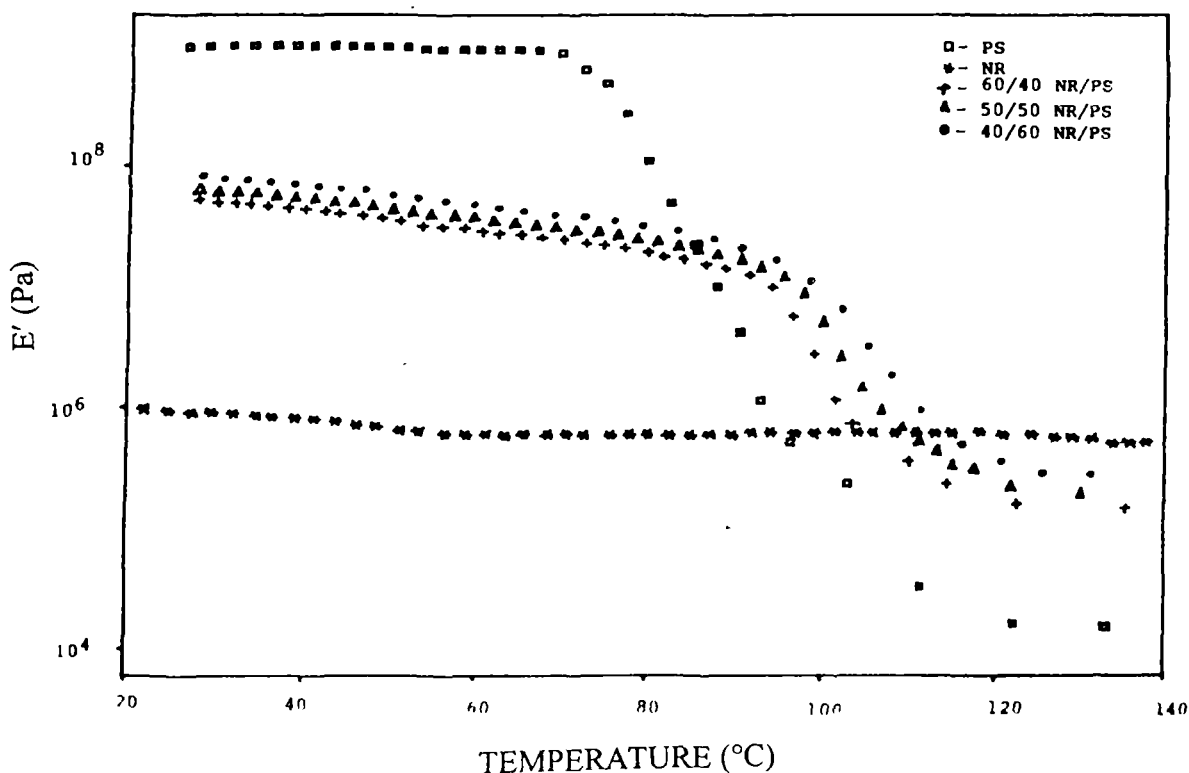
Figure 7.14.   Variation of storage modulus with temperature for different NR/PS blends at a frequency of 0.1 Hz (20-140°C).
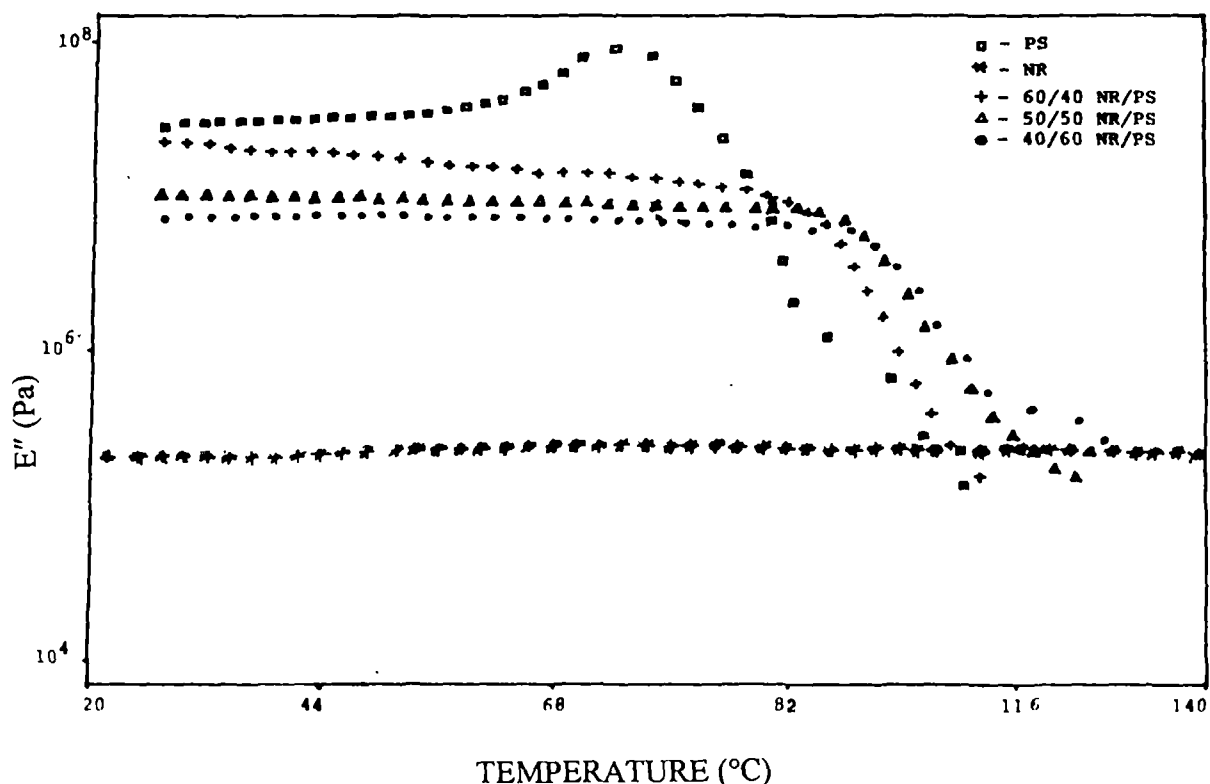
Figure 7.15. Variation of loss modulus with temperature for different NR/PS blends at a frequency of 0.1 Hz (20-140°C).

7.1.3 Effect of compatibilisation

As mentioned earlier, the dynamic mechanical properties of NR/PS blends have been studied with and without the addition of the compatibiliser. The effect of compatibiliser loading on tan δ of 50/50 NR/PS blends is given in Figure 7.16 in the temperature range of -70 to 30°C. In the case of non-compatibilised NR/PS blend, the peak maximum at -50°C, corresponds to the glass transition temperature of NR. Upon graft copolymer addition, the Tg values have been shifted to the high temperature region. The tan δ value of 50/50 NR/PS blend with 1.5% graft copolymer is higher compared to non-compatibilised blend. Above that concentration (3 and 4.5% copolymer) the tan δ values are less compared to the non-compatibilised blend. The shifting of Tg value of NR component towards the

high temperature region is associated with the interfacial activity of the graft copolymer which enhances the compatibility of the system.
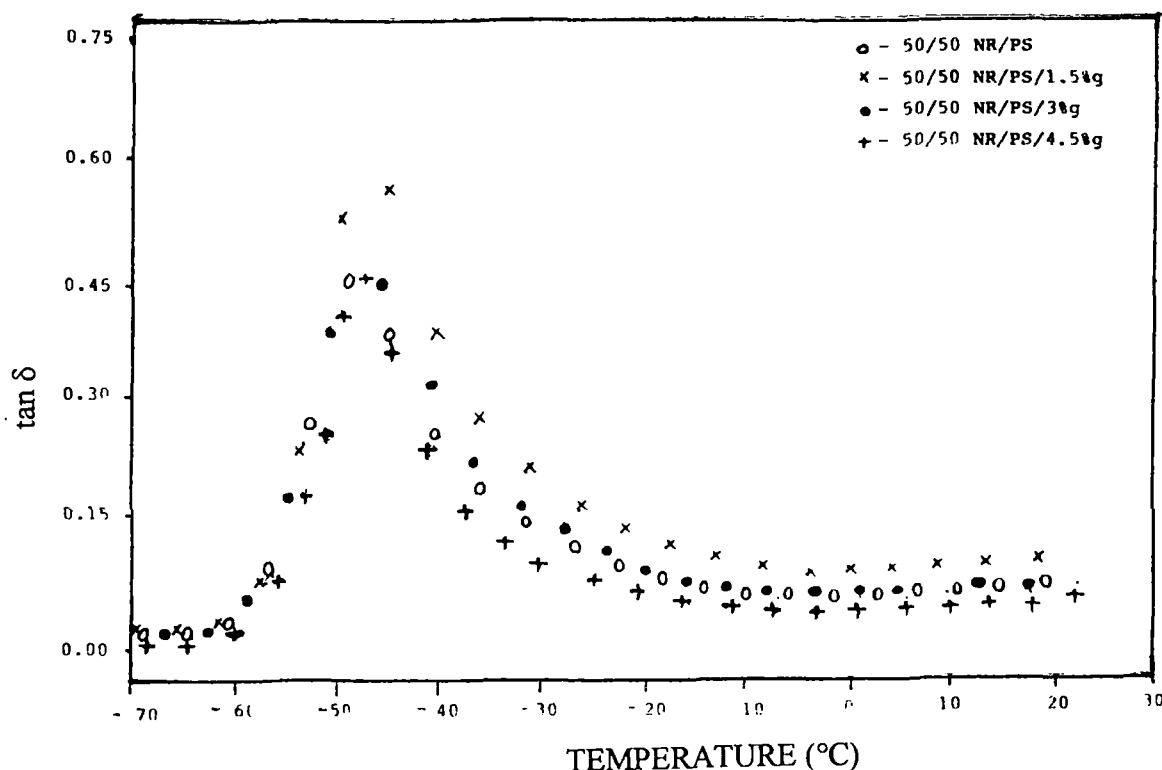
Figure 7.16. Variation of tan δ with temperature for different compatibilised NR/PS blends (-70 to 30°C).

The variation of tan δ as a function of temperature (20 to 140°C) for the compatibilised and non-compatibilised blends (50/50) is given in Figure 7.17. Both the compatibilised and non-compatibilised blends show the similar behaviour for tan δ curve. In the case of 3 and 4.5% compatibiliser loading, the Tg peak due to PS is shifted considerably to the high temperature region. In the case of blend with 1.5% compatibiliser, up to 100°C, the tan δ values are lower or comparable to the non-compatibilised blends. However, beyond 100°C the trend is exactly the reverse. In the case of blends with 3 and 4.5% compatibiliser, a reverse trend is obtained

throughout the temperature range. In the case of 4.5% compatibiliser loading, the Tg peak of PS is shifted considerably to the high temperature region. Addition of compatibiliser alters the Tg value of both natural rubber and polystyrene phases. The variation in Tg values due to NR and PS phases with compatibiliser loading at different frequencies are given in Table 7.1. The addition of the compatibiliser improves the blend properties by locating at the blend interface. This enhances interfacial adhesion and reduces the interfacial tension across the phase boundary. Beyond a certain concentration, i.e., the so-called critical micelle concentration (CMC) the compatibiliser has a tendency to form micelle. The variation of tan δ_{max} due to both NR and PS with compatibiliser loading is given in Figure 7.18. Here in both cases, tan δ_{max} increases up to 1.5% compatibiliser loading and thereafter it decreases. However, the increase associated with the NR phase is marginal.
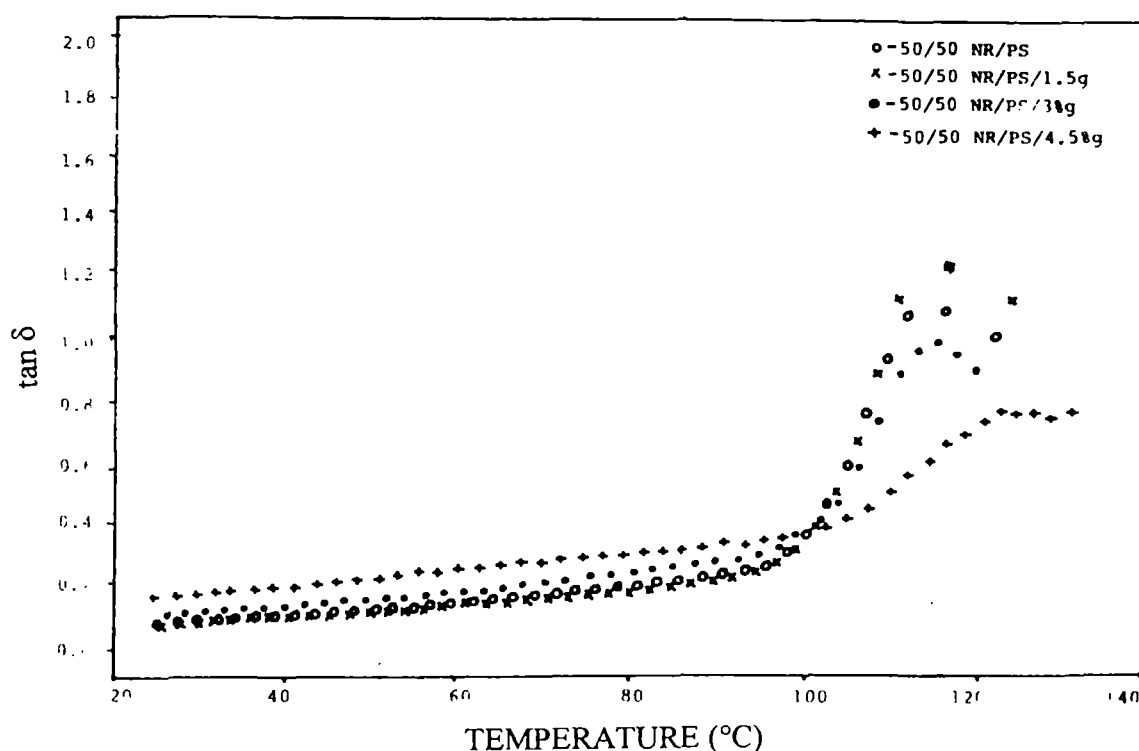
TEMPERATURE (°C)

Figure 7.17. Variation of tan δ with temperature for different compatibilised NR/PS blends (20 to 140°C).
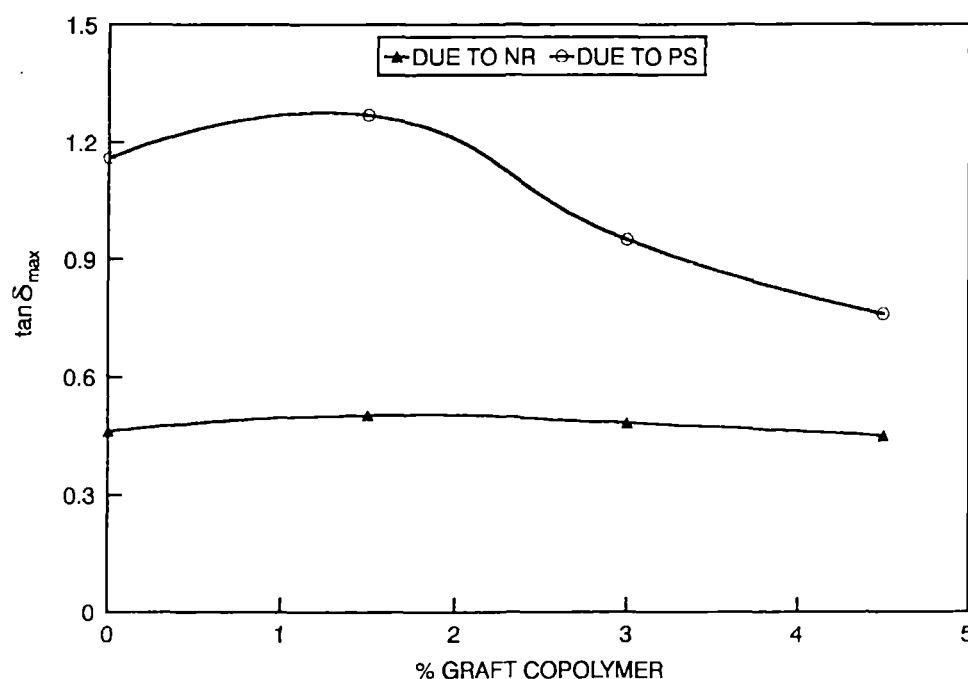
Figure 7.18. Variation of tan δ$_{maxi}$ due to NR and PS with compatibiliser loading.

The activation energies of compatibilised NR/PS blends are given in Table 7.2. It is seen that the activation energy due to NR phase is not showing much variation with compatibiliser loading below CMC. However, above CMC there is a sudden fall in value. The activation energy due to PS increases up to 1.5% graft loading and above that the values decreases.

The three dimensional pictures (Figures 7.19–7.22) give the variation of tan δ with temperature and frequency for 50/50 NR/PS blend with 0, 1.5, 3 and 4.5% compatibiliser, respectively. The peaks represent the glass transition temperatures due to NR phase in the blends. It is seen from the figures that the compatibiliser influences the glass transition peak of the natural rubber phase. With the increase of frequency the glass transition temperature of the system is progressively shifted to higher temperature region.
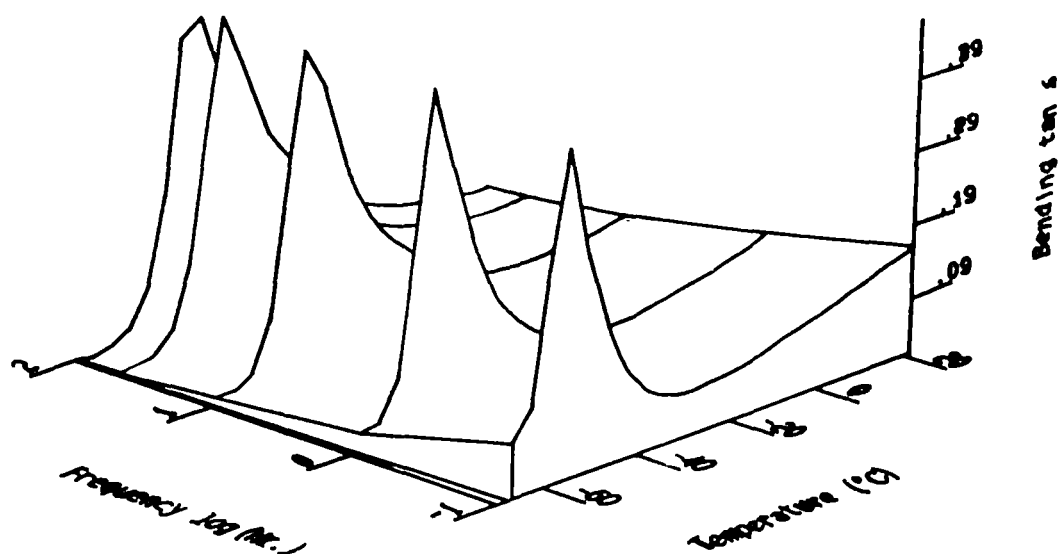
Figure 7.19. Three-dimensional plots of tan δ vs. temperature and frequency of 50/50 NR/PS blends without compatibiliser.
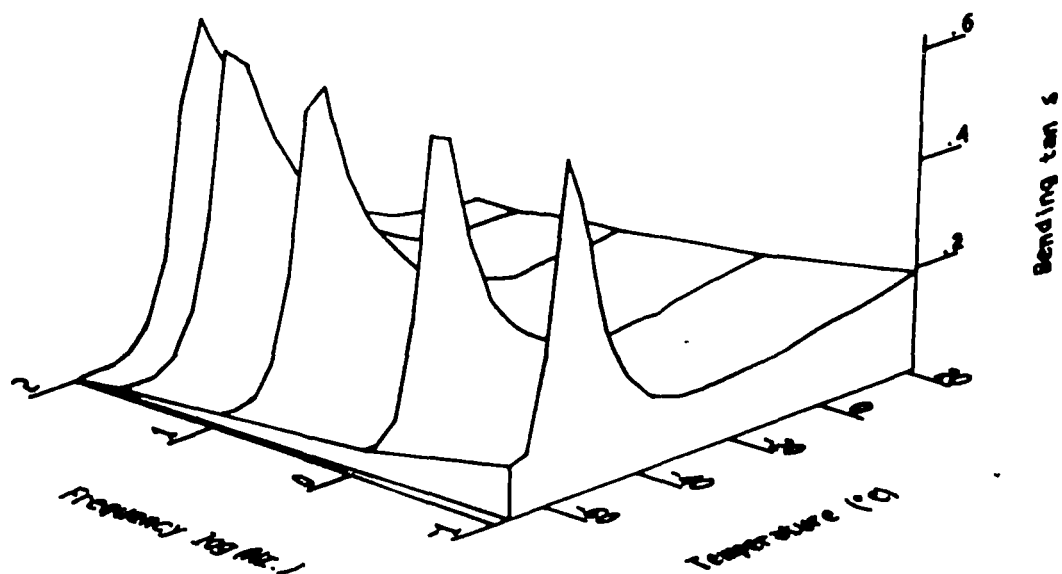
Figure 7.20. Three-dimensional plots of tan δ vs. temperature and frequency of 50/50 NR/PS blends with 1.5% compatibiliser.
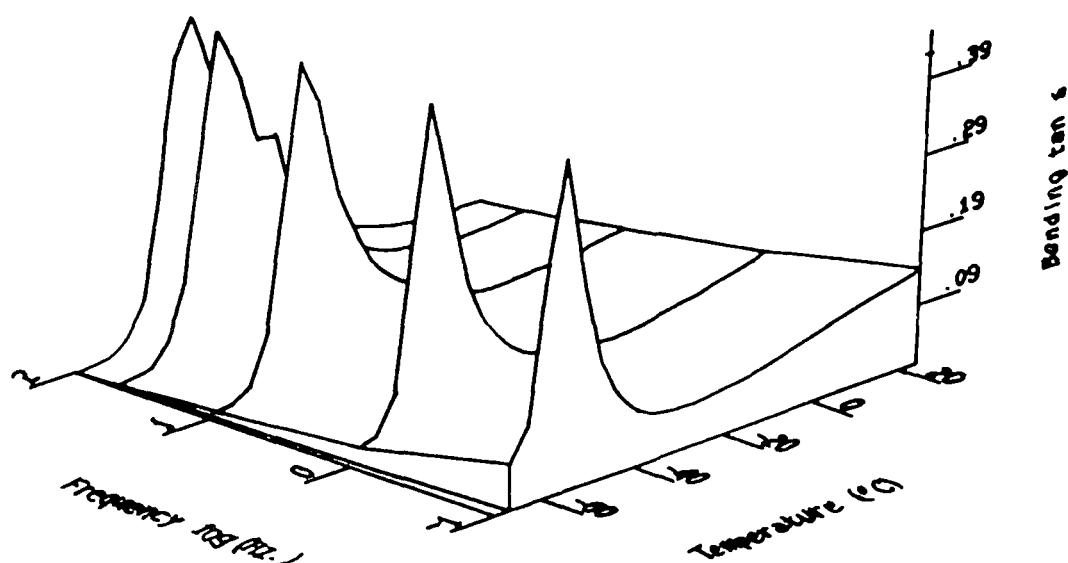
Figure 7.21.   Three-dimensional plots of tan δ vs. temperature and frequency of 50/50
NR/PS blends with 3% compatibiliser.
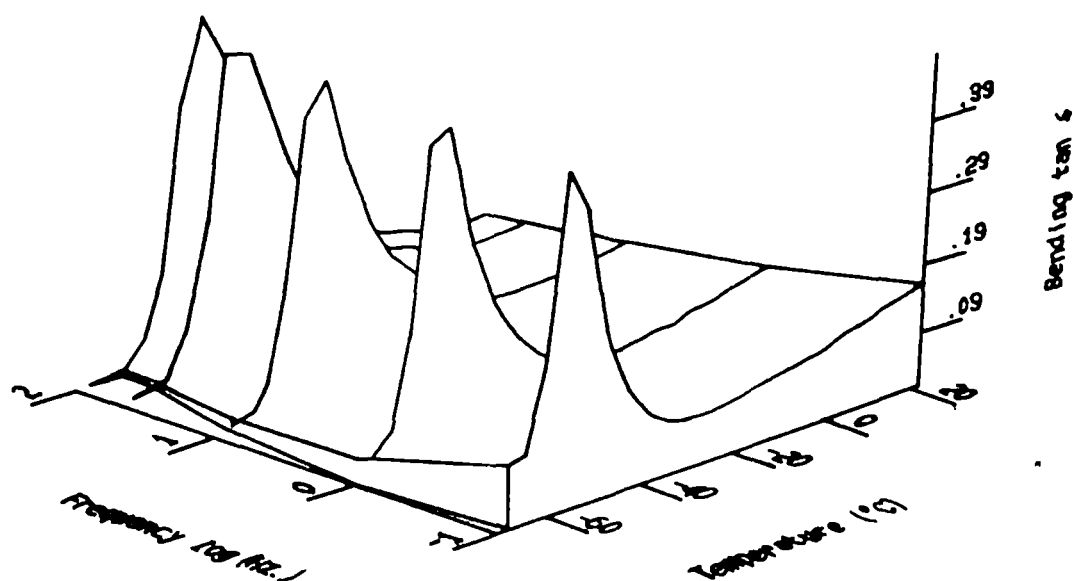
Figure 7.22.   Three-dimensional plots of tan δ vs. temperature and frequency of 50/50
NR/PS blends with 4.5% compatibiliser.

The variation of storage modulus (E′) and loss modulus (E″) with temperature in the range (-70 to 30°C) is given in Figures 7.23 and 7.24, respectively. The 2 sets of curves show the same trend throughout the temperature range. In the low temperature region, both the storage and loss modulii are lower in the case of compatibilised blend. The effect of graft copolymer loading on storage modulus and loss modulus in the high temperature region (20 to 140°C) are given in Figures 7.25 and 7.26, respectively. The compatibilised blend (1.5% graft loading) shows higher modulus compared to non-compatibilised blends and is mainly attributed to enhanced interactions between the phases due to the presence of the copolymer. Above that level (3 and 4.5% graft loading) the blends show a lower modulus value compared to non-compatibilised blend and can be related to the undesirable micelle formation as explained earlier. Similar observations have been reported by Brahimi et al.[4] The storage modulus of polyethylene/polystyrene blend is increased by compatibilisation using PS-PE block copolymers up to interface saturation concentration (CMC) and after that the modulus is decreased.
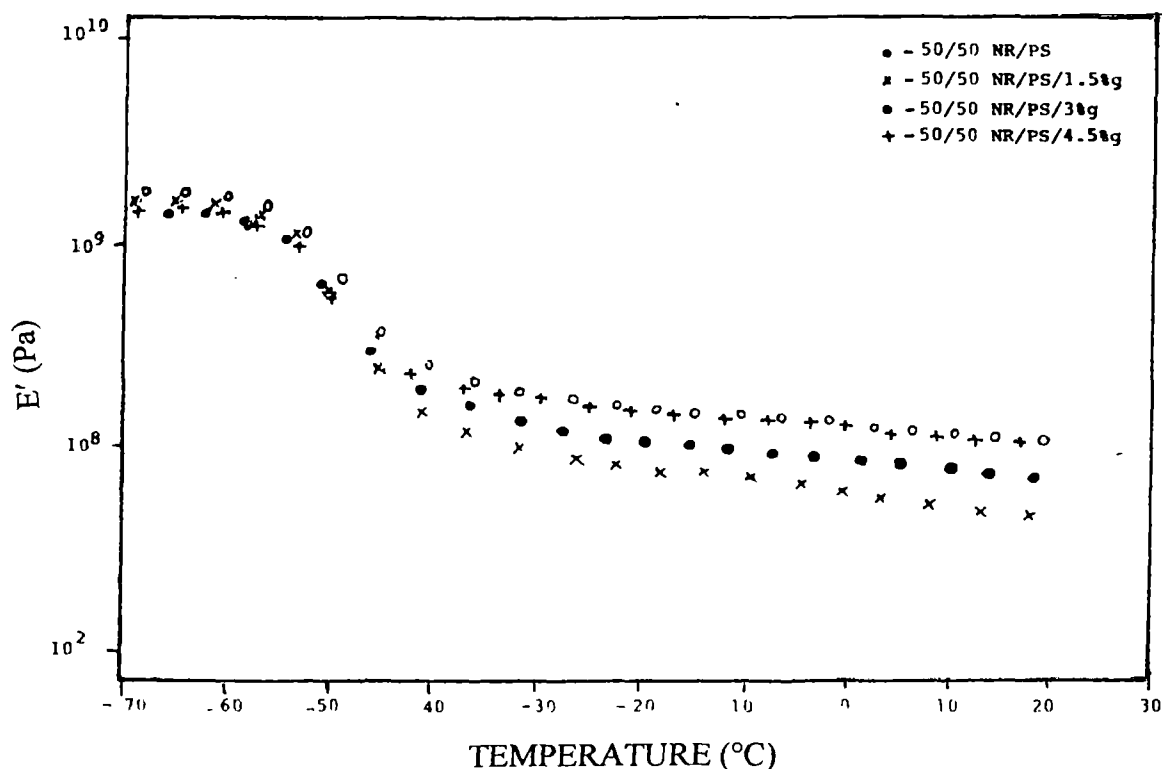
Figure 7.23. Variation of storage modulus with temperature (-70 to 30°C) of compatibilised 50/50 NR/PS blends.
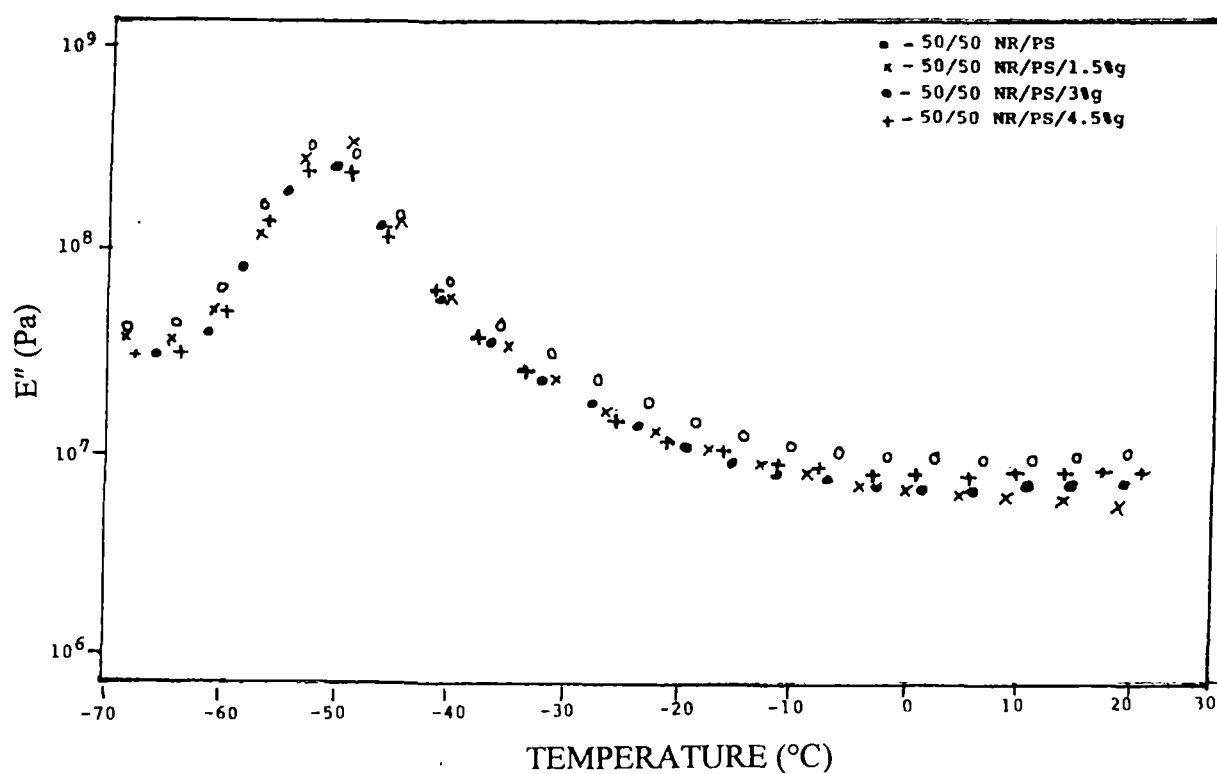
Figure 7.24. Variation of loss modulus with temperature (-70 to 30°C) of compatibilised 50/50 NR/PS blends.
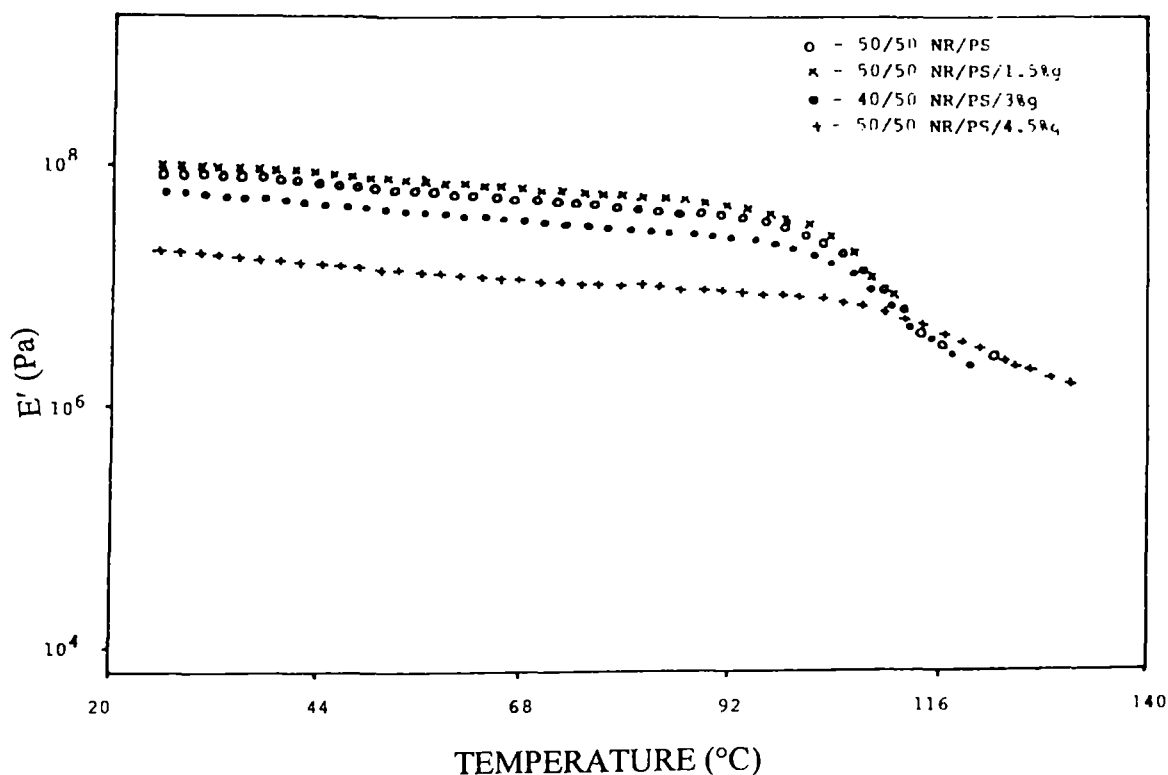
Figure 7.25. Variation of storage modulus with temperature (20 to 140°C) of compatibilised 50/50 NR/PS blends.
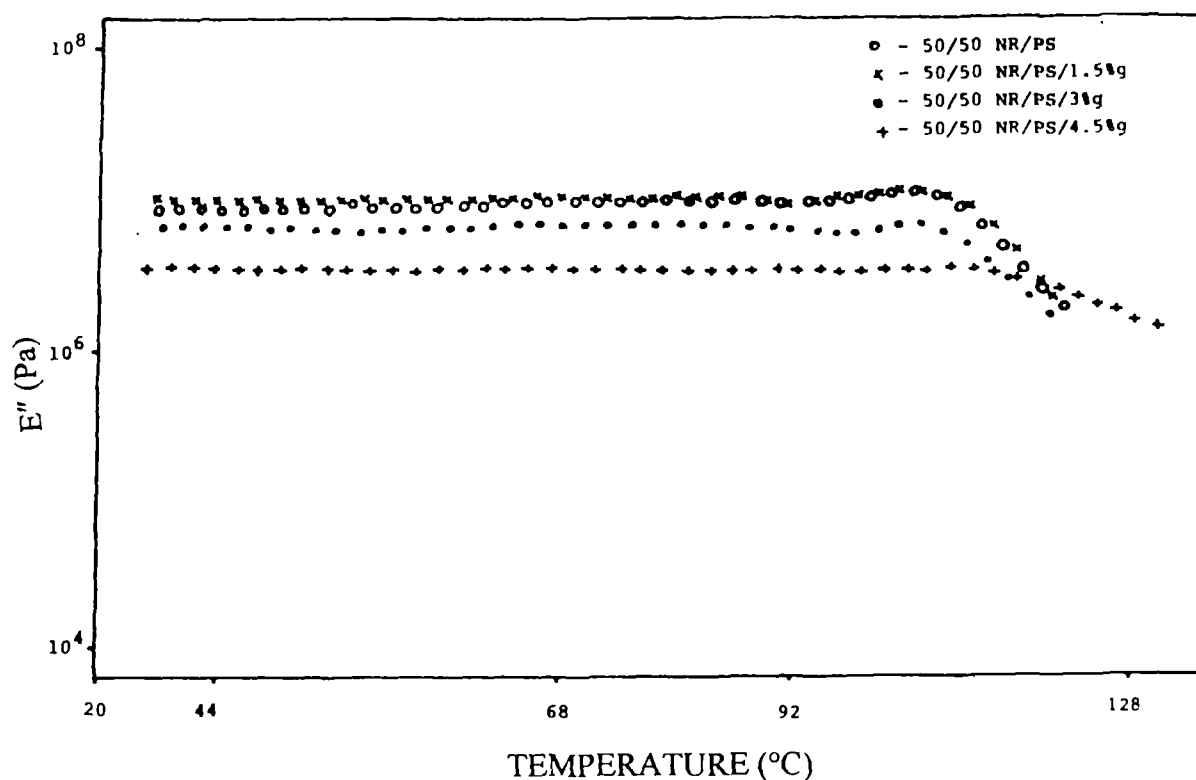
Figure 7.26. Variation of loss modulus with temperature (20 to 140°C) of compatibilised 50/50 NR/PS blends.

7.1.4 Modelling of viscoelastic properties

Different models like parallel, series, Halpin-Tsai, Takayanagi and Coran's model can be used to predict the mechanical properties of the blends.

The highest-upper-bound parallel model is given by the rule of mixtures.

$$M = M_1\phi_1 + M_2\phi_2 \tag{7.2}$$

where M is any mechanical property of the blend. M_1 and M_2 are the mechanical properties of components 1 and 2 respectively and ϕ_1 and ϕ_2 are their corresponding volume fractions. In this model the components are arranged parallel to one another so that the applied stress elongates each component by the same extent. In the lowest-lower bound series model, the blend components are arranged in series and the equation is given as follows

$$1/M_1 = \phi_1/M_1 + \phi_2/M_2 \tag{7.3}$$

Parameters M, M_1, M_2, ϕ_1 and ϕ_2 are the same as in the upper-limit model. According to the Halpin-Tsai equation,[6,7]

$$M_1/M = \frac{(1 + AiBi\phi_2)}{(1 - Bi\phi_2)} \tag{7.4}$$

where

$$B_i = \frac{(M_1/M_2) - 1}{(M_1/M_2) + Ai} \tag{7.5}$$

In this model subscripts 1 and 2 correspond to the continuous and dispersed phase respectively. The constant $A_i = 0.66$ when elastomer forms the dispersed phase in a continuous hard matrix. On the other hand, if the hard material forms the dispersed phase in a continuous elastomer matrix, then $A_i = 1.5$. In the case of incompatible blends, generally the experimental value is between the parallel upper bond (M_U) and the series lower bound (M_L) values.

According to Coran's model,[8]

$$M = f(M_U - M_L) + M_L \tag{7.6}$$

where f varies between zero and unity.

$$f = V_H \, n(nV_s + 1) \tag{7.7}$$

where n is related to phase morphology, V_H and V_s are the volume fractions of the hard and soft phases respectively

According to Takayanagi model[9]

$$M = (1 - \lambda) M_1 + \lambda(1 - \phi)/M_1 + (\phi/M_2) \tag{7.8}$$

As suggested by Cohen and Ramos, the degree of parallel coupling of the model can be expressed by

$$\% \text{ parallel} = \frac{\phi(1 - \lambda)}{(1 - \phi\lambda)} \times 100 \tag{7.9}$$

where M_1 is the property of the matrix phase, M_2 is the property of the dispersed phase and $\phi\lambda$ is the volume fraction of the dispersed phase and is related to the degree of series-parallel coupling.

According to Kerner's model[10]

$$E_r = E_m \left[\frac{\dfrac{\phi_d E_d}{[(7-5v_m)E_m+(8-10v_m)E_d]} + \dfrac{\phi_m}{15(1-v_m)}}{\dfrac{\phi_d E_m}{[(7-5v_m)E_m+(8-10v_m)E_d]} + \dfrac{\phi_m}{15(1-v_m)}} \right] \tag{7.10}$$

where E_r is the relative modulus, v_m is the Poisson's ratio, ϕ_d is the volume fraction of the dispersed phase, and ϕ_m is the volume fraction of the matrix. The subscripts m, d and b stand for the matrix, dispersed phase and blend respectively.

According to Paul's (upper limit)[11] model,

$$E_b \leq (1-\phi_d) E_m + \phi_d E_d \tag{7.11}$$

where E_b, E_m, E_d and ϕ_d has the same significance as above

According to Kunori et al.[12]

$$\sigma_b = \sigma_m (1-\phi_d) + \sigma_d \phi_d \tag{7.12}$$

where σ_b, σ_m and σ_d are the properties of the blend, matrix and dispersed phase respectively. ϕ_d has the same significance as above.

Figure 7.27 shows that experimental and theoretical curves of storage modulus of NR/PS blends as a function of NR content at 80°C and at a frequency of 10 Hz. Up to 50 wt % of NR, the experimental values are close to Halpin-Tsai model and beyond that it is close to the Coran's model, where n=2.
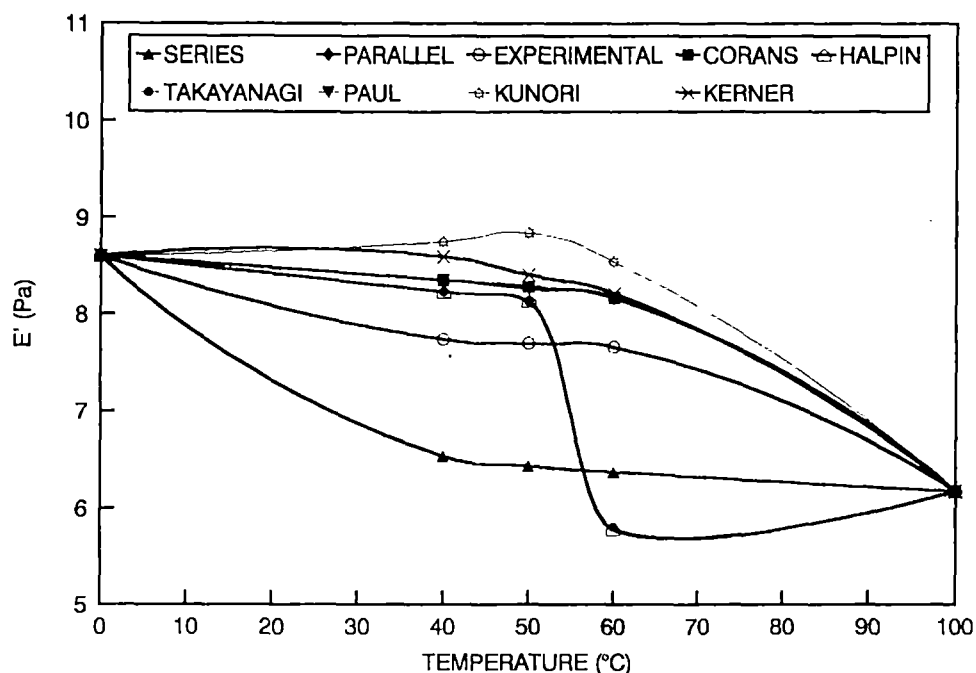
Figure 7.27. Various theoretical models of storage modulus at 80°C and at a frequency of 10 Hz (50/50 NR/PS blend).

7.1.5 Cole-cole analysis

Figure 7.28 shows the Cole-Cole plot where the loss modulus (E″) is plotted as a function of storage modulus (E′). It is reported that homogeneous polymeric systems show a semicircle diagram while a two phase system do not form a semicircle diagram.[13-15] It is seen that 50/50 NR/PS blend both compatibilised and non-compatibilised (Figures 7.28 and 7.29, respectively) show a behaviour different from that of a homogeneous system. These show that even though the compatibiliser addition can improve the interfacial adhesion between the two blend components, it can not make the system homogeneous on a molecular level. However, the system shows some tendency towards the formation of a semicircle upon the addition of the compatibiliser (Figure 7.29).
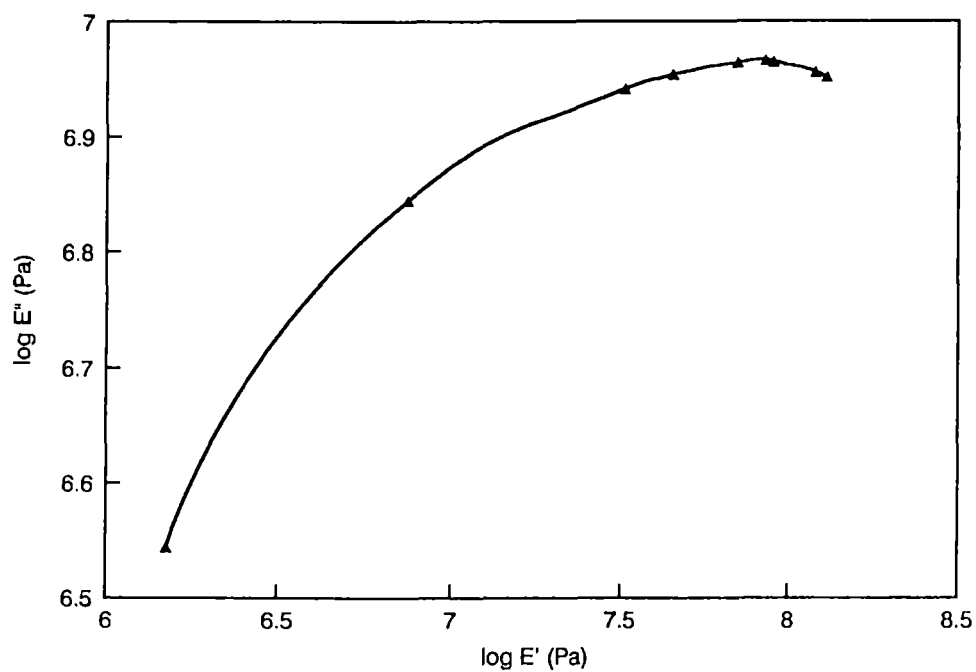
Figure 7.28. Cole-cole plots of loss modulus vs. storage modulus (non-compatibilised)
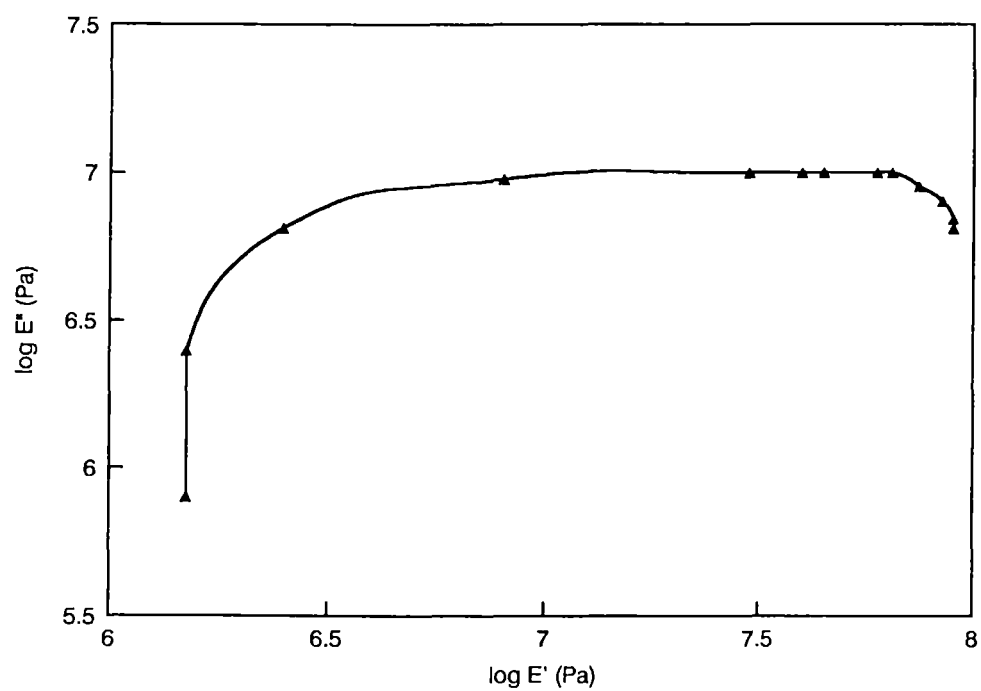
Figure 7.29. Cole-cole plots of loss modulus vs. storage modulus (compatibilised)

7.1.6 Time-temperature superposition

Due to the broad time-dependence involved, it is not feasible to directly measure the complete behaviour of the modulus as a function of time at constant temperature.[16] It is possible to construct a master curve via a shifting procedure based on the principle of time-temperature correspondence. According to this, the extension is identical to that which would be measured at long times at a particular temperature. Viscoelastic data collected at one temperature can be superimposed upon the data collected at different temperatures by shifting the curves (E' vs. log frequency). The modulus curve at a particular temperature is shifted along the frequency axis until overlaps with the next curve. One effectively has a measure of the complete modulus-time behaviour by applying the time-temperature correspondence principle to experimental measurements of polymer relaxation carried out on experimentally accessible time scales. Thus using the time temperature superposition principle, it is possible to predict the viscoelastic behaviour of a material well outside the frequency or time range of the mechanical equipment.

Master curves can be constructed by plotting $\log (t/a_T)$ vs. $\log ET_0/T$ where a_T is the shift factor, E is the storage modulus (E') at a particular temperature. The T_0 is the reference temperature on the Kelvin scale and T is the temperature of the experiment, t is the time and is related to frequency, f, as follows

$$t = \frac{1}{2\pi f} \qquad (7.13)$$

where f is the frequency of oscillation. Figure 7.30 shows the master curve for 50/50 NR/PS blend. It has been found that the variation of log E' vs. log f at different temperatures were merged into a single curve.
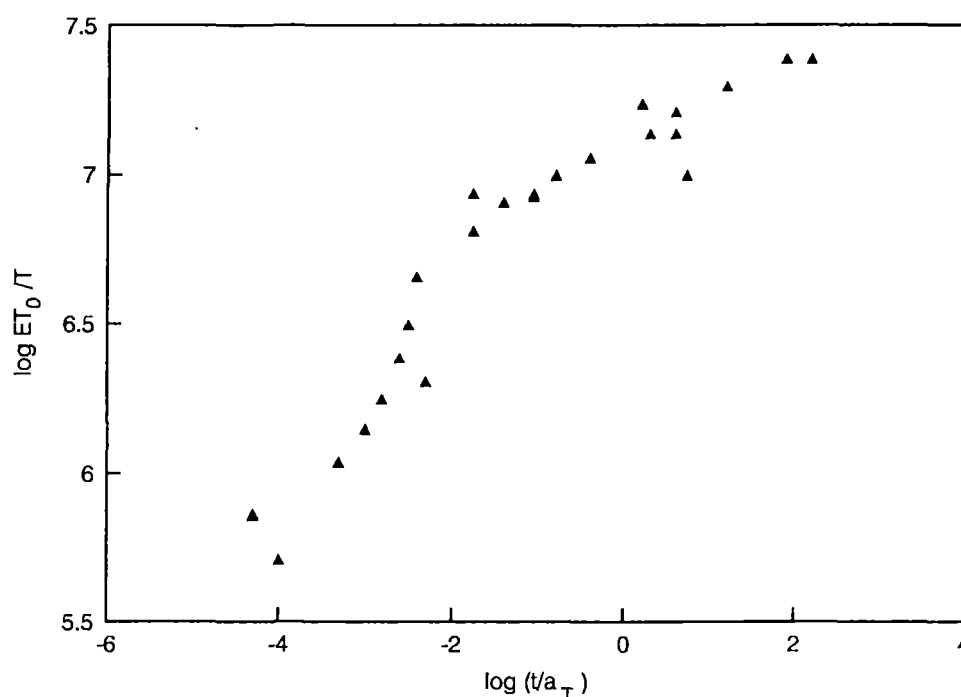
Figure 7.30. Time temperature superposition curve.

7.2 References

1. A. Schneider and J. Wirbser, *New Polymeric Mater.*, **2**, 149 (1990).

2. J. Karger-Kocsis and L. Kiss, *Polym. Eng. and Sci.*, **27**, 254 (1987).

3. L. Toy, M. Niinomi and M. Shen., *J. Macromol. Sci. Phys.*, **BII(3)**, 281 (1975).

4. B. Brahimi, A. Ait-Kadi, A. Ajji and R. Fayt, *J. Polym. Sci. Part B: Polym. Phys.*, **29**, 945 (1991).

5. R. N. Santra, B. K. Samantaray, A. K. Bhowmick and G. B. Nando, *J. Appl. Polym. Sci.*, **49**, 1145 (1993).

6. L. E. Nielson, *Rheol. Acta*, **13**, 86 (1974).

7. J. C. Halpin, *J. Compos. Mater.*, **3**, 732 (1970).

8. A. Y. Coran, *Handbook of Elastomers New Development and Technology* (Eds., A. K. Bhowmick and H. L. Stephens) Marcel Dekker, NY, 1988, p. 249.

9. R. M. Holsti-Miettinen, J. Y. Seppala, O. T. Ikkala and I. T. Reima., *Polym. Eng. Sci.*, **34**, 395 (1994).

10. E. H. Kerner, *Proc. Phy. Soc.*, **69B**, 808 (1956).

11. B. Paul, *Trans. Metallurg. Soc. AIME*, **218**, 36 (1960).

12. T. Kunori and P. H. Geil, *J. Macromol. Sci.—Phys.*, **B18**(1), 135 (1980).

13. L. Ibarra, M. Macias and E. Palma, *J. Appl. Polym. Sci.*, **57**, 831 (1995).

14. C. Wismie, G. Maria and P. Monge., *Eur. Polym. J.*, **21**, 479 (1985).

15. J. George, S. S. Bhagawan and S. Thomas, *J. Thermal Analysis*, **47**, 1121 (1996).

16. J. J. Aklonis and W. J. Macknight John (Eds.), *Introduction to Viscosity*, 2nd Edn, A Wiley Intenscience Publication, 1983, p. 44.

Chapter 8

Thermal Characteristics

Thermal behaviour of polymers is of much importance as a tool in materials characterisation. Thermal analysis of polymers is important as it plays a major role in the use of polymeric materials in many consumer oriented applications. Fabrication of a variety of articles and their end uses need a detailed understanding of the thermal degradation of polymers.

One of the widely accepted methods for studying the thermal properties of polymeric materials is thermogravimetry (TG). Thermogravimetric data will provide the number of stages of thermal breakdown, weight loss of the material in each stage, threshold temperature, etc.[1] Both thermogravimetry (TG) and derivative thermogravimetry (DTG) provide information about the nature and conditions of degradation of the material. Compatibility of the polymer blends can be studied by differential scanning calorimetry (DSC). This will give the glass transition temperature (Tg) and melting temperature (Tm) of the polymeric material. Miscible blends will show single, sharp transition peak (Tg) intermediate between that of the blend components. Separate peaks will be obtained for immiscible blends. In the case of borderline miscible blends, broad transition peaks are obtained.

Blending of polymers has been reported to have much influence on the thermal stability of individual polymers. The compatibility plays an important role in the overall thermal stability of the blends.[2,3] Several authors have analysed the thermal properties of blends.[4-6]

The aim of this chapter is to study the thermal properties of NR/PS blends with and without the addition of the compatibiliser (NR-g-PS). The thermal stability of the blends has been analysed by thermogravimetry. Differential scanning

calorimetry has been used to analyse the glass transition temperatures of the blends. The effects of blend composition and compatibiliser loading on the thermal properties have been analysed.

8.1 Results and discussion

8.1.1 Thermogravimetry (TG)

Thermogravimetric plots of NR and PS are given in Figures 8.1 and 8.2, respectively. Three regions of temperatures (up to 250°C, 250-450°C, and higher than 450°C) are considered in discussing the thermal stability of NR. Below 250°C, solid rubber is quite stable. In the absence of oxygen crude rubber may be kept for long periods with no loss of low-molecular weight products from thermal reactions. Degradation of NR occurs in two steps. First step degradation starts at about 267°C and will be completed at 458°C. During this stage 85.88% weight loss is observed and volatilisation becomes rapid and substantially complete distillation will be occurred. According to Bolland and Orr[7] there is little or no loss of unsaturation of bulk rubber in the temperature range of 200-270°C, although the rubber is undergoing both scission and crosslinking. The second step degradation starts at 460°C and will be completed at 600°C. During this stage, weight loss obtained is 11.11%. About 3.01% pot residue remains above 600°C which is insoluble and intractable and has been likened to cyclised rubber. The first step degradation occurs at a sharp rate compared to second step degradation. The weight loss observed at 300°C is 3.6% and that at 400°C is 78.5%. In the DTG curve, the major peak is observed at 373°C. This corresponds to the complete distillation of NR. Above 300°C, volatilisation becomes rapid. Complete distillation occurs in 30 minutes at temperature near 400°C. Degradation of NR can be explained by the following chemical reactions.[8] A variety of products are obtained; of which the common product is levulinaldehyde.
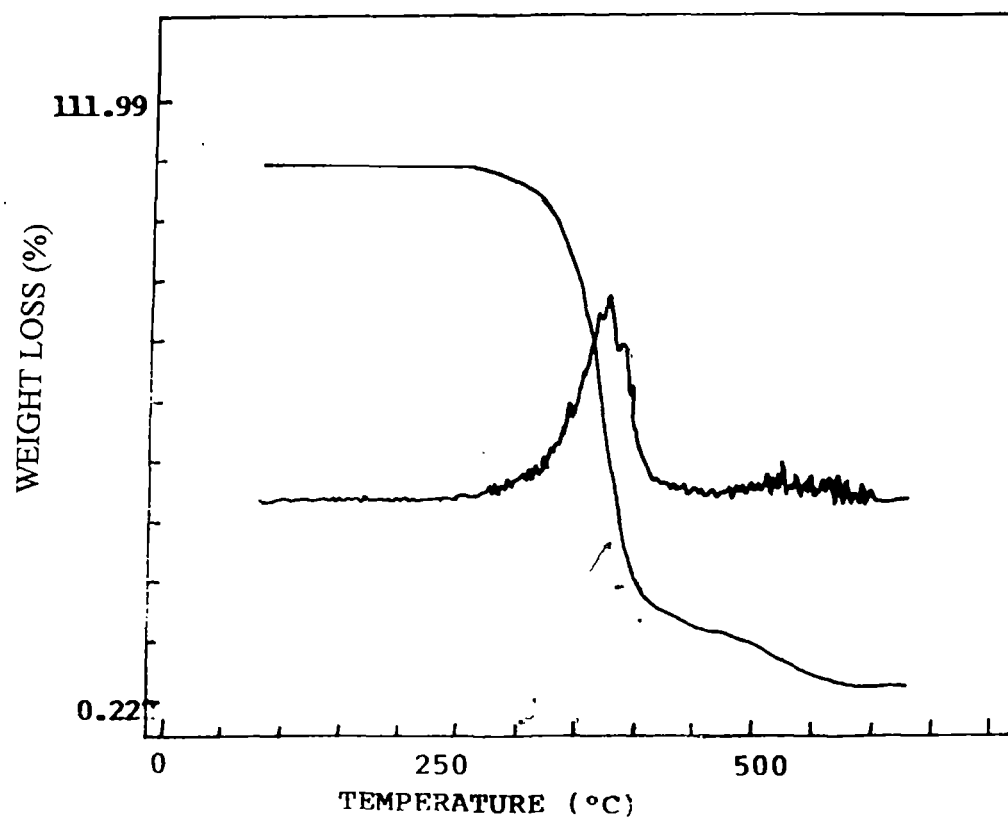
Figure 8.1.   TG and DTG curves of NR.
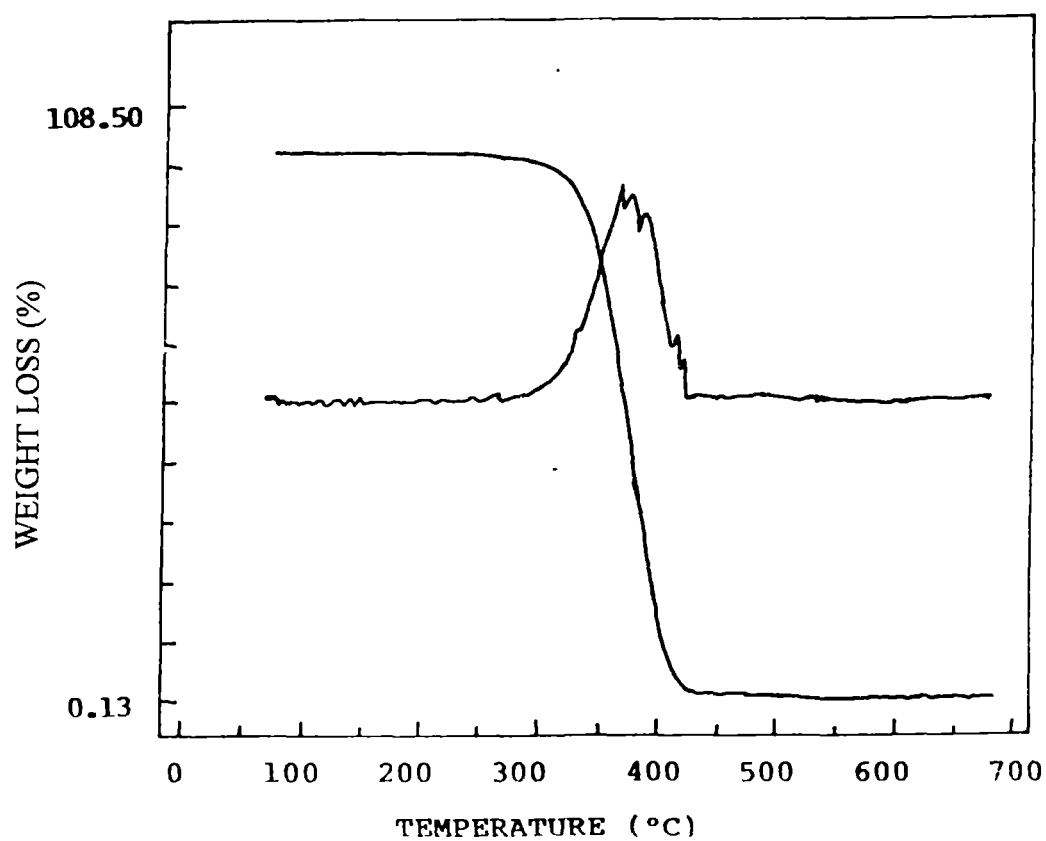
Figure 8.2.   TG and DTG curves of PS.

$$R\cdot \ + O_2 \rightarrow \ ROO\cdot$$

$$ROO\cdot \ + RH \rightarrow ROOH + R\cdot$$

$$2ROOH \rightarrow ROO\cdot \ + RO\cdot \ + H_2O$$

```
       CH3               CH3
        |                 |
wwCH2-C=CH-CH2-CH2-C=CHwww        ROO·
                                 ───────→
```

```
       CH3               CH3
        |                 |
wwCH2-C=CH-CH2-CH2-C=CHww          O2
                     • |          ───→
                      OOR
```

```
       CH3               CH3
        |                 |
wwCH2-C=CH-CH2-CH2-C-CHww
                      |  |         ───────→
                     •OO OOR
```

```
       CH3               CH3
        |•                |
wwCH2-C-CH-CH2-CH2-C-CHww           O2
         |            |  |         ───→
         O────────────O OOR
```

```
       CH3               CH3
        |                 |
wwCH2-C-CH-CH2-CH2-C-CHww           RH
      |  |            |  |         ───────→
     •OO O────────────O OOR
```

```
       CH3               CH3
        |                 |
wwCH2-C-CH-CH2-CH2-C-CHww
      |  |            |  |         ───────→
     HOO O────────────O OOR       -HO·
```

```
       CH3               CH3
        |                 |
wwCH2-C-CH-CH2-CH2-C-CHww
      | |            |  |          ───────→
     •O O────────────O OOR
```

```
       CH3               CH3
        |                 |
wwCH2-C  + O=CH-CH2-CH2-C  + CHww  + RO•
      ||                ||    ||
      O  Levulinaldehyde O    O
```
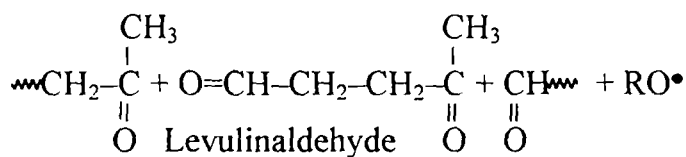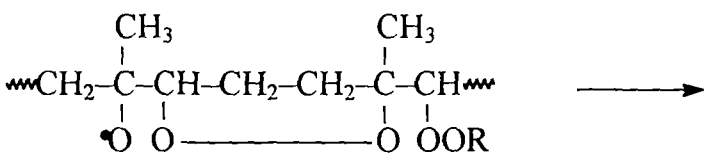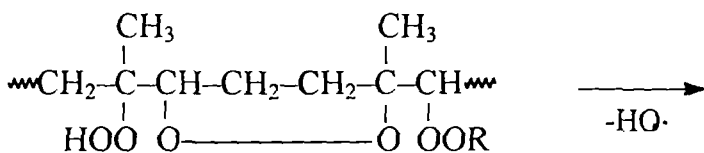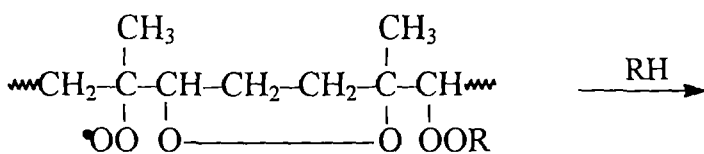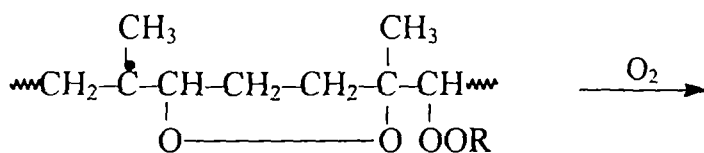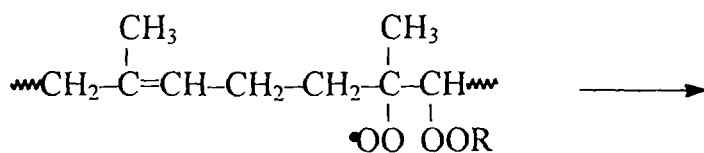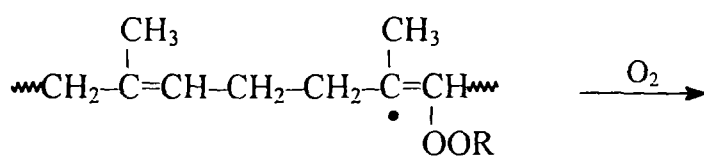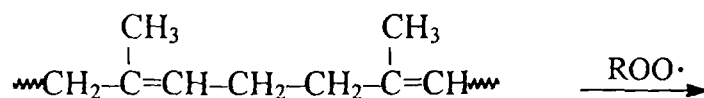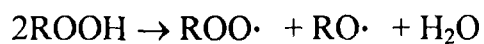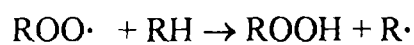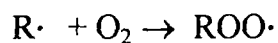
In the case of polystyrene, degradation is observed in a single step (Figure 8.2). Up to 240°C it is stable and thereafter a sharp degradation occurs. Degradation will be completed at 510°C and during this stage the weight loss observed is 99.05%, i.e., above 510°C no residue remains because the products of degradation are volatile. The weight loss at 300°C is 3.53% and that at 400°C is 84.9%. In the DTG curve, the major peak is observed at 372°C which corresponds to the complete chain scission to volatile monomers along with minute amounts of dimer, trimer, tetramer and pentamer. Polystyrene degrades at elevated temperature (above 300°C) to a mixture of low molecular weight compounds. These include styrene (40%), toluene (2.4%), methyl styrene (0.5%) and other products having an average molecular weight of 264.

In the case of PS, the degradation depends upon whether it is above or below 300°C. Between 200-300°C the molecular weight falls, but no volatile products are evolved. Below 300°C, random scission probably involves initial homolysis as shown below.

$$\sim\!\!\sim\!CH_2\!-\!CH\!-\!CH_2\!-\!CH\!-\!CH_2\!\!\sim\!\!\sim \rightarrow \sim\!\!\sim\!CH_2\!-\!CH\cdot \quad + $$

|
Ph

|
Ph

|
Ph

(A)

$$\cdot CH_2\!-\!CH\!-\!CH_2\!-\!CH\!\sim\!\!\sim \rightarrow \sim\!\!\sim\!CH_2\!-\!CH_2 + CH_2 = C\!-\!CH_2\!\!\sim\!\!\sim$$

|
Ph

|
Ph

|
Ph

|
Ph

(B)   (C)   (D)
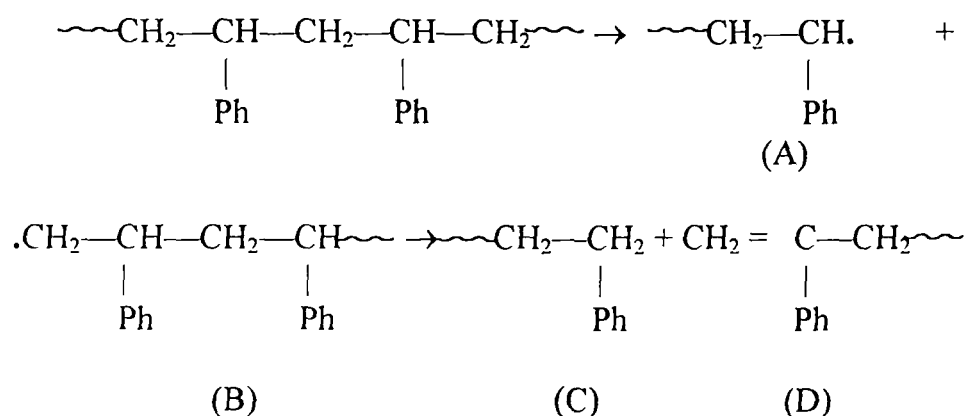
Since below 300°C no volatile products results, (A) and (B) are believed to undergo a cage disproportionation. In this temperature range depolymerisation does not occur. The products (C) and (D) are stable up to 300°C.

As compared to the degradation pattern of individual components, degradation behaviour of the blend is slightly different. It has been reported that a

marginal stability can be achieved by the incorporation of a second polymer.[9] The

TG and DTG plots of different NR/PS blends are given in Figures 8.3-8.5. All

DTG curves show two peaks, a minor peak and a major one. These correspond to

the respective monomer evolution. Table 8.1 gives the DTG peak values of

different blends. The first peak value near 400°C corresponds to NR degradation

and the second peak value near around 440°C corresponds to PS degradation. In

the case of blends, two peaks are obtained in all the cases, corresponding to the

degradation of the two component polymers NR and PS. It was found that as the

NR content increases, both these peak values increase. The temperatures at which

degradation start are 140, 193 and 250°C for S_{40}, S_{50} and S_{60} NR/PS blends

respectively. As the NR content increases, improvement in the initial

decomposition behaviour of the blends is observed.
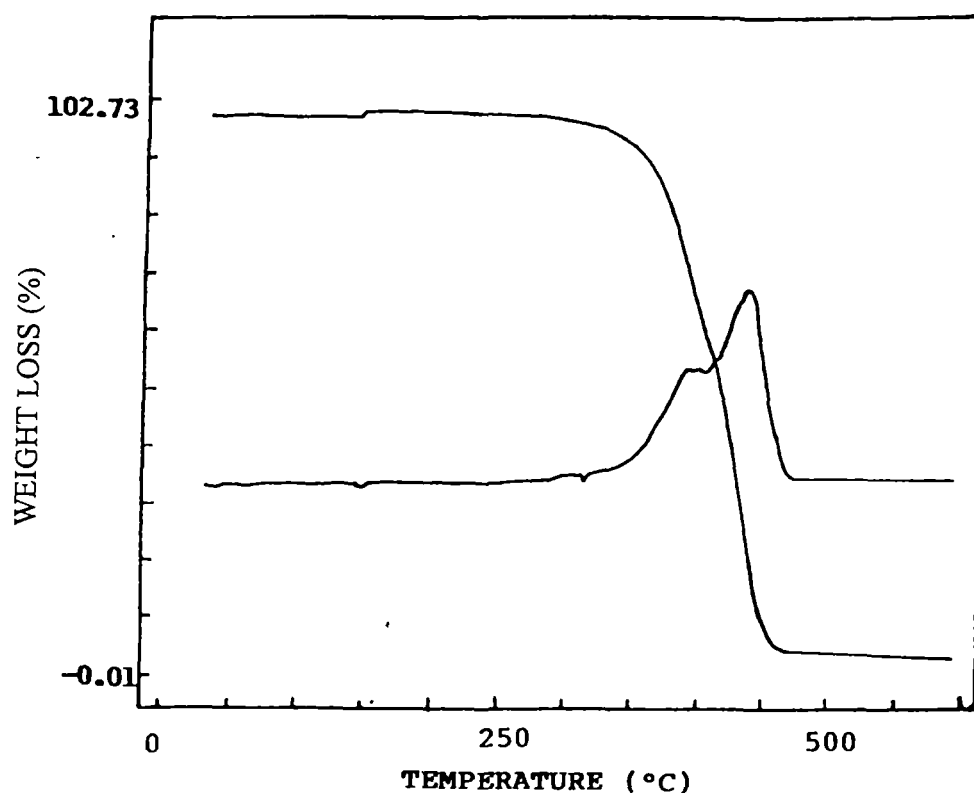
Figures 8.3.   TG and DTG curves S_{40}.
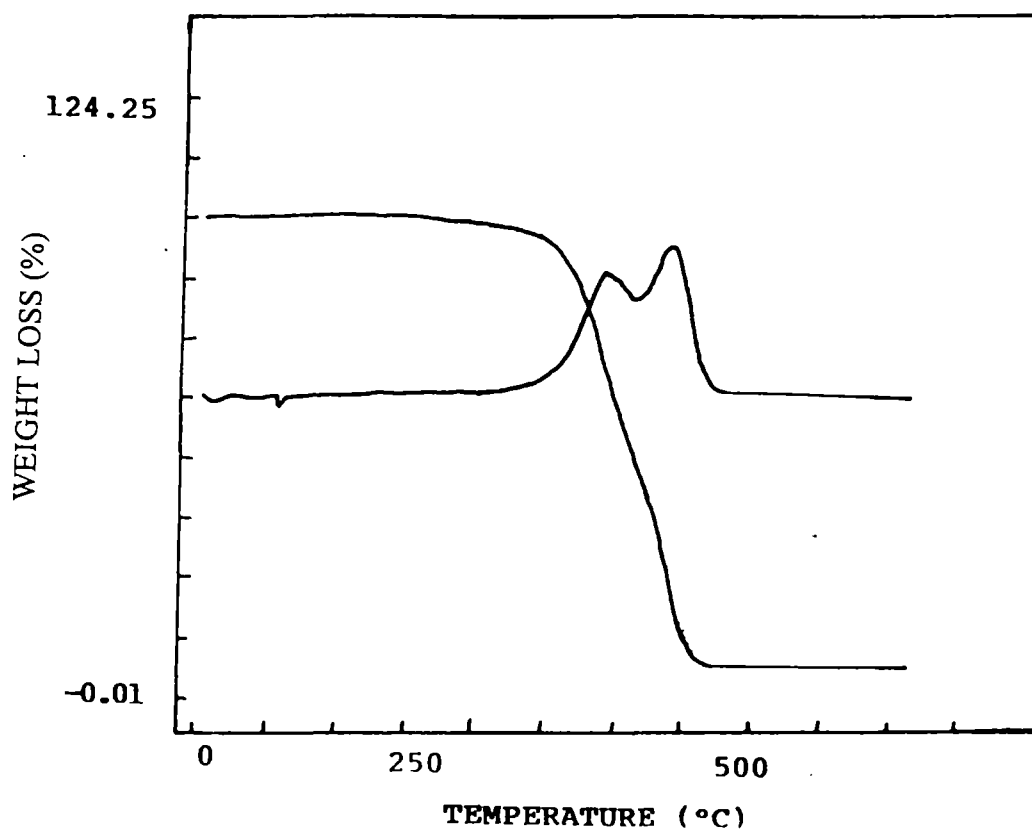
Figures 8.4. TG and DTG curves S_{50}
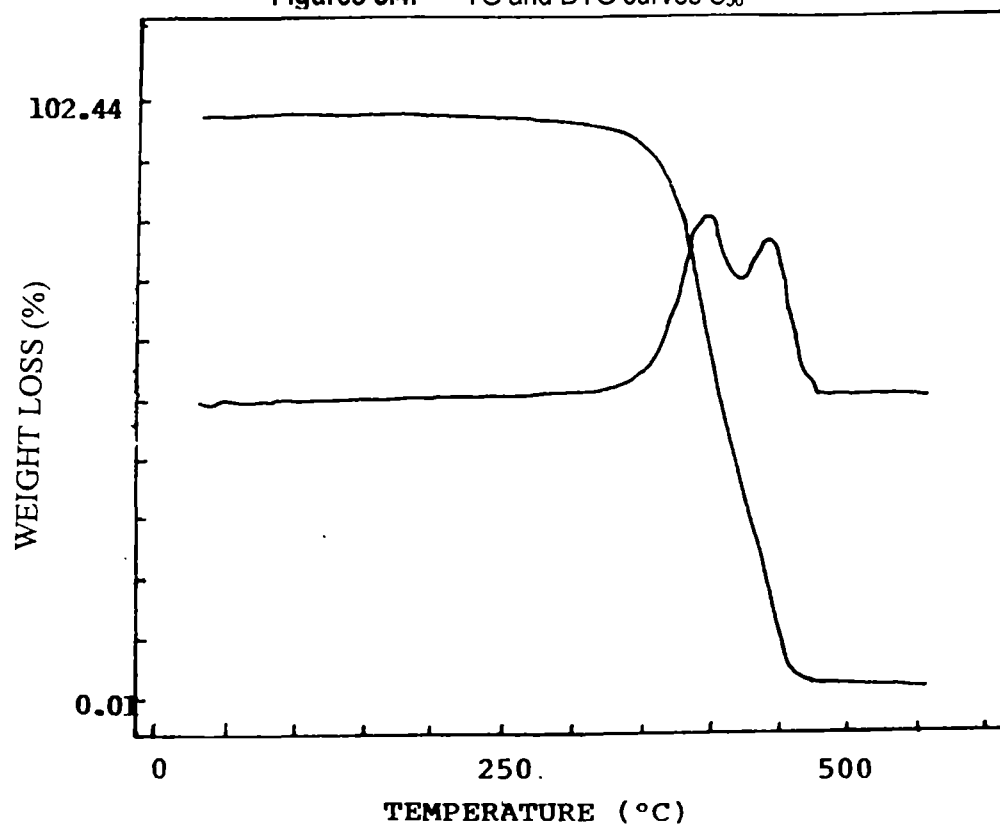
Figures 8.5. TG and DTG curves S_{60}

Table 8.1. DTG peak values of different NR/PS blends.

Samples	1st peak (°C)	2nd peak (°C)
S_{40}	391.2	434.6
S_{50}	392.8	437.8
S_{60}	393.9	440.6
SG_a	395.8	438.2
SG_b	395.9	440.9
SG_c	395.9	442.2

McNeill and Gupts[10] reported using thermogravimetry that both the rate of volatile formation and the rate of chain scission of polyisoprene are reduced when blended with polystyrene. In the pyrolysis of polyisoprene/ polystyrene blends, each component degrades in a manner different from that observed when polyisoprene is degraded separately. But the products of pyrolysis are identical both qualitatively and quantitatively. PS appears to be stabilised against thermal degradation at 340°C when blended with polyisoprene alone although its chain scission appears to be accelerated at 292°C. It can be explained by assuming that polyisoprene generates small radicals during chain scission in the first stage of degradation. As these radicals diffuse into the polystyrene phase, hydrogen abstraction takes place, and the radicals which would normally contribute to degradation of the polyisoprene (PI) are thus stabilised. Subsequently PS chains undergo scission at sites adjacent to the radical centres. The resulting PS radicals decompose slowly below 300°C. Above this temperature, there is an apparent inhibition of its depolymerisation by dipentene formed from the degradation of PI. This inhibition could result through the hydrocarbon abstraction by PS radicals from the dipentene or by coupling.

The weight loss of component polymers and the different blends are given in Table 8.2. It can be seen that at 300 and 400°C, the weight loss of the blend is lower than the blend components. It reveals that blending can improve the thermal

properties of the materials. As the NR content increases, the weight loss increases at both the temperatures. This is because NR is more susceptible to thermal degradation as compared to polystyrene.

Table 8.2. Weight loss of various NR/PS blends.

Sample	Weight loss at 300°C (%)	Weight loss at 400°C (%)
NR	3.60	78.5
PS	3.53	84.9
40/60 NR/PS (S_{40})	0.84	33.7
50/50 NR/PS (S_{50})	1.01	36.4
60/40 NR/PS (S_{60})	1.67	38.6

Compatibiliser has much influence on the thermal properties of the blends (Figures 8.6-8.9). For 50/50 NR/PS blends without compatibiliser, the degradation starts at 190°C. Upon the addition of 1.5% graft copolymer, the degradation temperature was raised to 214°C. Further addition of 1.5% graft copolymer (total 3%) raised the degradation temperature to 227°C. Finally the temperature at which degradation starts was raised to 250°C upon the addition of 4.5% graft copolymer. This is because, the graft copolymer addition improves the compatibility which in turn will be reflected in the thermal properties. Table 8.3 gives the weight loss at 300 and 400°C. Weight loss is decreased upon the addition of the compatibiliser throughout the temperature range which in turn is an indication of improvement of thermal properties. The morphology of the different NR/PS blends are shown in Figure 4.3 indicates the compatibilising action of the copolymer (NR-g-PS). In the case of blend without compatibiliser (Figure 4.3a) the domain size is higher. Upon compatibiliser loading, the domain size decreases (Figures 4.3b–4.3d) which is an indication of interfacial saturation.
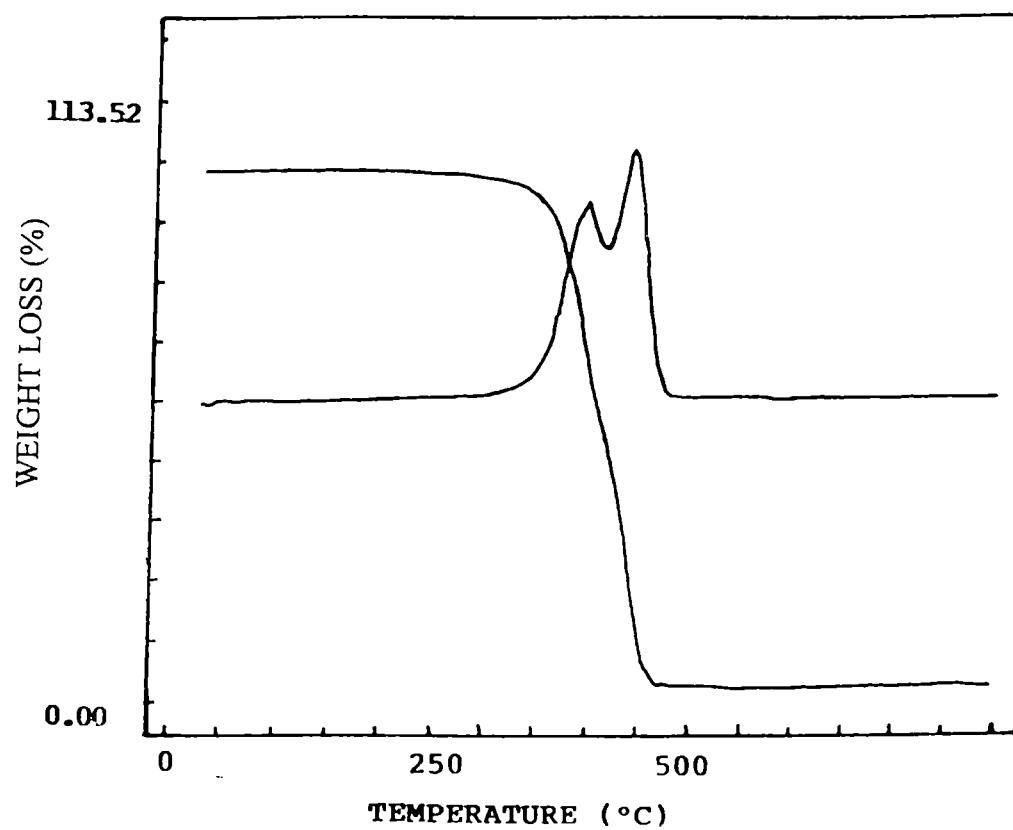
Figures 8.6.   TG and DTG curves SGa
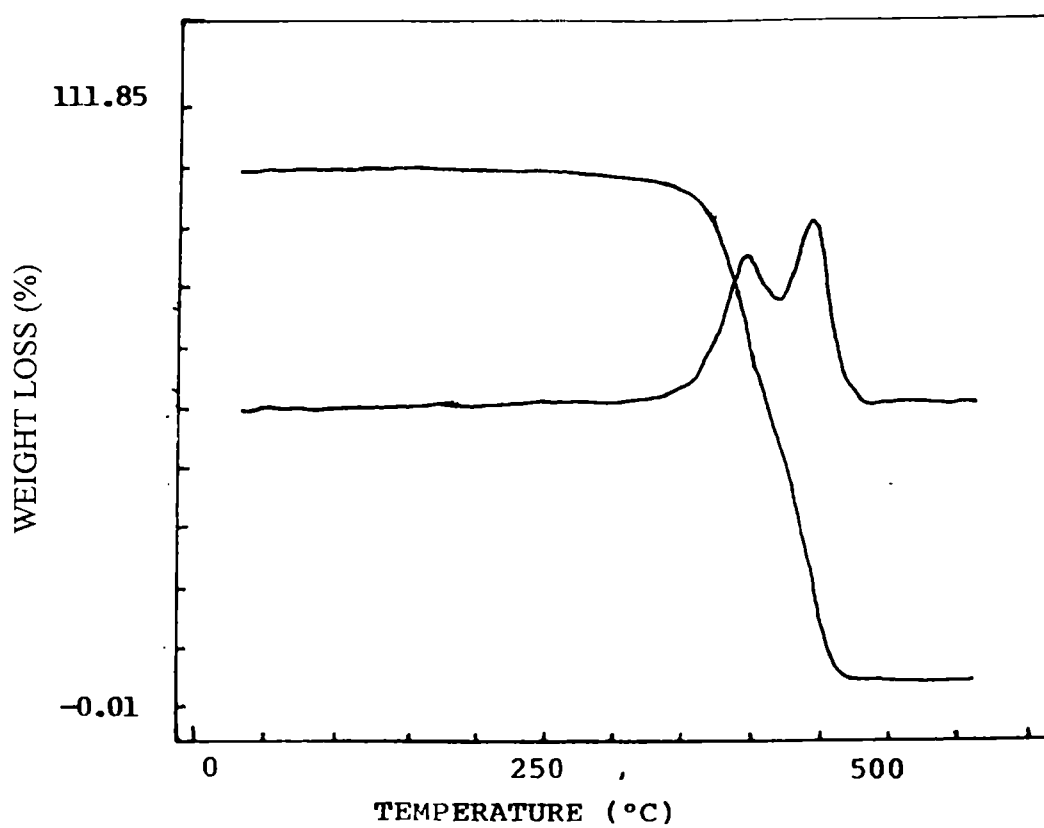
Figures 8.7.   TG and DTG curves SGb
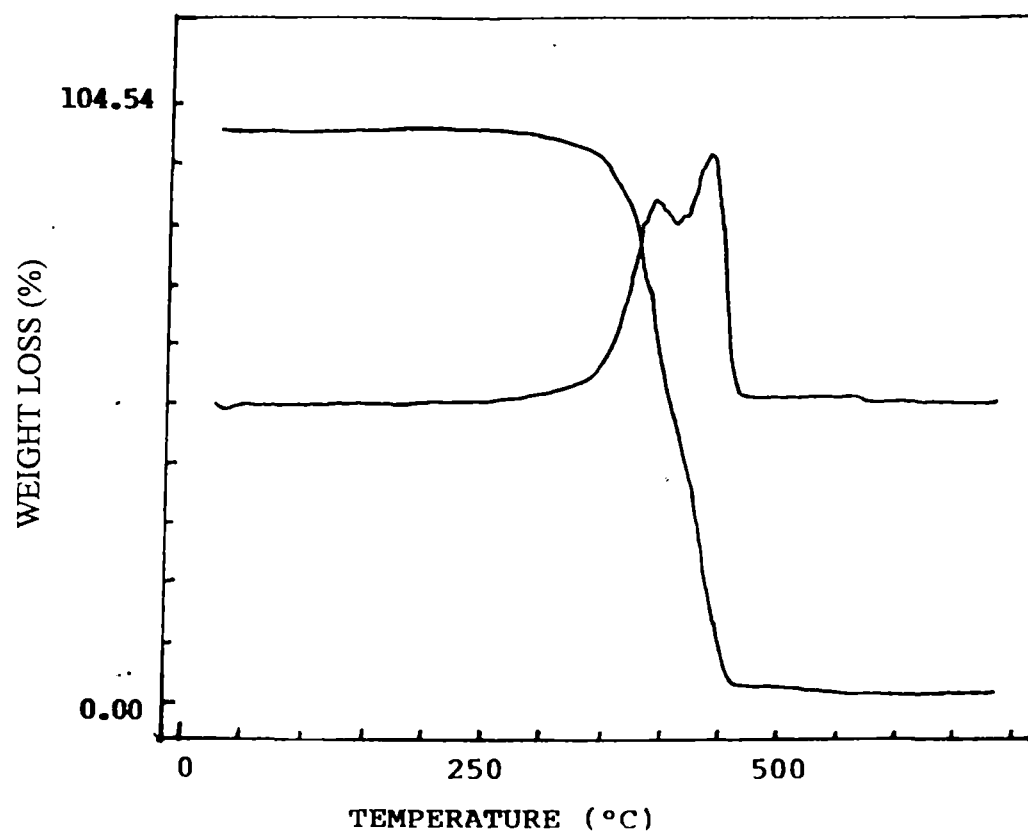
Figures 8.8.   TG and DTG curves SG$_c$
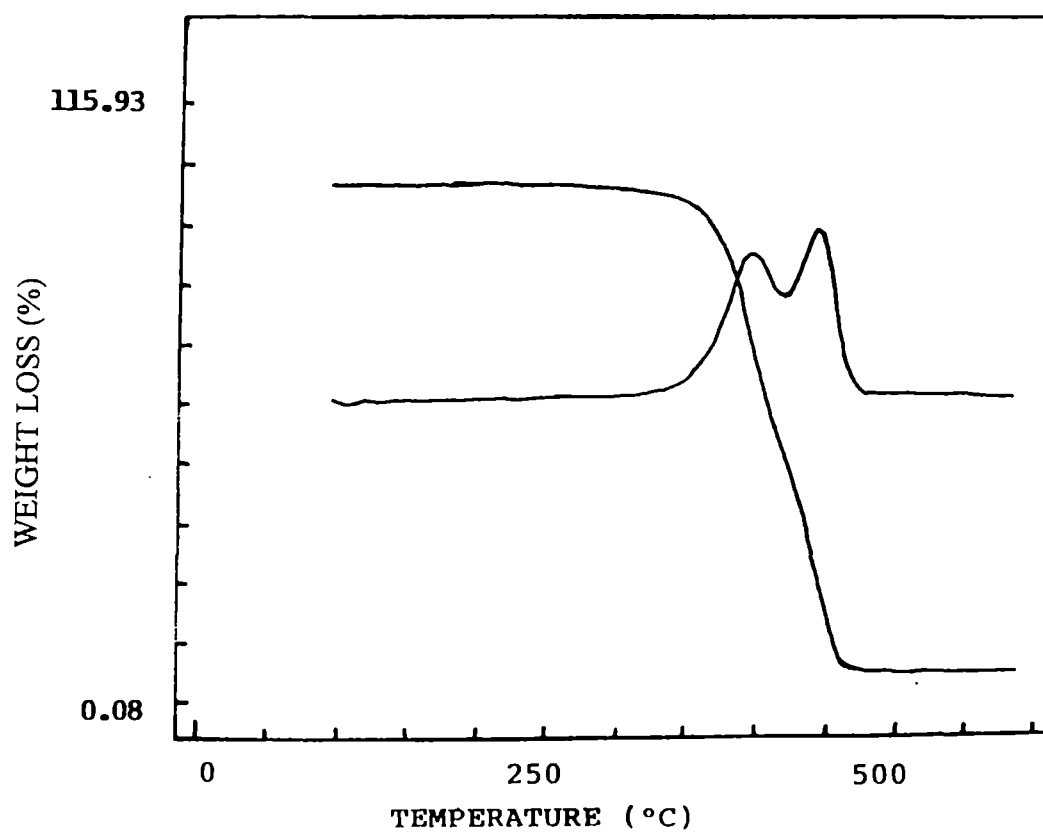
Figures 8.9.   TG and DTG curves SG$_d$

Table 8.3. Weight loss of NR/PS blends (compatibilised).

Percentage of graft copolymer	Weight loss at 300°C (%)	Weight loss at 400°C (%)
0	1.01	36.04
1.5	0.92	34.19
3	0.91	32.9

8.1.2 Differential scanning calorimetry studies (DSC)

The thermal behaviour of NR/PS blends with and without the addition of graft copolymer was analysed by DSC. Figure 8.10 shows the DSC traces of NR and PS. Glass transition temperature (Tg) was recorded at the half height of the corresponding heat capacity jump. The glass transitions of pure NR and PS are found to be -49 and + 101°C, respectively. Glass transition values of the various blends without and with the graft copolymer are given in Tables 8.4 and 8.5, respectively. The blends show two glass transitions even the presence of the graft copolymer are shown in Figures 8.11 and 8.12. This reveals that the blends are incompatible and phase separated. This is in agreement with the conclusions made by Paul[11] who suggested that if two polymers are far from being miscible, then no copolymer is likely to make one phase system, the main role of the copolymer is to act as an interfacial agent.

Table 8.4. Glass transition temperature of different NR/PS blends.

Sample	Tg value (°C)
NR	-49
PS	+102
S_{40}	-49 and +113
S_{50}	-52 and +101
S_{60}	-52 and +112

Table 8.5. Glass transition of different NR/PS blends (compatibilised).

Sample	Tg value (°C)
S_{50}	-52 and + 101
SG_a	-54 and + 118
SG_b	-55 and + 119
SG_c	-54 and + 112
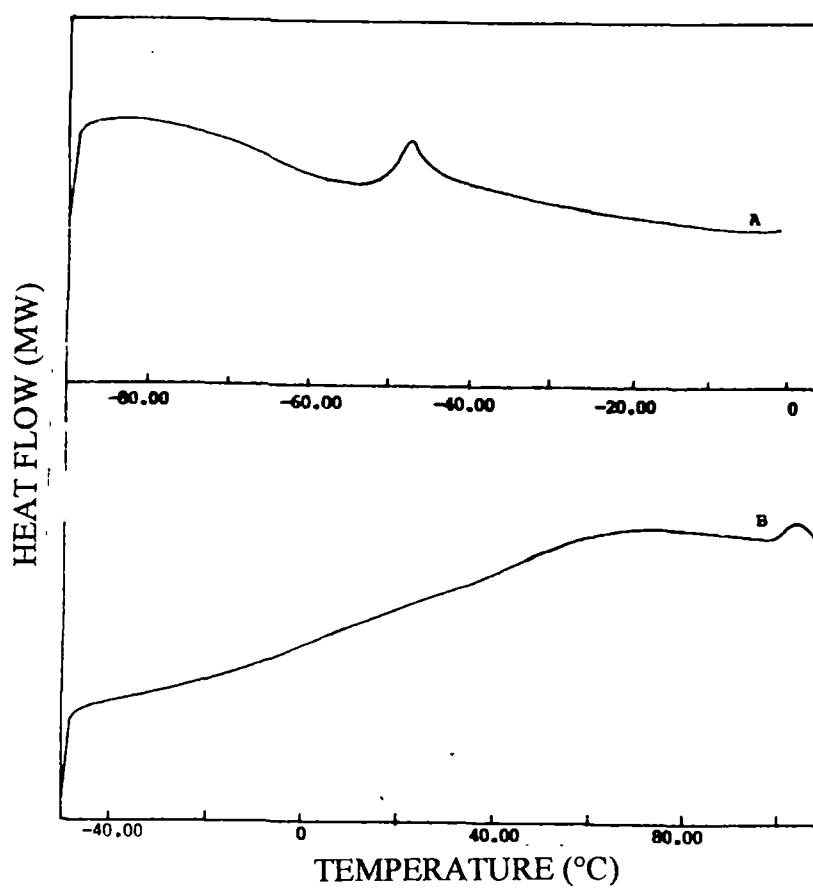
Figure 8.10. DSC curves of (A) NR and (B) PS.
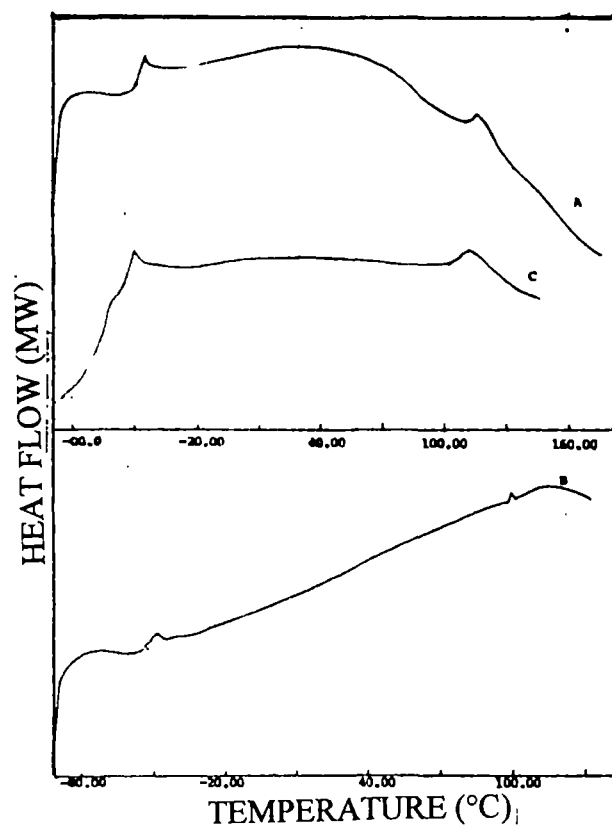
Figure 8.11. DSC curves of NR/PS blends (Non-compatibilised) (A) S_{40}, (B) S_{50}, (C) S_{60}.
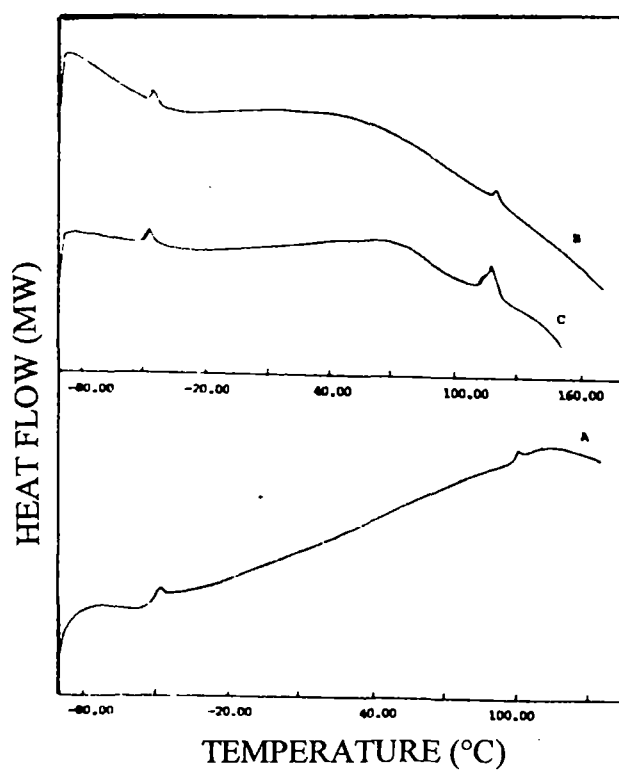
Figure 8.12. DSC curves of NR/PS blends (compatibilised) (A) S_{50}, (B) SG_a, and (C) SG_b.

8.2 References

1. I. C. McNeill, *Thermal Degradation, Comprehensive Polymer Science-6*, (Ed., G. Allen), Pergamon Press, New York, 1989, Ch. 15.

2. N. Grassie, I. C. McNeill and I. F. McLaren, *Eur. Polym. J.*, **6**, 679 (1970).

3. B. Dodson and I. C. McNeill, *J. Polym. Sci., Polym. Chem. Ed.*, **14**, 353 (1976).

4. P. P. Lizymol, and S. Thomas, *Polym. Degrad. Stab.*, **41**, 59 (1993).

5. K. T. Varughese, *Kautschuk + Gummi Kunststoffe*, **41(11)**, 1114 (1988).

6. T. O. Ahn, C. K. Kim, B. K. Kim,, H. M. Jeong and J. D. Huh, *Polym. Eng. Sci.*, **30** (1990) 341.

7. J. L. Bolland and W. J. C. Orr, *Trans. Inst. Rubber Ind.*, **21**, 133 (1945).

8. K. J. Saunders, *Organic Polymer Chemistry* (2nd Edn.), Chapman and Hall, New York, 1988, p. 460.

9. N. Grassie, *Encyl. of Polym. Sci. Technol.*, Vol. 4, John Wiley and Sons, Inc., New York, 1967, p. 159.

10. I. C. McNeill and S. N. Gupts, *Polym. Degrad. Stab.*, **2**, 95 (1980).

11. D. R. Paul, *Polymer Blends,* (Eds., D. R. Paul and S. Newman), Academic Press, New York, 1978, Ch. 12.

Chapter 9

Transport of Aliphatic Hydrocarbon Liquids Through Dynamically Crosslinked NR/PS Blends

Transport of organic solvents through polymeric materials is an important area, which finds applications in innumerable fields. Molecular transport of solvents through polymers has become the subject of several studies and a great attention has been drawn in the field of diffusion, sorption and permeation. There has been a tremendous increase in the use of polymers as structural engineering materials and a knowledge about the performance of polymers under the influence of external forces like the presence of solvents, temperature, etc. is essential. The sorption and transport of various solvents through polymeric materials are the basis of a wide variety of applications like food packaging, controlled drug release, reverse osmosis, etc.

A detailed study of the transport behaviour of penetrants through different rubbery polymers has been reported by Aminabhavi and coworkers.[1-4] The Fick's laws of diffusion has been found to control the transport behaviour in many cases. But there are cases in which the sorption studies show deviation from the typical Fickian trend.[5]

Mesorbian and Ammondson[6] reported the permeability of n-heptane, methyl salicylate and methyl alcohol through polyethylene-nylon blends.

Cabasso *et al.*[7] studied the sorption of benzene-cyclohexane mixtures through polymer blends composed of poly(phosphonates) and acetyl cellulose. The blends are found to be selectively absorbing benzene from benzene-cyclohexane mixtures.

Molecular transport of haloalkanes through blends of ethylene-propylene copolymer and isotactic polypropylene has been studied by Aminabhavi and Phayde.[8]

The main objective of the present chapter is to investigate the effect of dynamic crosslinking on the diffusion and sorption behaviour of aliphatic hydrocarbon liquids through natural rubber/polystyrene blends in the temperature range of 28-58°C. The effects of penetrant size, temperature, blend composition and crosslink density on the diffusion and sorption behaviour have also been investigated. The kinetic and thermodynamic data connecting the sorption, diffusion and permeation processes have been computed.

9.1 Results and discussion

9.1.1 Effect of vulcanising system

Figures 9.1 and 9.2 show the diffusion curves of 50/50 NR/PS blends at 28 and 48°C, respectively. The blends were vulcanised with different vulcanising systems, viz., sulphur, DCP and a mixed system of the two. The solvent used was mineral turpentine. In all the cases, the uptake increases linearly at first and later it levels off. This indicates the attainment of complete equilibrium. A similar trend is observed in the other two solvents, viz., petrol and diesel also. It is clear from Figures 9.1 and 9.2, that the sample crosslinked by sulphur absorbs the highest amount of solvent whereas that crosslinked by peroxide takes the lowest. The mixed system occupies an intermediate position. The same trend is observed at 48°C also, i.e., the Q_t mol per cent values decrease in the order sulphur > mixed > peroxide. The sorption behaviour of the samples can be attributed to the differences in (1) the dispersed particle size of the systems vulcanised by the three different techniques, (2) the nature of crosslinks and (3) crosslink density. As the dispersed particle size increases, the degree of close packing decreases leading to an increased free volume supporting the maximum solvent uptake. The size of the dispersed rubber phase varies in the order sulphur > mixed > peroxide. This supports the highest solvent uptake by the sulphur system and lowest uptake by the peroxide system.
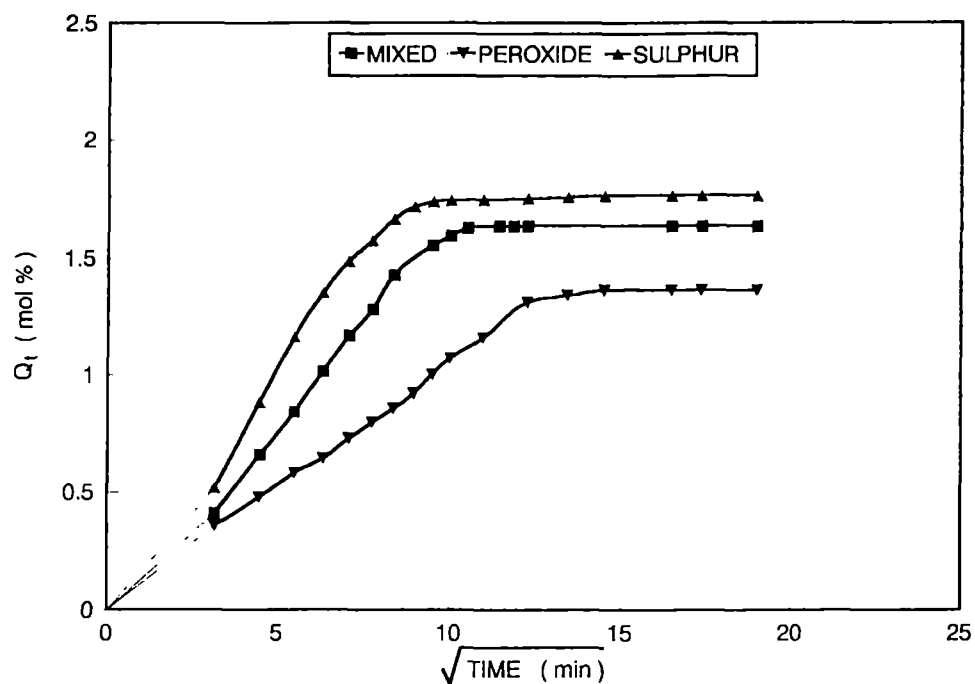
Figure 9.1. Mol per cent uptake of mineral turpentine by 50/50 NR/PS blends with different crosslinking systems at 28°C.
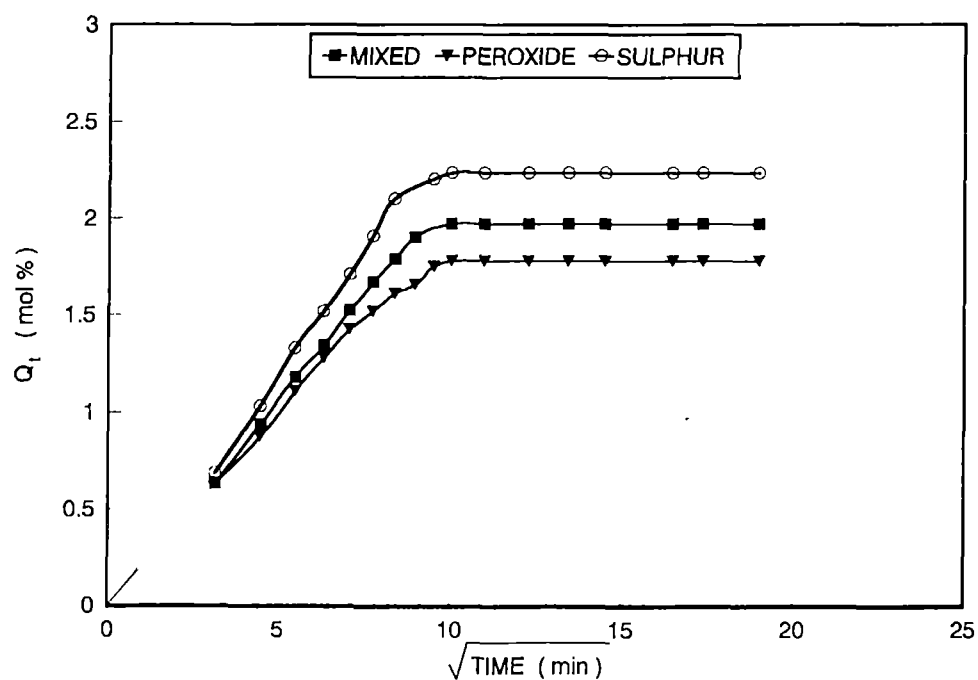
Figure 9.2. Mol per cent uptake of mineral turpentine by 50/50 NR/PS blends with different crosslinking systems at 48°C.

Additionally Morrison and Porter[9] showed that the sorption behaviour of rubber vulcanisates can be explained in terms of the nature of crosslinks between different rubber chains. The nature of different networks possible during crosslinking are shown in Figure 3.22. The mono, di and polysulphidic linkages in sulphur system impart high chain flexibility to the polymer network and this help to accommodate more solvents between the polymer chains. In the DCP system only rigid C-C linkages are present which hinder the penetration of solvent molecules through the polymer matrix and this accounts for the minimum solvent uptake. In mixed system all these mono, di, polysulphidic and C-C linkages are present and hence it shows an intermediate behaviour. The same trend is observed in the other two solvents also. The values of bond energies and bond lengths of different bonds support this view (Table 9.1). The longer and more labile polysulphidic linkages can accommodate more solvent. The polysulphidic linkages can undergo rearrangement under different strains. Therefore, it can take up more solvent.

Table 9.1. Bond length and bond energies of different types of chemical linkages.

Type of bond	Bond length (Å)	Bond energy (Kcal/mol)
C-C	1.54	85
C-S	1.81	64
S-S	1.88	57

We have further calculated the molar mass between the crosslinks (M_c) which gives a quantitative assessment of the crosslink density. For calculating M_c, it is essential to know the polymer-solvent interaction parameter χ which can be calculated using the following equation.[10]

$$\chi = \frac{(d\phi / dT)\{[\phi / (1-\phi)] + N\ln(1-\phi) + N\phi\}}{2\phi(d\phi / dT) - \phi^2 N(d\phi / dT) - \phi^2 / T} \qquad (9.1)$$

where ϕ is the volume fraction of the material in the swollen sample and N is calculated from ϕ as follows.

$$N = \frac{[\phi^{2/3}/3 - 2/3]}{[\phi^{1/3} - 2\phi/3]} \qquad (9.2)$$

Knowing the value of χ, the molar mass between the crosslinks (M_c) can be calculated using the following equation.[2,11]

$$M_c = \frac{-\rho_p v\phi^{1/3}}{[\ln(1-\phi) + \phi + \chi\phi^2]} \qquad (9.3)$$

where ρ_p is the density of the polymer, v is the molar volume of the solvent and ϕ is the volume fraction of the polymer in the fully swollen state.

The volume fraction of the polymer (ϕ) in the fully swollen state, is determined by the equation[12,13]

$$\phi = \frac{W_1/\rho_1}{W_1/\rho_1 + W_2/\rho_2} \qquad (9.4)$$

where W_1 and ρ_1 are the weight and density of the polymer sample respectively and W_2 and ρ_2 are the weight and density of the solvent. The value of ϕ is given in Table 9.2. The values of interaction parameter (χ) and (M_c) are given in Table 9.3. The estimated values of χ for sulphur, mixed and DCP systems are 1.38, 1.43 and 1.66, respectively, i.e., the χ value is highest for DCP system and lowest for sulphur system. This result is in agreement with the change in Q_∞ values for different vulcanising systems. The estimated values of (M_c) are also given in Table 9.3. These values are in the order sulphur > mixed > DCP. The order of which is the same as that of Q_∞ values. As M_c increases, the area between the different crosslinks increases, decreasing the number of crosslinks per chains. Hence the total volume of solvent molecules that can be accommodated between the crosslinks increases. Sulphur system shows the maximum value, the DCP system the minimum and the mixed system occupies the intermediate position.

Table 9.2.   Volume fraction (φ) and equilibrium sorption (Q∞) of swollen NR/PS blends.

Tempera- ture (°C)	φ			Q∞ (mol%)		
	Sulphur	Mixed	DCP	Sulphur	Mixed	DCP
. 28	0.20	0.22	0.27	1.76	1.63	1.23
48	0.18	0.20	0.21	2.07	1.80	1.73
58	0.17	0.19	0.20	2.23	1.97	1.77

Table 9.3.   Values of interaction (χ) parameter and molar mass between crosslinks (Mc).

Sample	χ	Mc
30/70 NR/PS/sulphur	1.51	1665
40/60 NR/PS/sulphur	1.57	1404
50/50 NR/PS/sulphur	1.38	3385
50/50 NR/PS/DCP	1.66	1749
50/50 NR/PS/sulphur/DCP	1.43	3264

The volume fraction of swollen material decreases in the order DCP > mixed > sulphur (Table 9.2). Since the volume fraction of swollen material is proportional to crosslink density and it can be concluded that as the volume fraction values decreases, the crosslink density decreases. Therefore, the solvent uptake follows the order DCP < mixed < sulphur.

In order to examine the changes in the matrix after attaining equilibrium in a solvent, the solvent saturated samples were desorbed fully. They were then reimmersed in the solvent to attain equilibrium saturation. The samples were then redesorbed. Thus, a sorption-desorption-resorption-redesorption technique has been employed to investigate the solvent effect. Mineral turpentine was used as the solvent. The plots of sorption-desorption-resorption-deresorption experiments

for sulphur cured samples are given in Figure 9.3. Desorption and resorption curves do not follow similar patterns. However, resorption and redesorption curves follow similar patterns. Compared to sorption process time to attain equilibrium and equilibrium sorption values are higher in the case of resorption process. During the sorption-desorption process, the polymer chains will undergo rearrangement and hence the subsequent resorption-redesorption process will be different from that of the former. Ferry[14] explained these effects based on the network relaxation in terms of the times required for the molecular rearrangements of the chains and that of the solvent diffusion into the polymer.
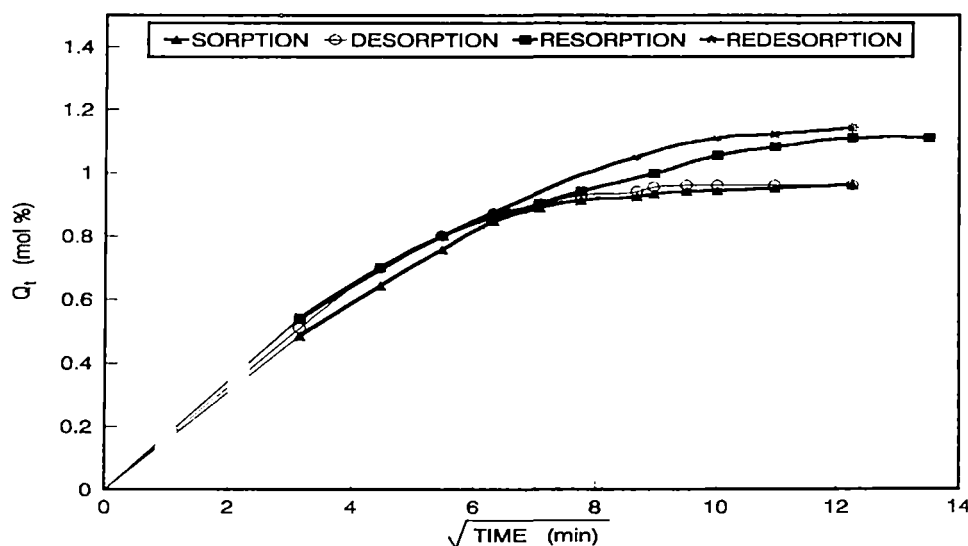
Figure 9.3. S-D-RS-RD curves for NR/PS/S blends.

9.1.2 Effect of penetrant size

The effect of different solvents such as petrol, mineral turpentine and diesel on the sorption behaviour of NR/PS blends have been studied in detail. As the size of the solvent molecules increases from petrol to diesel there is a decrease in the value of Q_t mol per cent. Figures 9.4 and 9.5 show the diffusion curves in 30/70 and 50/50 NR/PS blends, respectively. In both the cases, petrol shows the maximum value of Q_t mol per cent and diesel the minimum. Mineral turpentine occupies the intermediate positions. The decrease in Q_t mol per cent uptake with

increase in molecular weight of the solvent is due to the greater activation energy needed for activating the diffusion process. This is clearly understood from Table 9.4. It can be seen that the Q_∞ values decrease with increase in molecular weight of the solvent used. The behaviour is the same in all the different blend systems studied.
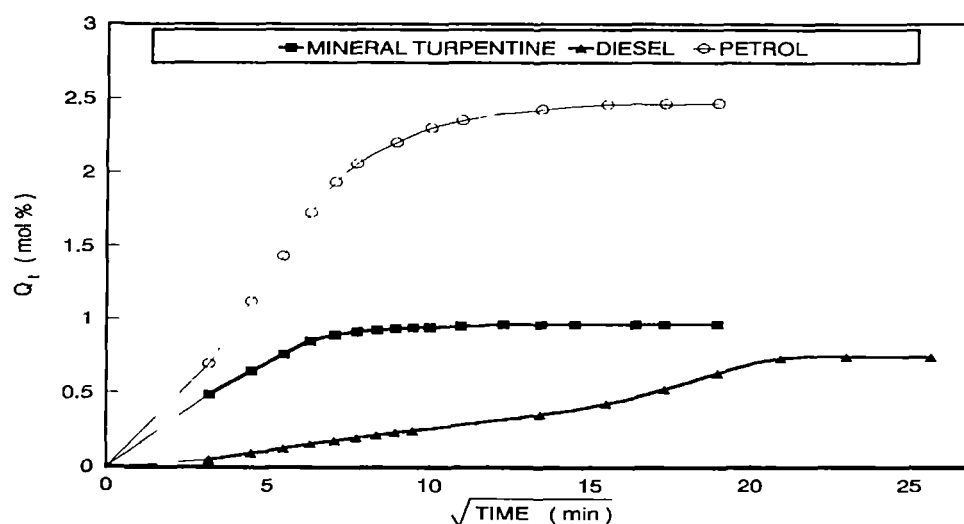
Figure 9.4.   Mol per cent uptake of petrol, diesel and mineral turpentine at 28°C by 30/70 NR/PS/S blend.
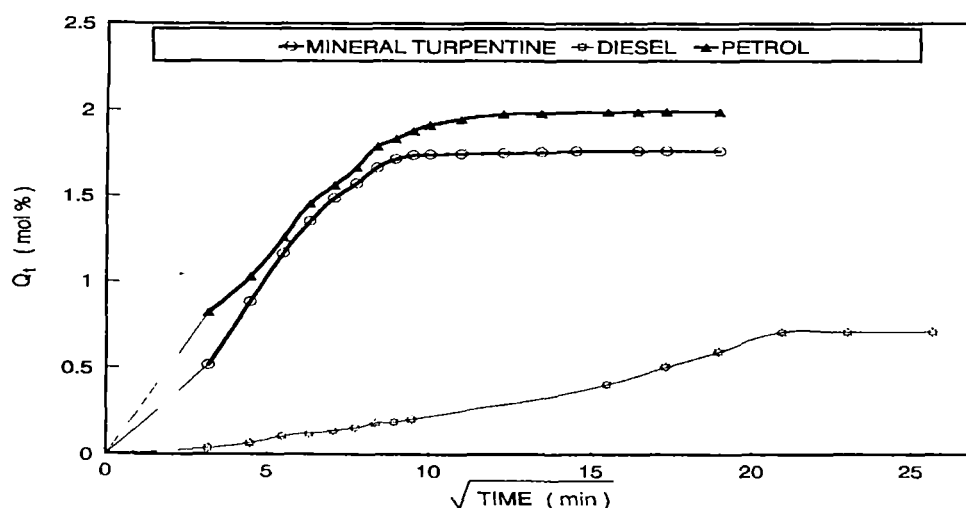
Figure 9.5.   Mol per cent uptake of petrol, diesel and mineral turpentine at 28°C by 50/50 NR/PS/S blend.

Table 9.4. Values of equilibrium sorption (Q∞) in different solvents.

Sample	Solvent	Q_∞ (mol%)
70/30/sulphur (28°C)	Petrol	2.48
	Mineral turpentine	0.96
	Diesel	0.73
50/50/sulphur (28°C)	Petrol	1.96
	Mineral turpentine	1.76
	Diesel	0.71

9.1.3 Mechanism of sorption

In order to understand the mechanism of transport of solvents through NR/PS blends, the results of sorption experiments were analysed using the following equation.[3,15,16]

$$\log (Q_t/Q_\infty) = \log k + n \log t \qquad (9.5)$$

where Q_t is the mol per cent sorption at time t and Q_∞ is that at equilibrium. k is a constant which depends upon the structural peculiarities of the system and its interaction with the solvent used. It gives some idea about the interaction between the blend components and solvents. The value of n gives us an idea about the mechanism of solvent transport. When the value of n=0.5, the sorption mechanism is termed as Fickian where the rate of polymer chain relaxation is higher than the diffusion rate of the penetrant. When n=1, the diffusion mechanism is said to be non-Fickian at which the chain relaxation is slower than the solvent diffusion. If the values lies between 1 and 0.5, then the mechanism is said to follow an anomalous trend where the polymer chain relaxation rate and the solvent diffusion rate are similar. The value of n and k obtained by the regression analysis using the data from the linear portions of the sorption curves are given in Table 9.5. In the

present study, the value of n is neither 0.5 nor 1. Instead it is between 0.3 and 1, thereby represent an anomalous transport trend. It can be seen that the n values decrease with a rise in temperature. There is no systematic variation in the value of n with respect to blend composition. In the case of dynamically vulcanised samples with different types of crosslinks, n values decrease with a rise in temperature and supports a Fickian mode of diffusion at high temperature. The n values of the DCP vulcanised samples are more close to the Fickian diffusion compared to the sulphur cured and mixed samples (Table 9.6). In general, the anomalous behaviour of the samples might be due to the leaching out of additives from the dynamically vulcanised samples. This sort of behaviour was also reported in the literature.[17] The time taken by the rubber chains in the blend to respond to the swelling stress and to rearrange themselves to accommodate the solvent molecules is also responsible for the anomalous behaviour of the samples.

Table 9.5. Analysis of sorption data of solvents through NR/PS blends at different temperatures.

Samples	Temperature (°C)	n	K (min^{-1})
30/70/sulphur	28	0.58	0.16
30/70/sulphur	48	0.48	0.28
30/70/sulphur	58	0.32	0.25
40/60/sulphur	28	0.86	0.01
40/60/sulphur	48	0.34	0.10
40/60/sulphur	58	0.28	0.13
50/50/sulphur	28	0.73	0.05
50/50/sulphur	48	0.55	0.08
50/50/sulphur	58	0.52	0.08

The value of k increases with rise in temperature suggesting an increase in the polymer-solvent interactions with temperature. In the case of dynamically vulcanised samples also, k value increase with rise in temperature (Table 9.6).

Table 9.6. Analysis of sorption data of dynamically crosslinked 50/50 NR/PS blends of different temperatures.

Samples	Temperature (°C)	n	k (min^{-1})
50/50/sulphur	28	0.73	0.05
50/50/sulphur	48	0.55	0.08
50/50/sulphur	58	0.52	0.08
50/50/DCP	28	0.44	0.10
50/50/DCP	48	0.55	0.08
50/50/DCP	58	0.39	0.13
50/50/sulphur/DCP	28	0.66	0.05
50/50/sulphur/DCP	48	0.52	0.08
50/50/sulphur/DCP	58	0.49	0.10

The effective diffusivity (D) of the polymer-solvent system is a kinetic parameter which can be calculated from the initial linear portions of the sorption curves using the following equation.[18]

$$\frac{Q_t}{Q_\infty} = 1 - \frac{8}{\pi^2} \sum_{n=0}^{\infty} 1/(2n+1)^2 \exp[-D(2n+1)^2\pi^2 t/h^2] \qquad (9.6)$$

where h is the initial sample thickness. Q_t, Q_∞ and t have the same meaning as before. For a short period of swelling, the following simplified equation can be used,[3,5,6]

$$D = \pi(h\theta/4Q_\infty)^2 \qquad (9.7)$$

where θ is the slope of the sorption curve before attainment of 50% equilibrium. Because of considerable swelling in a short period, a swelling correction is necessary to get the correct diffusion coefficient known as intrinsic diffusion coefficient (D*). This can be calculated using the following equation.

$$D^* = \frac{D}{\phi^{7/3}}$$ (9.8)

where D is the diffusivity and ϕ is volume fraction of rubber in the swollen sample. The estimated values of the intrinsic diffusion coefficient (D*) in the case of mineral turpentine are given in Table 9.7.

Table 9.7. Values of diffusion, sorption and permeation coefficients of different NR/PS blends.

Sample	Temperature (°C)	$D^* \times 10^7$ (cm^2/sec)	S (g/g)	$P \times 10^7$ (cm^2/sec)
30/70/sulphur	28	40.47	1.63	66.10
30/70/sulphur	48	13.13	1.80	23.71
30/70/sulphur	58	20.00	2.02	40.49
40/60/sulphur	28	27.86	1.51	42.22
40/60/sulphur	48	11.63	1.76	20.54
40/60/sulphur	58	9.25	1.95	18.09
50/50/sulphur	28	65.73	3.00	197.22
50/50/sulphur	48	14.99	3.52	52.80
50/50/sulphur	58	20.86	3.79	79.23
50/50/DCP	28	21.12	2.78	58.74
50/50/DCP	48	15.18	3.07	46.63
50/50/DCP	58	15.85	3.35	53.11
50/50/sulphur/DCP	28	10.41	2.09	21.83
50/50/sulphur/DCP	48	23.63	2.94	69.56
50/50/sulphur/DCP	58	12.29	3.02	37.16

The variation in D values depends upon the nature of crosslinks, temperature and penetrant size. However, we could not find any systematic trend in the values of D in terms of the nature of crosslinks and temperature. The effect of penetrant size on D values is given in Table 9.8. It is seen that the diffusion coefficient values decrease with increasing molecular size of the penetrant. According to the free volume theory,[19,20] the rate of diffusion depends upon the ease with which polymer chain segments exchange their positions with penetrant molecules. Mobility of the polymer chains also depends upon the free volume in the matrix. As the size of the penetrant molecule increases, the ease of exchange becomes less, leading to a decrease in the value of diffusion coefficient.

Table 9.8. Values of diffusion, sorption and permeation coefficients of NR/PS blends in different solvents.

Samples	Solvent	$D^* \times 10^7$ (cm^2/sec)	S (g/g)	$P \times 10^7$ (cm^2/sec)
50/50/sulphur	Petrol	100.9	1.96	198.79
(28°C)	Mineral turpentine	65.7	3.00	197.22
	Diesel	3.1	2.31	7.36
30/70/sulphur	Petrol	46.52	2.48	65.82
(28°C)	Mineral turpentine	40.47	1.65	66.18
	Diesel	4.1	2.40	10.07

Joshi and Astarita[21] developed a model which relates the diffusion coefficient with the concentration of solvent. In this attempt the model parameters were varied by incrementing over a particular range and the fit to the experimental data was subjected to a linear regression analysis to get the best values. Diffusion coefficients which resulted from equation (9.6) was plotted against concentration (wt %) for 50/50 NR/PS blends containing different types of crosslinks (Figure 9.6). The D values are decreasing with the concentration of NR and thus showing an anomaly from the normal trend. The decrease of diffusivity with concentration in all the systems reveal the fact that lack of response of NR/PS blend

systems with solvent stress. Above 60 wt % of NR_j sulphur system shows the minimum value of D and the mixed system shows the highest value. Peroxide system occupies the intermediate position. Between 60-70 wt % of NR, peroxide system occupies the highest position. Below 70 wt % of NR sulphur system occupies the highest position, mixed system the minimum and peroxide system the intermediate position.
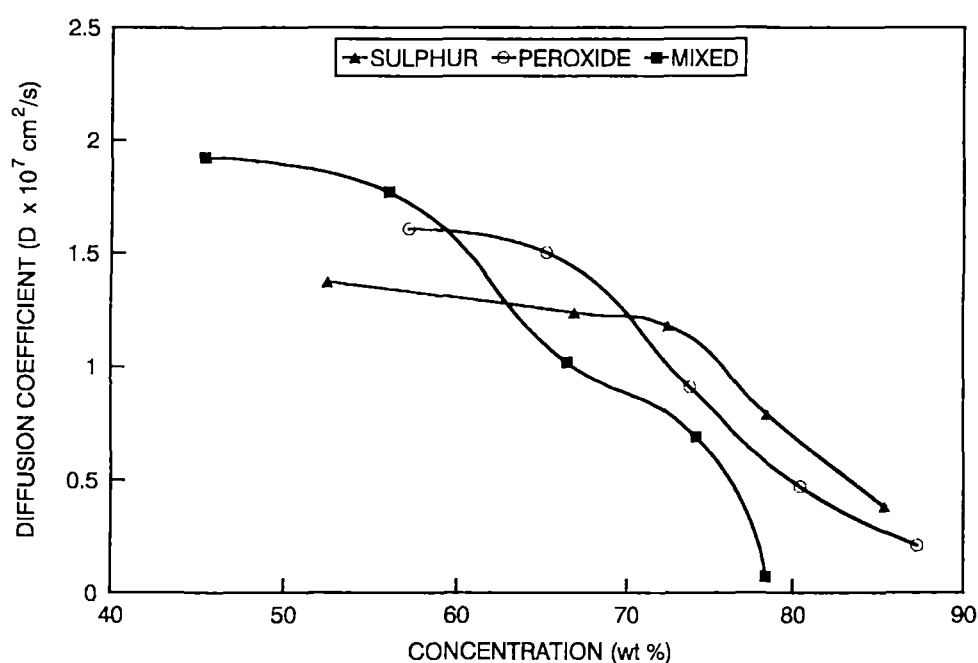
Figure 9.6. Concentration dependence of diffusivity at 28°C for different vulcanising systems using mineral turpentine as the solvent.

The solubility or the sorption of the penetrant molecule is also an important parameter as far as the permeation of a penetrant molecule into a polymer matrix is concerned. Sorption describes the initial penetration and dispersal of permeant molecules into the polymer matrix. Sorption coefficient (S) is obtained as the maximum saturation sorption value and can be calculated using the following equation,[17]

$$S = M_s/M_p \qquad (9.9)$$

where M_s is the mass of the penetrant molecule at equilibrium swelling and M_p is the mass of the polymer sample. The variation of sorption coefficient with temperature is given in Table 9.7. The value increases with temperature and this suggests an increase in the solvent uptake with temperature. It is found that the sorption coefficient is maximum for the sulphur system and minimum for the peroxide (DCP) system. The mixed system occupies the intermediate position. The higher value for sulphur system is an indication of the better accommodation of the solvent molecules in the highly flexible polymer matrix. The minimum value of sorption coefficient in the case of DCP system is due to the fact that the less flexible C-C network can accommodate minimum amount of the solvent. However, the variation of sorption coefficient (s) with penetrant size does not show a systematic trend.

The process of permeation is a combined process of diffusion and sorption and hence the permeability coefficient (P) depends upon both diffusivity (D) and sorptivity (S). It can be calculated using the following equation,[17,22]

$$P = D.S \tag{9.10}$$

This relationship holds for the permeation process when D obeys the Fick's law and S obeys Henry's law. Permeability coefficient values in different solvents are given in Table 9.8. It is found that the values decrease with increasing molecular size of the solvent. Among the three crosslinking systems, sulphur system shows the highest values and DCP system shows the minimum value of P as in the case of S. But there is no systematic trend in the variation of P with increasing temperature.

The diffusion coefficient (D) stands for the average capacity of the penetrant molecules to move among the polymer chain segments. The solubility parameter (δ) is the thermodynamic function and is depending upon the equilibrium sorption value. Permeability coefficient (P) reflects the net effect of sorption and diffusion. In the case of different NR/PS blends, D value do not show a regular trend whereas S and P show the same trend. From this it is possible to conclude that for the

permeation process of the system under study sorption predominates over diffusion. From the values of these different parameters, it is clear that the sulphur system is most permeable and the DCP system the least.

9.1.4 Effect of blend composition

The effect of blend composition on the sorption behaviour of different solvents was studied. The sorption curves of different NR/PS blends (sulphur system) at 28°C and 48°C are shown in Figures 9.7 and 9.8, respectively. In all the cases, solvent used is mineral turpentine. It is seen that both at 28°C and 48°C, 50/50 NR/PS blends show the maximum uptake followed by 30/70 and 40/60 blend systems. The same trend is observed at 58°C too (Table 9.9). This investigation could not be extended to other systems as the specimens get damaged during dynamic crosslinking. It is seen that as the temperature increases, Q_∞ value is increasing in all the three different blend systems.
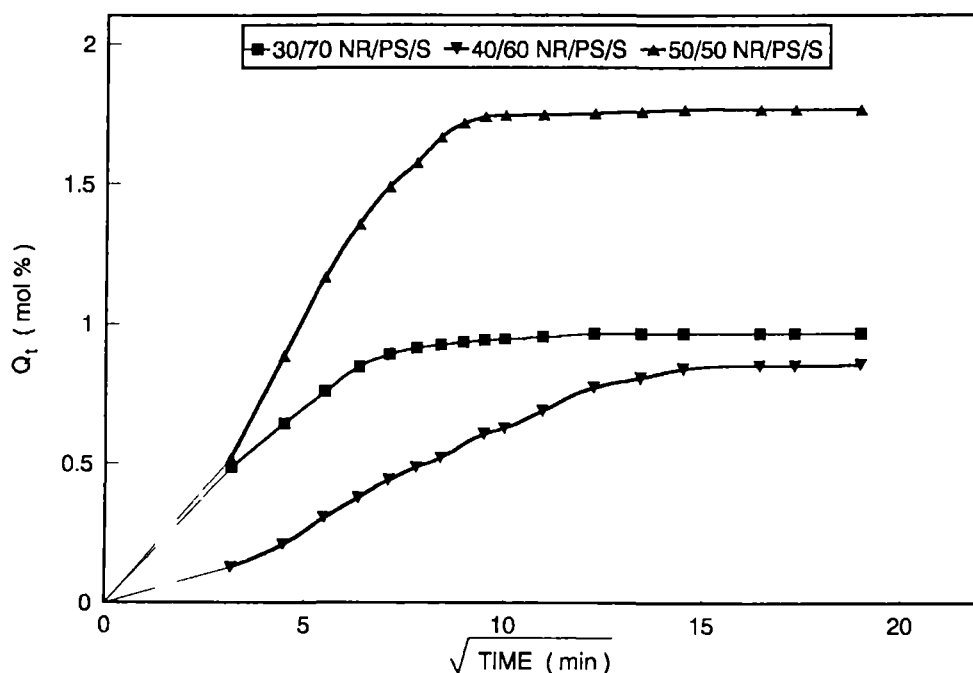
Figure 9.7. Mol per cent uptake of mineral turpentine by different blend systems at 28°C.
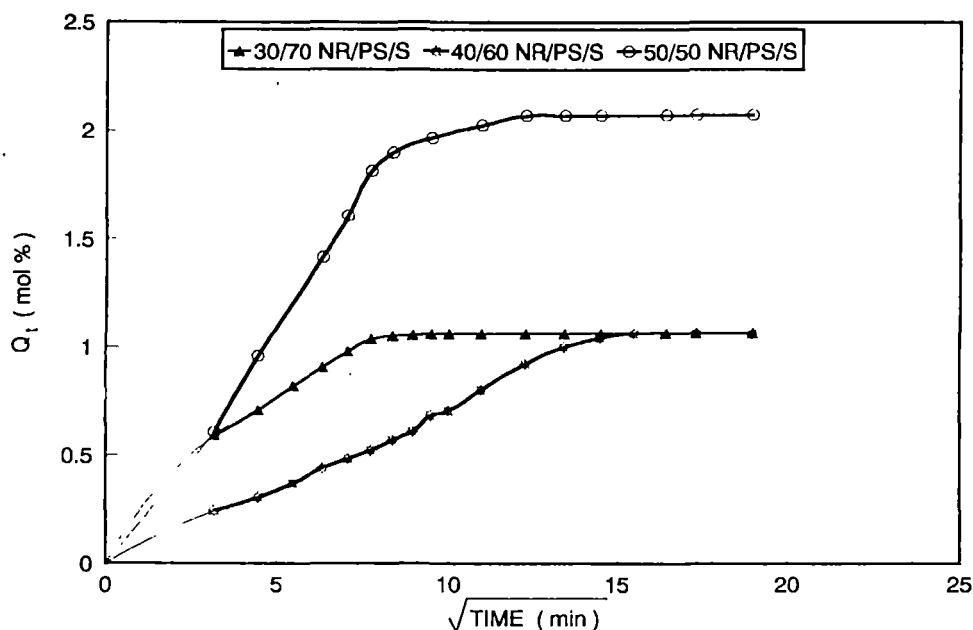
Figure 9.8.   Mol per cent uptake of mineral turpentine by different blend systems at 48°C.

Table 9.9.   Values of equilibrium sorption of different blends at different temperatures (Solvent: mineral turpentine).

Blend composition	Q_∞ (mol%)		
	28°C	48°C	58°C
30/70/sulphur	0.96	1.06	1.21
40/60/sulphur	0.89	1.03	1.17
50/50/sulphur	1.76	2.07	2.50

9.1.5   Effect of temperature

To study the effect of temperature, the sorption experiments were carried out at 38, 48 and 58°C in addition to 28°C. Figure 9.9 gives the diffusion curves of 50/50 NR/PS/S system at four different temperatures namely 28, 38, 48 and 58°C. It can be seen that the rate of diffusion as well as the maximum solvent uptake values (Q_∞) increase with increase of temperature. This is the same in 30/70

NR/PS/S system too (Figure 9.10). Other blend systems also show the same trend and the figures are not included to reduce the total number of figures. The slope of the linear portion of the sorption curves increases with temperature, indicating that the diffusion process is a temperature activated one.
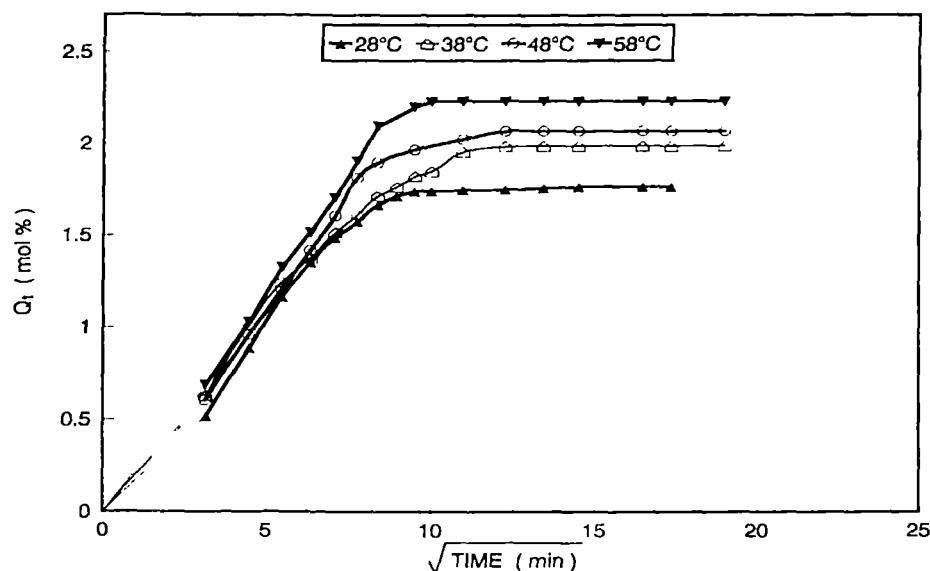
Figure 9.9. Mol per cent uptake of mineral turpentine by 50/50 NR/PS/S blend at different temperatures.
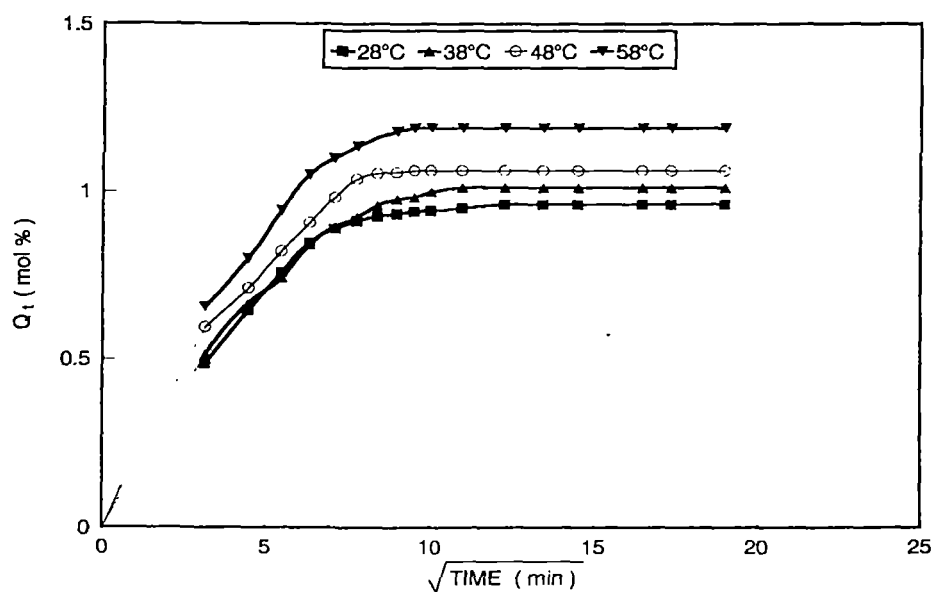
Figure 9.10. Mol per cent uptake of mineral turpentine by 30/70 NR/PS/S blend at different temperatures.

It is relevant to estimate the activation energy for diffusion E_D and that for permeation E_P from the Arrhenius relationship.[5]

$$\log X = \log X_0 - \frac{E_x}{2.303RT} \qquad (9.11)$$

where X stands for either D or P. X_0 represents either D_0 or P_0 and E_x is either E_D or E_P, i.e., the activation energy of the process under consideration. Arrhenius plots of log D or log P versus 1/T were constructed and from the slopes of these curves, the values of E_D or E_P were estimated by the linear regression analysis. E_D is found to be higher than E_P in all the cases and the values are given in Table 9.10. It is seen that the values increase from 30/70 to 50/50 NR/PS blends. The activation energies increases from 30/70 NR/PS to 50/50 NR/PS blends. The activation energies decrease in the order sulphur > DCP > mixed system.

Table 9.10. Activation parameters of diffusion, permeation of NR/PS blends.

Sample	E_D (kJ/mol)	E_P (kJ/mol)
30/70/sulphur	10.27	7.71
40/60/sulphur	13.33	11.92
50/50/sulphur	15.65	12.80
50/50/DCP	3.82	3.47
50/50/sulphur/DCP	3.81	1.63

9.1.6 Thermodynamic parameters

The molar equilibrium sorption coefficient (K_s) is a thermodynamic constant and is defined as[23]

$$K_s = \frac{\text{No. of moles of solvent sorbed at equilibrium}}{\text{Mass of the polymer}} \qquad (9.12)$$

The values of sorption coefficient (K_s) are given in Table 9.11 at different temperatures which is a measure of the uptake of solvent by the polymer. The highest values are obtained for the sulphur system and the minimum for the peroxide system. The mixed system occupies the intermediate position. As the temperature increases, the value of sorption coefficient increases in all the cases.

Table 9.11. Thermodynamic sorption constant.

Sample	Temperature °C	$K_s \times 10^2$ mol g^{-1}
30/70/sulphur	28	0.00961
	48	0.01062
	58	0.01908
40/60/sulphur	28	0.00891
	48	0.01038
	58	0.01503
50/50/sulphur	28	0.01764
	48	0.02071
	58	0.02234
50/50/DCP	28	0.01232
	48	0.01731
	58	0.01777
50/50/sulphur/DCP	28	0.01635
	48	0.01806
	58	0.01971

Using the Van't Hoff relation[2,24] it is possible to calculate the values of enthalpy (ΔH) and entropy (ΔS) for the transport process.

$$\log K_s = \frac{\Delta S}{2.303\,R} - \frac{\Delta H}{2.303\,RT} \tag{9.13}$$

Van't Hoff plot of log K_s versus $1/T$ for the different blend systems have been made. The slope and intercept of the plots give the values of ΔS and ΔH, respectively. From the values of ΔH and ΔS, the standard free energy (ΔG) of the process has been obtained using the relation,

$$\Delta G = \Delta H - T\Delta S \tag{9.14}$$

The values of ΔS, ΔH and ΔG are given in Table 9.12.

Table 9.12. Van't Hoffs parameters entropy, enthalpy and free energy.

Sample	$-\Delta S$ (J/mol)	$-\Delta H$ (J/mol)	ΔG (J/mol)
30/70/sulphur	16.81	16890.51	11829.44
40/60/sulphur	4.65	13330.51	11929.48
50/50/sulphur	11.769	6566.10	10108.78
50/50/DCP	0.785	10723.76	10960.30
50/50/sulphur/DCP	17.541	5032.96	10313.04

The free energy values (ΔG) are found to be positive. The free energy value decreases in the order DCP > mixed > sulphur. It can be concluded that the sorption process is more spontaneous in sulphur system and less possible in DCP system.

Standard enthalpy values (ΔH) are found to be negative and hence the sorption process can be described as an exothermic one. The values of standard entropy (ΔS) are also found to be negative and it indicates the retainment of liquid state structure of solvents even in the sorbed state within the polymer. The positive values of ΔG suggest that the sorption process in all these systems was not spontaneous.[3]

A structural rearrangement in polymer matrix occurs when a solvent diffuse through it and might induce the kinetic behaviour. The diffusion and sorption of

solvents through polymer matrix is a rate controlled kinetic process and can be studied by the following first order kinetic rate equation.[17,24]

$$dc/dt = k_1 (C_\infty - C_t) \qquad (9.15)$$

On integration equation (13) changes to

$$k_1 t = 2.303 \log [C_\infty/(C_\infty - C_t)] \qquad (9.16)$$

where k_1 is the first order rate constant C_t and C_∞ are the concentrations at time t and equilibrium, respectively. From the slope of the plot of log $(C_\infty - C_t)$ Vs. time, we can estimate the value of k_1 (Table 9.13).

Table 9.13. Kinetic data for crosslinked NR/PS blends.

Sample	Temperature (°C)	$k_1 \times 10^3$ (min^{-1})
30/70/sulphur	28	42.2
	48	55.4
	58	31.9
40/60/sulphur	28	12.8
	48	8.8
	58	7.1
50/50/sulphur	28	37.8
	48	32.3
	58	20.2
50/50/DCP	28	13.7
	48	31.2
	58	32.2
50/50/sulphur/DCP	28	21.6
	48	15.7
	58	28.0

Among sulphur systems, the rate constant values are lower for 40/60 sulphur system which is in agreement with the swelling data. The rate constant values decrease in the order sulphur > mixed > peroxide which is in the same order as that

of the swelling data. With increase of temperature, there is no regular trend in the rate constant values. It is found that at higher temperature rate constant values are decreased.

9.1.7 Comparison with theory

In order to examine the deviation of experimental results from those predicted by theory, theoretical sorption curves were created by fitting the value of diffusion coefficient into the following equation[18]

$$\frac{Q_t}{Q_\infty} = 1 - \frac{8}{\pi^2} \sum_{n=0}^{\infty} 1/(2n+1)^2 \exp[-D(2n+1)^2\pi^2 \, t/h^2] \tag{9.17}$$

where Q_∞, Q_t, n, D, h, etc. have the same significance as described before. The experimental sorption curves of 30/70 NR/PS/S blends (mineral turpentine – 48°C), 50/50 NR/PS/DCP blends (mineral turpentine – 48°C) and 30/70 NR/PS/DCP blends (mineral turpentine – 58°C) are compared with the theoretical curves (Figures 9.11–9.13). A fairly good agreement has been observed between the theoretical and experimental results. A similar trend was observed with the other systems too.
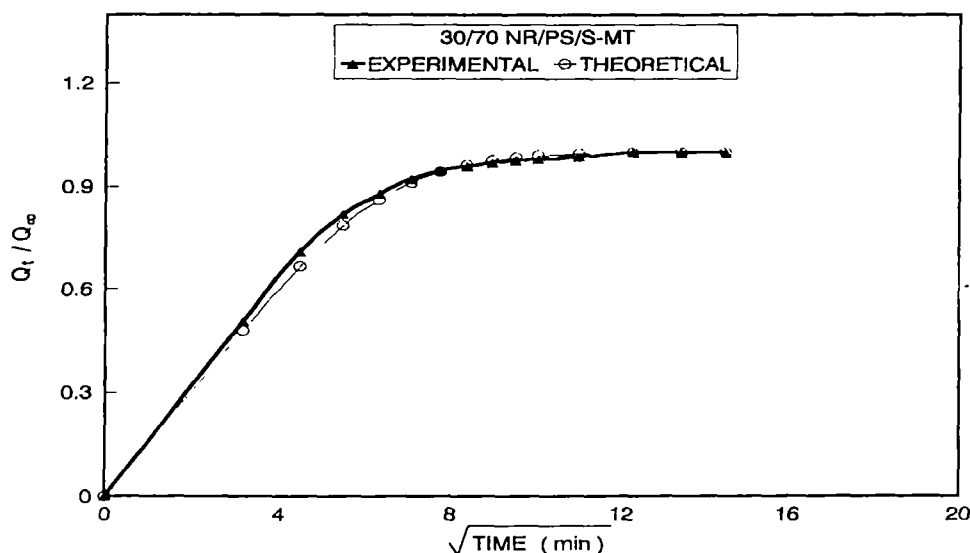
Figure 9.11. Comparison between experimental and theoretical curve for 30/70 NR/PS/S (MT, 48°C).
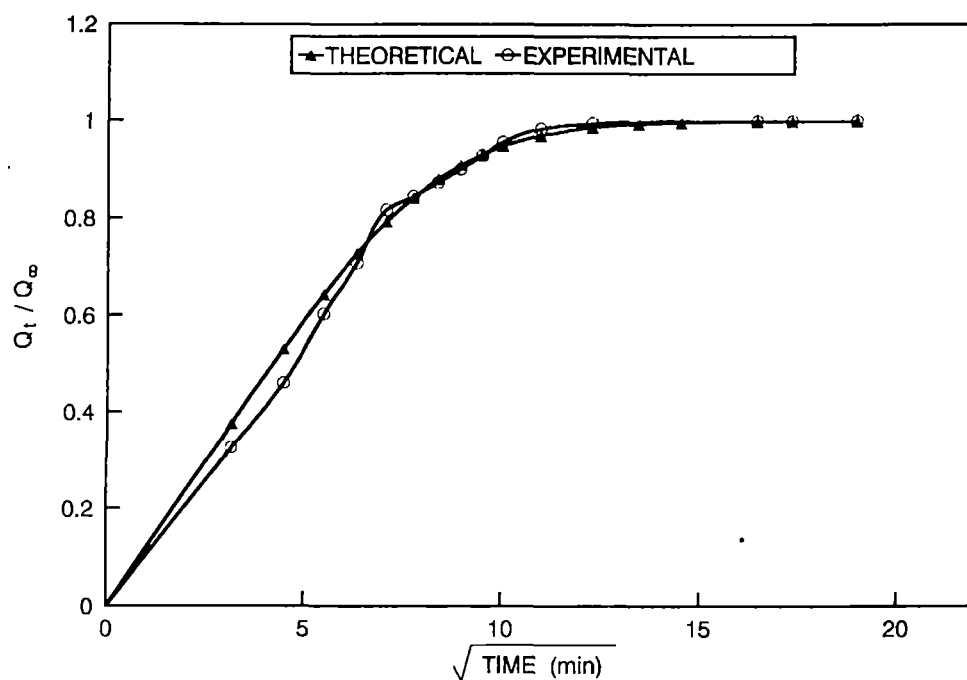
Figure 9.12. Comparison between experimental and theoretical curve for 50/50 NR/PS/DCP (MT, 48°C).
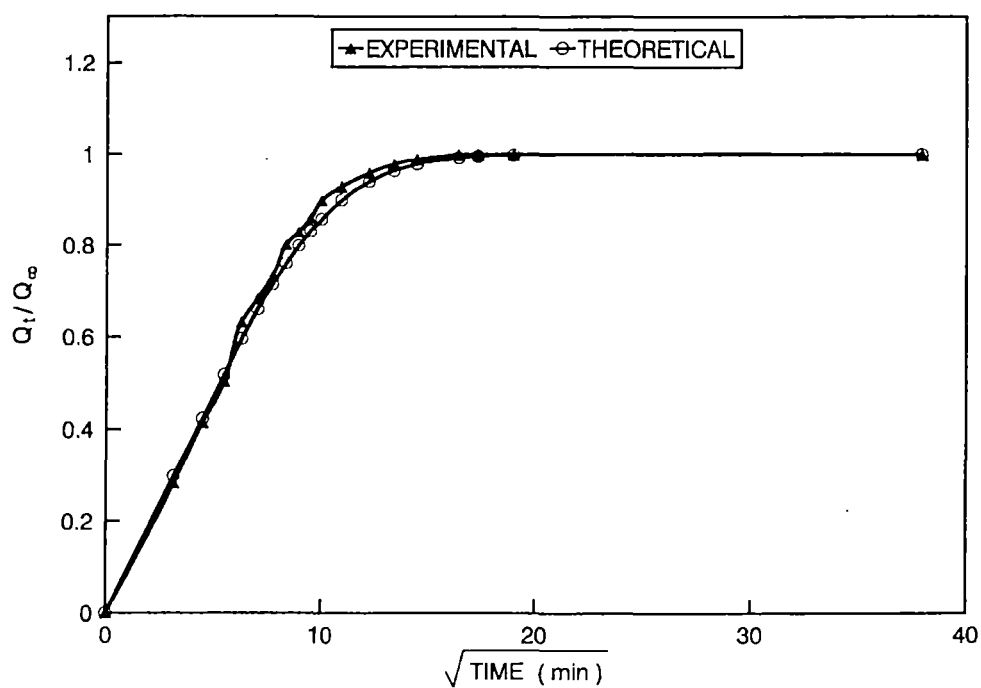
Figure 9.13. Comparison between experimental and theoretical curve for 30/70 NR/PS/DCP (MT, 58°C).

9.2 References

1. S. B. Harogoppad and T. M. Aminabhavi, *Polym. Commun.*, **32**, 120 (1991).

2. R. S. Khinnavar and T. M. Aminabhavi, *J. Appl. Polym. Sci.*, **42**, 2321 (1991).

3. S. B. Harogoppad and T. M. Aminabhavi, *J. Appl. Polym. Sci.*, **42**, 2329 (1991).

4. R. S. Khinnavar, T. M. Aminabhavi, R. H. Balundgi, S. S. Shukla and A. Kulac, *J. Hazard. Mater.*, **28**, 281 (1991).

5. T. M. Aminabhavi and R. S. Munnoli, *J. Hazard. Mater.*, **38**, 223 (1994).

6. R. B. Mesorbian and C. J. Ammondson, *U. S. Patent* No. 3, 093, 255, June 11 (1963).

7. I. Cabasso, J. Jagur-Grodzinski and D. Vofsi, *J. Appl. Polym. Sci.*, **18**, 2117 (1974).

8. T. M. Aminabhavi and H. T. S. Phayde, *J. Appl. Polym. Sci.*, **57**, 1419 (1995).

9. N. J. Morrison and M. Porter, *Rubber Chem. Technol.*, **57**, 63 (1994).

10. U. S. Aithal, T. M. Aminabhavi and P. E. Cassidy, *Barrier Polymers and Structures*, Am. Chem. Soc. Symp. Ser., 423 (Ed., W. J. Koros) 197th National Meeting, Dallas, Tx. Am. Chem. Soc., Washington, DC, 1989, p. 351.

11. P. J. Flory and J. Rehner Jr., *J. Chem. Phys.*, **11**, 521 (1943).

12. A. P. Mathew, S. Packirisamy, M. G. Kumaran and S. Thomas, *Polymer*, **36**, 4935 (1995).

13. S. R. Jain, V. Sekhar and V. N. Krishnamurthy, *J. Appl. Polym. Sci.*, **48**, 1515 (1993).

14. J. D. Ferry, *Viscoelastic Properteis of Polymers*, John Wiley and Sons, New York, 1970.

15. J. S. Chiou and D. R. Paul, *Polym. Eng. Sci.*, **26**, 1218 (1986).

16. L. M. Lucht and N. A. Peppas, *J. Appl. Polym. Sci.*, **33**, 1557 (1987).

17. S. B. Harogoppad and T. M. Aminabhavi, *Macromolecules*, **24**, 2595 (1991).

18. A. N. Gent and R. H. Tobias, *J. Polym. Sci. Polym. Phys. Edn.*, **20**, 2317 (1982).

19. S. B. Harogoppad and T. M. Aminabhavi, *Polymer*, **32**, 870 (1991).

20. H. Fujita and A. Kishimoto, *J. Polym. Sci.*, **25**, 547 (1958).

21. S. Joshi and G. Astarita, *Polymer*, **20**, 455 (1979).

22. T. M. Aminabhavi and R. S. Khinnavar, *Polymer*, **34(5)**, 1006 (1993).

23. G. W. C. Hung, *Microchem. J.*, **19**, 130 (1974).

24. M. Aminabhavi and S. B. Harogoppad, *J. Chem. Educ.*, **68**, 343 (1994).

Chapter 10

Conclusion and Future Outlook

10.1 Conclusion

Polymer blends have gained much interest and ofcourse have become a new branch of macromolecular science. The field of polymer blends is quite attractive due to the fact that already existing polymers can be used and thus the costly development of new polymers from new monomers can be avoided. Further blending is the most simplest and cheapest route of combining the properties of different polymeric materials.

Although blending looks very attractive, most of the polymer blends are immiscible and incompatible leading to heterophase polymer blends. This heterogeneity is an unfavourable one and this may lead to problems that reflect in the overall performance of the resultant material. The high interfacial tension and poor adhesion between the phases are responsible for the poor dispersion and lack of stability to gross phase segregation which are associated with incompatible blends.

There are different techniques to alleviate the above mentioned problems. Addition of a third component (block or graft copolymer) which is capable of having interaction with the blend components is a well-known method. Development of such a compatible blend system requires a thorough understanding of the copolymer behaviour at the blend interface.

The core point of the thesis consists of the interfacial activity of the compatibiliser (NR-g-PS) in incompatible natural rubber/polystyrene blends. The influence of the compatibiliser on the mechanical, rheological, morphological, thermal, and sorption characteristics of the blends were analysed.

The special features and different types of elastomer blend, problems and solutions of blend incompatibility, techniques of compatibilisation, basic features of compatibilisation, theoretical aspects of compatibilisation, etc. have been discussed in the introduction part of the thesis. In addition to this, earlier studies of compatibilisation of TPEs have been reviewed in detail. The details of the materials used and experimental techniques adopted in the present investigation are given in detail.

The morphology and mechanical properties of unvulcanised NR/PS blends have been analysed with special reference to the effect of blend ratio, processing conditions (solution casting vs. melt mixing) and vulcanising systems. In the case of melt mixed samples, the mixing torque increased with increase of rubber content. The increase in mixing torque with increase in rubber content is due to the higher viscosity of NR phase as compared to PS. The mixing temperature shows an initial and intermediate drop due to the introduction of the material and then it increases with mixing time. The dynamically cured samples show higher mixing torque compared to uncured samples. The morphology of the blends indicates a two-phase structure in which rubber phase is dispersed in the continuous PS matrix at its lower proportions and the reverse is the case at higher proportions of NR, i.e., phase inversion takes place. The nature of casting solvents on the morphology and properties has been studied. Domain size and polydispersity are highest for $CHCl_3$ casted samples and lowest for C_6H_6 casted samples. The CCl_4 casted samples take intermediate position. In spite of these, CCl_4 casted blends show inferior properties compared to $CHCl_3$ casted blends. This may be associated with the occlusion of the casting solvents due to their high boiling point (CCl_4, BP 77°C). The changes in morphology in different casting solvents are associated with the different levels of interactions of the blend components with the solvent. In the case of melt mixed samples the tensile and tear strength decrease with increase of rubber content whereas the impact strength increases with increase of rubber content. The same trend is observed in the case of solution casted blends. Although the domain size is smaller in melt mixed samples, the mechanical properties are inferior to solution casted samples. The mechanical and thermal degradation are the major reasons for

the inferior properties of melt mixed samples. The solution casted samples show variation in their properties depending upon the extent of interaction between the blend component and casting solvent. The experimental data was compared with different theoretical models like series, parallel, Coran's, etc. It has been found that the experimental data are close to Halpin-Tsai model in the case of tear strength both at low and high rubber content. In the case of tensile strength at low rubber content the experimental data are close to parallel model and at high rubber content the data are close to the Coran's model, in which n = 2. Dynamically cured samples show increase in mechanical properties compared to uncured samples. Among the varies dynamically crosslinked samples, peroxide system showed the minimum value of impact strength and sulphur system exhibited the maximum value and this could be related to the flexibility of crosslinks in different vulcanised systems. The dynamically cured samples showed very high modulus as compared to uncured samples. The behaviour of different vulcanising systems towards the mechanical properties could be related to the blend morphology, crosslink density and nature of crosslinks.

The compatibilising activity of NR-g-PS in heterogeneous NR/PS blends has been studied in detail. The graft copolymer (NR-g-PS) was characterised by both FTIR and H'NMR spectroscopy. Both the morphology and mechanical properties of NR/PS blends have been investigated. Concentration and molecular weight of the copolymer, composition of the blend, mode of addition of compatibiliser, homopolymer molecular weight and processing conditions were the controlling parameters on blend morphology. Copolymer addition reduces the domain size of the dispersed phase and finally gets levelled off at higher concentrations which is an indication of interfacial saturation. The experimental results were in agreement with the predictions of Noolandi and Hong. The area occupied by the compatibiliser molecule at the interface (Σ) has been estimated. As the molecular weight of the homopolymer decreases, the interfacial area occupied by the copolymer (Σ) increases, and hence more reduction in the domain size was observed. The Σ values were also influenced by the blend composition, mode of

addition and the nature of the casting solvents. By the selection of a suitable solvent having close solubility parameter to that of the homopolymers, the interaction of the compatibiliser with the interface could be enhanced. The mechanical property analysis are in agreement with the morphological changes. It was found that the tensile strength and modulus increase upon the addition of the compatibiliser and finally get levelled off at higher concentration. Attempts were made to deduce the conformation of the compatibiliser at the blend interface. Different models were discussed and found that the actual conformation is neither fully extended nor flat. A portion of the copolymer penetrates into the corresponding homopolymer and the rest of it remains at the interface.

Rheological properties of the blends have been investigated using a capillary rheometer and melt flow indexer. Blends were prepared by both melt mixing and solution casting techniques. In both cases, the shear viscosity decreased with increase of shear stress indicating pseudoplastic nature. The viscosity of the system was found to increase with increase of rubber content. The solution casted blends showed higher viscosity compared to melt mixed samples. Mechanical degradation of both NR and PS at high temperature and shear must have contributed to the lower viscosity of melt blended samples as compared to solution casted samples. At lower shear rates, the viscosities of the blends are higher than those of the component polymers. However, at higher shear rates, the system exhibits a negative deviation. Thus the viscosity-composition curve of both solution and melt mixed blends showed that the viscosity of the blends are non additive functions of viscosities of NR and PS. The negative devaition in viscosity is associated with very poor physical and chemical interactions across the phase boundaries. Morphology analysis reveal that the particle size reduced significantly at high shear rate. The experimental viscosity values have been compared with theoretical predictions. Melt viscosity of the blends increases upon the addition of a few per cent of the compatibiliser (NR-g-PS) followed by a decrease at higher loading. The increase in viscosity has been explained on the basis of the high interfacial

interaction between the blend components. The micelle formation is responsible for the decrease in viscosity at higher graft loading. The SEM analysis of the extrudate surface reveal that the domain size decreases with increase of copolymer loading, and finally gets levelled off at higher copolymer loading. Arrhenius plots and activation energy measurements gave information about the temperature dependence of different blend systems. Melt elastic parameters like die swell, principal normal stress differences, recoverable shear strain, etc. were calculated for both compatibilised and noncompatibilised blends. Melt flow index studies are in agreement with the capillary rheometer data. Master curves have been constructed using the MFI and rheometer data and this could be used to construct the rheograms of the NR/PS systems by simply knowing the MFI data.

The stress-relaxation behaviour of various NR/PS blends in tension has been studied as a function of the effect of strain level, ageing, composition and compatibiliser loading. The rate of relaxation was found to increases with strain level. It was observed that ageing produced interesting effects on the relaxation pattern. Aged samples follow a two-stage relaxation pattern. The rate of relaxation increases with temperature due to the degradation of the sample. The relaxation pattern of different blends depend upon the NR content and phase morphology. The compatibilised blends show a different pattern of relaxation compared to non-compatibilised blends. The compatibilised blends below CMC, followed a two-stage relaxation pattern whereas above CMC the blends showed a three-stage relaxation pattern which is associated with the micelle formation. The compatibilised blends indicated an increase in the rate of relaxation because of the presence of a broader interface and improved interfacial interaction.

The dynamic mechanical properties of NR/PS blends were analysed in detail. It was found that at all frequencies the tan δ values increase with increase in temperature up to the glass transition of NR and thereafter it levels off in the low temperature region (-70 to 30°C). In the high temperature region it was found that at all frequencies the tan δ values increase with increase in temperature up to the

glass transition of polystyrene and thereafter the values decrease. The tan δ values were found to increase with increase of frequency. The storage modulus decreases with increase of temperature at all frequencies due to the decreasing stiffness of the samples. In all cases as expected, as the frequency increases, the Tg values due to the blend components shifts towards the high temperature region. In all cases, as the frequency increases, the storage modulus values increase and the variation is more pronounced in the transition region. Loss modulus value also increase with increase of frequency. At the low temperature region, the loss modulus values are higher at the low frequencies and lower at higher frequencies. However, in the high temperature region reverse is the case. As the frequency increases, E″ peak temperature due to NR phase shifts towards the high temperature region. The damping behaviour increases as the NR content increases. The storage modulus of different NR/PS blends decreased with increase of NR content. The modulus values decrease with temperature and finally levels off at high temperature. In the case of blends with 1.5% compatibiliser, the tan δ values are higher compared to noncompatibilised blends at all frequencies. At low temperature region, addition of 3% compatibiliser decreases the damping behaviour of the blends due to its interfacial activity. But the trend is reversed in the high temperature region because the interfacial activity of the compatibiliser is weakened at high temperature. At higher compatibiliser loading, the tan δ values are increased, due to the formation of micelles which is highly undesirable. Addition of 3% compatibiliser enhances the modulus value. Different theoretical models such as series, parallel, Coran's, Halpin-Tsai, etc. were used to fit the experimental viscoelastic data. It was found that, up to 50 wt % NR, the experimental values are close to Halpin-Tsai model and beyond that the values are close to the Coran's model.

Cole-Cole plots of compatibilised and non-compatibilised blends showed the heterogeneous nature of the system. However, the compatibilised system shows a tendency to form a homogeneous phase. The time-temperature superposition master curve was constructed via the shifting procedure based on the principle of

time-temperature correspondence. Thus it was enabled to have a complete modulus-time behaviour at a constant temperature.

Thermogravimetric analysis and differential scanning calorimetric analysis were carried out to study the thermal behaviour of NR/PS blends. The effects of blend composition and compatibiliser loading on the thermal behaviour of blends were analysed. It was found that blending improved the thermal properties of the blends. The weight loss of the blends was found to be lower than that of the blend components. The addition of compatibiliser influenced the thermal behaviour. The weight loss of the blends at various temperatures was found to be decreased upon the addition of the compatibiliser. Further, the initial decomposition temperature was raised upon the addition of the compatibiliser. DSC studies indicated the existence of two glass transitions for the non-compatibilised and compatibilised blends. Even with the addition of technological compatibiliser (NR-g-PS) the NR/PS blends are thermodynamically incompatible.

Diffusion and transport of three solvents namely, petrol, mineral turpentine and diesel through dynamically crosslinked NR/PS blends were analysed in Chapter 9. Three vulcanising systems namely, sulphur, mixed and DCP have an important role in the sorption phenomena. Sulphur system shows the highest solvent uptake and the DCP system the minimum. The mixed system occupies the intermediate position. This has been explained based on the flexibility of the crosslinked networks. As the penetrant size increases, the solvent uptake decreases. Solvent uptake is maximum for petrol and minimum for diesel. Mineral turpentine occupies the intermediate position. The value of molar mass between the crosslinks (M_c) was estimated for different blend systems and found that it varies in the same order as that of Q_∞, i.e., sulphur > mixed > DCP. As the temperature increases, the equilibrium sorption increases in all the cases. The Arrhenius parameters were computed. The Van't Hoffs relationship was used to estimate the entropy, enthalpy and free energy of sorption. Rubber-solvent interaction parameter was estimated. Effect of blend composition on sorption

behaviour was studied and found that the 50/50 NR/PS blend shows the maximum solvent uptake.

10.2 Future outlook

10.2.1 Influence of block copolymer on compatibilisation

In the present investigation, we have carried out the technological compatibilisation of the immiscible natural rubber/polystyrene blends via. non-reactive compatibilisation technique, i.e., by the addition of natural rubber-graft-polystyrene. It is well known that the block copolymers are more effective than graft copolymers as far as the interfacial activity is concerned. It is possible to prepare the block copolymer of NR and PS and its interfacial activity could be studied in detail. However, expensive anionic polymerisation technique should be used for the copolymer synthesis. The influence of segmental mass ratio, molecular weight, etc. on the morphology and properties is worth probing.

10.2.2 Interfacial tension measurement

It is expected that the copolymer addition will reduce the interfacial tension in an immiscible blends. The action of a compatibiliser in an immiscible blend can be well followed by the measurement of interfacial tension across the phase boundary with and without the copolymer using highly specialised pendant drop apparatus. This can be followed with the help of a video digital image processing technique. Other techniques such as breaking thread method and embedded fibre retraction technique can also be used for the interfacial tension measurements.

10.2.3 Interfacial thickness measurements

Addition of copolymer to an immiscible blend leads to an increase in the interfacial thickness by the localisation of the copolymer at the blend interface. The techniques of ellipsometry has been used by several researchers to measure the interfacial thickness between two polymer layers. The same can be adopted in this

case too. The measurements can be carried out using an automated ellipsometer with a series of bilayer specimens. Small angle X-ray scattering (SAXS) and neutron scattering (SANS) measurements can also be used to estimate the interfacial thickness with and without the addition of the copolymer.

10.2.4 Location of the copolymer

The copolymer may locate at the blend interface or may present in the bulk. In the second case it may exists either as the dispersed phase or as the continuous one. In some cases, it may exist both at the interface and at the bulk. In all these cases, the location of the copolymer is important. There are several methods which can be successful utilised to locate the copolymer. These include fluorescence spectroscopy, fluorescence microscopy and transmission electron microscopy.

10.2.5 Fabrication of useful products

The use of NR/PS blends for applications such as automobile body parts, dashboards, bumpers, aircraft mouldings, etc. is worth attempting.

Appendix

List of Publications

I.   Papers published in International Journals

1.   The technological compatibilisation of natural rubber/polystyrene blends by the addition of natural rubber-g-polystyrene. .
R. Asaletha, M .G. Kumaran and S. Thomas, *Rubber Chem. Technol.,* 68(4), 671 (1995).

2.   Effect of casting solvents and compatibiliser loading on the morphology and properties of natural rubber/polystyrene blends.
R. Asaletha, M .G. Kumaran and S. Thomas, *Polym. Plast. Proc. Technol. Eng.,* 34(4), 633 (1995).

3.   Melt rheoglogy of natural rubber/polystyrene/natural rubber-graft-polystyrene blends.
R. Asaletha, M .G. Kumaran and S. Thomas, *J. Appl. Polym. Sci.* (In Press)

4.   Thermal analysis of natural rubber/polystyrene blends: Thermogravimetric and Differential scanning calorimetric studies.
R. Asaletha, M .G. Kumaran and S. Thomas, *Polym. Degr. Stab.* (In Press).

5.   Thermoplastic elastomers from polystyrene and natural rubber: Morphology and mechanical properties
R. Asaletha, M .G. Kumaran and S. Thomas, *Eur. Polym. J.* (Communicated).

6.   Transport behaviour of aliphatic hydrocarbon liquids through dynamically crosslinked natural rubber/polystyrene blends.
R. Asaletha, M .G. Kumaran and S. Thomas, *J. Appl. Polym. Sci.* (Communicated).

7.   Stress relaxation behaviour of natural rubber/polystyrene blends.
R. Asaletha, M .G. Kumaran and S. Thomas, *J. Polym. Sci. Polym. Phys.* (Communicated).

8.   Morphology and dynamic mechanical properties of natural rubber/polystyrene/ natural rubber-graft-polystyrene blends.
R. Asaletha, G. Groeninckx, Sabu Thomas and M. G. Kumaran, *Polymer* (Communicated).

II. Other publications (Chapter for a Book)

1. Compatibilisation of thermoplastic elastomer blends, Handbook of Engineering Polymeric Materials (Ed., Cheremisinoff), Marcel Dekker, USA, Ch. 42, p. 633, 1997.
    R. Asaletha, Z. Oommen and S. Thomas.

III. Papers presented in International and National Conferences

1. Interfacial activity of natural rubber-graft-polystyrene in heterogeneous natural rubber/polystyrene blend.
    International Symposium on Macromolecules (MACRO '95), VSSC, Thiruvananthapuram, January 11-13, 1995.

2. Morphology and properties of natural rubber/polystyrene blends: Influence of compatibiliser loading and casting solvents.
    82nd Indian Science Congress held at Calcutta, January 3-8, 1995.

3. Compatibilisation of NR/PS blends.
    7th Kerala Science Congress held at Palakkad, January 27-29, 1995.

4. Natural rubber/polystyrene blends: Rheological studies.
    83rd Indian Science Congress held at Patiala, January 3-8, 1996.

5. Natural rubber-polystyrene blends. Technological compatibilisation studies.
    8th Kerala Science Congress held at Kochi, January 27-29, 1996.

6. Melt rheology of natural rubber/polystyrene blends.
    European Symposium on Polymer Blends, Maastricht, The Netherlands, May 12-15, 1996.

7. Thermoplastic elastomers: Blends of natural rubber/polystyrene.
    International Conference on Rubbers: Rubber '97, Taj Bengal, Calcutta, December 12-14, 1997.

8. Dynamic mechanical thermal analysis of NR/PS/NR-g-PS blends.
    International Symposium on Advances in Polymer Science and Technology (MACRO '98), CLRI, Chennai, January 5-9, 1998.

THE TECHNOLOGICAL COMPATIBILIZATION OF NATURAL RUBBER/POLYSTYRENE BLENDS BY THE ADDITION OF NATURAL RUBBER-*graft*-POLYSTYRENE

R. Asaletha and Sabu Thomas*

School of Chemical Sciences, Mahatma Gandhi University, Priyadarshini Hills P.O.,
Kottayam-686 560, Kerala, India

AND

M. G. Kumaran

Rubber Research Institute of India, Kottayam, Kerala-686 009, India

ABSTRACT

Compatibility of natural rubber (NR)/polystyrene (PS) blend is poor and can be enhanced by the addition of a graft copolymer of natural rubber and polystyrene (NR-*graft*-PS). The effects of homopolymer molecular weight, copolymer molecular weight, copolymer concentration, processing conditions and mode of addition on the morphology of the dispersed phase have been investigated by means of optical microscopy. The addition of a small percentage of the compatibilizer decreases the domain size of the dispersed phase. The effect levels off at higher concentrations. The leveling off could be an indication of interfacial saturation. The experimental results were compared with the theoretical predictions of Noolandi and Hong. The addition of the graft copolymer improves the mechanical properties of the blend and attempts were made to correlate the mechanical properties with the morphology of the system. Attempts were also made to understand the conformation of the qraft copolymer at the interface.

INTRODUCTION

Thermoplastic elastomers (TPEs) are a relatively new class of materials which combine the excellent processing characteristics of the thermoplastics and the elastic characteristics of the rubbers. They can be obtained by blending the constituent materials. Various parameters like the selection of the rubber and thermoplastic, blend ratio, processing conditions, etc., affect the properties of the TPEs.

Nowadays blending of different polymers which will combine the properties of the constituent materials is a commonly accepted method. Even though blending is an easy method for the preparation of TPEs, most of the TPE blends are immiscible. Very often the resulting materials exhibit poor mechanical properties due to the poor adhesion between the phases. Over the years different techniques have been developed to alleveate this problem. These include (1) the addition of a third homopolymer or graft or block copolymer which is miscible with the two phases, and (2) the introduction of covalent bonds between the homopolymer phases. The first approach can be considered as nonreactive compatibilization and the second as reactive compatibilization. This paper, in fact, deals with the nonreactive compatibilization technique instituted by the addition of graft copolymer.

There are several studies in literature in which the addition of copolymer increases the technological compatibility of immiscible polymer pairs. Incorporation of a copolymer usually improves the interaction between the constituent homopolymers and thereby slows down the phase separation process.[1-4] It was reported by Paul[5,6] that the copolymer addition will provide finer dispersion, improve interfacial adhesion, stability against gross segregation and will reduce the interfacial tension.

In a pioneering work, Riess and coworkers reported on the compatibilizing action of copolymers in polystyrene/poly(methylmethacrylate) and polystyrene/polyisoprene

---

* Author to whom all correspondence should be addressed.

blends.[7,8] They have reported that block copolymers are more effective than graft copolymers in the above systems. They further concluded that the solubilization occurs only when the molecular weight of the homopolymers are less than or comparable to the molecular weight of the corresponding segment in the block copolymer.

Compatibilizing action of poly(styrene-block-isoprene) in polystyrene/polyisoprene blend has been reported by Inoue and coworkers.[9,10] Morphology of the system was analyzed and it was found that a fine morphology is obtained by the addition of a few percentage of the block copolymer. Teyssie and coworkers [11-13] have examined the compatibilizing action of copolymers in a large number of systems. They suggested that molecular weight and structure of the copolymer are the controlling parameters which will effect the efficiency of the compatibilizer. They have compared the efficiency of tapered and pure block copolymer in polystyrene/polyethylene system and was found that tapered block copolymer is more effective than the pure block copolymer.

Patterson, Hu and Grindstaff[14] have studied the poly(dimethylsiloxane)/poly-(oxyethylene-block-oxypropyl ene) blends, compatibilized by the addition of poly(dimethyl siloxane-block-oxyethylene). The lowering of the interfacial tension upon the addition of the copolymer was reported by several researchers. For example, Gailard and coworkers[15] have reported on the reduction in interfacial tension in polystyrene/polybutadiene/styrene ternary blend by the addition of poly(styrene-block-butadiene) copolymer. Studies of Willis and Favis dealt with polystyrene–maleic anhydride/bromobutyl rubber blends which was compatibilized by the addition of dimethylaminoethanol. More recently,[17-19] forward recoil spectroscopy, small angle x-ray scattering, neutron reflectivity methods were successfully used to analyze the interface of various polymer blends in the presence and absence of copolymers.

Coran and Patel[20-22] reported a series of thermoplastic elastomer compositions. These include blends of nylon and various synthetic rubbers like ethylene–vinyl acetate, ethylene–propylene–diene monomer rubber, chlorinated polyethylene, polyurethane rubber, etc.[23] Coran and Patel[24] further reported on thermoplastic elastomers from blends of polystyrene and various rubbers such as IIR, ethylene–propylene–diene monomer, natural rubber, styrene–butadiene rubber, butyl rubber, acrylate rubber, chloroprene rubber, nitrile rubber, and poly(trans-pentenamer) rubber. The mechanical properties of the blends were correlated with parameters like critical surface tension for wetting, crystallinity, tensile strength of the hard phase and critical entanglement spacing.

Technological compatibilization of disimilar rubber–plastic blends were also discussed in detail by Coran and Patel.[25] For example, in the case of the polyolefin/nitrile rubber system, compatibilization using phenolic modified, maleic modified, triethylenetetramine modified, and chlorine treated powdered polyolefin was discussed. The in-situ formed modified polyolefin–rubber copolymer acts as the compatibilizer in the above cases. Dynamic vulcanization as a technique for compatibilization was adopted by Gessler[26] and Fischer.[27]

Finally Leibler,[28,29] Noolandi and Hong[30-32] developed thermodynamic theories concerning the effect of copolymers in heterogeneous polymer blends. According to Leibler, the reduction in interfacial tension is due to the adsorption of copolymers at the interface. An assymmetric copolymer will be less active as a compatibilizer compared to a symmetric one. The aim of Noolandi and Hong's theory was to obtain an expression for interfacial tension reduction. The reduction in interfacial tension for a range of copolymer and homopolymer molecular weights was calculated. The results were then compared with the experimental results of Riess and coworkers.

In this paper we report on thermoplastic elastomers from blends of natural rubber (NR) and polystyrene (PS) which are highly incompatible. Until now, no serious attention has been given to the compatibilizing action of copolymers in these blends. The effects of the graft copolymer of NR and PS (NR-graft-PS) on the mechanical and morphological properties of NR/PS blends have been analyzed. The influence of copolymer concentration, molecular weight of homo and copolymers, mode of addition and nature of casting solvents on the morpoholgy and properties of the blends has been quantitatively investigated. Attempts

were made to deduce the graft copolymer conformation at the interface. Finally, the experimental results were compared with the current theories of Noolandi and Hong.

EXPERIMENTAL

Polystyrene was supplied by Poly Chem Ltd., Bombay, India. Natural rubber (ISNR-5) was supplied by Rubber Research Institute of India, Kottayam. The characteristics of the materials used are given in Table 1.

The graft copolymer of NR and PS (NR-graft-PS) was prepared by polymerizing styrene in rubber latex using ^{60}Co ν radiation as the initiator.[39] Styrene monomer was made into an emulsion which was then mixed with NR latex of known dry rubber content (DRC) at room temperature and exposed to ^{60}Co ν radiation for 16 h. The dose rate was 0.1166 Mrd/min. The free homopolymers natural rubber and polystyrene were removed from the crude sample by extraction with petroleum ether and methyl ethyl ketone, respectively.

BLEND PREPARATION AND CHARACTERIZATION

Natural rubber (NR) and polystyrene (PS) were blended together in a common solvent: chloroform (A 5% solution was made for casting). Different compositions of the blends: 40/60, 50/50 and 60/40, were made with and without the addition of the graft copolymer. To study the effect of casting solvent, blends were also made from carbon tetrachloride. Natural rubber, polystyrene and the graft copolymer were mixed in chloroform. The mixture was kept overnight and then stirred for eight hours with a magnetic stirrer. Films were cast on a glass plate and dried in a vacuum oven at 80°C for 48 h, and then at 120°C for a further 4 h. The morphologies of the samples were studied by optical microscopy and the mechanical properties were determined according to ASTM standard procedures using a Zwick Universal Testing Machine.

The influence of the mode of addition of the graft copolymer was studied in three ways. In the first case the minor phase (PS) and the graft copolymer were premixed, kept overnight and stirred for 7 h; then NR was added to the mixed solution, kept overnight again and stirred for a further 7 h. In the second case, the same was repeated by premixing the major phase (NR) and graft copolymer. In the third case, the graft copolymer was added to the NR/PS blend directly. The morphologies of all the systems were examined as mentioned earlier. The effect of homopolymer and graft copolymer molecular weight on compatibilization was studied by using natural rubber, polystyrene and NR-graft-PS of different molecular (Table I).

TABLE I

CHARACTERISTICS OF THE MATERIALS USED

Material	Density (g/cm^3)	Solubility parameter (cal/cm^3)$^{1/2}$	Molecular weight (M_n)
NR$_0$	0.90	7.75	7.79×10^5
NR$_6$	0.90	7.75	3.7×10^5
NR$_{10}$	0.90	7.75	2.49×10^5
NR$_{16}$	0.90	7.75	1.62×10^5
PS$_1$	1.04	8.56	3.51×10^5
PS$_2$	1.04	8.56	2.073×10^5
G$_1$ (NR-graft-PS)	—	—	3.95×10^5
G$_2$ (NR-graft-PS)	—	—	1.009×10^5
CHCl$_3$	—	9.30	—
CCl$_4$	—	8.60	—

RESULTS

GRAFT COPOLYMER CHARACTERIZATION

Graft copolymer (NR-*graft*-PS) was characterized by FTIR spectroscopy, ^{1}H NMR spectroscopy and gravimetric methods. The qrafting efficiency and percentage of PS grafted were 49% and 20%, respectively. This has been estimated by gravimetric anlaysis as reported earlier.[34]

The FTIR spectrum shows peaks at 3026 and 2855 cm^{-1} which correspond to aromatic C—H stretching in PS. Peaks at 1601 cm^{-1} and 1541 cm^{-1} correspond to C=C stretching of the aromatic ring of PS. The peaks at 1452 and 1375 cm^{-1} correspond to the aliphatic C—H stretching in NR.

The ^{1}H NMR spectrum obtained at 90 MHz shows chemical shifts at 1–2, 4.6–4.8, and 6.6 ppm corresponding to alkyl protons of NR, vinyl protons and aromatic protons of polystyrene, respectively.

EFFECT OF GRAFT COPOLYMER CONCENTRATION ON MORPHOLOGY

NR/PS blends are completely immiscible. Large polystyrene domains are dispersed in the continuous NR matrix. The compatibility of the above system can be improved by the addition of a compatibilizer *i.e.*, a graft copolymer of NR and PS (NR-*graft*-PS). It was seen that the size of the dispersed polystyrene domains decreases with the increasing percentage of the graft copolymer. Figure 1 shows the optical microphotographs of 50/50 NR/PS blends with and without the additon of the copolymer. In this blend the NR is the continuous phase and PS is the dispersed phase. The number average domain size measurements were done by noting the diameter of about 100 domains at random in each blend system. The average domain size decreases with increasing concentration of the compatibilizer and finally levels
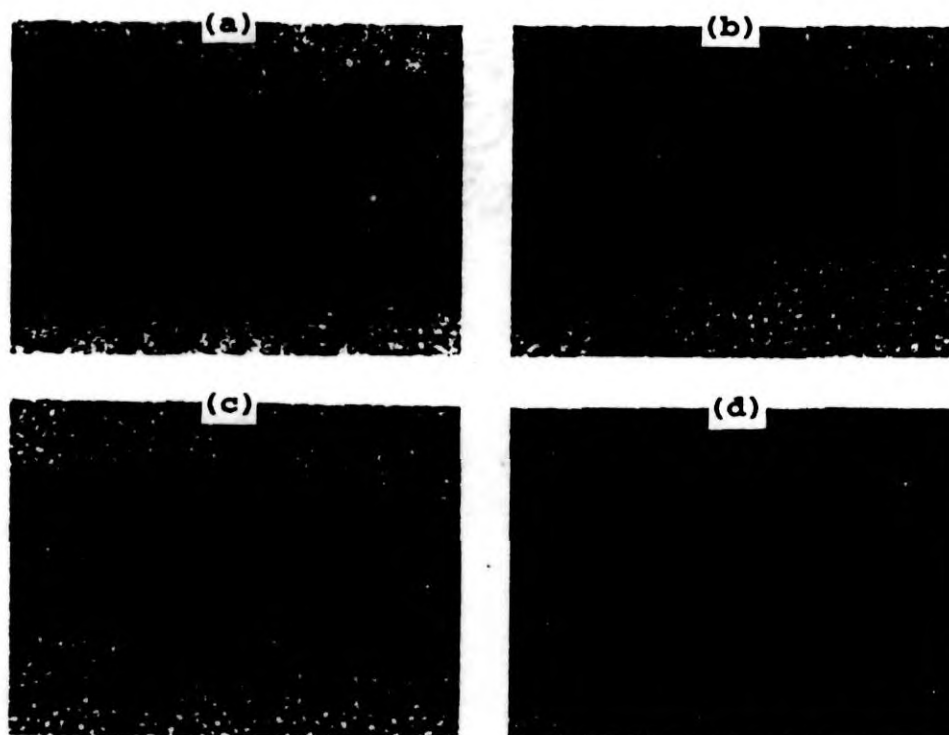

FIG. 1. — Optical photographs of 50/50 NR/PS blends with variable amounts of graft copolymer; (a) 0%; (b) 1.5%; (c) 3%; (d) 6%.

off at higher concentrations (Figure 2). This leveling point can be considered as the so-called apparent critical micelle concentration (CMC) *i.e.*, concentration of the copolymer at which micelles are formed. This sort of micelle formation is highly undesirable. From Figure 2, the CMC values were, in fact, estimated from the intersection of the straight line drawn in the low concentration and the leveling off line at high concentration. It is important to indicate that generally CMC is estimated from the plot of interfacial tension versus copolymer concentration. Since the interfacial tension is directly proportional to the domain size, the estimation of CMC from the plot of domain size versus concentration is justified.[35]

Let us now look at 50/50 blend in detail. Here the leveling point (CMC) was found to be at 0.8% compatibilizer loading. The domain size of the blend without graft copolymer is 26.88 μm. Addition of 1.5% graft reduces the domain size to 3.493 μm; *i.e.*, a reduction of 82.7% occurs. Addition of another 1.5% causes a reduction of 38% in the domain size. Finally the domain size levels off at higher concentrations. In the case of 60/40 and 40/60 NR/PS blends the percentages of graft copolymer required to saturate the interface (*i.e.*, CMC) are 1.5% and 0.6%, respectively.

The domain size distribution for 50/50 NR/PS blend with and without the addition of the compatibilizer is given is Figure 3. Table II gives the standard deviation values of the blend (50/50) with and without the addition of the copolymer. These values decrease with increasing loading of the copolymer. The uncompatibilized blend contains large numbers of bigger particles. The polydispersity is higher for the blend without compatibilizer and is much reduced at higher concentration of the compatibilizer, which is evident from the width of the distribution curve. Similar studies have been reported by Willis and Favis[36] and by Djakovic *et al.*[37]

Figure 4 shows the effect of compatibilizer on the interparticle distance of dispersed domains in the 50/50 NR/PS blend system. The interparticle distance decreases with increasing concentration of the compatibilizer and finally levels off at higher compatibilizer loading.

EFFECT OF HOMOPOLYMER AND GRAFT COPOLYMER MOLECULAR WEIGHTS ON MORPHOLOGY

The compatibilizing effect of the graft copolymer in NR/PS blends depends very much on the molecular weight of the homopolymer. Generally, the amount of the graft copolymer
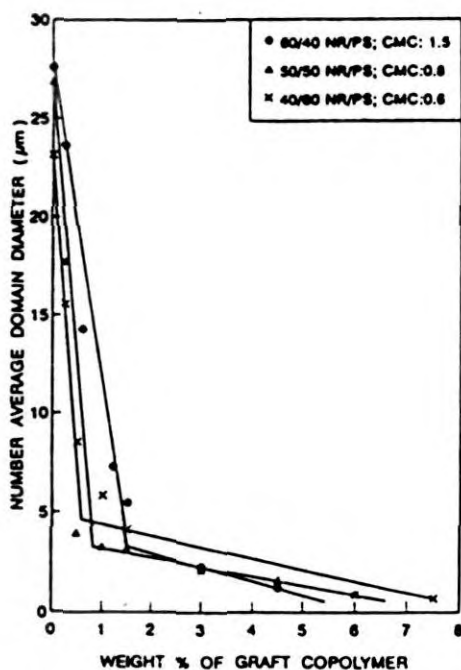
FIG. 2. — Effect of copolymer concentration on the average domain size of the dispersed phase for different NR/PS blends.
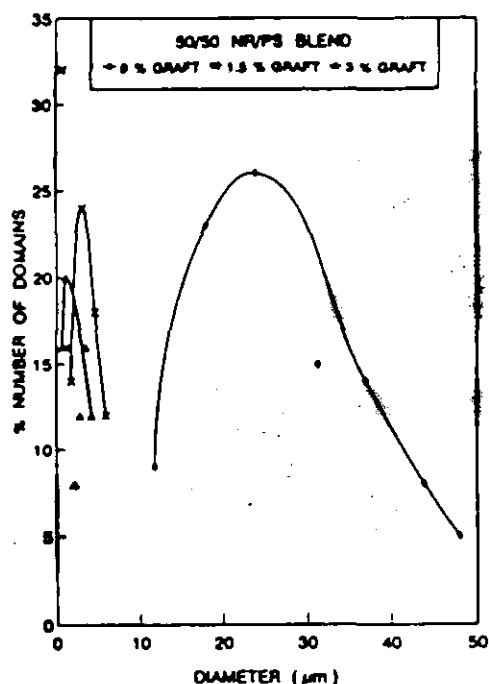
FIG 3. — Effect of copolymer concentration on the average domain size distribution of 50/50 NR/PS blends.

required for compatibilization is proportional to the molecular weight of the homopolymer. Natural rubbers and polystyrenes of the following molecular weights were used to study the effect of homopolymer molecular weight on the compatibilizing action of the graft copolymer — natural rubber: $NR_0 = 7.79 \times 10^5$; $NR_6 = 3.7 \times 10^5$; $NR_{10} = 2.49 \times 10^5$; $NR_{16} = 1.62 \times 10^5$; and polystyrene: $PS_1 = 3.51 \times 10^5$; $PS_2 = 2.073 \times 10^5$.

The amount of graft copolymer required to saturate unit volume of the interface (CMC) was found to decrease with decrease in molecular weight (Figures 5 and 6) of the homopolymers. The average domain size decreases with an increase in graft loading. The influence of polystyrene molecular weight on CMC values and domain size is given Table III.

Molecular weight of the copolymer (NR-*graft*-PS) influences the interfacial saturation point. We have used graft copolymers of molecular weight $G_1 = 3.95 \times 10^5$ and $G_2 = 1.009 \times 10^5$. The amount of graft copolymer needed for interface saturation decreases with increase in molecular weight of the compatibilizer. The critical micelle concentration was found to be 1.5% in the case of 60/40 NR/PS blends compatibilized with sample G_1. The same blend system with sample G_2 gives a higher CMC value; *i.e.*, a 3% compatibilizer loading was required to saturate unit volume of the interface.

TABLE II

STANDARD DEVIATION VALUES OF 50/50 NR/PS BLEND

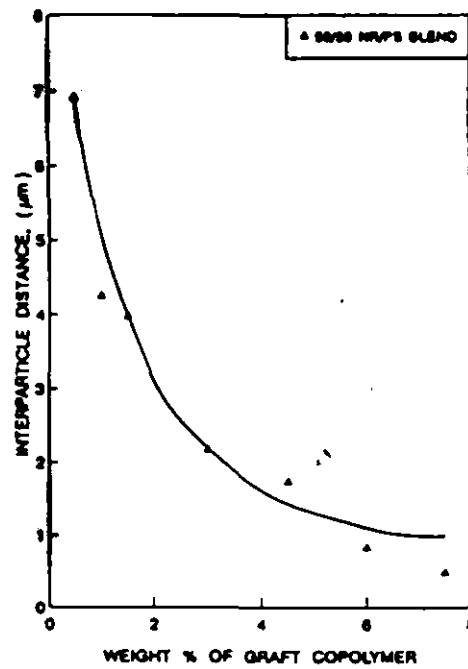| % Graft copolymer	Average domain size (μm)	Standard deviation
0.5	3.5	25.45
1	3.2	23.40
1.5	3.4	24.95
3	2.1	7.40
4.5	1.6	11.70
6	0.9	2.15

Fig. 4. — Effect of copolymer concentration on the interparticle distance
of the dispersed phase of 50/50 NR/PS blend.

EFFECT OF MODE OF ADDITION OF GRAFT COPOLYMER ON MORPHOLOGY

Morphology of the blend depends very much on the mode of preparation of the blends.
Variation in the conditions of blend preparation can change the morphology. Cimmino et
al.[38] have observed a drastic change in the domain size of nylon/rubber blends when prepared
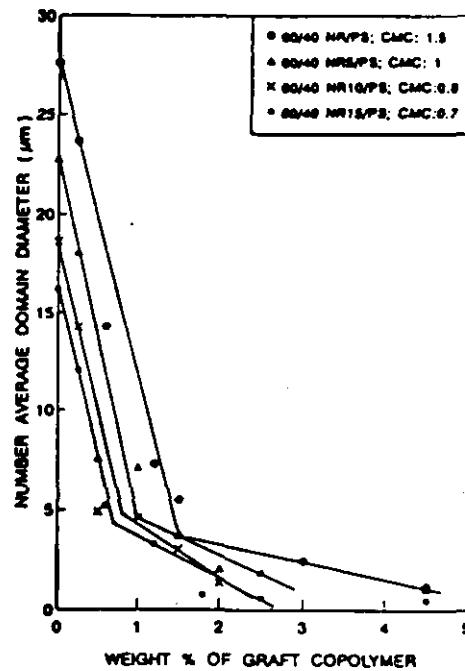in two steps compared to one-step mixing.

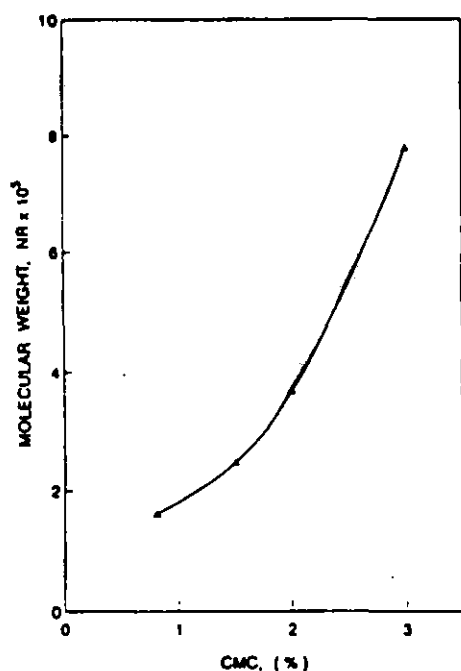Fig 5. — Influence of NR molecular weight on morphology of different NR/PS blends.

FIG. 6. — Effect of NR molecular weight on the apparent critical micelle concentration, CMC.

The two-step mixing can be done in two ways. Blending the solution of the dispersed phase (PS) with the compatibilizer first and then blending with the matrix polymer (NR). In the second case the matrix polymer is blended with the compatibilizer first and then blending with the dispersed polymer. Solutions were blended and then evaporated to get thin films. Preblending the compatibilizer with the dispersed phase (PS) is found to improve the interaction between the copolymer and the dispersed phase.

The particle size and CMC of NR_0/PS blends were measured in the two-step mixing and were compared the values with those of one-step mixing. In the case of 60/40 NR/PS blends (one-step) the CMC was attained at 1.5% of the graft copolymer. When the copolymer phase was preblended with the dispersed phase, the CMC was attained at 1.3% of the graft copolymer loading and there is much reduction in the domain size of the dispersed phase. In one-step mixing, the particle size of the domains at 1.5% graft copolymer loading was found to be 5.08 μm whereas in two-step mixing the corresponding value is 3.70 μm; at 2.5% graft loading, the values are 2.45 μm and 1.84 μm, respectively. When the matrix polymer was preblended with the copolymer, the CMC was the same as in the case of one-step mixing (1.5%) (see Table IV).

The above findings reveal that the mode of addition of the compatibilizer has an important role in the morphology of the blends. Compared to one-step mixing, in two-step mixing i.e., by preblending the compatibilizer with the dispersed phase, the amount of the compatibilizer

TABLE III

EFFECT OF MOLECULAR WEIGHT OF PS on CMC VALUES

Sample	Mol wt. (M_n)	CMC (%)	Domain radius (r) at CMC (μm)
PS₁	3.51×10^5	1.5	1.80
PS₂	2.07×10^5	1.2	1.28

TABLE IV

DISPERSED PHASE RADIUS (r) AT CMC AND 'Σ' VALUES OF THE SYSTEM

Polymer blends	Solvent	CMC (m) (%)	Radius r at CMC (μm)	'Σ' (nm²)
40/60 (NR$_0$/PS$_1$/G$_1$)	CHCl$_3$	0.6	1.30	100.9
50/50 (NR$_0$/PS$_1$/G$_2$)	CHCl$_3$	0.8	1.71	71.9
60/40 (NR$_0$/PS$_1$/G$_1$)[a]	CHCl$_3$	1.5	2.54	30.98
60/40 (NR$_0$/PS$_1$/G$_1$)[b]	CHCl$_3$	1.3	1.85	49.10
60/40 (NR$_0$/PS$_1$/G$_1$)[c]	CHCl$_3$	1.5	2.45	32.12
60/40 (NR$_0$/PS$_1$/G$_1$)	CCl$_4$	1.1	1.30	82.55
60/40 (NR$_0$/PS$_1$/G$_2$)	CHCl$_3$	3.0	0.65	15.46
60/40 (NR$_4$/PS$_1$/G$_1$)	CHCl$_3$	1.0	2.36	50.02
60/40 (NR$_{10}$/PS$_1$/G$_1$)	CHCl$_3$	0.8	2.45	60.08
60/40 (NR$_{18}$/PS$_1$/G$_1$)	CHCl$_3$	0.7	2.60	64.97

[a] One-step mixing.
[b] Two-step mixing NR to PS + G.
[c] Two-step mixing PS to NR + G.

diffused into the interface can be increased and the distance travelled by the compatibilizer to reach the blend interface can be minimized. This leads to better interfacial interaction of the compatibilizer and results in a finer morphology. A speculative model has been given to illustrate this behavior (Figure 7).

EFFECT OF CASTING SOLVENTS ON MORPHOLOGY

Casting solvent plays an important role in the morphology of blends. The same blend system can give different morphologies in different casting solvents.

We have selected two solvents for comparison: chloroform and carbon tetrachloride. There is much difference in the resulting domain size for the two solvent systems. Films cast from carbon tetrachloride show a finer morphology than chloroform cast films (Figure 8). The difference in the behavior may be due to the difference in the level of interaction between the copolymers and solvents. This has been well addressed by the pioneering studies of Robard and Patterson.[39]
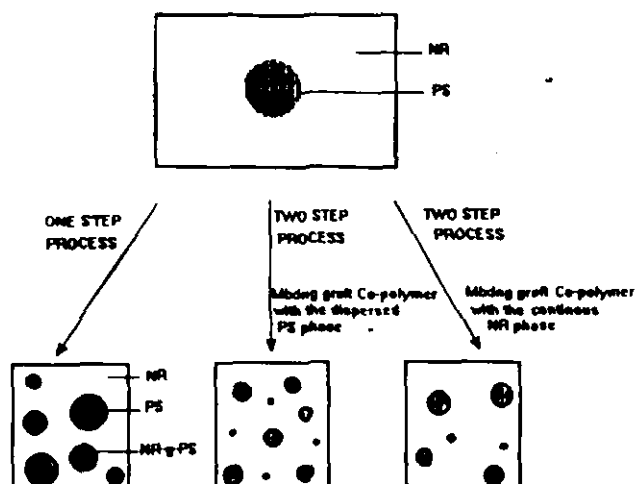

Fig. 7. — Speculative model illustrating the compatibilization efficiency under different modes of copolymer addition.
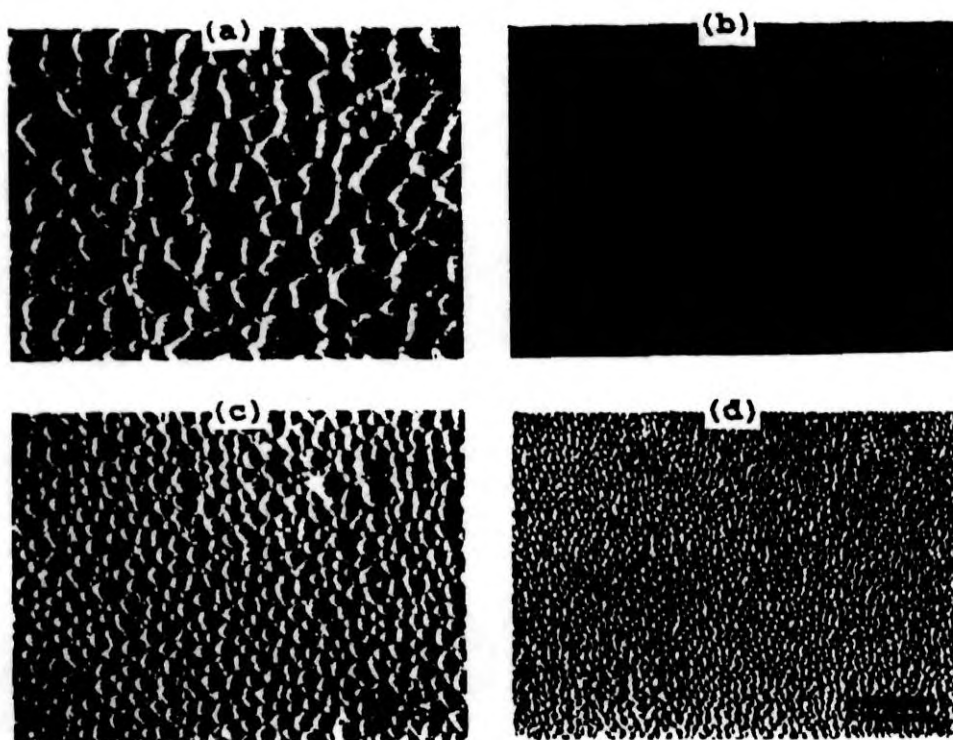
FIG. 8. — Optical photographs of 60/40 NR/PS films casted from CCl₄ and CHCl₃ containing variable amounts of graft copolymer; (a), 0% graft from CHCl₃; (b), 1.2% graft from CHCl₃; (c), 0% graft from CCl₄; (d), 1.2% graft from CCl₄.

In both cases the addition of graft copolymer reduces the domain size.[40] The concentration of the graft copolymer required to saturate unit volume of the interface is less for carbon tetrachloride cast film (CMC — 1.1%) than for chloroform cast film (CMC — 1.5%). The sizes of the domains of the uncompatibilized blends of chloroform cast and carbon tetrachloride cast films are 27.6 μm and 17.6 μm, respectively. This behavior is due to the fact that the solubility parameter of CCl₄ (δ = 8.6) is closer to those of the polymers (PS, δ = 8.56; NR, δ = 7.75) than is the solubility parameter of CHCl₃ (δ = 9.3).

MECHANICAL PROPERTIES

Blend morphology has a significant effect on the mechanical properties of the blends. Many research studies have been reported on the morphology–mechanical property relationships of polymer blends. Paul, Locke and Vinson[41] have studied the mechanical properties of PE/PVC blends containing chlorinated PE as compatibilizer. Mechanical properties of nylon/PP was studied by Ide and Hasegawa.[42] Lock and Paul[43] studied the improvement in mechanical properties of PS/PE blends by the addition of qraft copolymer. In all the above cases, the graft copolymer improved interfacial adhesion and hence the mechanical properties of the blends.

The influence of addition of graft copolymer on tensile strength and modulus was studied. Figure 9 shows the variation in tensile strength and modulus with percentage of the compatibilizer loading. Table V shows that the tensile strength and modulus increase with the addition of the copolymer and finally level off at higher concentrations. The impact strength increases up to 3% compatibilizer loading and then it decreases at higher concentration (Table V). These changes are in accordance with the morphology of the blends. Addition of the copolymer results in an improvement in tensile strength, modulus and impact strength due to the enhanced interfacial bonding between PS and NR through the graft copolymer.
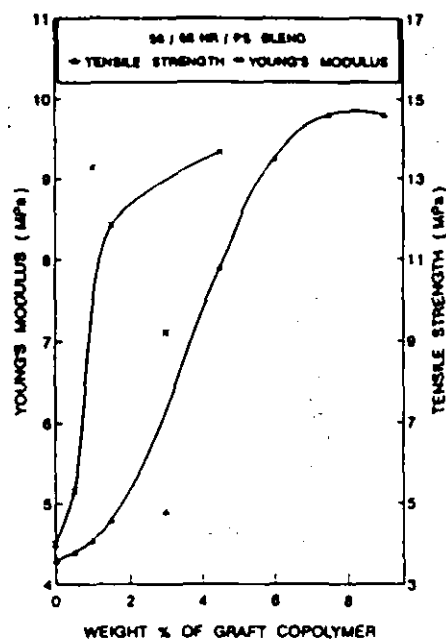
FIG 9 — Effect of copolymer concentration on the tensile strength and modulus of 50/50 NR/PS blend.

DISCUSSION

In the case of heterogeneous polymer blends, several research studies have concentrated on the compatibilizing action of the block and graft copolymers. The high interfacial tension existing between the phases which is responsible for macrophase separation can be reduced by the addition of the compatibilizer. There are different parameters which govern the interfacial saturation. These include molecular weight of the homopolymers, molecular weight of the copolymer, polymer(s) structural details, mode of addition of compatibilizer, processing conditions, affinity of the copolymer for the dispersed phase, orientation of the copolymer at the interface, etc.

The experimental and theoretical studies on the compatibilization of immiscible blends report on the so-called interfacial saturation by the addition of copolymers. For example in the case of polyethylene/natural rubber blends,[44] 5% of the compatibilizer (polyethylene-

TABLE V
MECHANICAL PROPERTIES OF 50/50 NR/PS BLENDS

Wt. % graft polymer	Stress at % elongation (MPa)			Tensile strength (MPa)	Elongation at break (%)	Tensile impact strength (J/mm²)
	15%	30%	50%			
0	1.24	1.78	2.37	3.60	454	0.30 × 10⁵
1	—	—	—	—	—	1.43 × 10⁵
1.5	1.54	1.82	2.45	3.86	194	1.64 × 10⁵
3	1.96	2.05	2.75	4.5Q	190	2.10 × 10⁵
4.5	1.99	2.28	3.07	10.10	252	1.63 × 10⁵
6	2.56	2.78	3.24	13.24	247	1.39 × 10⁵
7.5	3.20	3.47	3.88	13.15	241	1.37 × 10⁵

block-polyisoprene) was found to be sufficient for interfacial saturation. The compatibilizing action of poly(styrene-*block*-1,2-butadiene) in heterogeneous polystyrene/1,2-polybutadiene blends was reported by Spiros, Gancarz and Koberstein.[45] Interfacial tension reduced parallel with copolymer addition up to the critical micelle concentration (CMC) and thereafter leveled off at higher concentration. Beyond the CMC, further addition of the copolymer leads to micelle formation.

Willis and Favis[16] reported that about 5% of the ionomer is sufficient for polyolefin/ polyamide blend system for interfacial saturation. Fayt, Jerome and Teyssie[11,12] found equilibration of domain size by the addition of 0.5%–1% by weight of the compatibilizer. The recent studies of Thomas and Prud'homme[46] and Oommen and Thomas[47] also report on the interfacial saturation by the addition of copolymers in PS/PMMA and NR/PMMA systems, respectively. The theoretical predictions of Noolandi and Hong[30-32] indicated that micellar aggregation of the copolymer takes place at the interface of the blend beyond a critical concentration of the copolymer (CMC).

Almost all the experimental and theoretical studies related to the compatibilization of heterogeneous blends, including the present work, suggest that there is a critical concentration of the compatibilizer required to saturate the blend interface (CMC) beyond which addition of the compatibilizer leads to undesirable micelle formation which very often reduces the total performance of the blend system.

One can also explain the interfacial saturation point using Taylor's Equation.[36]

$$W_e = \frac{\eta_m d n \dot{\gamma}}{2\gamma_{12}};$$ (1)

where W_e is the critical Weber number; η_m is the viscosity of the matrix, $\dot{\gamma}$ is the shear rate; γ_{12} is the interfacial tension, and dn is the number average diameter of the dispersed phase. On the addition of the compatibilizer, the interfacial tension decreases and there is a consequent particle break down (deformation). However, at a particular compatibilizer loading there is a balance of interfacial tension and particle deformation. Thus, there is a critical value of W_e below which no particle deformation occurs and at this point, the compatibilizer occupies the maximum interfacial area. Therefore, there is a maximum quantity of the compatibilizer required to saturate the blend interface and beyond this level further addition of compatibilizer will not reduce the particle size. The studies of Favis and Willis[48] and White[49] also report similar observations.

The compatibilizer added to a heterogeneous blend locates at the interface and reduces the interfacial energy. Based on thermodynamics, Noolandi and Hong[30-32] developed an expression for interfacial tension reduction. Accordingly, the interfacial tension reduction $\Delta\gamma$ in a heterogeneous binary blend A/B — upon the addition of a copolymer, A-*block*-B — is given by

$$\Delta\gamma = d\phi_c\left[\left(\frac{1}{2}\chi + \frac{1}{Zc}\right) - \frac{1}{Zc}\exp\left(Zc\,\frac{\chi}{2}\right)\right];$$ (2)

where d is the width at half height of the copolymer profile reduced by Kuhn statistical segment length; χ is the Flory Huggins interaction parameter between the A and B segment of the AB copolmer; and Zc is the degree of polymerization of the copolymer. According to this theory, the interfacial tension reduction $\Delta\gamma$ is proportional to the copolymer volume fraction ϕ_c until the system reaches the CMC. However, beyond the CMC $\Delta\gamma$ levels off with ϕ_c. Although this expression was developed for block copolymers, our recent investigations indicated that this theory can be applied to graft copolymers as well.[47] Since interfacial tension reduction is directly proportional to particle size reduction Δd, it can be shown that

$$\Delta d = Kd\phi_c\left[\left(\frac{1}{2}\chi + \frac{1}{Zc}\right) - \frac{1}{Zc}\exp\left(Zc\,\frac{\chi}{2}\right)\right];$$ (3)

where K is the proportionality constant. The plot of experimental values of Δd vs. ϕ_c is given in Figure 10. It can be seen that at low concentration of the compatibilizer Δd decreases
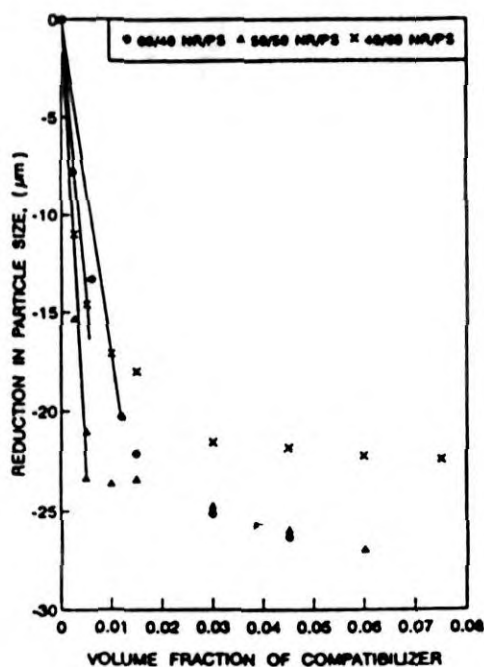
FIG. 10. — Effect of graft copolymer volume fraction on particle size reduction.

linearly with copolymer loading and at high concentration Δd levels off as indicated by Noolandi and Hong.

Valuable information can be obtained by calculating the area, Σ, occupied by the copolymer molecule at the blend interface. Let us consider a binary blend that contains a volume fraction ϕ_A of polymer A as spherical domains of radius r in a matrix B. The total interfacial area per unit volume of the original blend is equal to $3 \phi_A/\gamma$. If each copolymer molecule occupies an area, Σ, at the interface, the mass M of the copolymer required to saturate unit volume of the blend is given by the following equation[6]:

$$\Sigma = \frac{3\phi_A M}{mrN};$$ (4)

where M is the molecular weight of the copolymer and N is Avogadro's number. In the present study, since CMC is the interfacial saturation point, it would be reasonable to consider CMC to have the value m.

The radius r of the dispersed domain at CMC, the CMC values (m values), and Σ are given in Table IV. The CMC values are estimated from Figure 2 by the intersection of the straight line drawn at the low concentration and the leveling-off line at high concentration.

It can be noticed that the area occupied by the compatibilizer molecule at the interface (Σ) increases as the molecular weight of the homopolymer decreases (Figure 11). The 'Σ' values also depend on the mode of addition of the compatibilizer to the blend system. In the two step process where the copolymer is preblended with the dispersed phase, the Σ value is 49.10 nm^2. This indicates that the interaction of the copolymer and homopolymer is higher in the two-step process, compared to the one-step process where $\Sigma = 30.98$ nm^2. Greater interaction would increase interfacial area and reduce interfacial tension.

The nature of the casting solvent can also influence the 'Σ' values. In the case of CCl$_4$ Σ is higher (82.55 nm^2) compared to chloroform (30.98 nm^2). In a good solvent like CCl$_4$, interaction between the copolymer and homopolymer is greater than in chloroform and hence the interfacial area occupied by the copolymer is larger. Similarly the copolymer molecular weight is also a controlling parameter. When the copolymer molecular weight is reduced,
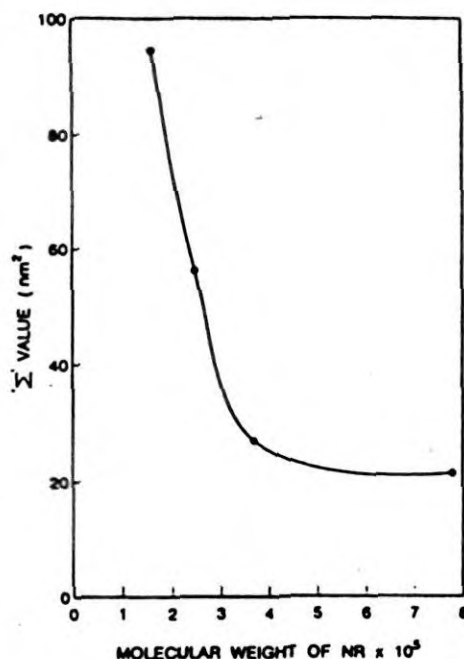
FIG. 11. — Effect of homopolymer molecular weight on the calculated area occupied
by the copolymer molecule at the blend interface, Σ.

the interaction between the copolymer and homopolymer is reduced. Hence the area occupied
by the copolymer at the interface is ($\Sigma = 15.46$ nm^2) lower than the area of a copolymer
with a higher molecular weight ($\Sigma = 30.98$ nm^2).

One can also comment on the conformation of the copolymer based on the Σ values.
Figure 12 depicts three different physical models representing the conformation of the co-
polymer at the blend interface. Model (a) indicates a conformation in which the graft co-
polymer extends into the corresponding homopolymer phases. In this case the occupied area
at the interface is the cross-sectional area of the extended copolymer molecule. This is ap-
proximately equal to 0.6 nm^2. In the (b) model [Figure 12(b)], the copolymer lies flat at the
interface and here the occupied area is the lateral surface area of the entire copolymer
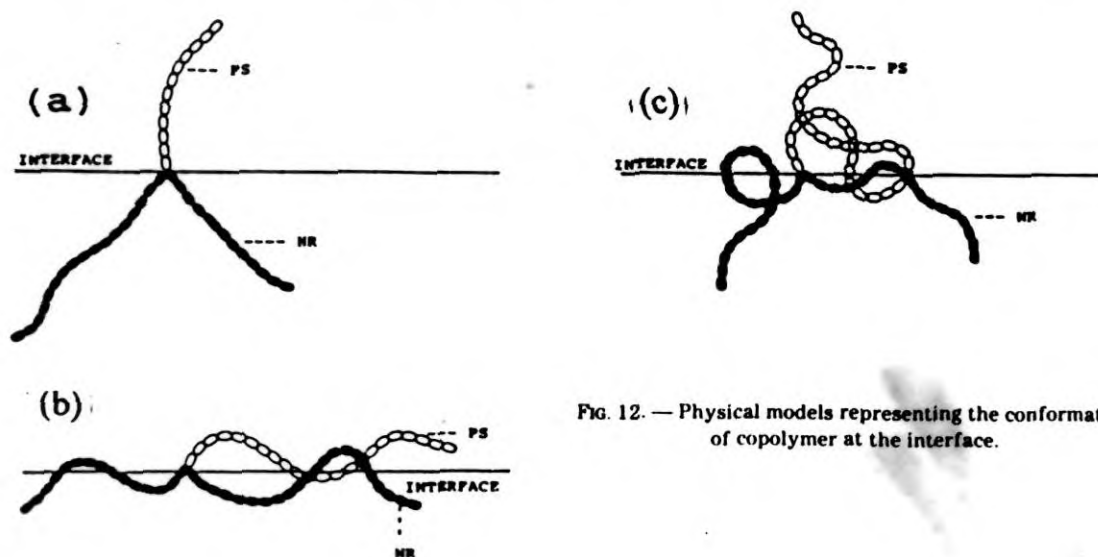

FIG. 12. — Physical models representing the conformation
of copolymer at the interface.

molecule. By considering each segment of the graft copolymer as a spherical random coil, we have calculated the lateral surface area of the copolymer by using the experimental values of the root-mean-square radius of gyration of the PS block reported in literature.[46] The lateral surface area was approximately equal to 106 nm^2.

A comparison of the experimental and calcuated values of interfacial area will give the actual conformation of the copolymer at the blend interface. The experimental values of Σ as obtained from Equation (4), lie between 15.46 and 100.9 nm^2 (see Table IV). This is intermediate to those of models (a) and (b) (0.6 and 106 nm^2) reported in the literature. This suggests that the actual conformation of the copolymer at the blend interface is neither fully extended nor completely flat. The actual position can be represented by model (c) in Figure 12, in which a portion of the copolymer remains at the interface and the rest penetrates into the corresponding homopolymer phases. This model is in agreement with the model suggested by Oommen and Thomas.[47] However, by controlling the physical parameters such as molecular weight of the homopolymer and copolymer, mode of preparation of the blends, casting solvents, etc., one can dictate the area occupied by the copolymer at the interface. For example, as the molecular weight of the copolymer increases or the molecular weight of the homopolymer decreases, the area occupied by the copolymer at the interface increases (see Table IV). For example, copolymer G_1 occupies an area of 30.98 nm^2, which is much higher than G_2 which occupies an area of 15.46 nm^2.

It is also important to consider the fact that as the molecular weight of the copolymer increases, macromolecular interactions, such as chain entanglement, hinder the complete penetration of each segment into the corresponding homopolymer phases. This suggests that the copolymer cannot penetrate completely into the homopolymer phases and therefore, it is expected that part of the copolymer may stay at the interface. This could lead to an increase in interfacial thickness which would be maximum in the case of copolymers having the highest molecular weight. According to Wu,[35] interfacial tension (γ_{12}) and interfacial thickness (L) are related by the following equation:

$$\gamma_{12} = 7.6/L0.86. \qquad (5)$$

This indicates that the superior compatibilizing action of the high molecular weight graft copolymer is associated with the larger increase in interfacial thickness and consequent reduction in interfacial tension. Russel et al.[18] also have reported that addition of copolymer increases the interfacial thickness of PS/PMMA blends. In this study the interfacial thickness was measured by neutron reflectivity. The thickness of the interface increased 50% by the addition of the copolymer. Recent experimental results of Anastesiadis, Gancarz and Koberstein[50] also support the conformation represented in Figure 12(c). They have reported on the compatibilizing action of poly(styrene-block-1,2-butadiene) in PS/1,2-poly(butadiene) and found that about 24% of the contour length of the copolymer chain is located at the blend interface and the rest penetrates into the corresponding homopolymer phases.

CONCLUSION

The compatibilizing activity of NR-graft-PS in heterogeneous NR/PS blends has been studied in detail. Both the morphology and mechanical properties of NR/PS blends have been investigated. Concentration and molecular weight of the copolymer, composition of the blend, mode of addition of compatibilizer, homopolymer molecular weight, and processing condition were the controlling parameters on blend morphology. Copolymer addition reduces the domain size of the dispersed phase and finally levels off at higher concentrations, an indication of interfacial saturation. The experimental results were in agreement with predictions of Noolandi and Hong.

The area occupied by the compatibilizer molecule at the interface (Σ) has been estimated. As the molecular weight of the homopolymer decreases, interfacial area occupied by the copolymer (Σ) increases, and hence more reduction in the domain size occurs. The 'Σ' values were also influenced by the blend composition, mode of addition and the nature of the casting

solvents. By the selection of a suitable solvent, having a solubility parameter close to that of the homopolymers, the interaction of the compatibilizer with the interface can be enhanced.

The mechanical properties are in agreement with the morphological changes. It was found that the tensile strength and modulus increases upon the addition of the compatibilizer and finally levels off at higher concentration.

Attempts were made to establish the conformation of the compatibilizer at the blend interface. Different models were discussed. The actual conformation is neither fully extended nor flat. A portion of the copolymer penetrates into the corresponding homopolymer and the rest remains at the interface.

· ACKNOWLEDGMENTS

REFERENCES

[1] G. E. Molau, in "Block Polymers," S. L. Aggarwal, Ed., Plenum Press, New York, 1970, p. 79.

[2] G. E. Molau and H. Keskkula, *Appl. Polym. Symp.* n.7, 35 (1968).

[3] G. E. Molau, *J. Polym. Sci., Part A* **A3**, 1267 (1965).

[4] G. E. Molau, *J. Polym. Sci., Part A* **A3**, 4235 (1965).

[5] D. R. Paul, in "Polymer Blends," D.R. Paul and S. Newman, Eds., Academic Press, New York, 1978, ch. 12.

[6] D. R. Paul and S. Newman, Eds. "Polymer Blends," Academic Press, New York, 1978, v. 1.

[7] G. Riess, J. Kohler, C. Tournut, and A. Banderet, *Makromol. Chem.* **101**, 58 (1967).

[8] J. Kohler, G. Riess, and A. Banderet, *Eur. Polym. J.* **4**, 173 (1968).

[9] T. Inoue, T. Soen, T. Hashimoto, and H. Kawai, *Macromolecules* **3**, 87 (1970).

[10] M. Moritani, T. Inoue, M. Motegi, and H. Kawai, *Macromolecules* **3**, 433 (1970).

[11] R. Fayt, R. Jerome, and Ph. Teyssie, *J. Polym. Sci., Polym. Phys. Ed.* **20**, 2209 (1982).

[12] R. Fayt, R. Jerome, and Ph. Teyssie, *Polym. Eng. Sci.* **27**, 328 (1987).

[13] R. Fayt, P. Hadjiandreou, and Ph. Teyssie, *J. Polym. Sci., Polym. Chem. Ed.* **23**, 337 (1985).

[14] H. T. Patterson, K. H. Hu, and T. H. Grindstaff, *J. Polym. Sci., Part C*, n. **34**, 31 (1971).

[15] P. Gailard, Sauter M. Ossenbach, and G. Riess, *Makromol. Chem. Rapid Commun.* **1**, 771 (1980).

[16] J. M. Willis and F. D. Favis, *Polym. Eng. Sci.* **30**, 1073 (1990).

[17] K. R. Shull, E. J. Mramer, G. Hadiziioanon, and W. Tang, *Macromolecules* **23**, 4780 (1990).

[18] T. P. Russel, A. Menelle, W. A. Hamilton, G. S. Smith, S. K. Satija, and C. F. Majkrzak, *Macromolecules* **24**, 5721 (1991).

[19] M. L. Fernandez, J. S. Higgins, J. Penfold, R. C. Ward, C. Shackelton, and D. Walsh, *Polymer* **29**, 1923 (1988).

[20] A. Y. Coran and R. Patel, RUBBER CHEM. TECHNOL. **56**, 1045 (1983).

[21] A. Y. Coran and Patel, RUBBER CHEM. TECHNOL. **56**, 210 (1983).

[22] A. Y. Coran and R. Patel, RUBBER CHEM. TECHNOL. **53**, 141 (1980).

[23] A. Y. Coran, R. Patel, and D. Williams-Headd, RUBBER CHEM. TECHNOL. **58**, 1014 (1985).

[24] A. K. Bhowmick and H. L. Stephens, "Handbook of Elastomers," Marcel Dekker, Inc., New York and Basel, 1988, ch. 8.

[25] A. Y. Coran and R. Patel, RUBBER CHEM. TECHNOL. **56**, 1045 (1983).

[26] N. R. Legge, G. Holden, and H. E. Schroeder, "Thermoplastic Elastomers," Hanser, Munich Vienna, New York, 1987, ch. 7.

[27] W. K. Fisher (to Uniroyal, Inc.), U.S. 3,758,643 (Sept. 11, 1973).

[28] L. Leibler, *Makromol. Chem., Macromol. Symp.* **16**, 17 (1985).

[29] L. Liebler, *Macromolecules* **15**, 1283 (1982).

[30] J. Noolandi, *Polym. Eng. Sci.* **24**, 70 (1984).

[31] J. Noolandi and K. M. Hong, *Macromolecules* **15**, 482 (1982).

[32] J. Noolandi and K. M. Hong, *Macromolecules* **17**, 1531 (1984).

[33] W. Cooper, P. R. Sewell, and G. Vaughan, *J. Polym. Sci.* **41**, 167 1959).

[34] M. Goni, Gurru Chaga, J. Sam Roman, M. Valero, and G. M. Guzman, *Polymer* **34**, 512 (1993).

[35] S. Wu, *Polym. Eng. Sci.* **27**, 335 (1987).

[36] J. M. Willis and B. D. Favis, *Polym. Eng. Sci.* **28**, 1416 (1988).

[37] L. Djakovic, P. Dokie, I. S. Radivojevic, and V. Sovilij, *Colloid Polym. Sci.* **265**, 993 (1987).

[38] S. Cimmino, F. Coppola, L. D'orazio, R. Greco, G. Maglio, M. Malinconico, C. Man Carella, E. Martuscali, and G. Ragosta, *Polymer* **27**, 1874 (1986).

[39] A. Robard and D. A. Patterson, *Macromolecules* 10, 1021, (1977).

[40] R. Asaletha, M. G. Kumaran, and S. Thomas, *Polym. Plast. Technol. Enq.* (in press).

[41] D. R. Paul, C. E. Locke, and C. E. Vinson, *Polym. Eng. Sci.* 13, 202 (1973).

[42] F. Ide and A. Hasegawa, *J. Appl. Polym. Sci.* 18, 963 (1974).

[43] C. E. Locke and D. R. Paul, *J. Appl. Polym. Sci.* 17, 2591 (1973).

[44] C. Qin, J. Yin, and B. Huang, *Polymer* 31, 663 (1990).

[45] H. A. Spiros, Irena Gancarz, and J. T. Koberstein, *Macromolecules* 22, 1449 (1989).

[46] S. Thomas and R. E. Prud'homme, *Polymer* 33, 4260 (1992).

[47] Z. Oommen and S. Thomas, *Polym. Eng. Sci.* (in press).

[48] B. D. Favis and J. M. Willis, *J. Polym. Sci. Polym. Phys. Ed.* 28, 2259 (1990).

[49] J. L. White, *Polym. Eng. Sci.* 13, 46 (1973).

[50] S. A. Anastesiadis, I. Gancarz, and J. T. Koberstein, *Macromolecules* 22, 1449 (1989).

EFFECT OF CASTING SOLVENTS AND COMPATIBILIZER LOADING ON THE MORPHOLOGY AND PROPERTIES OF NATURAL RUBBER/ POLYSTYRENE BLENDS

R. ASALETHA and M. G. KUMARAN

Rubber Research Institute of India
Kottayam—686 009, Kerala, India

SABU THOMAS*

School of Chemical Sciences
Mahatma Gandhi University
Priyadarshini Hills PO
Kottayam—686 560, Kerala, India

Abstract

Thermoplastic elastomers from blends of natural rubber (NR) and polystyrene (PS) have been prepared by the solution-casting technique. The blend of NR and PS is an incompatible one and can be made compatible by the addition of NR-*g*-PS. The compatibilizing action of NR-*g*-PS in NR/PS blends has been studied with special reference to the effect of the nature of the casting solvents and compatibilizer loading. Chloroform and carbon tetrachloride were selected as the casting solvents. The nature of the casting solvent has a profound influence on the compatibilizing action of the graft

* To whom all correspondence should be addressed.

633

copolymer. This has been explained based on the preferential interaction of the solvent with one of the components in the mixture. The domain size of the dispersed polystyrene phase was decreased by the addition of a few percent of the compatibilizer, followed by a leveling off at higher concentrations. The leveling off is an indication of interfacial saturation. The mechanical properties of the blends were improved by the addition of the compatibilizer.

INTRODUCTION

The blending of polymers has become an important industrial technique which is an economic and versatile way to produce materials having a wide range of properties. Thermoplastic elastomers prepared from blends of rubber and plastic have created very much interest in the industrial sector. Many of the thermoplastic elastomer blends are incompatible and hence exhibit poor mechanical properties. This problem can be alleviated by the addition or the in situ formation of a compatibilizer [1, 2]. Suitably selected compatibilizers will locate at the interface between the blend components, reduce the interfacial energy, and result in improved interfacial adhesion. The compatibilizer can be a graft copolymer, block copolymer, or a third component which can interact with both blend phases.

Several studies have been reported on the action of compatibilizers in heterogeneous blends. Molau et al. [3-5] reported on the ability of block copolymers to emulsify polymer dispersions in solution and reduce phase separation. Gailard and coworkers [6, 7] studied the interfacial tension reduction in the polystyrene/polybutadiene/styrene ternary system by the addition of poly(styrene-b-butadiene). Patterson et al. [8] have reported on the incompatible methyl-terminated poly(dimethyl siloxane)/poly(oxyethylene-b-oxypropylene) system, which was made compatible by the addition of poly(dimethyl siloxane-b-oxymethylene). Anastasiadis et al. [9] reported on the compatibilizing action of polystyrene-b-polybutadiene in the polystyrene/1,2-polybutadiene system. Studies of Coumans et al. [10] deal with the polyethylene/polystyrene blend system and its emulsification by the corresponding block copolymer.

Willis and Favis [11, 12] reported on the processability–morphology relationship in different blend systems. The morphology of compatibi-

lized polyolefin/polyamide blends was found to be dependent on the concentration of the compatibilizer [11]. The morphology and impact properties of polystyrene–maleic anhydride/bromobutyl rubber blends have been studied as a function of interfacial modification [12].

The nature of the casting solvent has a major influence on the morphology and properties of the dispersed phase of heterogeneous blends. Caravatti et al. [13] studied the influence of casting solvents on the miscibility and phase separation behavior of polystyrene/poly(vinylmethylether) blends. They used chloroform and toluene as casting solvents, and reported on the characterization of heterogeneous polystyrene/poly(vinylmethylether) system by two-dimensional proton spin diffusion spectroscopy for the study of heterogeneity in blends. In heterogeneous systems, spin diffusion between components in different domains depends on domain size, which provides insight into the domain structure of polymers. In the case of polystyrene/poly(vinylmethylether), when cast from chloroform, the diffusion spectrum indicated the absence of spin diffusion between the two polymers and there was no evidence of mixed domain in the blend. However, when cast from toluene, the diffusion spectrum revealed the presence of mixed domains in which component polymers were in close contact on a microscopic scale. Chiou et al. [14] have reported the miscibility of bisphenol-A–polycarbonate with poly(methylmethacrylate). They have adopted various techniques such as solution casting (CH_2Cl_2, THF as casting solvents), melt mixing, and precipitation methods for the blend preparation.

Chen and Morewetz [15] reported on blends of styrene copolymers and terpolymers carrying hydrogen bond donors with polymethacrylates. The miscibility of the polymers depended strongly on the casting solvents. Blends were cast from toluene, dioxane, and chloroform, and the intimacy of the mixing of the components of these blends was characterized by nonradiative energy transfer (NET) from the carbazole to the anthracene flurophore. It has been observed that the same polymer blend can give different morphologies in different systems depending upon the solvents from which the film was cast, and this is due to the preferential interaction of the solvents with one of the components in the mixture [16–18]. Solutions of polystyrene–poly(vinylmethylether) pairs in benzene and tetrachloroethene [16] are clear, and here $|\Delta\chi|$ (the difference in strengths of the polymer–solvent interaction) was found to be small. However, phase separation was observed for the same blend system (PS/PVME) in chloroform, trichloroethene, and di-

chloromethane, where $|\Delta\chi|$ is large. Oommen et al. [19] reported on the effect of casting solvents in the preparation of a natural rubber/polymethylmethacrylate blend which was made compatible by the addition of natural rubber-g-poly(methylmethacrylate). They selected chlorobenzene and toluene as the casting solvents. It was found that chlorobenzene cast film gives finer morphology, and that the amount of compatibilizer required for interfacial saturation is less in this case than that in toluene-cast film.

Thomas and Prud'homme [20] reported on the effect of processing conditions on the phase morphology of polystyrene/poly(methylmethacrylate)/polystyrene-b-poly(methylmethacrylate) blends. It was found that films cast from chloroform had a coarser morphology than those cast from 1,2-dichloroethane. The compatibilizing effect was more efficient in 1,2-dichloroethane.

This paper deals with the effect of processing conditions and compatibilizer loading on the morphology and mechanical properties of natural rubber/polystyrene blends. Morphology and mechanical properties of blends were analyzed in two casting solvents, chloroform and carbon tetrachloride.

EXPERIMENTAL

The raw materials required for this study include polystyrene, supplied by Poly Chem India Ltd., Bombay; and natural rubber (ISNR-5), supplied by the Rubber Research Institute of India, Kottayam. The characterization data on the polystyrene and natural rubber are given in Table 1.

Graft copolymer (NR-g-PS) was prepared by the method adopted by Cooper et al. [21] using ^{60}Co γ-radiation as the initiator. Styrene monomer was made into an emulsion which was then mixed with NR latex of known dry rubber content (DRC) at room temperature and exposed to ^{60}Co γ-radiation for 16 h (dose rate 0.1166 mrad/h). The free homopolymers natural rubber and polystyrene were removed from the crude sample by extraction with petroleum ether and methylethylketone, respectively. The grafting efficiency was found to be 49% and the percentage of polystyrene grafted was 20. These values were obtained gravimetrically as reported earlier [22].

The graft copolymer obtained was characterized by Fourier-transform infrared spectroscopy (FTIR) and nuclear magnetic resonance (H^1

TABLE 1
Characteristics of the Materials Used

Material	Density (g/cc)	Solubility parameter $(Cal/cm^3)^{1/2}$	Intrinsic viscosity (dL/g)	Molecular weight (MW)
NR	0.90	7.75	4.25	7.79×10^5
PS	1.04	8.56	1.241	3.51×10^5
NR-g-PS	—	—	3.09	3.49×10^5
CCl₄	—	8.6	—	—
CHCl₃	—	9.3	—	—

NMR) spectroscopic studies. The FTIR spectrum shows the following absorption peaks corresponding to various stretchings in the molecule. The peak at 3026 cm^{-1} corresponds to the aromatic C—H stretching in polystyrene. Peaks at 1452 cm^{-1} and 1493 cm^{-1} correspond to the aliphatic (C—H) stretching of PS. Peaks at 1601 cm^{-1}, 1493 cm^{-1}, and 1541 cm^{-1} correspond to (C=C) stretching of the aromatic ring of PS. The peak at 1375 cm^{-1} corresponds to (C—H) stretching of natural rubber, and those at 837 cm^{-1} and 1244 cm^{-1} correspond to (C=C) and (C—C) stretching of NR, respectively. The proton NMR spectrum obtained at 90 MHz shows chemical shifts at 1-2, 4.6-4.8, and 6.6 ppm, corresponding to alkyl protons of NR, and to vinyl protons and aromatic protons of polystyrene, respectively.

Natural rubber and polystyrene were blended together (60/40 composition) in a common solvent, chloroform or carbon tetrachloride with and without the addition of the graft copolymer. The samples were made on a glass plate and dried in vacuum oven at 80°C for 48 h and then at 120°C for a further 4 h. The morphology of the blend was studied by optical microscopy. The tensile properties were measured in a Zwick universal testing machine at a cross head speed of 50 mm/min.

RESULTS AND DISCUSSION

Morphology

Effect of graft copolymer as a compatibilizer depends on the molecular weight, concentration, composition, and conformation of the graft copolymer at the interface. The compatibilizing action of graft copolymer

is also affected by the processing conditions (nature of casting solvents, mode of addition, etc.). The compatibilizing activity of the NR-*g*-PS in NR/PS blends was analyzed by noting the domain size of the dispersed PS phase in the continuous NR matrix. The domain size of the dispersed PS was measured from optical photographs. In the morphology study, about 100 domains were selected at random and the diameter of each domain was measured.

Figures 1(a)–1(e) show the domain morphology of carbon tetrachloride-cast 60/40 NR/PS blends containing 0, 1.2, 3, 4.5, and 7.5% graft copolymer, respectively. Figures 2(a)–2(e) show the corresponding sample made from chloroform. Films cast from carbon tetrachloride show finer morphology compared to those cast from chloroform. The sizes of the uncompatibilized blend of chloroform-cast and carbon tetrachloride-cast films are 27.6 μm and 17.6 μm, respectively. As discussed earlier, the morphology of a binary blend strongly depends on the nature of the casting solvent, and the same blend can give different morphologies in different solvents [13, 17]. The domain size of the film cast from carbon tetrachloride is smaller than that cast from chloroform. The difference in behavior is due to the difference in solubility parameter values, which are given in Table 1. The solubility parameter difference between polystyrene and carbon tetrachloride is 1.02 (ΔA_1) and that between polystyrene and chloroform is 0.38 (ΔB_1). The difference in solubility parameter between NR and carbon tetrachloride is 1.00 (ΔA_2) and that between NR and chloroform is 2.40 (ΔB_2). The ΔA_1 − ΔA_2 value and ΔB_1 − ΔB_2 value between the homopolymers and solvents are 0.02 and 2.02 for carbon tetrachloride and chloroform, respectively. This suggests that the homopolymers have no preferential interaction with carbon tetrachloride. However, in the case of chloroform, the homopolymers have different levels of interactions. Polystyrene more strongly interacts with chloroform than NR since the solubility parameter of PS is very close to that of chloroform. Therefore, carbon tetrachloride-cast films give finer morphology.

By the addition of 1.2% graft copolymer to the blend, the domain size of chloroform cast film was reduced to 7.29 μm; i.e., a reduction of 73.5% occurs. For carbon tetrachloride-cast film, addition of 1.2% graft copolymer reduces the domain size to 2.28 μm; i.e., a reduction of 86.9% occurs. Addition of a further 1.8% graft copolymer causes a domain size reduction of 66.3% in the case of chloroform-cast film and 69.4% for the carbon tetrachloride-cast film. The size of the domains finally levels off at higher concentrations of the compatibilizer.)The
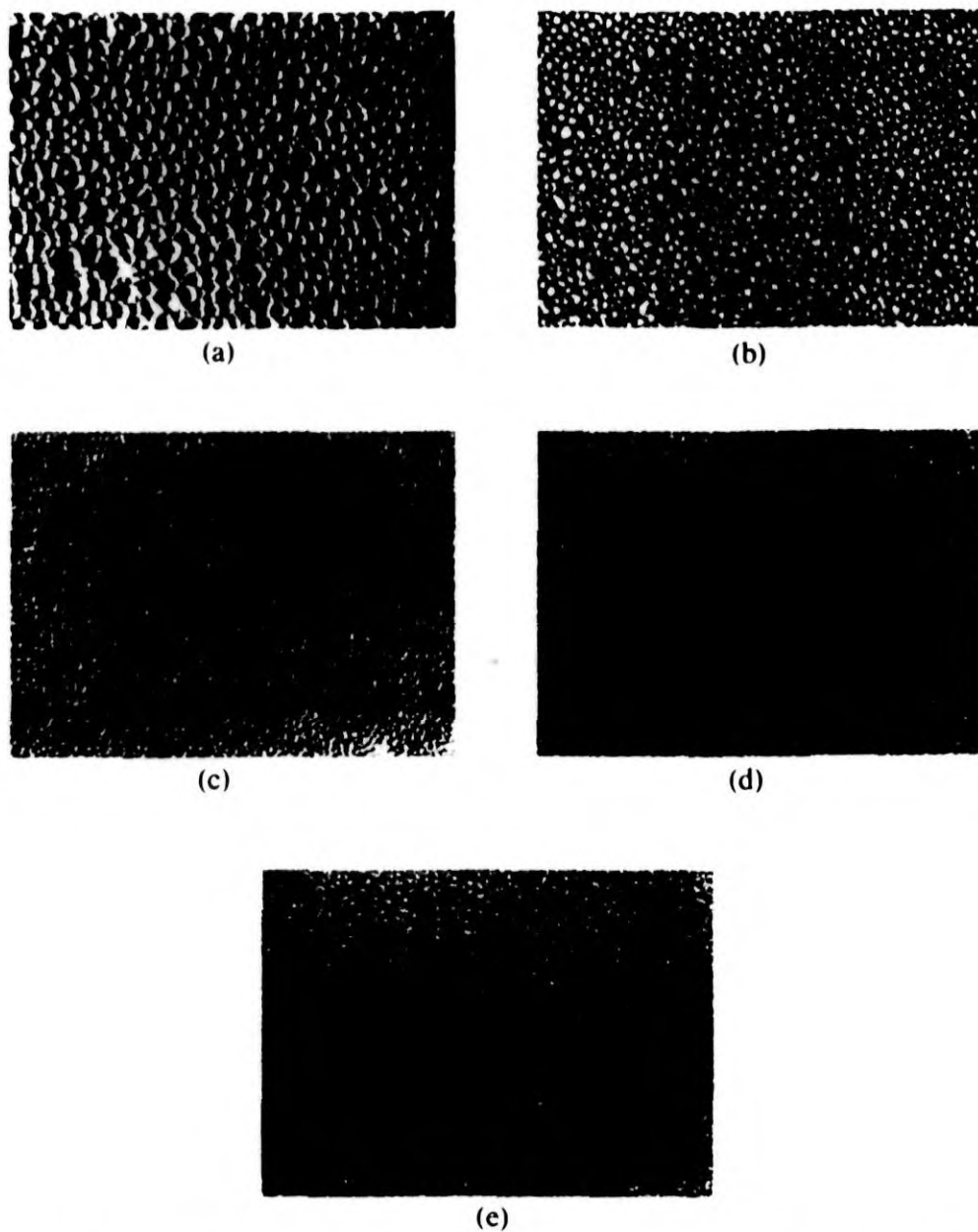
FIG. 1.   Optical micrographs of NR/PS blends containing (a) 0%, (b) 1.2%, (c) 3%, (d) 4.5%, and (e) 7.5% graft copolymer. Carbon tetrachloride-cast film.
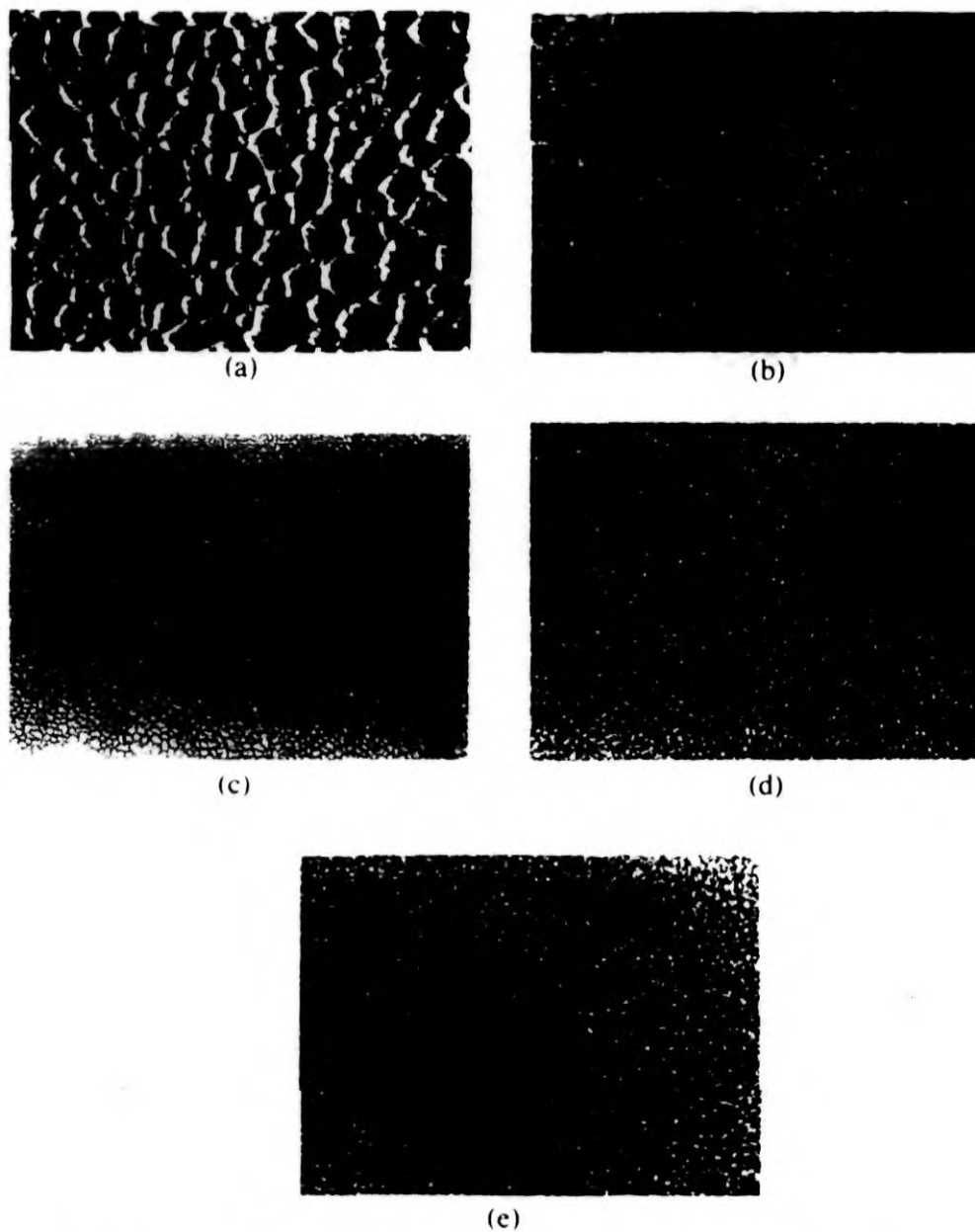
FIG. 2. Optical micrographs of NR/PS blends containing (a) 0%, (b) 1.2%, (c) 3%, (d) 4.5%, and (e) 7.5% graft copolymer. Chloroform-cast film.

domain size as a function of the graft copolymer content is given Fig. 3. The leveling off occurs at about 4.5% graft copolymer loading for chloroform- and 3% for carbon tetrachloride-cast film. This leveling point can be taken as the critical micelle concentration (CMC), i.e., the concentration at which micelles are formed. Further addition of the compatibilizer beyond CMC may not modify the interface much but may create micelle formation which is highly undesirable. The leveling
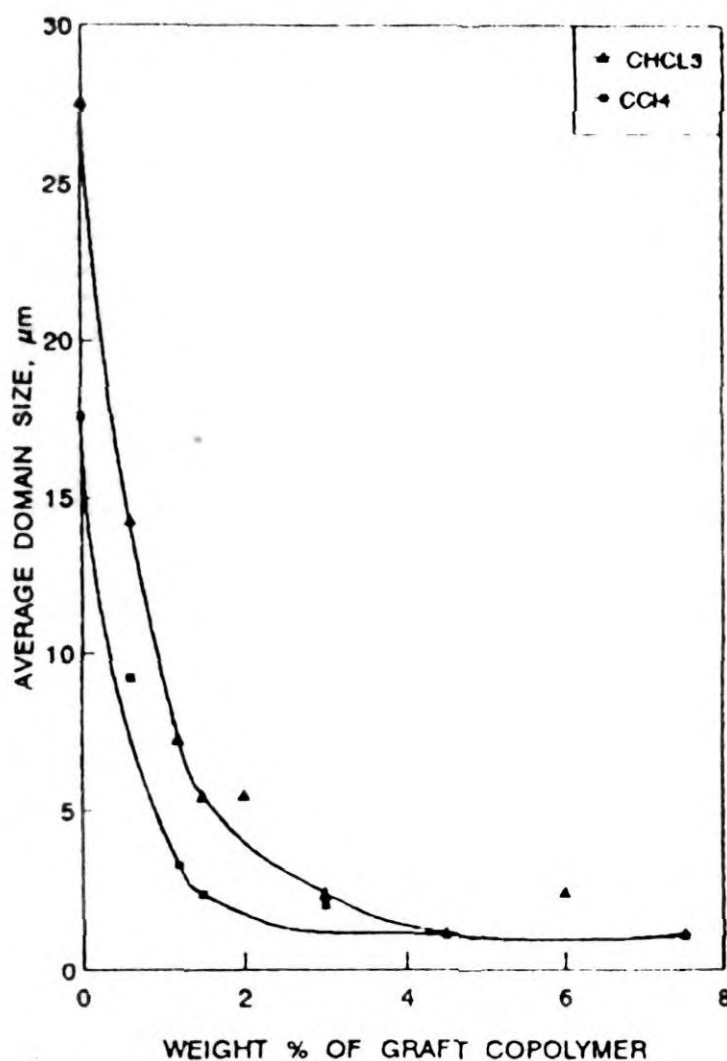

FIG. 3. Effect of compatibilizer loading and casting solvent on the dispersed phase size of NR/PS blends.
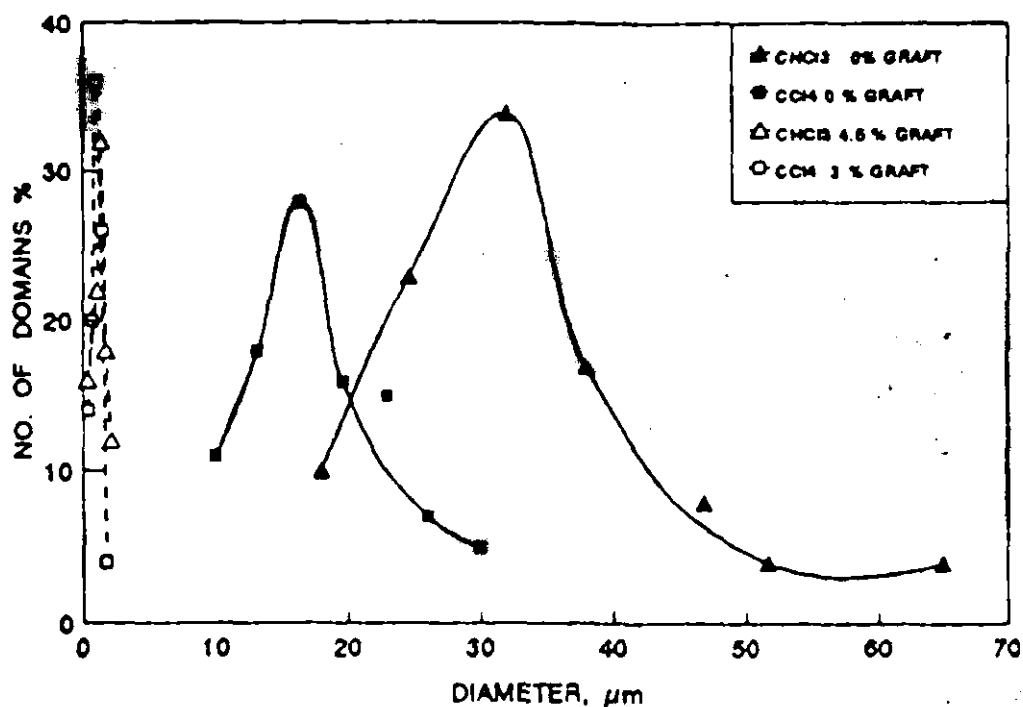
FIG. 4. Particle size distribution of NR/PS blends cast from $CHCl_3$ and CCl_4.

TABLE 2
Domain Size of Dispersed Phase

Weight percent of graft	CHCl₃		CCl₄	
	Average size (μm)	Standard deviation	Average size (μm)	Standard deviation
0	27.60	11.06	17.60	7.11
0.6	14.30	1.96	9.24	1.29
1.2	7.29	1.84	3.28	0.96
1.5	5.48	1.10	2.41	0.59
3.0	2.45	1.09	2.08	0.44
4.5	1.22	0.53	1.12	0.39

off is also an indication of interfacial saturation. It is also important to note that over the entire range of compatibilizer loading up to CMC, CCl_4 cast film shows finer morphology than $CHCl_3$-cast film.

The domain size distribution is given in Fig. 4. The polydispersity is higher for blends without graft copolymer as evidenced by the large width of the distribution curve. The domain size distribution curve of chloroform-cast film is broader than that of carbon tetrachloride-cast
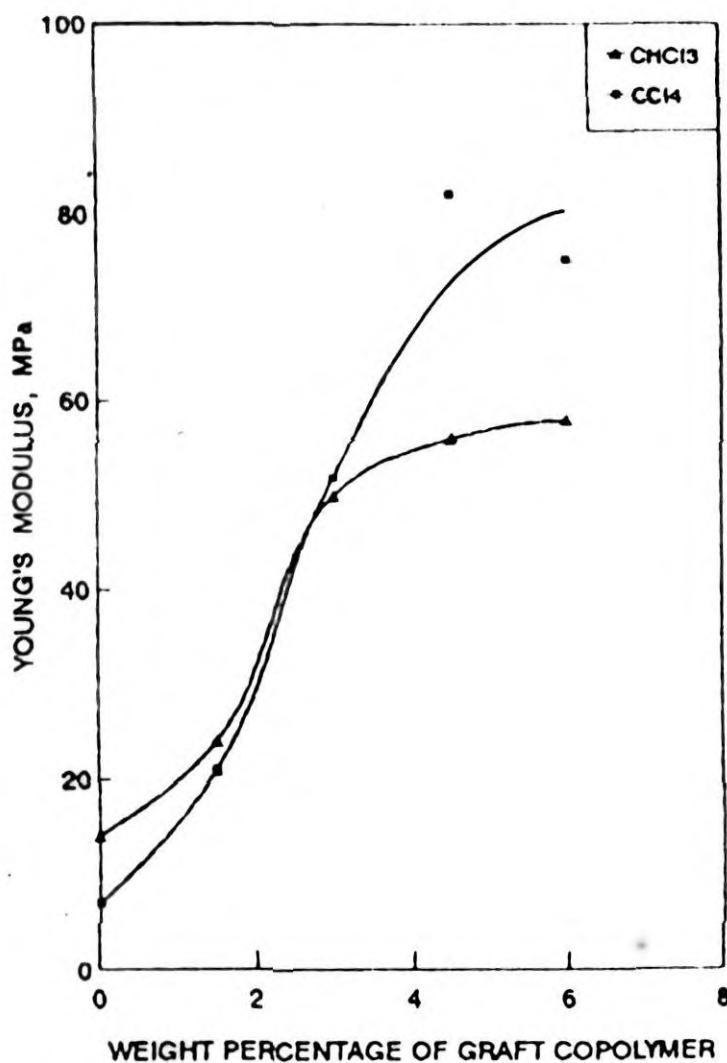

FIG. 5. Effect of compatibilizer loading on Young's modulus values.

film. Polydispersity is much reduced at 4.5% graft copolymer concentration for chloroform-cast film and at 3% graft copolymer concentration for carbon tetrachloride-cast film. The standard deviation values given in Table 2 also support the above findings.

Mechanical Properties

Figure 5 shows the Young's modulus values as a function of the weight percent (wt%) of graft copolymer. Among the compatibilized blends,
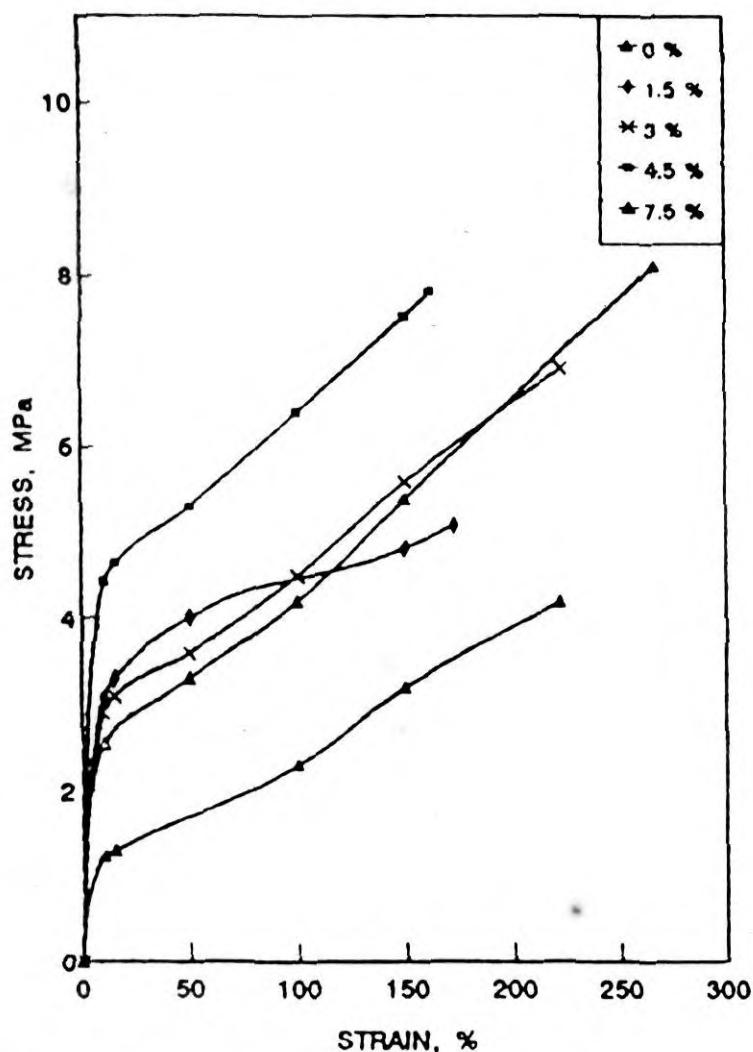

FIG. 6. Stress–strain behavior of CCl₄-cast NR/PS blends.

the Young's modulus values are slightly higher in the case of carbon tetrachloride-cast film than chloroform-cast film. In both cases the values increase with increasing concentration of the graft copolymer, followed by a leveling off.

Figures 6 and 7 show the stress–strain curves of the samples cast from carbon tetrachloride and chloroform, respectively. In both cases the stress–strain curves show a similar behavior. The stress–strain curves have in general elastic and inelastic regions. All the samples exhibit high initial modulus followed by a gradual increase in stress
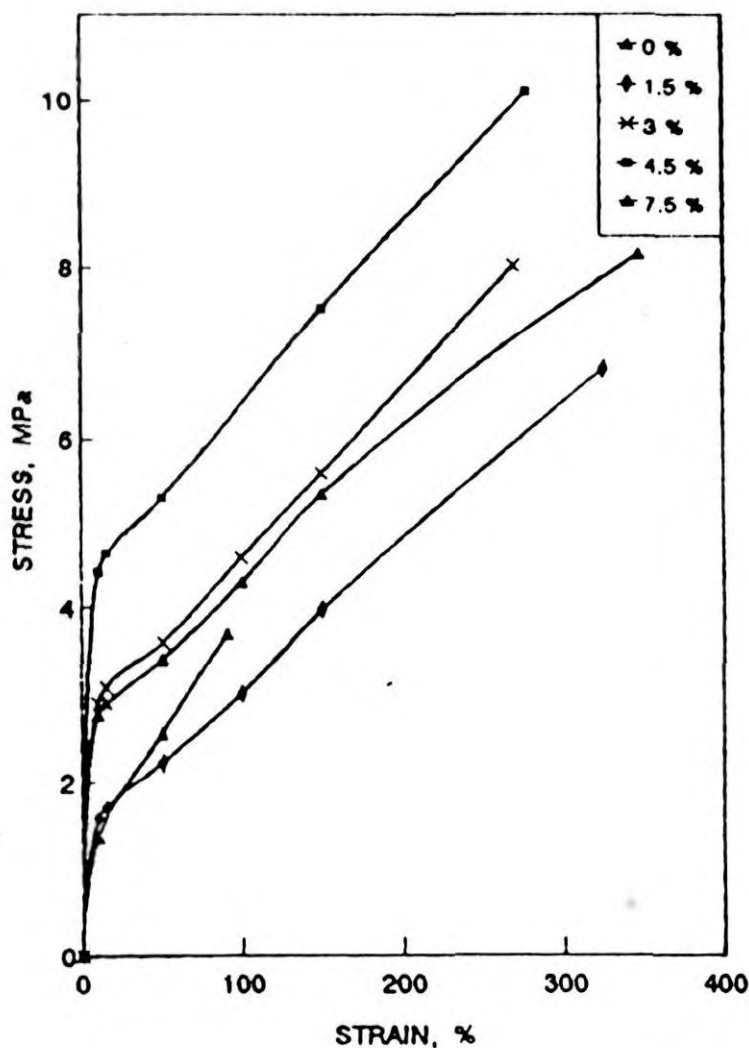

FIG. 7. Stress–strain behavior of CHCl₃-cast NR/PS blends.

with strain. In the case of carbon tetrachloride-cast film (Fig. 6), tensile strength increases up to 3% compatibilizer loading and then levels off due to micelle formation, which is highly undesirable. In the case of chloroform-cast film (Fig. 7) the trend is the same, and in this case tensile strength increases up to 4.5% compatibilizer loading and then levels off.

Table 3 shows the mechanical properties of the two systems. Tensile strength increases with increasing concentration of the compatibilizer in both cases. In the case of chloroform-cast film, tensile strength levels off at about 4.5% graft loading whereas in the case of carbon tetrachloride, leveling off occurs at about 3% graft loading. Though a finer particle size is obtained in the case of carbon tetrachloride compared to chloroform, the tensile properties are better in chloroform-cast film. This may be due to the occlusion of carbon tetrachloride in the cast film due to its high boiling point. This will act as a plasticizer and result in lower tensile properties. The elongation at break increases upon addition of the compatibilizer in both cases. This is associated with the microbridge formation between the PS domains and the NR matrix through the compatibilizer.

TABLE 3

Mechanical Properties of 60/40 NR/PS Blend

Nature of solvent	Weight percent of graft copolymer	Tensile strength (MPa)	Elongation at break (%)
CHCl₃	0	3.70	77
	1.2	4.83	308
	1.5	6.81	325
	3.0	8.00	270
	4.5	10.14	279
	6.0	10.24	351
CCl₄	0	3.39	161
	1.2	4.87	178
	1.5	5.24	173
	3.0	7.00	200
	4.5	7.88	163
	6.0	7.40	206

CONCLUSION

The effect of casting solvents on the compatibilizing action of NR-*g*-PS in heterogeneous NR/PS blend has been analyzed. It was found that the addition of the graft copolymer has strong influence on the morphology and mechanical properties of the blends. Carbon tetrachloride-cast film has a fine domain distribution compared to chloroform-cast film, and the domain size is much less in the former case. In both cases the domain size is decreased by the addition of a few percent of the copolymer, followed by a leveling off at higher concentration. The critical micelle concentration was found to be 4.5% in the case of chloroform- and 3% in the case of carbon tetrachloride-cast film. The differences are associated with the preferential interaction of the solvent with the component polymers. The mechanical properties of the blends are improved by the addition of compatibilizer.

ACKNOWLEDGMENTS

REFERENCES

1. D. R. Paul, in *Polymer Blends* (D. R. Paul and S. Newman, eds.), Academic Press, New York, 1978, Ch. 12.
2. D. R. Paul and J. W. Barlow, *Am. Chem. Soc. Adv. Chem. Ser.*, *176*, 315 (1979).
3. G. E. Molau, *J. Polym. Sci.*, *A3*, 1267 (1965).
4. G. E. Molau, *J. Polym. Sci.*, *A3*, 4235 (1965).
5. G. E. Molau and W. M. Wittbrodt, *Macromolecules*, *1*, 260 (1968).
6. P. Gailard, M. Ossenbach-Sauter, and G. Riess, *Makromol. Chem. Rapid Commun.*, *1*, 771 (1980).
7. P. Gailard, M. Ossenbach-Sauter, and G. Riess, in *Polymer Compatibility and Incompatibility: Principles and Practice* (K. Sole, ed.), MMI Symp. Ser. 2, Harwood, New York, 1982.

8. H. T. Patterson, K. H. Hu, and T. H. Grindstaff, *J. Polym. Sci. C, 34,* 31 (1971).

9. S. H. Anastasiadis, I. Gancarz, and J. T. Koberstein, *Macromolecules, 22,* 1449 (1989).

10. W. J. Coumans, D. Heikens, and S. D. Sjoerdsma, *Polymer, 21,* 103 (1980).

11. J. M. Willis and B. D. Favis, *Polym. Eng. Sci., 28*(21), 1416 (1988).

12. J. M. Willis and B. D. Favis, *Polym. Eng. Sci., 30*(17), 1073 (1990).

13. P. Caravatti, P. Neuenschwander, and R. R. Ernst, *Macromolecules, 18,* 119 (1985).

14. J. S. Chiou, D. R. Paul, and J. W. Barlow, *Polymer, 23,* 1543 (1982).

15. C. T. Chen and H. Morewetz, *Macromolecules, 22,* 159 (1989).

16. M. Bank, J. Leffingwell, and C. Thies, *Macromolecules, 4,* 43 (1971).

17. D. Heikens, *Kem. Ind., 31,* 165 (1982).

18. A. Robard and D. A. Patterson, *Macromolecules, 10,* 1021 (1977).

19. Z. Oommen, S. Thomas, and M. R. G. Nair, *Polym. Eng. Sci.* (in press).

20. S. Thomas and R. E. Prud'homme, *Polymer, 33*(20), 4260 (1992).

21. W. Cooper, P. R. Sewell, and G. Vaughan, *J. Polym. Sci., 41,* 167 (1959).

22. M. Goni, Gurrchaga, J. San Roman, M. Valero, and G. M. Guzman, *Polymer, 34,* 512–517 (1993).

Curriculum Vitae

Name ASALETHA R.

Age and Date of Birth 30, 29.5.1967

Permanent Address Kollalackal House
Puthuppally P. O., Kottayam
Kerala - 686 011, INDIA

Address for Correspondence Lecturer
School of Technology and Applied Sciences
Mahatma Gandhi University, Mannanam, Kottayam
Kerala - 686 561, INDIA
Fax: 91-481-561190
Phone: 0473-342274

Education M.Sc. Chemistry, Distinction

Research Interests

1. Transport process through polymers, its kinetics and thermodynamics.
2. Polymer blends: Characterization and properties
3. Polymer composites: Fabrication and properties
4. Interpenetrating networks: Latex IPNs and characterization

Work Experience

Five years research experience in Polymer Technology/Chemistry.

Skills

Instrumentation: Most of rubber/plastic processing and characterissation machineries.

Awards

1. Senior Research Fellowship, CSIR, New Delhi.
2. Young Scientist Award, Indian Science Congress Association.

Memberships

1. Indian Science Congress Association
2. Mahatma Gandhi University Chemical Society
3. Indian Society for Technical Education